

SYVAC3-CC4 THEORY

NWMO TR-2011-20

June 2011

Nuclear Waste Management Organization

nwmo

NUCLEAR WASTE
MANAGEMENT
ORGANIZATION

SOCIÉTÉ DE GESTION
DES DÉCHETS
NUCLÉAIRES

Nuclear Waste Management Organization
22 St. Clair Avenue East, 6th Floor
Toronto, Ontario
M4T 2S3
Canada

Tel: 416-934-9814
Web: www.nwmo.ca

SYVAC3-CC4 THEORY

NWMO TR-2011-20

June 2011

ABSTRACT

Report Number: NWMO TR-2011-20
Title: SYVAC3-CC4 THEORY
Company: Nuclear Waste Management Organization
Date: June 2011

Abstract

This report describes the theory for the Canadian Concept Generation 4 (CC4) system model for postclosure safety assessment of a deep geologic repository for used CANDU fuel. The system model is composed of several linked submodels – the wasteform and containers, the engineered barriers in the repository, the geosphere, and the biosphere.

The CC4 model was developed to address the configuration of a deep geologic repository for used nuclear fuel with emplacement of durable containers, surrounded by dense clay and backfill. The repository is located deep underground in stable, saturated rock. The submodels of the wasteform, containers and engineered barriers describe the failure of some containers through small defects, degradation of the used fuel, contaminant (radionuclide) release through the defects in the container, and migration of contaminants through buffer and backfill materials. The geosphere model describes the movement of contaminants from the repository via the groundwater in both the rock mass and in the fracture system, to the surface environment. The biosphere model describes the movement of contaminants between surface water, soils, atmosphere, vegetation, animals and humans, and the consequent radiological dose to a reference person and generic biota living near the repository.

Earlier versions of this system model were used for the case studies presented in the AECL Environmental Impact Statement and Second Case Studies, in the OPG Third Case Study, and in the NWMO Glaciation Study. This report describes Version CC4.08 of the system model.

TABLE OF CONTENTS

	<u>Page</u>
ABSTRACT	v
1. INTRODUCTION	1
1.1 BACKGROUND	1
1.2 SCOPE	3
1.3 REFERENCES	3
2. WASTEFORM AND CONTAINER MODEL	5
2.1 MODEL OVERVIEW	5
2.2 NUCLIDE INVENTORIES	5
2.3 CONTAINER FAILURE	7
2.3.1 Failure Characteristics.....	7
2.3.2 Failure Rate.....	8
2.4 WASTE DEGRADATION	9
2.4.1 Fuel Wasteform	9
2.4.2 Zircaloy Waste Matrix	11
2.4.3 Metallic Wasteforms	12
2.4.4 Soft Wasteforms.....	12
2.5 SOLUBILITIES OF NUCLIDES	12
2.5.1 Equilibrium Constants.....	13
2.5.2 Speciation of Groundwater	13
2.5.3 Elemental Solubilities	18
2.6 NUCLIDE RELEASE INTO CONTAINER	25
2.6.1 Release from UO ₂ Matrix.....	25
2.6.2 Release from Zircaloy Cladding.....	26
2.6.3 Release from Other Wasteforms	27
2.7 RELEASE FROM CONTAINER	28
2.7.1 Release Processes	28
2.7.2 Constant Nuclide Concentration in Container	28
2.7.3 Time-Dependent Nuclide Concentration in Container without Precipitation	30
2.7.4 Isotopic Ratios for Co-Precipitation.....	33
2.7.5 Release from Container after Precipitation	34
2.8 INTERFACE WITH VAULT MODEL	35
2.9 REFERENCES	35

3. VAULT MODEL	38
3.1 MODEL OVERVIEW	38
3.2 VAULT SECTOR PROPERTIES	38
3.2.1 Excavation Damaged Zone Physical Properties	40
3.2.2 Transverse Darcy Velocities.....	41
3.2.3 Axial Darcy Velocities.....	42
3.3 TRANSPORT THROUGH BUFFER, BACKFILL AND EDZ	42
3.3.1 Mass Balance Equation and Parameters.....	43
3.3.2 Boundary Conditions and Solution	45
3.4 INTERFACE WITH SURROUNDING GEOSPHERE	46
3.5 REFERENCES	46
4. GEOSPHERE MODEL	48
4.1 INTRODUCTION	48
4.2 MODEL OVERVIEW	50
4.3 TRANSPORT MODEL	54
4.3.1 Transport Equation.....	54
4.3.2 Transport Calculation Using Response Functions	54
4.3.3 Boundary Conditions	55
4.3.4 Response Functions for Time Dependent Parameters	57
4.3.5 Parameters in the Transport Equation.....	61
4.4 WELL MODEL	66
4.4.1 Overview.....	66
4.4.2 Maximum Well Capacity.....	67
4.4.3 Drawdowns in the Aquifer.....	67
4.4.4 Surface Water Captured.....	69
4.4.5 Plume Capture Fractions.....	69
4.4.6 Site-Specific Effects of the Well.....	73
4.5 MATRIX DIFFUSION	74
4.5.1 Requirements for Application.....	74
4.5.2 Quasi-Equilibrium Regime.....	77
4.5.3 Thick-Rock Regime	77
4.5.4 Hydrodynamic Regime.....	78
4.5.5 Transitions Between the Regimes	78
4.6 COLLOIDS	79
4.7 INTERFACE WITH VAULT MODEL	80
4.8 INTERFACE WITH BIOSPHERE MODEL	81

4.9 REFERENCES	83
5. BIOSPHERE MODEL	86
5.1 MODEL OVERVIEW	86
5.2 GEOSPHERE-BIOSPHERE INTERFACE	88
5.2.1 Modelling Well Usage.....	89
5.2.2 Nuclide Concentrations in the Discharges to the Biosphere	92
5.3 THE SURFACE WATER SUBMODEL	94
5.3.1 General	94
5.3.2 Lake Water.....	96
5.3.3 Lake Sediment	97
5.3.4 Concentration in Bioturbated Sediment Layer	98
5.3.5 Concentration in Sediment over a Discharge.....	99
5.3.6 Use of Sediments in Fields.....	99
5.4 THE SOIL SUBMODEL	100
5.4.1 Overview of the Soil Model	100
5.4.2 Soil Inflow Terms.....	105
5.4.3 Loss Terms	111
5.4.4 Contaminant Concentrations in the Field Soils	115
5.5 THE ATMOSPHERE SUBMODEL	116
5.5.1 General	116
5.5.2 Particulates	118
5.5.3 Indoor suspension from water (<i>ISW</i>)	119
5.5.4 Terrestrial Degassing (<i>TG</i>).....	119
5.5.5 Aquatic Degassing (<i>AG</i>).....	120
5.5.6 Indoor Radon Gas Sources (<i>IRN</i>).....	121
5.5.7 Noble Gas Groundwater Release (<i>GWR</i>).....	121
5.5.8 Fires	121
5.5.9 Total.....	123
5.5.10 Deposition Flows	124
5.6 THE FOOD-CHAIN AND DOSE SUBMODEL	125
5.6.1 General	125
5.6.2 Ingrowth	127
5.6.3 Human Ingestion and Inhalation Rate.....	129
5.6.4 Terrestrial Plant/Animal Pathways.....	129
5.6.5 Human Drinking Water Pathway.....	135
5.6.6 Human Soil Ingestion Pathway.....	135
5.6.7 Human Inhalation Pathway.....	135
5.6.8 Human External Doses.....	136
5.6.9 Mass/Radioactivity Conversion Factor.....	138
5.6.10 Internal Dose Arising from ¹²⁹ I	139
5.6.11 Internal Dose Arising from ¹⁴ C	140
5.6.12 Internal Dose Arising from ³⁶ Cl	140
5.6.13 Internal Dose Arising from ³ H	141
5.6.14 Total Doses to Humans	141

5.7 CHEMICAL TOXICITY	142
5.8 RADIOLOGICAL IMPACTS ON NON-HUMAN BIOTA	143
5.8.1 Reference Biota.....	143
5.8.2 Mathematical Formulation	144
5.8.3 Internal Exposure of Plants.....	145
5.8.4 Internal Exposure of Terrestrial Animals	146
5.8.5 Internal Exposure of Fish.....	147
5.8.6 Immersion in Water	147
5.8.7 Immersion in Soil or Sediment.....	148
5.8.8 Immersion in Air	148
5.8.9 Immersion in Vegetation.....	149
5.8.10 Determination of Total External Doses	149
5.8.11 Calculation of Total Radiological Doses	150
5.8.12 Groundwater Limits to ¹⁴C, ³⁶Cl and ¹²⁹I Internal Doses for Non-Human Biota	150
5.8.13 Model for Tritium	151
5.9 REFERENCES.....	151
6. MASS ACCUMULATION AND DISTRIBUTION.....	154
6.1 MASS IN CONTAINER	154
6.2 MASS IN ENGINEERED BARRIERS	155
6.3 MASS IN GEOSPHERE.....	156
6.4 MASS IN BIOSPHERE	157
7. RADIOTOXICITY INDICATORS.....	160
7.1 RADIOTOXICITY CONCENTRATION IN LAKE WATER	160
7.2 RADIOTOXICITY FLUX FROM GEOSPHERE	160
7.3 REFERENCES.....	161
ACKNOWLEDGEMENTS.....	162
APPENDIX A: CONVOLUTION AND COMPARTMENT MODELS	163
APPENDIX B: LAPLACE TRANSFORM INVERSION	165
APPENDIX C: BIOSPHERE SUBMODEL PARAMETERS	167

LIST OF TABLES

	<u>Page</u>
Table 2.1: Example Binomial Distribution Calculation of Number of Failed Containers.....	9
Table 2.2: Species Used in Determining Solubilities.....	21

LIST OF FIGURES

	<u>Page</u>
Figure 1.1: Illustration of the multi-barrier repository concept for a deep geologic repository showing the multi-barrier design concept	2
Figure 2.1: Standard 37-element CANDU used fuel bundle. Each bundle is 102-mm diameter and 495 mm long, and holds about 19 kg of UO ₂	6
Figure 2.2: Used fuel container concept showing outer copper shell, steel inner vessel, and used fuel bundles held in steel baskets. This design is about 1.25 m diameter by 3.9 m long and holds 360 bundles (Garisto et al. 2011).....	6
Figure 2.3: Distribution of various radionuclides within a used fuel element	25
Figure 3.1: Cross-sectional view of three candidate emplacement room layouts, showing the main material components.....	39
Figure 3.2: Emplacement room geometry used in the CC4 vault model	40
Figure 4.1: (a) 3-D and (b) 2-D views of the geosphere network used to model a hypothetical repository placed within the Whiteshell Research Area (Davison et al. 1994).....	48
Figure 4.2: A schematic example of a CC4/GEONET representation of a two-dimensional geosphere model (surface relief exaggerated)	50
Figure 4.3: Illustration of the principal properties of a transport segment.....	51
Figure 4.4: Illustration of the insertion of sediment and overburden layers. Figure (A) shows a transport segment passing through a layer of bedrock leading to a discharge. Figure (B) shows the introduction of nodes added to define sediment and overburden layers in the geosphere transport network	52
Figure 4.5: Schematic illustration of a vertical cross-section through the well reference nodes	53
Figure 4.6: Illustration of the boundary conditions for which response functions have been developed for use in transport of contaminants across 1-D segments	56
Figure 4.7: Schematic illustration in cross-section of piezometric surfaces in the well aquifer with and without a well present	68
Figure 4.8: Schematic plan view showing capture line, capture nodes and dividing streamline in the aquifer	70
Figure 4.9: Plan view of groundwater streamlines in the aquifer supplying the well with moderate well demand (upper figure) and higher well demand (lower figure). The stagnation points are shown by the symbol □	72
Figure 4.10: Illustration of the magnitude of the effective retardation factor, R, as a result of matrix diffusion effects as a function of travel distance, L, showing the three regimes: hydrodynamic, thick rock and quasi-equilibrium. There is a long transition region between the thick rock and the quasi-equilibrium regimes (after Lever et al. 1982)	76
Figure 4.11: Illustration of a cluster of associated discharges - aquatic, terrestrial and wetland.....	82
Figure 5.1: Conceptual view of biosphere model (Davis et al. 1993)	88

Figure 5.2: Transport processes considered in the lake (surface water) submodel (Goodwin et al. 1994)96

Figure 5.3: Transport processes considered in the soil submodel (Goodwin et al. 1994) 101

Figure 5.4: Illustration of the upland surface soil model: (a) dimensions, (b) water flow, and (c) contaminant flow. 106

Figure 5.5: Illustration of the shallow soil model: (a) dimensions, (b) water flow, and (c) contaminant flow. In this model, the water table fluctuates seasonally into the surface soil region, so the groundwater discharge is assumed to go directly into the surface soil 107

Figure 5.6: Transport processes considered in the atmosphere submodel (Goodwin et al. 1994)..... 117

SYVAC3-CC4 THEORY

1. INTRODUCTION

1.1 BACKGROUND

This report describes the Canadian Concept - Generation 4 (CC4) system model for postclosure safety assessment of a deep geologic repository for used CANDU fuel. The system model is composed of several linked submodels – the wasteform, the containers, the engineered barriers in the repository, the geosphere, and the biosphere.

The system model was developed to address the configuration of a deep geologic repository for used nuclear fuel with in-room emplacement of durable containers, surrounded by dense clay and backfill. The repository is located deep underground in stable, saturated rock. An illustrative figure of such a repository is provided in Figure 1.1. The wasteform and container model describes the failure of some containers through small defects, degradation of the used fuel by water, and contaminant release from the container via water. The vault model describes the movement of contaminants through buffer and backfill materials, and a possible damaged rock zone around the room. The geosphere model describes the movement of contaminants from the repository via the groundwater, through both the rock mass and fractures, to the surface environment. The biosphere model describes the concentration of contaminants in surface water, soils, atmosphere, vegetation and animals, and estimates the consequent radiological dose to a reference person and generic biota living near the repository. Peak element concentrations in water, air and soil are also calculated.

An earlier version of this model was implemented as a computer code (CC3) and used for the safety assessment submitted to the Canadian environment assessment panel in 1994 for the AECL concept for used fuel disposal (Goodwin et al. 1994). A revised model, referred to as PR4, as a “prototype” for CC4, was used for the AECL Second Case Study (Goodwin et al. 1996). The system model has continued to be updated and improved. CC4, Version 4.04 was used for the OPG Third Case Study (Gierszewski et al. 2004).

In CC4 Version 4.07 the capability of the previous versions was extended by permitting the simulation of changes in state in the geosphere and biosphere. A change in state means that some characteristic properties of the system could be significantly different at stipulated points in time. The CC4 Version 4.07 submodels can represent the changed states, approximating the transformations as abrupt events. One specific example of interest is glaciation, and the CC4 Version 4.07 model permits the investigation of how the performance of the repository might be affected by a succession of one or more glacial cycles, each of which may contain different states such as temperate, permafrost and ice sheet states. The principal new input requirement for CC4.07 was the triplet set:

$$\{S_i^G, S_i^B, t_i^S\}, \quad (1.1)$$

which defines a sequence of states for the geosphere, S_i^G , and the biosphere, S_i^B , each with a state duration time of t_i^S years. The first states S_1^G and S_1^B occur at the start of the simulation time and the summation over the state duration times should equal or exceed the end of the simulation time. Note that S_i^G and S_i^B represent state descriptors, such as “geosphere

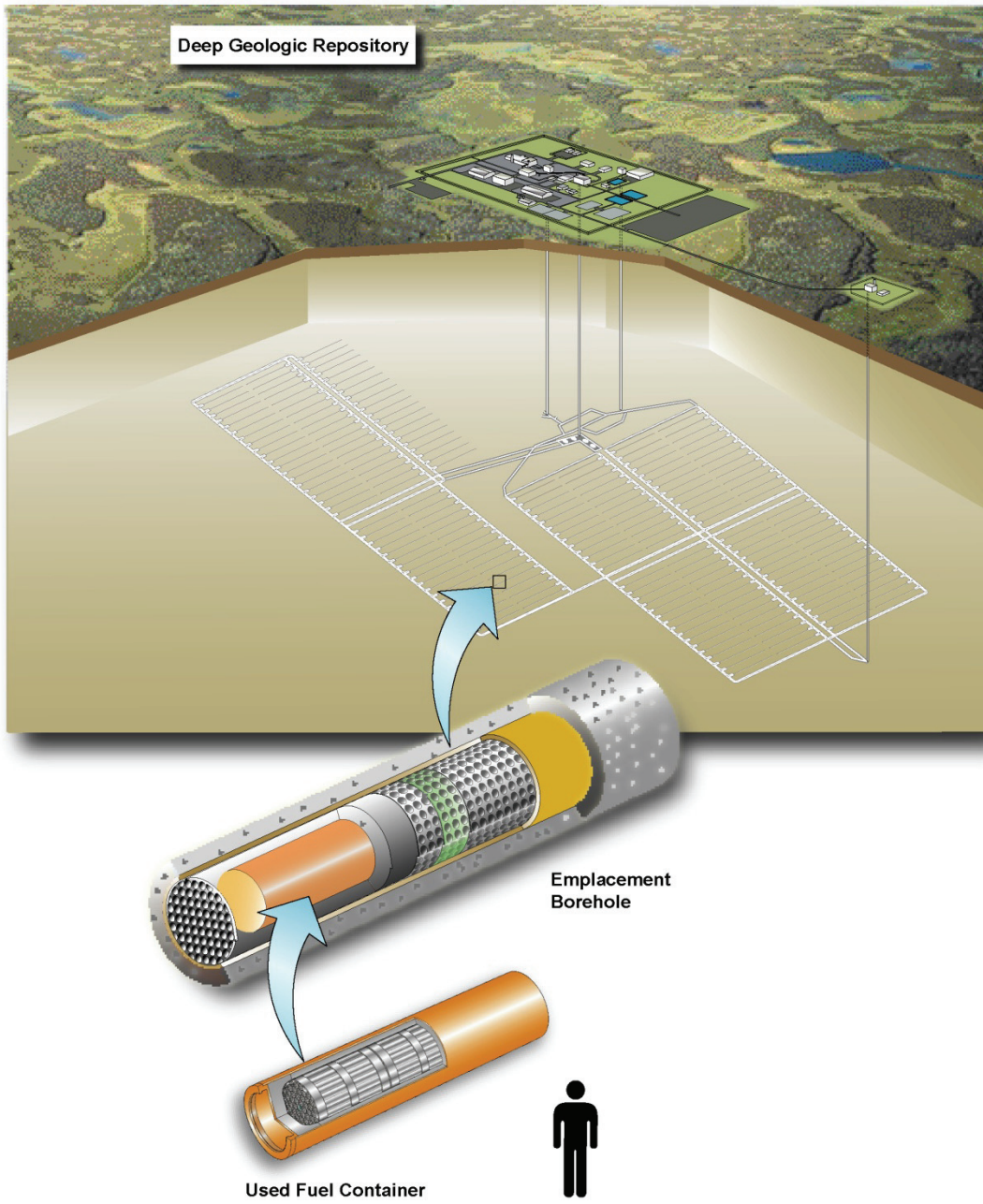


Figure 1.1: Illustration of the multi-barrier repository concept for a deep geologic repository showing the multi-barrier design concept

permafrost” and “biosphere temperate”. In principle, they should be related, meaning that the geosphere and biosphere should have similar states at the same point in time. CC4 Version 4.07 was used for the glaciation study described in Garisto et al. (2010).

This report describes CC4 Version 4.08. This version of the code will be used in the forthcoming Fourth Case Study and includes several minor modifications, including:

- (i) The calculation of the concentrations in air of ^{222}Rn and ^{129}I due to volatilization from surface water bodies was modified to parallel the calculations used for other volatile radioisotopes. This change means that these volatilization losses are taken into account when calculating the ^{222}Rn and ^{129}I concentrations in the water body and when estimating the biosphere mass balance.
- (ii) In previous versions of the CC4 model, a minimum depth for a groundwater supply well could be specified, based on stratigraphic or topographic restrictions. This option has been removed in the CC408.
- (iii) Airborne radionuclide concentrations due to suspension of terrestrial particulates were previously estimated using whichever field had the maximum soil concentration. In CC4.08, these concentrations are computed using the soil concentration of the field from which the particulates are suspended.

1.2 SCOPE

This report gives the main equations implemented in the system model computer code, with their underlying assumptions. References are given where more detailed or background information is published. Recommended values for the parameters are specific to each safety assessment, and are not included here.

The report describes the CC4 model in four main sections – the wastefrom and container in Section 2, the repository engineered barriers in Section 3, the geosphere in Section 4, and the biosphere in Section 5. These sections also include a description of how changes in state are accommodated in the submodels: Section 2.3.1 is concerned with the simulation of container failure, and Sections 4.1 and 5.1 with properties of the geosphere and biosphere respectively. Section 6 describes the mass distribution information available from the model, and Section 7 describes complementary safety indicators.

1.3 REFERENCES

- Garisto, F., J. Avis, T. Chshyolkova, P. Gierszewski, M. Gobien, C. Kitson, T. Melnyk, J. Miller, R. Walsh and L. Wojciechowski. 2010. Glaciation scenario: Safety assessment for a deep geological repository for used fuel. Nuclear Waste Management Organization Technical Report NWMO TR-2010-10. Toronto, Canada.
- Gierszewski, P., J. Avis, N. Calder, A. D'Andrea, F. Garisto, C. Kitson, T. Melnyk, K. Wei and L. Wojciechowski. 2004. Third case study - Postclosure safety assessment. Ontario Power Generation Report 06819-REP-01200-10109-R00. Toronto, Canada.
- Goodwin, B.W., D. McConnell, T. Andres, W. Hajas, D. LeNeveu, T. Melnyk, G. Sherman, M. Stephens, J. Szekely, P. Bera, C. Cosgrove, K. Dougan, S. Keeling, C. Kitson, B. Kummen, S. Oliver, K. Witzke, L. Wojciechowski and A. Wikjord. 1994. The

disposal of Canada's nuclear fuel waste: Postclosure assessment of a reference system. Atomic Energy of Canada Limited Report AECL-10717, COG-93-7. Pinawa, Canada.

Goodwin, B.W., T. Andres, W. Hajas, D. LeNeveu, T. Melnyk, J. Szekely, A. Wikjord, D. Donahue, S. Keeling, C. Kitson, S. Oliver, K. Witzke and L. Wojciechowski. 1996. The Disposal of Canada's Nuclear Fuel Waste: A study of postclosure safety of in-room emplacement of used CANDU fuel in copper containers in permeable plutonic rock. Volume 5: Radiological Assessment. Atomic Energy of Canada Limited Report AECL-11494-5, COG-95-552-5. Pinawa, Canada.

2. WASTEFORM AND CONTAINER MODEL

2.1 MODEL OVERVIEW

The reference wasteform is a CANDU used fuel bundle, consisting of irradiated UO_2 encased in Zircaloy cladding (Figure 2.1). Radionuclides are contained in either the UO_2 fuel matrix or the Zircaloy cladding (including the end-plates).

Depending on the design, a few hundred used fuel bundles are placed into a used fuel container. The reference container concept has a corrosion-resistant copper shell and a structural steel inner vessel (Figure 2.2).

The container model tracks the decay and possible eventual release of radionuclides in the used fuel as a result of container failure. It models the following processes:

- failure of some containers at a specified time through a small defect that allows water to enter the containers and contact the fuel;
- instant release of a fraction of contaminants in the UO_2 fuel and Zircaloy cladding on contact with water;
- release of remaining radionuclides as the UO_2 and Zircaloy corrodes;
- corrosion of UO_2 based on a kinetic model related to the time-dependent dose rate;
- corrosion of the Zircaloy cladding based on a solubility-limited dissolution model;
- precipitation of contaminants inside the failed container if solubility limits are exceeded;
- radioactive decay and ingrowth; and
- transport by diffusion of dissolved contaminants through the container defect and into the surrounding buffer.

The model does not account for any effect of the Zircaloy cladding on delaying or inhibiting fuel corrosion, or for sorption on surfaces within the container. It assumes that groundwater flow is sufficiently slow within the container volume that advective transport is negligible, and that the container shell, although punctured, retains its general integrity such that the release of contaminants must occur through a small defected area.

Calculations are made for a representative failed container, with the output being the release rate of radionuclides from the container into the surrounding buffer. This radionuclide outflow is used as the source term for analysis of radionuclide transport through the engineered barriers in the repository as described in the next section. The calculations allow for linear decay chains.

2.2 NUCLIDE INVENTORIES

The initial inventory of a nuclide i in the container in wasteform w , $I_{0,w}^i$, is

$$I_{0,w}^i = I_{0,ww}^i \cdot M_{ctr,w} \quad (2.1)$$

where $I_{0,ww}^i$ is the initial inventory of nuclide i in wasteform w per kg of wasteform w , and $M_{ctr,w}$ is the mass of wasteform w in a container.

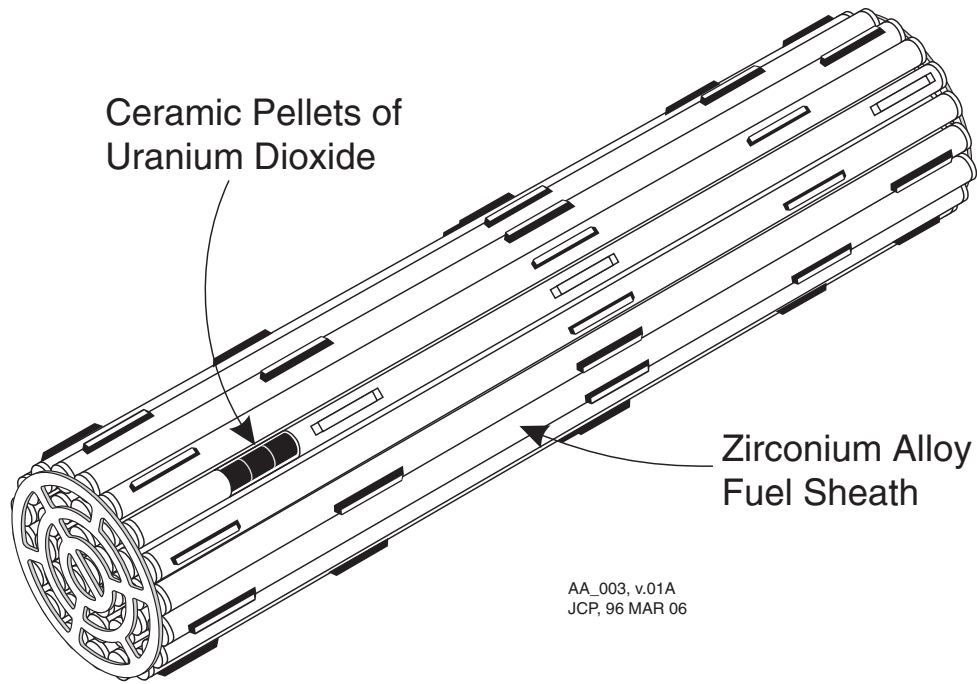


Figure 2.1: Standard 37-element CANDU used fuel bundle. Each bundle is 102-mm diameter and 495 mm long, and holds about 19 kg of UO_2

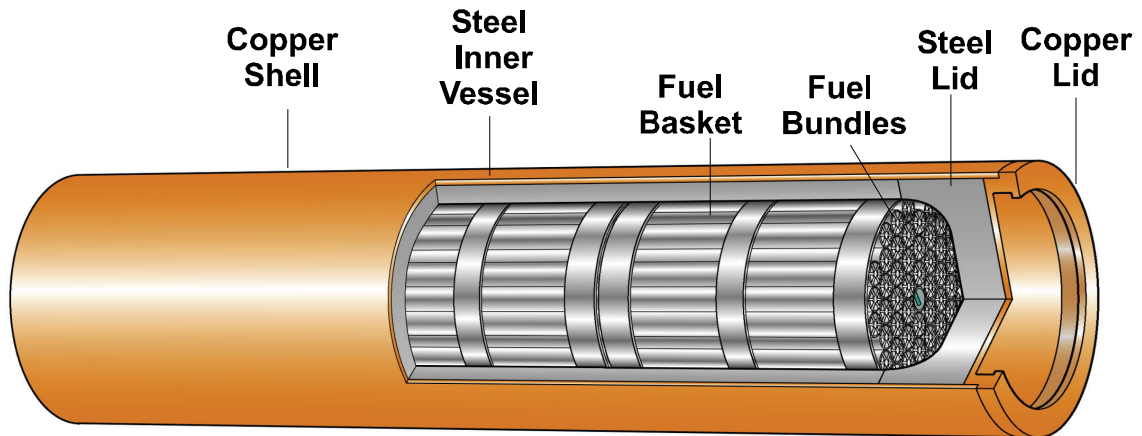


Figure 2.2: Used fuel container concept showing outer copper shell, steel inner vessel, and used fuel bundles held in steel baskets. This design is about 1.25 m diameter by 3.9 m long and holds 360 bundles (Garisto et al. 2011)

Since radionuclides decay at different rates, and some nuclides decay into other nuclides, the amounts of the nuclides change with time. The nuclide inventory in wasteform w , $I_w^i(t)$ for a linear decay chain (nuclides $1, 2, \dots, i$) is given by Bateman (1910):

$$I_w^i(t) = \sum_{q=1}^i (B^{iqw} e^{-\lambda^q t}), \quad (2.3)$$

where the sum goes over all decay chain precursors of nuclide i , and

$$B^{iqw} = \sum_{j=1}^q (I_{0,w}^j X^{iqj}) \quad (2.4a)$$

$$X^{iqj} = \begin{cases} 1 & \text{if } j = q = i \\ \prod_{r=j}^{i-1} \lambda^r \left[\prod_{r=j, r \neq q}^i (\lambda^r - \lambda^q)^{-1} \right] & \text{otherwise} \end{cases} \quad (2.4b)$$

In Equation (2.4b), it is assumed that no two decay constants have the same value so that $(\lambda^r - \lambda^q)$ is never zero. This is true for all known radionuclides with half-lives longer than 1 day.

2.3 CONTAINER FAILURE

2.3.1 Failure Characteristics

The containers are made from a durable material. Under the expected conditions in the repository, they would not fail for thousands of years (e.g. McMurry et al. 2003). As long as the container remains intact the radionuclides are confined.

The CC4 safety assessment model, however, considers the consequences of failure of some containers. Specifically, the model considers that the failed containers are characterized by small defects that occur randomly among the containers with the same probability per container.

The actual failure process is not modelled. Instead, the initial time of failure (or delay time) t_F is provided as a model input, with all failed containers within a given repository sector failing at the same time. It should be noted that the failure time t_F does not correspond to the actual time when a defect is formed in the container wall, since it may take some further time for water to enter the container and contact the fuel. Rather, t_F could also account for factors such as the time until the repository saturates and groundwater comes into physical contact with fuel. At this time, there is sufficient water within the container to support radionuclide release from the fuel and provide a continuous water pathway between the container interior and the surrounding buffer. Radionuclides dissolved in the water can diffuse through this pathway as described later in this report.

Over time, further corrosion of the container could occur, especially since the interior of the container can be wetted by water entering through the initial defect. For example, there could be growth of iron corrosion products, leading to enlargement of the defect, and at some point loss of structural integrity of the container (McMurry et al. 2004). Structural integrity could also

be compromised during a glacial cycle, possibly caused by enhanced mechanical pressures from an overlaying ice sheet. From a radionuclide transport perspective, the pathway for nuclide release may become larger, although possibly partly blocked by corrosion products.

In the CC4 model, the potential increase in the size of the defect is not modelled and the current model only includes a constant defect size.

2.3.2 Failure Rate

Since each container can have only two states - intact or failed - and the container failures are independent of each other (by assumption), then the number of failed containers can be obtained from a binomial distribution.

In the language of the binomial distribution, if the quantity j is the number of "occurrences" of a given state (container failures in this case) in N "trials" (total number of containers), each having probability p of this state "occurring" (probability of container failure), then the probability that there will be j "occurrences" is the binomial probability distribution:

$$B(j; N, p) = \frac{N!}{j!(N-j)!} p^j (1-p)^{N-j} \quad (2.5)$$

and the probability that there will be up to and including m "occurrences" is the cumulative binomial probability distribution:

$$P(m; N, p) = \sum_{j=0}^m \frac{N!}{j!(N-j)!} p^j (1-p)^{N-j} \quad (2.6)$$

For example, consider a case with 10 containers, each having probability of failure 0.2. The binomial distribution failure pattern is given in Table 2.1. The table indicates that the probability of no failed containers is 10.7%, of 1 failed container is 27%, and of 10 (out of 10) failed containers is 1 in 10 million.

For the CC4 safety assessment model, the total number of containers in each sector N_T^s and the probability of container failure P_F are input. A failure quantile Q_F^s is chosen randomly over $[0,1]$ (uniform probability) or supplied as input. Equations (2.6) and (2.7) can then be solved to give N_F^s , the number of failed containers in repository sector s :

$$\begin{cases} 0 \leq Q_F^s \leq P(0; N_T^s, P_F) & \text{then } N_F^s = 0, \text{ else} \\ P(N_F^s - 1; N_T^s, P_F) < Q_F^s \leq P(N_F^s; N_T^s, P_F) & \text{with } 1 \leq N_F^s \leq N_T^s \end{cases} \quad (2.7)$$

Referring again to the example in Table 2.1, if the failure quantile is sampled randomly from a uniform distribution in the range $[0,1]$, then for each sampling, there would be a different number of containers failing, from 0 to 10. Over many such samplings, the average number of containers failing would be 2. However, only 30% of the samplings would have exactly 2 failures; in 38% of the samplings, the number of failed containers would be less than 2, while in the remaining 32% the number of failed containers would be greater than 2.

Table 2.1: Example Binomial Distribution Calculation of Number of Failed Containers

Number of Failures j	Probability of j Failures $B(j;N,p)$	Probability of up to j Failures $P(j;N,p)$	Contribution to Average $j \cdot B(j;N,p)$
0	0.107	0.107	0.000
1	0.268	0.375	0.268
2	0.302	0.677	0.604
3	0.201	0.878	0.603
4	0.088	0.966	0.352
5	0.026	0.992	0.130
6	0.006	0.998	0.036
7	0.001	0.999	0.007
8	0.00007	1.000	<0.001
9	0.000004	1.000	<0.001
10	0.0000001	1.000	<0.001
Sum			2.000

2.4 WASTE DEGRADATION

There may be a number of different wastefoms present in the repository. The main wastefoms are the UO_2 fuel matrix and the Zircaloy cladding. Although these are both part of the used fuel bundle and are not separated within the container, they have different radionuclide inventories and different degradation rates and are therefore considered separately.

Other optional secondary wastefoms allowed within the CC4 model are a metal and a soft wastefom. For example, the metal could be used to represent irradiated steel components or the used fuel container material or co-disposed used Co-60 rods, while the soft wastefom would represent any readily decomposable materials that may be present in some portion of the repository.

2.4.1 Fuel Wasteform

The UO_2 ceramic fuel matrix is durable, and dissolves slowly in water. The most important factor in the rate of dissolution of UO_2 is the redox conditions in the surrounding groundwater (Shoesmith et al. 1997, 2007). Reducing conditions are expected to prevail in and around the container under the influence of the reducing groundwater, and consumption of any residual oxygen by reaction with the copper and steel container materials or with ferrous and organic material in the sealing materials. Under these conditions, the UO_2 would dissolve very slowly.

However, conditions at the used fuel surface could remain oxidizing for a long time due to the production of oxidants near the fuel by radiolysis of water (Johnson et al. 1996). (This water would have reached the fuel only after failure of the container and fuel cladding.) Radiolysis of groundwater would be caused by the α -, β -, and γ -radiations emitted by the used fuel (Johnson et al. 1996).

The Second Case Study used a radiolysis-based dissolution model based on electrochemical data (Johnson et al. 1996). It was replaced with a simpler empirical model for radiolysis-driven

dissolution based on the concept of an effective G-value (Johnson and Smith 2000, Kolar et al. 2000). The effective G-value (G_{EFF}) is defined as the yield of oxidizing radiolysis products that result in fuel dissolution. This G_{EFF} approach was used in the Third Case Study (Garisto et al. 2004).

However, the experimental data needed to support the selected G_{EFF} values used in the Third Case Study are not extensive. Therefore, the current model adopts a different empirical approach which is supported by a more extensive set of experimental data. In this approach, the rate of dissolution of the used fuel matrix due to α -, β - and γ -radiolysis is modelled as approximately linear in the corresponding dose rates, i.e.,

$$c_{UO_2}(t) = A_{fuel}[G_{\alpha} f_{\alpha} D_{\alpha}(t+t_c)^{a\alpha} + G_{\beta} f_{\beta} D_{\beta}(t+t_c)^{a\beta} + G_{\gamma} f_{\gamma} D_{\gamma}(t+t_c)^{a\gamma} + R_{Uchem}] \quad (2.8)$$

where

- $c_{UO_2}(t)$ is the total used fuel dissolution rate [$\text{mol}_U \cdot \text{a}^{-1}$];
- A_{fuel} is the effective surface area of the dissolving fuel, per container [m^2];
- $D_{\alpha}(t + t_c)$, $D_{\beta}(t + t_c)$ and $D_{\gamma}(t + t_c)$ are the time-dependent dose rates [$\text{Gy} \cdot \text{a}^{-1}$];
- t is the time after repository closure [a];
- t_c is the time between fuel removal from reactor and repository closure [a];
- G_{α} , G_{β} and G_{γ} are empirical rate constants for fuel dissolution in the presence of alpha, beta and gamma radiation fields, respectively [$\text{mol}_U \cdot \text{m}^{-2} \cdot \text{Gy}^{-1}$];
- f_{α} , f_{β} and f_{γ} are the alpha dose, beta dose, and gamma dose variability factors, accounting for uncertainties in the radiation field strengths due to, for example, uncertainties in the nuclide inventories, and are approximately equal to unity [-];
- $a\alpha$, $a\beta$, and $a\gamma$ are fitting parameters for the dependence of the fuel dissolution rate on the alpha, beta, and gamma dose rates, and are approximately equal to one [-]; and
- R_{Uchem} is the chemical fuel dissolution rate, i.e., the dissolution rate of the fuel in the absence of radiolysis [$\text{mol}_U \cdot \text{m}^{-2} \cdot \text{a}^{-1}$].

Data on beta- and gamma-based dissolution are available in Johnson et al. (1996) and data on alpha-dissolution in Shoesmith (2007). These data are described in Garisto et al. (2011, Appendix E). The beta/gamma contribution is expected to be dominant for the first 500 years (Garisto et al. 2009). After this time, the fission products will have largely decayed and most of the remaining radioactivity in the fuel will be due to the actinides. Since actinides tend to decay by alpha decay, at long times alpha radiolysis will control the fuel dissolution rate. (Note that there is no dissolution until the container is breached and water comes in contact with the fuel.) H_2 generated by corrosion of iron within the container may reduce the effective dissolution rate, and can be included via the dissolution rate constants (Shoesmith, 2008).

The UO_2 degradation rate only applies after a container has failed and continues while some inventory of UO_2 fuel remains in the failed container. The end or cut-off time, when no UO_2 inventory remains, is conveniently calculated using the compartment model described in Appendix A. When using this compartment model, the function $F^N(t)$ is equal to a Dirac delta

function multiplied by the initial inventory of UO_2 , equivalent to the emplacement of the entire used fuel wastefrom into the compartment at $t = 0$. The function $F^{MAX}(t)$ is the degradation rate obtained from Equation (2.8) for times after container failure, $t \geq t_F$. The resulting function $F^{OUT}(t)$ obtained from the compartment model is the UO_2 degradation rate in a failed container, $c_{\text{UO}_2}(t)$, limited by the initial inventory.

2.4.2 Zircaloy Waste Matrix

The Zircaloy cladding naturally forms a thin layer of protective ZrO_2 on its surface in contact with water. Consequently, it dissolves very slowly in water (Shoemith and Zagidulin. 2010). Since the Zircaloy is a small contributor to the total radioactivity within the container, it is convenient to conservatively assume that the Zircaloy dissolves at a rate that ensures that the Zr concentration in the water inside the container is maintained at its solubility limit C_{sol}^{Zr} .

(Zirconium is the dominant element in Zircaloy.) The rate of degradation of the cladding is therefore equal to the rate of release of dissolved Zr from the container. The maximum (steady) output or release rate of Zr from the container, F^{MAX} , is determined as described later in Section 2.6 based on a constant concentration C_{sol}^{Zr} within the container:

$$F^{MAX} = \min(F_{BLR}, F_{PLR}) \quad \text{for } t > t_F \quad (2.9)$$

where

t_F is the time of failure of the container,

F_{BLR} is steady-state release rate for buffer-limited release, $F_{BLR} = 4r_{hole} \cdot C_{sol}^{Zr} \cdot Di_{buffer}$,

F_{PLR} is the steady-state release rate for pinhole-limited release, $F_{PLR} = \frac{\pi r_{hole}^2 \cdot C_{sol}^{Zr} \cdot Di_{defect}}{L_{hole}}$,

r_{hole} is the effective radius of the defect in the container wall,

L_{hole} is the effective length of the defect,

Di_{defect} is the intrinsic diffusivity of Zr in the defect,

Di_{buffer} is the intrinsic diffusivity of Zr in the buffer.

Although in reality there would be some transient release rate leading up to this constant concentration and release rate, it is assumed that the steady release rate is instantly reached at $t=t_F$. This steady release rate continues until all the Zircaloy has been dissolved and released at time t_{nr}

$$c_{Zr}(t) = \begin{cases} 0 & t < t_F \\ F^{MAX} & t_F \leq t \leq t_{nr} \\ 0 & t_{nr} < t \end{cases} \quad (2.10)$$

The compartment model in Appendix A can be used to calculate $c_{Zr}(t)$. As before, $F^{IN}(t)$ is set equal to the product of a Dirac delta function and the initial Zircaloy cladding inventory, equivalent to placing the entire Zircaloy inventory into the compartment at $t = t_F$. The variable F^{MAX} in Appendix A is given by Equation (2.9). For Zircaloy, there is no parent nuclide and no decay rate. The resulting function $F^{OUT}(t)$ is the Zircaloy corrosion rate, $c_{Zr}(t)$.

2.4.3 Metallic Wasteforms

The metal waste degradation rate $c_{metal}(t)$ [mol/a] is modelled by a constant corrosion rate with a time scale of τ_{cm} for complete dissolution after contact with water at t_F :

$$c_{metal}(t) = \begin{cases} 0 & t < t_F \\ \frac{I_{0,metal}}{\tau_{cm}} & t_F \leq t \leq t_F + \tau_{cm} \\ 0 & \tau_{cm} < t \end{cases} \quad (2.11a)$$

where $I_{0,metal}$ is the initial amount of the metal wasteform in a container [mol], and τ_{cm} is the time scale for complete dissolution of the metal [a].

2.4.4 Soft Wasteforms

The soft waste degradation rate $c_{soft}(t)$ [mol/a] is assumed to be fast, at a constant rate over short time span τ_{soft} , which may be zero. However, if τ_{soft} is zero, the matrix degrades instantly and all the radionuclide content is released instantly on contact with groundwater. Thus,

$$c_{soft}(t) = \begin{cases} I_{0,soft} \delta(t - t_F) & \tau_{soft} = 0 \\ I_{0,soft} / \tau_{soft} & \tau_{soft} > 0, \quad t_F \leq t \leq t_F + \tau_{soft} \\ 0 & \tau_{soft} > 0, \quad t > t_F + \tau_{soft} \end{cases} \quad (2.11b)$$

where $I_{0,soft}$ is the initial amount of the soft wasteform in a container [mol].

2.5 SOLUBILITIES OF NUCLIDES

The solubility of a nuclide is a property of the underlying chemical element. For example, both ^{234}U and ^{238}U have the same solubility - that of uranium.

The solubilities of five important low-solubility elements - uranium, neptunium, plutonium, thorium and technetium – can be calculated by CC4 from chemical and thermodynamic data (which are model inputs). For all other elements, solubilities are input to the model. Note that solubilities input in molal units (mol/kg) must be converted to molar units (mol/m³) before they are used by the model, by multiplying the input concentrations by the density of water to yield solubility C_{sol}^L for element L in mol/m³. Also, in the following text, $[A]$ means the concentration of A in molal units, i.e., (mol/kg).

The theory summarized in this chapter for determination of the solubilities of the five elements is fully described in Lemire and Garisto (1989). Only the equations implemented in the model are summarized in this chapter.

The main inputs are the groundwater pH, and concentrations of $NaCl$, Na_2SO_4 and $CaCl_2$, total dissolved inorganic carbon, total F and total P.

Values for some parameters are input based on three ionic strength regimes:

$$\begin{aligned} Z &< Z^A \\ Z^A &\leq Z \leq Z^B \\ Z^B &< Z \end{aligned} \quad (2.12)$$

where Z is the ionic strength of the groundwater, and the reference ionic strength values Z^A and Z^B are inputs to the model. Based on the ionic strength, Z , of the groundwater in the model calculations, the parameter values are taken from the relevant ionic strength regime.

2.5.1 Equilibrium Constants

For the concentrations of the aqueous species of the complexes of the 5 elements, an equilibrium constant for the relevant dissolution reaction producing each complexed species is required.

The equilibrium constants K of the relevant species for the solubility calculations are determined for all three ionic strength regimes, at temperature T using:

$$\log(K) = \frac{T_0}{T} [\log(K_0) + m(T - T_0)] \quad (2.13)$$

where K_0 is the equilibrium constant at the reference temperature T_0 taken to be 298.15°K (25°C), and m is an empirically determined slope for the temperature dependence. A different value for K_0 and m may be used for each ionic strength regime.

Reaction rates and water densities are calculated at a repository average temperature. Pressure effects are small over the relevant range and are neglected.

2.5.2 Speciation of Groundwater

The concentrations of the major components of groundwater $NaCl$, Na_2SO_4 and $CaCl_2$ are input into the model. The initial ionic concentrations of the major ions are then given by

$$\begin{cases} [Na^+]_0 = [NaCl] + 2[Na_2SO_4] \\ [Ca^{+2}]_0 = [CaCl_2] \\ [Cl^-]_0 = [NaCl] + 2[CaCl_2] \\ [SO_4^{-2}]_0 = [Na_2SO_4] \end{cases} \quad (2.14)$$

and the ionic strength, Z , based on these major groundwater components is determined from

$$Z = [NaCl] + 3[Na_2SO_4] + 3[CaCl_2] \quad (2.15)$$

The value obtained for Z is used to select values from the appropriate range of ionic strengths for each equilibrium constant used in the following calculations.

For the calculation of the groundwater speciation, the solubility products of gypsum CaSO_4 , calcite CaCO_3 , fluorite CaF_2 , and hydroxyapatite $\text{Ca}_5(\text{PO}_4)_3\text{OH}$ are considered. In addition, the calculations require values for the second protonation constant of phosphate PO_4^{3-} , the first and second protonation constants of carbonate CO_3^{2-} , and the ion product of water, K_w .

2.5.2.1 Calcium Sulphate Concentrations

The initial values for the concentrations for the major groundwater components Na_2SO_4 and CaCl_2 may represent a solution supersaturated with respect to gypsum CaSO_4 . The initial ion product $[\text{Ca}^{+2}]_0[\text{SO}_4^{-2}]_0$ is compared to the solubility product equilibrium constant for gypsum, K_{CaSO_4} , calculated above in Equation (2.13) for the ionic strength regime indicated by Z . If the ion product is greater than the solubility product,

$$[\text{Ca}^{+2}]_0[\text{SO}_4^{-2}]_0 > K_{\text{CaSO}_4} \quad (2.16)$$

then some gypsum precipitates and both Ca^{+2} and SO_4^{-2} ions are removed from the groundwater solution in equal amounts. If the quantity of precipitated gypsum is x_{pp} mol/kg, the resulting final ion product $[\text{Ca}^{+2}][\text{SO}_4^{-2}]$ satisfies

$$[\text{Ca}^{+2}][\text{SO}_4^{-2}] = K_{\text{CaSO}_4} \quad (2.17)$$

where

$$\begin{cases} [\text{Ca}^{+2}] = [\text{Ca}^{+2}]_0 - x_{pp} \\ [\text{SO}_4^{-2}] = [\text{SO}_4^{-2}]_0 - x_{pp} \end{cases} \quad (2.18)$$

Equation (2.17) is a quadratic equation in x_{pp} which has solution

$$x_{pp} = \frac{([\text{Ca}^{+2}]_0 + [\text{SO}_4^{-2}]_0) - \sqrt{([\text{Ca}^{+2}]_0 + [\text{SO}_4^{-2}]_0)^2 - 4([\text{Ca}^{+2}]_0[\text{SO}_4^{-2}]_0 - K_{\text{CaSO}_4})}}{2} \quad (2.19)$$

and the final concentrations $[\text{Ca}^{+2}]$ and $[\text{SO}_4^{-2}]$ are given by Equation (2.18). The groundwater ionic strength, Z , is adjusted for the loss of ions. The adjustment in ionic strength is given by

$$Z \rightarrow Z - 4x_{pp} \quad (2.20)$$

If the initial ion product is less than the solubility product, K_{CaSO_4} then no gypsum precipitates, x_{pp} is zero, and Z does not need adjustment.

The adjusted value of Z is used in selecting equilibrium constant values for subsequent calculations of minor anion concentrations. However, it is assumed that any adjusted value does not affect the determination of gypsum precipitation in this section and the calculations in Equations (2.17) to (2.19) are not repeated with an adjusted value for Z .

It is assumed that gypsum is the only mineral to affect the concentration of calcium ions (Lemire and Garisto 1989) and that the effects of the minor anions and possible precipitation of the calcium containing minerals of hydroxyapatite, fluorite and calcite do not significantly affect the final value for calcium ion concentration, $[Ca^{+2}]$.

2.5.2.2 Minor Anion Concentrations

Carbonate, fluoride, and phosphate are anions that, through complexation, may enhance the solubility of the actinides and fission products. All three anions form relatively insoluble calcium minerals that may control the concentrations in groundwater of these anions.

All three anions can be protonated in solution and the degree of protonation is controlled by the hydrogen ion concentration, $[H^+]$, or pH . The pH of the groundwater is an input to the model, as is the total inorganic fluorine, $[F_T]$, total inorganic phosphorus, $[P_T]$, and total inorganic carbon, $[C_T]$. From pH , the concentration of hydrogen ions is

$$[H^+] = 10^{-pH} \quad (2.21)$$

2.5.2.3 Fluoride Concentration

Protonation of fluoride is insignificant in the pH range of interest. Fluorite, CaF_2 , is assumed to be the solubility-limiting mineral controlling the fluoride concentration in groundwater (Lemire and Garisto 1989). Its solubility product equilibrium constant K_{CaF_2} is derived from Equation (2.13) for the ionic strength regime indicated by Z .

The concentration of Ca^{+2} is assumed to be insignificantly affected by any precipitation of fluorite, so the saturation concentration of F^- , denoted $[F^-]_s$, is given by

$$[F^-]_s = \sqrt{K_{CaF_2} / [Ca^{+2}]} \quad (2.22)$$

where $[Ca^{+2}]$ was determined above. If the value of total fluorine concentration, $[F_T]$, is greater than $[F^-]_s$, then some fluorite precipitates and the concentration of fluoride in groundwater is equal to $[F^-]_s$. Otherwise, the concentration of fluoride in groundwater is equal to $[F_T]$.

2.5.2.4 Hydrogen Phosphate Concentration

Protonation of phosphate makes the major species in the pH range of interest HPO_4^{-2} and $H_2PO_4^-$. Assuming these two species initially make up the total inorganic phosphorus $[P_T]$,

$$[P_T] = [H_2PO_4^-] + [HPO_4^{-2}] \quad (2.23)$$

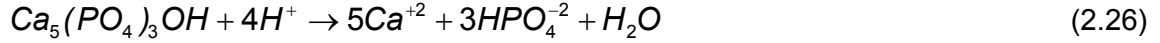
then the initial concentration of HPO_4^{-2} is given by

$$[HPO_4^{-2}]_0 = [P_T] / (K_{p2} [H^+] + 1) \quad (2.24)$$

where K_{p2} is the second protonation constant of PO_4^{-3} . That is, K_{p2} is the equilibrium constant, calculated from Equation (2.13) for the selected temperature and ionic strength regime Z , for the protonation reaction



The mineral limiting the phosphate concentrations is assumed to be hydroxyapatite, $Ca_5(PO_4)_3OH$ whose solubility product, K_{HAp} , is based on the dissolution reaction



The concentration of Ca^{+2} is assumed to be insignificantly affected by any precipitation of hydroxyapatite, and thus the saturation concentration of HPO_4^{-2} is found from

$$[HPO_4^{-2}]_s = \sqrt[3]{K_{HAp} [H^+]^4 / [Ca^{+2}]^5} \quad (2.27)$$

where the value for K_{HAp} is obtained from Equation (2.13), and where $[Ca^{+2}]$ was determined above. If the value of initial concentration of HPO_4^{-2} obtained from Equation (2.24), is greater than $[HPO_4^{-2}]_s$, then some hydroxyapatite precipitates, and the concentration of HPO_4^{-2} in the water is equal to $[HPO_4^{-2}]_s$. Otherwise, the concentration of HPO_4^{-2} in groundwater is equal to the initial concentration, $[HPO_4^{-2}]_0$

The equilibrium concentration of $H_2PO_4^-$ is found from the second protonation reaction equilibrium, Equation (2.25).

2.5.2.5 Carbonate Concentration

Protonation of carbonate makes all three species CO_3^{-2} , HCO_3^- , and H_2CO_3 significant in the pH range of interest. Assuming these three species make up the total inorganic carbon $[C_T]$

$$[C_T] = [H_2CO_3] + [H_2CO_3^-] + [CO_3^{-2}] \quad (2.28)$$

then the initial concentration of CO_3^{-2} is given by

$$[CO_3^{-2}]_0 = [C_T] / (K_{c1} K_{c2} [H^+]^2 + K_{c2} [H^+] + 1) \quad (2.29)$$

where K_{c1} and K_{c2} are the first and second protonation constants of CO_3^{-2} . That is, these are the equilibrium constants obtained from Equation (2.13) for the protonation reactions



The mineral limiting the carbonate concentrations is assumed to be calcite, $CaCO_3$.

The concentration of Ca^{+2} is assumed to be insignificantly affected by any precipitation of calcite, and thus the saturation concentration of CO_3^{-2} is found from

$$[CO_3^{-2}]_s = K_{CaCO_3} / [Ca^{+2}] \quad (2.32)$$

where the solubility product of calcite, K_{CaCO_3} is obtained from Equation (2.13) and $[Ca^{+2}]$ was determined above. If the value of the initial concentration of CO_3^{-2} obtained from Equation (2.29) is greater than $[CO_3^{-2}]_s$, then some calcite precipitates and the concentration of CO_3^{-2} in groundwater is equal to $[CO_3^{-2}]_s$. Otherwise, the concentration of CO_3^{-2} in groundwater is equal to the initial concentration, $[CO_3^{-2}]_0$.

The equilibrium concentration of HCO_3^- is found from the first protonation reaction equilibrium

$$[H_2CO_3] = K_{c1} [CO_3^{-2}] [H^+] \quad (2.33)$$

2.5.2.6 Sodium, Chloride, and Hydroxide Concentration

The pH refers only to the concentration of hydrogen ions; the corresponding concentration of hydroxide ions is obtained from the ion product for water, where the value for K_w is obtained from Equation (2.13)

$$[OH^-] = K_w / [H^+] \quad (2.34)$$

The other minor species were introduced as anions and, in general, the sodium ion concentration must be increased to maintain charge balance. In the unlikely case there is an excess of cations, then the chloride concentration is increased to maintain charge balance. The sum of the cation charges, S^C , and the sum of the anion charges, S^A , are separately obtained.

$$\begin{cases} S^C = [Na^+]_0 + 2[Ca^{+2}] + [H^+] \\ S^A = [Cl^-]_0 + 2[SO_4^{-2}] + [F^-] + [HCO_3^-] + 2[CO_3^{-2}] + [H_2PO_4^-] + 2[HPO_4^{-2}] + [OH^-] \end{cases} \quad (2.35)$$

If $S^A > S^C$, the Na^+ ion concentration is increased by $(S^A - S^C)$. However, if $S^C > S^A$, then the Cl^- ion concentration is increased by $(S^C - S^A)$.

2.5.2.7 Ionic Strength

Having now the final concentration in the groundwater for all major and minor ions, the final ionic strength is determined

$$Z = \frac{1}{2} ([Na^+] + [Cl^-] + [F^-] + [H_2PO_4^-] + [HCO_3^-] + [H^+] + [OH^-] + 2([Ca^{+2}] + [SO_4^{-2}] + [HPO_4^{-2}] + [CO_3^{-2}])) \quad (2.36)$$

2.5.2.8 Oxidation Potential

The dependence of electrochemical potentials on ionic concentration is temperature dependent. At the reference temperature T_0 at which the reference potentials are determined, taken to be 298.15°K (25°C), the slope factor $S = -RT_0/F = -0.05916$ Volts, where R is the gas constant and F is the Faraday. At other temperatures, the slope is adjusted using (Lemire and Garisto 1989).

$$S = -0.05916 \cdot \frac{T}{T_0} \quad [\text{Volts}] \quad (2.37)$$

The oxidation potential, Eh , of the groundwater is found from

$$Eh = Eh_0 + S \cdot pH \quad (2.38)$$

where Eh_0 , which is an input to the model, is the groundwater oxidation potential at $pH = 0$.

2.5.3 **Elemental Solubilities**

For most elements, the solubility is provided as input to the model. However, for the five elements U, Pu, Np, Th and Tc, the solubility can be calculated self-consistently assuming equilibrium of the aqueous species of these elements with an appropriate reference solid. By the Ostwald step rule, amorphous solids are kinetically favoured to precipitate first and, thus, the metal solubility is initially controlled by the solubility of the amorphous solid metal dioxide. (Subsequent decreases in metal solubility, resulting from the aging of the amorphous precipitate into a more thermodynamically stable solid, are not considered here.)

The elemental solubility is determined as the sum of the concentrations of the various metal solution species that could exist in equilibrium with the solid metal dioxide at a given temperature and water composition. In addition to the inorganic complexing groundwater ions, Cl , SO_4^{-2} , F , HPO_4^{-2} , CO_3^{-2} , OH , and H^+ , whose concentrations have been determined above, allowance is made for two trace-level species that could represent organic complexing ligands. The concentration of the radionuclides is expected to be too low to significantly change the previously calculated concentrations for these inorganic species (except for U, see below).

2.5.3.1 Boundary Potentials

The equilibria for U, Pu, Np, Th and Tc are based on equilibria with the solid metal dioxides UO_2 , PuO_2 , NpO_2 , ThO_2 and TcO_2 . For uranium, this metal dioxide is defined as $UO_2(\text{fuel})$, which is a material that is effectively neither fully crystalline nor fully amorphous but whose calculated solubility agrees well with experimental and field data (Bruno et al. 1997). For plutonium, neptunium and thorium, the amorphous forms of the solid dioxides are assumed to control the solubilities of the corresponding elements (Lemire and Garisto 1989). Lastly, we assume the solubility of hydrated technetium dioxide ($TcO_2 \cdot 1.6H_2O$) controls the technetium solubility (Garisto and Gierszewski 2002).

Although these solids are reasonable estimates for relevant deep groundwater conditions, for Tc and U in particular it is possible that conditions might favour different solids controlling the solubility (Lemire and Garisto 1989). For instance, Tc (*metal*) might be the stable solid for technetium under more reducing conditions, and UO_3 (schoepite), for uranium under more

oxidizing conditions. Therefore, for these two elements, the electrochemical potential of the boundary between the two possible controlling solids is required for comparison with the solution Eh so that the correct controlling solid is identified.

The potential, E_{Tc} , at the boundary between the solids Tc and TcO_2 at temperature T is

$$E_{Tc} = E_{0,Tc} + E_{m,Tc} \cdot (T - T_0) \quad (2.39)$$

where $E_{0,Tc}$ is the value at $T_0 = 298.15^\circ\text{K}$ in the ionic strength regime indicated by Z , and $E_{m,Tc}$ is an empirically determined slope (Lemire and Garisto 1989). For $Eh < E_{Tc}$, Tc (*metal*) is assumed to be the solid controlling the technetium solubility.

The potential, E_U , at the boundary between the solids UO_2 and UO_3 is similarly

$$E_U = E_{0,U} + E_{m,U} \cdot (T - T_0) \quad (2.40)$$

where $E_{0,U}$ is the value at $T_0 = 298.15^\circ\text{K}$ in the ionic strength regime indicated by Z , and $E_{m,U}$ is an empirically determined slope (Lemire and Garisto 1989). For $Eh > E_U$, UO_3 is assumed to be the solid controlling the uranium solubility.

2.5.3.2 Solubility Factors

Solubility Factor for UO_3

The concentration of a Uranium solution species, U_i , in equilibrium with solid UO_3 , $[U_i]_{UO_3(s)}$, can be expressed in terms of the concentration of the same species in equilibrium with the solid UO_2 , $[U_i]_{UO_2(fuel)}$, as

$$[U_i]_{UO_3(s)} = (U_F)^{N_{U_i}} [U_i]_{UO_2(fuel)} \quad (2.41)$$

where N_{U_i} is the number of Uranium atoms in the chemical formula for the species U_i , and U_F is a solubility factor for Uranium given by

$$\log U_F = -2(E_U - Eh_0)/S \quad (2.42)$$

The coefficient -2 results from the net oxidation state change of U in going from UO_3 to UO_2 .

Solubility Factor for Elemental Tc

The concentration of a Technetium solution species, Tc_i , in equilibrium with solid elemental Tc, $[Tc_i]_{Tc(s)}$, can be expressed in terms of the concentration of the same species in equilibrium with the solid TcO_2 , $[Tc_i]_{TcO_2(s)}$:

$$[Tc_i]_{Tc(s)} = (T_F)^{N_{Tc_i}} [Tc_i]_{TcO_2(s)} \quad (2.43)$$

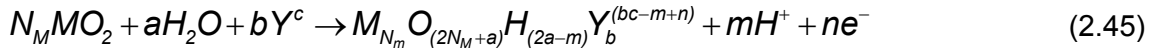
where N_{Tc_i} is the number of Technetium atoms in the chemical formula for the species Tc_i , and T_F is a solubility factor for Technetium given by:

$$\log T_F = 4(E_{Tc} - Eh_0)/S \quad (2.44)$$

The coefficient +4 results from the net oxidation state change of Tc in going from elemental Tc to TcO_2 .

2.5.3.3 Contributions of Solution Species

The dissolution of a metal dioxide in aqueous solution with a single complexing ligand can be described by dissolution reactions of the general form (Lemire and Garisto 1989):



where $M_{N_M} O_{(2N_M+a)} H_{(2a-m)} Y_b^{(bc-m+n)}$ is an aqueous solution species and Y^c is a complexing ligand with ionic charge c .

The equilibrium concentration of this solution species is given by

$$[M_{N_M} O_{(2N_M+a)} H_{(2a-m)} Y_b^{(bc-m+n)}]_{MO_2(s)} = K_{diss} [Y^c]^b / [H^+]^m [e^-]^n \quad (2.46)$$

Using the definitions $Eh = S \log_{10}[e^-]$ and $pH = -\log_{10}[H^+]$,

$$[M_{N_M} O_{(2N_M+a)} H_{(2a-m)} Y_b^{(bc-m+n)}]_{MO_2(s)} = K_{diss} \cdot 10^{m \cdot pH} \cdot 10^{-n \cdot Eh/S} [Y^c]^b \quad (2.47)$$

The value for K_{diss} is obtained from Equation (2.13). The subscript notation of $MO_2(s)$ emphasizes that the concentrations determined by Equation (2.47) are in equilibrium with the solid metal dioxide. The stoichiometric coefficients N_M , b , m and n for each such reaction considered are required inputs to the model.

2.5.3.4 Total Elemental Solubilities

The total solubility, C_{sol}^M , of each of the five elements ($M = U, Np, Pu, Th, Tc$) is obtained by summing the equilibrium aqueous concentration of each of the n_M solution species considered for each element M :

$$C_{sol}^M = \rho_w \sum_i^{n_M} N_{M_i} [M_i]_{MO_2(s)} \quad (2.48)$$

where N_{M_i} is the stoichiometric number of metal atoms in the chemical formula of the solution species M_i , and there are n_M such solution species considered for element M . Values for $[M_i]$, the concentration of the solution species, are obtained from Equation (2.47). Note that for subsequent use in the CC4 model, the dimensions of these total solubilities are expressed in molar units (mol/m^3) using the multiplier ρ_w (kg/m^3) for the density of water.

This model assumes that the amount of dissolved element is small enough that it does not affect the concentration of the ligand species, nor the solution Eh and pH .

The recommended solution species are shown in Table 2.2. The Tc species are from Garisto and Gierszewski (2002). The U, Np, Pu and Th species are from Lemire and Garisto (1989), except for removal of the aqueous phosphate complexes of the form $X(HPO_4)_n^{4-2n}$ for $X=Np, U$ or Pu and, for U , replacement of the $UO_2(HPO_4)_2^{2-}$ species by $UO_2HPO_4^-$ (Lemire et al. 2001). Table 2.2 indicates that $n_{Tc} = 6$ solution species are considered for Tc, 15 species considered for Np, 5 species for Pu, 10 species for Th, and 24 species for U.

For uranium, the value of the solubility factor U_F indicates whether UO_2 or UO_3 is the controlling solid species. If $U_F \geq 1$ ($Eh \leq E_U$), then we calculate the solubility based on $UO_2(\text{fuel})$ using Equation (2.48) with $M = U$. If $U_F < 1$, then we calculate the solubility based on $UO_3(s)$, utilizing Equation (2.41), resulting in

$$C_{sol}^U = \rho_w \sum_i^{n_U} N_{U_i} (U_F)^{N_{U_i}} [U_i]_{UO_2(\text{fuel})} \quad (2.49)$$

Table 2.2: Species Used in Determining Solubilities

Element		Solution Species			
Neptunium (18 species)	Np^{+3}	NpO_2^+	$Np(OH)_2^{+2}$	$Np(OH)_4(\text{aq})$	
	$NpO_2(OH)_2^-$	$NpO_2(OH)(\text{aq})$	NpF_2^{+2}	$NpO_2F(\text{aq})$	
	$Np(SO_4)_2(\text{aq})$	$NpO_2SO_4^-$	$NpO_2CO_3^-$	$NpO_2(CO_3)_2^{-3}$	
	$NpO_2(CO_3)_3^{-5}$	$NpO_2(HPO_4)^-$	$NpO_2Cl(\text{aq})$		
Plutonium (5 species)	Pu^{+3}	$PuOH^{+2}$	$Pu(OH)_4(\text{aq})$	$Pu(H_2PO_4)^{+2}$	
	$PuSO_4^+$				
Technetium (6 species)	TcO_4^-	$TcO(OH)^+$	$TcO(OH)_2(\text{aq})$	$TcO(OH)_3^-$	
	$Tc(OH)_2CO_3(\text{aq})$	$Tc(OH)_3CO_3^-$			
Thorium (10 species)	$ThOH^{+3}$	$Th(OH)_2^{+2}$	$Th(OH)_3^+$	$Th(OH)_4(\text{aq})$	
	ThF_3^+	$ThF_4(\text{aq})$	$Th(SO_4)_2(\text{aq})$	$Th(HPO_4)_2(\text{aq})$	
	$Th(HPO_4)_3^{-2}$	$Th(CO_3)_5^{-6}$			
Uranium (24 species)	UO_2^{+2}	UO_2^+	$UO_2(OH)^+$	$(UO_2)_3(OH)_7^-$	
	$UO_2(OH)_2(\text{aq})$	$UO_2(OH)_4^{-2}$	$U(OH)_4(\text{aq})$	$U(OH)_5^-$	
	UO_2Cl^+	UO_2F^+	$UO_2F_2(\text{aq})$	$UO_2F_3^-$	
	$UO_2F_4^{-2}$	UF_3^+	$UF_4(\text{aq})$	$UO_2CO_3(\text{aq})$	
	$UO_2(CO_3)_2^{-2}$	$(UO_2)_3(CO_3)_6^{-6}$	$UO_2(CO_3)_3^{-4}$	$U(CO_3)_5^{-6}$	
	$UO_2SO_4(\text{aq})$	$UO_2(SO_4)_2^{-2}$	$UO_2HPO_4(\text{aq})$	$UO_2PO_4^-$	

Similarly, for technetium, the value of the solubility factor T_F indicates whether TcO_2 or Tc (*metal*) is the controlling solid species. If $T_F \geq 1$ ($Eh \geq E_{Tc}$), then we calculate the solubility based on $TcO_2(s)$ using Equation (2.48) with $M = Tc$. If $T_F < 1$, then we calculate the solubility based on $Tc(metal)$, utilizing Equation (2.43), resulting in

$$C_{sol}^{Tc} = \rho_w \sum_i^{N_{Tc}} N_{Tc_i} (T_F)^{N_{Tc_i}} [Tc_i]_{TcO_2(s)} \quad (2.50)$$

2.5.3.5 Correction of Uranium Solubility for Carbonate Limits

The solubility model described above assumes that the total concentration of a radionuclide in solution is very small compared to the concentration of groundwater species such as HCO_3^- . For uranium, this assumption is not true for some groundwater compositions. In particular, the calculated total concentration of the U(VI) carbonate complexes could exceed the initial total carbonate concentration. In these cases, the calculated uranium solubility is unrealistically high. Therefore, the uranium solubility calculated using Equations (2.48) or (2.49) must be corrected in some cases.

The correction is carried out using the mathematical algorithm described in this section. The algorithm assumes that the total carbonate concentration in solution (including uranium carbonate complexes) is equal to the calculated total carbonate concentration in the contact groundwater, i.e., after precipitation of calcite (see Section 2.5.2.5).

It should be noted that the concentrations of the uranium complexes of the other complexing anions, e.g., F^- and HPO_4^{2-} , never exceed the concentrations of the anions themselves. This is likely because the uranium complexes of these anions are weaker than the carbonate complexes. Thus, the concentrations of these uranium complexes are calculated correctly and are not modified.

It is necessary to run the algorithm only if the total carbonate concentration in solution, including the carbonate associated with the U(VI) carbonate complexes, exceeds the initial total carbonic acid concentration in the contact groundwater by a significant amount. The total carbonic acid concentration in the contact groundwater, C_{T^*} , is calculated using $[CO_3^{-2}]^*$ and the formula

$$C_{T^*} = (K_{c1} K_{c2} [H^+]^2 + K_{c1}[H^+] + 1) [CO_3^{-2}]^* \equiv CF^* [CO_3^{-2}]^* \quad (2.51)$$

where $[CO_3^{-2}]^*$ is obtained as described in Section 2.5.2.5, and K_{c1} and K_{c2} are the first and second protonation constants of CO_3^{-2} (see Equation 2.28), and the equivalence sign is used to define CF^* . As usual, square brackets are used to denote species concentrations, i.e., $[CO_3^{-2}]^*$ represents the molal concentration of CO_3^{-2} in solution.

The four carbonate complexes of U(VI) included in the solubility model are: UO_2CO_3 , $UO_2(CO_3)_2^{-2}$, $(UO_2)_3(CO_3)_6^{-6}$ and $UO_2(CO_3)_3^{-4}$. It is convenient to define the four variables k_1^* , k_2^* , k_3^* and k_4^* as follows

$$k_1^* = (U_F)^{NU_i} [UO_2CO_3]_{UO_2(fuel)} / [CO_3^{-2}]^* \quad (2.52a)$$

$$k_2^* = (U_F)^{NU_i} [UO_2(CO_3)_2^{-2}]_{UO_2(fuel)} / ([CO_3^{-2}]^*)^2 \quad (2.52b)$$

$$k_3^* = (U_F)^{NU_i} [(UO_2)_3(CO_3)_6^{-6}]_{UO_2(fuel)} / ([CO_3^{-2}]^*)^6 \quad (2.52c)$$

$$k_{4^*} = (U_F)^{NUi} [UO_2(CO_3)_3^{-4}]_{UO_2(fuel)} / ([CO_3^{-2}]^*)^3 \quad (2.52d)$$

where the U_F factors in Equations (2.52) are only included if $U_F < 1$ (Equation 2.42).

The total carbonate concentration in solution, CU_{tot^*} , including the U(VI) carbonate complexes without correction for limited carbonate, is given by

$$CU_{tot^*} = CF^* [CO_3^{-2}]^* + k_{1^*} [CO_3^{-2}]^* + 2 k_{2^*} ([CO_3^{-2}]^*)^2 + 6 k_{3^*} ([CO_3^{-2}]^*)^6 + 3 k_{4^*} ([CO_3^{-2}]^*)^3 \quad (2.53)$$

This amount will be larger than the initial amount of carbonate in the contact groundwater since the carbonate species are not corrected for the formation of U carbonates. If the amounts of U carbonates are not too large, then this is a reasonable approximation. However, in some cases, the calculated amount of U carbonates in solution can be large, and the value of CU_{tot^*} would be much larger than C_{T^*} . Thus, a test should be made to determine if the correction to the uranium solubility needs to be applied. Given the accuracy of the correction (see below), the correction should be applied only if

$$CU_{tot^*} > 1.25^* C_{T^*} \quad (2.54)$$

The purpose of the algorithm described below is to find the value of $[CO_3^{-2}]_u$ for which

$$C_{T^*} = CF^* [CO_3^{-2}]_u + k_{1^*} [CO_3^{-2}]_u + 2 k_{2^*} ([CO_3^{-2}]_u)^2 + 6 k_{3^*} ([CO_3^{-2}]_u)^6 + 3 k_{4^*} ([CO_3^{-2}]_u)^3 \quad (2.55)$$

That is, the final amount of carbonate in solution, including carbonate associated with uranium carbonates species, is equal to the initial amount of carbonate in the groundwater.

First Order Approximation

In many cases for which $CU_{tot^*} \gg 1.25^* C_{T^*}$, only two of the U(VI) carbonate species are dominant: $(UO_2)_3(CO_3)_6^{-6}$ and $UO_2(CO_3)_3^{-4}$. For these cases,

$$CU_{tot^*} \approx 6 k_{3^*} ([CO_3^{-2}]^*)^6 + 3 k_{4^*} ([CO_3^{-2}]^*)^3 \quad (2.56a)$$

and therefore mass balance of carbonate requires (from Equation 2.55)

$$C_{T^*} \approx 6 k_{3^*} ([CO_3^{-2}]_{u1})^6 + 3 k_{4^*} ([CO_3^{-2}]_{u1})^3 \quad (2.56b)$$

where $[CO_3^{-2}]_{u1}$ is the first order approximation to $[CO_3^{-2}]_u$.

Writing $[CO_3^{-2}]_{u1} = x [CO_3^{-2}]^*$, with $0 < x < 1$, it is found from Equations (2.56a) and (2.56b) that

$$C_{T^*} = (CU_{tot^*} - 3 k_{4^*} ([CO_3^{-2}]^*)^3) x^6 + 3 k_{4^*} ([CO_3^{-2}]^*)^3 x^3 \quad (2.57)$$

Defining

$$\lambda = 3 k_{4^*} ([CO_3^{-2}]^*)^3 / CU_{tot^*} = 3 [UO_2(CO_3)_3^{-4}]^* / CU_{tot^*}, \quad (2.58)$$

it is found that x satisfies the equation

$$(1 - \lambda) x^6 + \lambda x^3 - C_{T^*}/CU_{tot^*} = 0. \quad (2.59)$$

This equation is quadratic in x^3 and can be solved first for x^3 and then for x . The positive root of the equation is required and, therefore,

$$x = \left(\frac{-\lambda + \sqrt{\lambda^2 + 4(1-\lambda)C_{T^*}/CU_{tot^*}}}{2(1-\lambda)} \right)^{1/3}. \quad (2.60)$$

$[CO_3^{-2}]_{u1}$ can then be found using

$$[CO_3^{-2}]_{u1} = x [CO_3^{-2}]^*. \quad (2.61)$$

where CU_{tot^*} is calculated using Equation (2.56a).

Second Order Approximation

The first order approximation to $[CO_3^{-2}]_u$ can be improved by using a Taylor expansion. This is equivalent to using the Newton-Raphson method.

The total carbonate concentration calculated using the first order approximation, CU_{tot1} , is given by

$$CU_{tot1} = CF^* [CO_3^{-2}]_{u1} + k_1^* [CO_3^{-2}]_{u1} + 2k_2^* ([CO_3^{-2}]_{u1})^2 + 6k_3^* ([CO_3^{-2}]_{u1})^6 + 3k_4^* ([CO_3^{-2}]_{u1})^3. \quad (2.62)$$

Taking the derivative of CU_{tot1} with respect to $[CO_3^{-2}]_{u1}$ gives

$$D_{u1} \equiv dCU_{tot1}/d[CO_3^{-2}]_{u1} = (CF^* + k_1^*) + 4k_2^* [CO_3^{-2}]_{u1} + 36k_3^* ([CO_3^{-2}]_{u1})^5 + 9k_4^* ([CO_3^{-2}]_{u1})^2. \quad (2.63)$$

The second order approximation, $[CO_3^{-2}]_{u2}$, for $[CO_3^{-2}]_u$ is then found by solving the equation

$$C_{T^*} = CU_{tot1} + D_{u1} ([CO_3^{-2}]_{u2} - [CO_3^{-2}]_{u1}). \quad (2.64)$$

The solution of Equation (2.64) gives

$$[CO_3^{-2}]_{u2} = [CO_3^{-2}]_{u1} + (C_{T^*} - CU_{tot1}) / D_{u1} \quad (2.65)$$

where $[CO_3^{-2}]_{u1}$, CU_{tot1} and D_{u1} are given by Equations (2.61), (2.62) and (2.63), respectively.

The algorithm described in this section was tested against the non-linear equation solver in Microsoft Excel for many probabilistically selected contact groundwaters. In all tested cases, the calculated total carbonate concentration, after the contact groundwater comes to equilibrium with the UO_2 solid, was in good agreement with the total carbonic acid concentration found in the contact groundwater itself. The largest observed difference was less than 30%.

The corrected solubility of uranium, $C_{sol,cor}^U$, can be calculated using

$$C_{sol,cor}^U = C_{sol}^U + \rho_w * k_1^* \{ [CO_3^{-2}]_{u2} - [CO_3^{-2}]_{u1} \} + k_2^* \{ ([CO_3^{-2}]_{u2})^2 - ([CO_3^{-2}]_{u1})^2 \} + 3k_3^* \{ ([CO_3^{-2}]_{u2})^6 - ([CO_3^{-2}]_{u1})^6 \} + k_4^* \{ ([CO_3^{-2}]_{u2})^3 - ([CO_3^{-2}]_{u1})^3 \}. \quad (2.66)$$

2.6 NUCLIDE RELEASE INTO CONTAINER

2.6.1 Release from UO₂ Matrix

The radionuclides formed within the UO₂ fuel pellet are distributed among various locations by the end of the reactor irradiation, as illustrated in Figure 2.3 (McMurry et al. 2003). While the bulk of the radionuclides are held within the UO₂ grains, certain metals have formed metallic particulates, and the balance (notably the more volatile nuclides) have collected in grain boundaries, cracks and external gaps around the fuel. When the cladding is breached and the fuel is contacted by water, the location of the nuclides affects the rate at which they are released into the groundwater.

In particular, we distinguish a rapid release and a slow release process. The rapid or “instant” release applies to all nuclides within the gaps, cracks and grain boundaries, which are assumed to be quickly accessed by water, and dissolved. The slow release applies to all nuclides within the grains and the intermetallic particles, which are only released as the UO₂ grains themselves dissolve. The latter mechanism is referred to as “congruent” release. These two mechanisms are described further below.

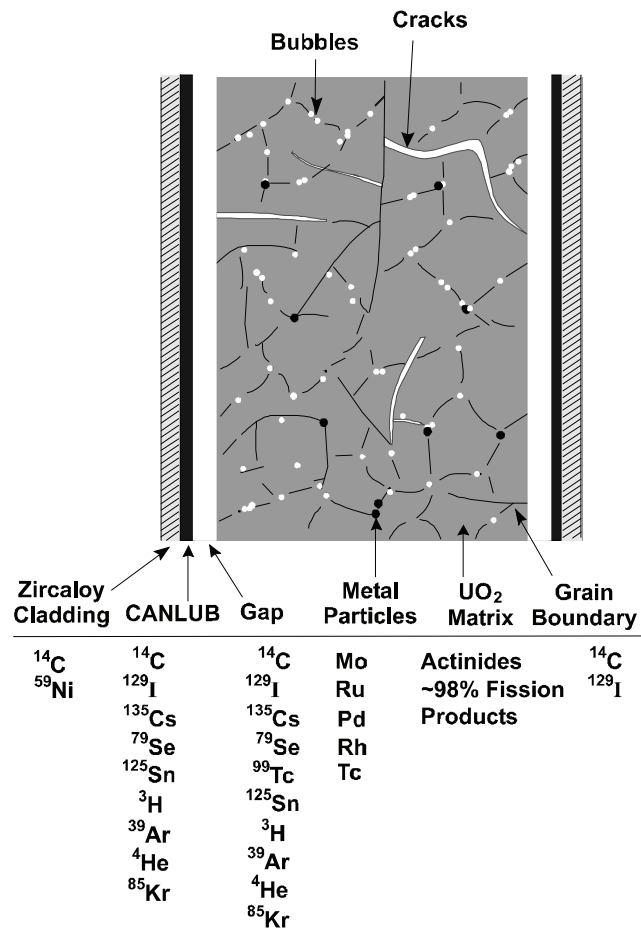


Figure 2.3: Distribution of various radionuclides within a used fuel element

Instant Release from UO₂

The rate of release of nuclide i from the UO₂ matrix by instant release in any given failed container is a delta function at the time of container failure:

$$F_{IR,UO_2}^i(t) = f_{IR,UO_2}^i I_{UO_2}^i(t) \delta(t - t_F) \quad [\text{mol/a}] \quad (2.67)$$

where

t_F is the time of container failure [a],

f_{IR,UO_2}^i is the fraction of the nuclide i released instantly from the UO₂ matrix upon contact with water [-],

$I_{UO_2}^i(t)$ is the inventory of nuclide i at time t in the UO₂ fuel in a container [mol], and

$\delta(t)$ is the Dirac delta function.

Congruent Release from UO₂

The remaining nuclides are released as the UO₂ matrix itself dissolves. The congruent dissolution release rate of nuclide i from the UO₂ matrix in the failed container at time t is

$F_{CD,UO_2}^i(t)$ [mol/a]:

$$F_{CD,UO_2}^i(t) = (1 - f_{IR,UO_2}^i) I_{UO_2}^i(t) \frac{C_{UO_2}(t)}{I_{0,UO_2}} \quad t \geq t_F \quad (2.68)$$

where

I_{0,UO_2} is the initial inventory of UO₂ in a container [mol], and

$C_{UO_2}(t)$ is the UO₂ matrix degradation rate in the failed container at time t [mol/a].

2.6.2 Release from Zircaloy Cladding

Radionuclides formed within the Zircaloy cladding by activation are generally uniformly distributed across the thin cladding, and are released into the container as the Zircaloy cladding itself dissolves (i.e., congruent dissolution). The rate of degradation of the Zircaloy matrix was determined in Section 2.4.2. However, some nuclides (e.g., ¹⁴C) may be trapped in the original surface oxide layer, and released more rapidly. The release of nuclides from the Zircaloy cladding is then a combination of instant release and congruent dissolution release:

$$F_{IR,Zr}^i(t) = f_{IR,Zr}^i I_{Zr}^i(t) \delta(t - t_F) \quad (2.69a)$$

$$F_{CD,Zr}^i(t) = (1 - f_{IR,Zr}^i) I_{Zr}^i(t) \frac{C_{Zr}(t)}{I_{0,Zr}} \quad t \geq t_F \quad (2.69b)$$

where

$f_{IR,Zr}^i$ is the instant release fraction of nuclide i in Zr cladding [-],

- $I_{0,Zr}$ is the initial inventory of Zr cladding in a container [mol],
 $I_{Zr}^i(t)$ is the inventory of nuclide i in Zr cladding in a container at time t [mol] assuming only ingrowth and decay (i.e., no loss into the container),
 $c_{Zr}(t)$ is the Zircaloy cladding dissolution rate in the failed container [mol/a].

2.6.3 Release from Other Wasteforms

In addition to the main used fuel wasteform, the model includes optional metal and soft wasteforms. In the metal wasteform, the nuclide release is modelled generally as an instant release process and a congruent dissolution process. The dissolution rate of the metal matrix is defined by a constant corrosion rate (Section 2.4.3), $c_{metal}(t)$. The soft waste is treated similarly but is assumed to more rapidly degrade on contact with water. The nuclides from these materials are released into the interior of the container.

Release from Metal

The rate of release of nuclide i from the metal matrix in a failed container is instant release or congruent release:

$$F_{IR,metal}^i(t) = f_{IR,metal}^i I_{metal}^i(t) \delta(t - t_F) \text{ [mol/a] and} \quad (2.70a)$$

$$F_{CD,metal}^i(t) = (1 - f_{IR,metal}^i) I_{metal}^i(t) \frac{c_{metal}(t)}{I_{0,metal}} \quad t \geq t_F \quad (2.70b)$$

where

- t_F is the time of container failure [a],
 $f_{IR,metal}^i$ is the fraction of nuclide i released instantly from the metal upon contact with water [-],
 $I_{metal}^i(t)$ is the inventory of nuclide i at time t in the metal wasteform in a container [mol],
 $I_{0,metal}$ is the initial metal inventory in the metal wasteform in a container [mol],
 $c_{metal}(t)$ is the metal corrosion rate at time t [mol/a].

Release from Soft Material

The release of nuclide i from the soft waste is rapid over the short time period t_{soft} . The release rate is formally treated similarly to the release from metal waste form with:

$$F_{IR,soft}^i(t) = f_{IR,soft}^i I_{soft}^i(t) \delta(t - t_F) \text{ [mol/a] and} \quad (2.70c)$$

$$F_{CD,soft}^i(t) = (1 - f_{IR,soft}^i) I_{soft}^i(t) \frac{c_{soft}(t)}{I_{0,soft}} \quad t \geq t_F \quad (2.70d)$$

where the second equation reduces to an additional instant release if t_{soft} is zero, and where $I_{soft}^i(t)$ is the inventory of nuclide i at time t in the soft wasteform in a container [mol], and the other symbols are defined similarly to the metal waste form.

2.7 RELEASE FROM CONTAINER

2.7.1 Release Processes

The container fails when a hole is breached through its walls, allowing groundwater to eventually contact the used fuel. The size of the breach will depend on the failure mechanism.

The CC4 model focuses on the case of a small defect, such as an undetected manufacturing defect present when the containers are emplaced. The evolution of conditions within the container as a result of this defect can be complex, and it is likely that the formation of a complete groundwater pathway for nuclide transport from used fuel to the container exterior would take tens of thousands of years after the defect has formed (McMurry et al. 2004). In the present model, we assume that the water pathway forms at time t_F , nominally the time of container failure (see Section 2.3.1).

The release rate of nuclides from the container can be estimated from: the release of nuclides from the wasteforms into the container interior by the various processes described in previous sections; the radioactive ingrowth and decay, sorption, precipitation and re-dissolution of nuclides within the container; and the loss of dissolved nuclides through the water-filled defect. Since the container remains surrounded by a low-permeability clay layer, nuclide releases from the container are constrained by the rate of nuclide diffusion through the defect and out into the surrounding clay.

It is convenient to consider nuclide release from a defective container in three progressively more complex stages: the special case of a constant nuclide concentration in the container, the more general case of a time-varying concentration without precipitation, and then the effects of precipitation.

2.7.2 Constant Nuclide Concentration in Container

A special case for the nuclide release rate from the container is when there is a constant nuclide concentration in the water within the container. For example, this applies if the nuclide concentration is being held at its solubility limit within the container.

The nuclide release rate from the container is then bounded by two cases.

- Release is limited by the mass transport in the clay buffer medium surrounding the container, referred to as "buffer-limited release".
- Release is limited by the small size of the "pinhole" defect itself, referred to as "pinhole-limited release".

The release rates for these two cases are described in LeNeveu (1996). Here, only the steady-state solutions are used, so they are valid for times greater than some initial time period. In practice, these initial times are so small as to be insignificant when compared with the time scale of the modelling. Furthermore, the transient release rate is less than the steady-state release rate.

The case with the lower release rate provides the principal mass transport resistance and is taken as the relevant model for the release rate from the container. The particular model can vary between nuclides. That is, the release rate of nuclides from the container through the defect is the minimum value of F_{BLR} and F_{PLR} obtained from Equations (2.71) and (2.73) below. This minimum value is applied for all times $t > t_F$.

Buffer-limited Release

For buffer-limited release from a constant concentration source, the steady-state release rate, F_{BLR} , is given by (LeNeveu 1996, Equation 28, with “ π ” replaced by “4” for conservatism):

$$F_{BLR} = \frac{4r_{hole}^2 C_0 D_{i_{buffer}} g_{buffer}}{[1 - e^{-g_{buffer} r_{hole}}]} \quad (2.71a)$$

where

$$g_{buffer} = \sqrt{\frac{\lambda K_{buffer}}{D_{i_{buffer}}}} \quad (2.71b)$$

and

- r_{hole} is the effective radius of the defect,
- C_0 is the constant nuclide concentration in the container interior,
- $D_{i_{buffer}}$ is the intrinsic diffusivity for the nuclide in the buffer surrounding the container,
- K_{buffer} is the capacity factor in the buffer surrounding the container,
- λ is the nuclide decay constant.

If the nuclide does not decay, then F_{BLR} reduces to

$$F_{BLR} = 4r_{hole}^2 C_0 D_{i_{buffer}} \quad (2.72)$$

Pinhole-limited Release

For pinhole-limited release, the steady-state release rate, F_{PLR} , depends on the transport properties of the defect and is given by (LeNeveu 1996, Equation 15)

$$F_{PLR} = \frac{2\pi r_{hole}^2 C_0 D_{i_{hole}} g_{hole} e^{-g_{hole} L_{hole}}}{[1 - e^{-2g_{hole} L_{hole}}]} \quad (2.73a)$$

where

$$g_{hole} = \sqrt{\frac{\lambda K_{hole}}{D_{i_{hole}}}} \quad (2.73b)$$

where

- L_{hole} is the effective length of the pinhole,
- $D_{i_{hole}}$ is the intrinsic diffusivity for the nuclide within the defect, and,
- K_{hole} is the capacity factor for nuclide sorption within the defect.

If the nuclide does not decay, then F_{PLR} reduces to

$$F_{PLR} = \frac{\pi r_{hole}^2 C_0 D_{i_{defect}}}{L_{hole}} \quad (2.74)$$

Diffusion and Sorption

Two key transport-related properties for describing nuclide transport are diffusion and sorption.

Diffusion is characterized in terms of the intrinsic diffusivity

$$D_i = \varepsilon \tau D_o \quad (2.75a)$$

where ε is the porosity available for diffusion in the material, τ is the tortuosity, and D_o is the free-water diffusivity. In general, D_i may vary with nuclide, because of differences in the free-water diffusivity or because of effects such as anion exclusion in clays in which the effective porosity available for diffusion of negatively charged species is reduced because the clay minerals tend to have negative surface charges.

Diffusivity increases with temperature. Values at 100°C may be about three times higher than at room temperature. This temperature effect scales with temperature T and porewater viscosity $\mu(T)$ as (Rohsenow and Choi, 1961, p.383):

$$D_i = D_{i_{298K}} \frac{T}{298K} \frac{\mu_{298K}}{\mu(T)} \quad (2.75b)$$

The capacity factor, K , is related to the amount of sorption of a nuclide on solid substrates

$$K = \varepsilon R = (\varepsilon + \rho K_d) \quad (2.76)$$

where R is a retardation factor, ε is the porosity, ρ is the bulk density and K_d is the nuclide sorption coefficient. No temperature effects are presently included.

2.7.3 Time-Dependent Nuclide Concentration in Container without Precipitation

General solution

In general, the concentration of the nuclides in the container will vary with time. The amount of a nuclide in the container can be calculated using a compartment model representing the interior of the container (Appendix A). The general equation for the amount A^i of nuclide i accumulated within the container is:

$$\frac{dA^i(t)}{dt} = [F_{IN}^i(t) + \lambda^p A^p(t)] - \lambda^i A^i(t) - F_{OUT}^i(t) \quad (2.77)$$

The input into the container interior is the total release rate of nuclide i from the wasteform(s) into the container $F_{IN}^i(t)$, plus ingrowth from decay of parents $\lambda^p A^p(t)$ where p is the parent of nuclide i and $A^p(t)$ is the amount of this parent in the container as a function of time.

The general output flow from the compartment with decay but without precipitation is the convolution of the input rate with the container release response function:

$$F_{OUT}^i(t) = \int_0^t [F_{IN}^i(\tau) + \lambda^p A^p(\tau)] G^i(t - \tau) d\tau \quad (2.78)$$

where $G^i(t)$ is the container response function for nuclide i . That is, the response function describes the outflow from the container as a result of a unit impulse input of nuclide i into the container at time $t=0$.

As with the constant container concentration considered in the previous section, the general container release response $G(t)$ is bounded by two cases.

1. Release is limited by the mass transport in the medium surrounding the container, ("buffer-limited release"). The medium surrounding the container is considered to be of semi-infinite extent with a $C = 0$ boundary condition at infinite distance and the "inlet" boundary condition is applied at the exit of the defect.
2. Release is limited by the small size of the "pinhole" defect itself ("pinhole-limited release"). A $C = 0$ (swept away) boundary condition is applied at the exit of the pinhole and the "inlet" boundary condition is applied at the entrance to the pinhole.

The release mechanism with the lower release rate provides the principal mass transport resistance and is taken as the relevant model for the release rate from the container. The particular model can vary between nuclides.

The response function solutions for these two cases are described in detail in LeNeveu (1996). In the response functions presented here, only the first terms of an expansion in time are included, so they are valid for times greater than some initial time period. In practice, these initial times are so small as to be insignificant when compared with the time scale of the modelling.

Buffer-Limited Release Container Response

For buffer-limited release, the container release response function, G_{BLR} , is given by

$$G_{BLR}(t) = a_{BLR} \exp[-(a_{BLR} + \lambda)t] \quad (2.79)$$

where

$$a_{BLR} = \frac{4D i_{buffer} r_{hole}}{K_{ctr} V_{ctr}} \quad (2.80)$$

and

- λ is the nuclide decay constant,
 Di_{buffer} is the intrinsic diffusivity for the nuclide in the buffer around the container,
 r_{hole} is the radius of the hole or defect in the container shell,
 K_{ctr} is the capacity factor for sorption of the nuclide inside the container,
 V_{ctr} is the free volume inside the container.

Equations (2.79) and (2.80) are from LeNeveu (1996, Equation 30), with π replaced by "4" for conservatism. Equation (2.79) is accurate for times $t > 100 K_{buffer} r_{hole}^2 / Di_{buffer}$ for a release starting at $t=0$. For example, for a 1-mm radius hole, buffer with a large capacity factor of $K_{buffer} \sim 1000$, and an intrinsic diffusivity of $Di_{buffer} \sim 0.1 \text{ m}^2/\text{a}$, the model is applicable for $t > 1$ year.

Pinhole-limited Release Container Response

For pinhole-limited release, the container release response function, G_{PLR} , is given by (LeNeveu 1996):

$$G_{PLR}(t) = a_{PLR} \exp[-(a_{PLR} + \lambda)t] \quad (2.81)$$

where

$$a_{PLR} = \frac{\pi r_{hole}^2 Di_{hole}}{K_{ctr} V_{ctr} L_{hole}} \quad (2.82)$$

and L_{hole} is the length of the defect through the container shell.

This response function is valid for $\pi K_{hole} r_{hole}^2 L_{hole} / K_{ctr} V \ll 1$. In the absence of sorption inside the container, the first ratio is the volume of the pinhole defect to the void volume of the container. With sorption inside the container, the ratio has an even smaller value. Hence, for small defects, this condition is generally true, while for large defects the buffer is likely more limiting anyway.

Equations (2.81) and (2.82) are accurate for times $t > L_{hole}^2 K_{hole} / Di_{hole}$ for a release starting at $t=0$. For example, for a 25-mm long hole, an open defect with no sorption ($K_{hole} \sim 1$), and an intrinsic diffusivity of $Di_{hole} \sim 0.1 \text{ m}^2/\text{a}$, the model is applicable for $t > 0.01$ years.

General Container Response Function

More generally, the container release response function is

$$G_{Ctr}(t) = \alpha e^{-(\alpha+\lambda)t} \quad (2.83)$$

where

- α is the container release rate constant [$1/\text{a}$], given by $\alpha = \min(a_{BLR}, a_{PLR})$
 and a_{BLR} and a_{PLR} are given by Equations (2.80) and (2.82).

Container Compartment Model

The compartment model (Appendix A) can be used to solve Equation (2.77) for the amount of nuclide i in the container.

Radionuclide releases from the wastefoms provide the inputs to the interior of the container following the ingress of water into the container after time (delay) t_F . The degradation rates of these wastefoms were determined in Section 2.4. In general, we assume that wastefoms have a fast “instant” release and a slower release process. Due to the differences in the time scales for the two release processes, it is then numerically useful to evaluate the container inventory considering these two contributions separately.

$$F_{IN}^i(t) = F_{IR}^i(t) + F_{SR}^i(t) \quad (2.84)$$

where

$F_{IR}^i(t)$ is the instant release rate of nuclide i into the container [mol/a] (e.g., Equations (2.67) or (2.69a)),
 $F_{SR}^i(t)$ is the remaining “slow” release rate of nuclide i into the container, notably congruent dissolution with the wastefom and ingrowth [mol/a].

The container release rate for instant release nuclides is from Equations (2.78) and (2.83). The contribution due to parent is assumed to be negligible.

$$F_{OUT,IR}^i(t) = f_{IR,W}^i \cdot I_W^i(t_F) \cdot \alpha \cdot e^{-(\alpha+\lambda^i)(t-t_F)} \quad , \quad t \geq t_F \quad (2.85)$$

The maximum container release rate due to congruent dissolution released nuclides and ingrowth is:

$$F_{OUT,SR}^i(t) = \int_0^t [F_{SR}^i(\tau) + \lambda^p A^p(\tau)] G^i(t-\tau) d\tau \quad (2.86)$$

where $G^i(t)$ is the response function for nuclide i [1/a], defined in Equation (2.83) and $F_{SR}^i(t)$ is defined in Equation (2.84). (Note that the container release is zero for times less than t_F as the input terms are zero.) Due to the time dependence of the input function, this convolution integral must be numerically evaluated.

The container release without precipitation due to “slow” release, $F_{OUT,SR}^i(t)$, and the accumulated amount in the container can be determined using the compartment model.

2.7.4 Isotopic Ratios for Co-Precipitation

There may be more than one isotope of a chemical element being released inside the container. All such isotopes contribute towards the elemental solubility limits. If precipitation occurs, all isotopes co-precipitate together.

Since significant isotopic separation is not expected in the wasteform release processes, the fractional amount of each isotope in solution can be determined from the inventory of these isotopes in the wasteform. However, these isotope ratios vary with time due to radionuclide decay and ingrowth. Thus the time dependent fraction of a particular isotope i , $r_i^j(t)$, is given by

$$r_i^j(t) = \frac{I^j(t)}{\sum_j I^j(t)}, \quad j = \text{isotope of same element as } i \quad (2.87)$$

For nuclides with short half-lives that are considered to be in secular equilibrium, the inventory included in the summation is that calculated from the inventory of a precursor by the secular equilibrium relationship.

$$I^j(t) = \lambda^i \cdot I^i(t) / \lambda^j, \quad \text{where } j \text{ is in secular equilibrium with precursor } i \quad (2.88)$$

The isotope ratio determined by Equation (2.87) should in general include any stable isotopes of the element that are present in the wasteform or in the background composition of the groundwater. The solubility for nuclide i would be overestimated if these stable isotopes are not included.

The summation in Equation (2.87) is done only over the nuclides in a single wasteform. The wasteforms are considered to degrade at different timescales, and therefore they are conservatively assumed to not influence precipitation of isotopes in other wasteforms. The solubility of an element, determined as described in Section 2.5, is then fractionated by the ratios determined by Equation (2.87) to determine the effective solubility limit for each isotope (per wasteform). Note that the isotope ratios will change with time due to decay, and therefore the solubility limit for an isotope will change with time.

2.7.5 Release from Container after Precipitation

Precipitation of nuclides inside the container is accounted for by invoking another compartment model calculation.

The process is to compare the release rate from the container defect under a constant concentration boundary condition (i.e., the solubility limit of the nuclide) in Section 2.7.2, with the release rate determined in Section 2.7.3 without consideration of solubility limits.

In applying this solubility limited release rate for comparison, the time dependent isotopic ratios determined in the previous Section 2.7.4 are applied as a multiplying factor.

If the resulting solubility limited release rate is the smaller one, then precipitation occurs, a precipitate accumulates, and the smaller solubility limited release rate is used. If the solubility limited release rate is the larger one, then the general solution (unconstrained by precipitation) release rate determined in Section 2.7.3 is used; this condition can only occur when no precipitate is present. Radioactive decay and ingrowth from a parent nuclide must also be considered in determining the amount of a precipitate.

This comparison of release rates, with accumulation and depletion of precipitate, including the effects of decay and ingrowth, is precisely the calculation performed by the compartment model described in Appendix A. For this comparison, the constrained maximum release rate, $F_{MAX}^i(t)$, is taken to be the product of the solubility limited release rate determined as described in Section 2.7.2 and the time varying isotopic ratio. The "input" rate, $F_{IN}^i(t)$, is taken to be the release rate unconstrained by solubility determined in Section 2.7.3. The compartment model does precisely the comparison required and gives the desired release rate, $F_{OUT}^i(t)$, having taken into account possible precipitation. The accumulated amount of precipitate, if any, is also determined by the compartment model.

This release rate, $F_{OUT}^i(t)$, is the final value for the release from the container, through the pinhole defect, into the surrounding buffer material.

2.8 INTERFACE WITH VAULT MODEL

The container model is based on the reference design concept where the container is surrounded by a layer of dense clay buffer. This buffer serves to isolate the container from the surrounding vault and geosphere, providing both a stable chemical environment and an impermeable layer to groundwater flow.

In the present model, the buffer allows water to enter and fill the failed containers. The saturation rate is not modelled, but is treated through a specified delay time, t_f . The buffer will affect the chemistry of the porewater that enters the container; this groundwater composition is provided as input and then equilibrated as described in Section 2.6.

The direct interface from the vault model into the container model is through the limitation of the nuclide releases from the container based on diffusion through the buffer.

The main interface from the container model to the vault model is the calculated time-dependent source term describing the release of radionuclides from the failed containers and into the buffer.

2.9 REFERENCES

- Bateman, H. 1910. Solution of a system of differential equations occurring in the theory of radioactive transformation. Proc. of Cambridge Phil. Society 15, 423.
- Bruno, J., E. Cera, J. de Pablo, L. Duro, S. Jordana and D. Savage. 1997. Determination of radionuclide solubility limits to be used in SR 97. Uncertainties associated with calculated solubilities. SKB Technical Report, TR 97-33. Stockholm, Sweden.
- Garisto, F. and P. Gierszewski. 2002. Technetium-99: Review of properties relevant to a Canadian geologic repository. Ontario Power Generation Report 06819-REP-01200-10081-R00. Toronto, Canada.
- Garisto, F., J. Avis, T. Chshyolkova, P. Gierszewski, M. Gobien, C. Kitson, T. Melnyk, J. Miller, R. Walsh and L. Wojciechowski. 2010. Glaciation scenario: Safety assessment for a

- deep geological repository for used fuel. Nuclear Waste Management Organization Technical Report NWMO TR-2010-10. Toronto, Canada.
- Garisto, F., J. Avis, A. D'Andrea, P. Gierszewski, and T. Melnyk. 2004. Third case study – Reference data and codes. Ontario Power Generation Report 06819-REP-01200-10107-R00. Toronto, Canada.
- Garisto, F., D.H. Barber, E. Chen, A. Inglot, and C.A. Morrison. 2009. Alpha, beta and gamma dose rates in water in contact with used CANDU fuel. Nuclear Waste Management Organization Technical Report NWMO TR-2009-27. Toronto, Canada.
- Garisto, F., M. Gobien, E. Kremer and C. Medri. 2011. Fourth case study: Reference data and codes. Nuclear Waste Management Organization Technical Report NWMO TR-2011-18. Toronto, Canada. (In Progress)
- Johnson, L.H., D.M. LeNeveu, F. King, D.W. Shoesmith, M. Kolar, D.W. Oscarson, S. Sunder, C. Onofrei and J.L. Crosthwaite. 1996. The disposal of Canada's nuclear fuel waste: A study of postclosure safety of in-room emplacement of used CANDU fuel in copper containers in permeable pluton rock; Volume 2: Vault Model. Atomic Energy of Canada Limited Report, AECL-11494-2, COG-95-552-2. Pinawa, Canada.
- Johnson, L.H. and P.A. Smith. 2000. The interaction of radiolysis products and canister corrosion products and the implications for spent fuel dissolution and radionuclide transport in a repository for spent fuel. NAGRA Technical Report NTB 00-04. Wettingen, Switzerland.
- Kolar, M., D.M. LeNeveu and F. King. 2000. An interim performance assessment model for used fuel. Ontario Power Generation Report 06819-REP-01200-10034-R00. Toronto, Canada.
- Lemire, R.J. and F. Garisto. 1989. The solubility of U, Np, Pu, Th and Tc in a geological disposal vault for used nuclear fuel. Atomic Energy of Canada Limited Report, AECL-10009. Pinawa, Canada.
- Lemire, R.J., J. Fuger, H. Nitsche, P. Potter, M.H. Rand, J. Rydberg, K. Spahiu, J.C. Sullivan, W.J. Ullman, P. Vitorge and H. Wanner. 2001. Chemical Thermodynamics 4; Chemical thermodynamics of neptunium and plutonium. Elsevier Science, Amsterdam, Holland.
- LeNeveu, D.M. 1996. Mass transfer rates from a pinhole in a waste container for an inventory-limited and a constant concentration source. Atomic Energy of Canada Limited Report, AECL-11540, COG-96-68. Pinawa, Canada.
- McMurry, J., B. Ikeda, S. Stroes-Gascoyne and D. Dixon. 2004. Evolution of a Canadian deep geologic repository: Defective container scenario. Ontario Power Generation Report 06819-REP-01200-10127-R0. Toronto, Canada.
- McMurry, J., D. Dixon, J. Garroni, B. Ikeda, S. Stroes-Gascoyne, P. Baumgartner and T. Melnyk. 2003. Evolution of a Canadian deep geologic repository: Base scenario. Ontario Power Generation Report 06819-REP-01200-10092-R0. Toronto, Canada.

Rohsenow, W. and H. Choi. 1961. Heat, mass, and momentum transfer. Prentice-Hall Inc., Englewood Cliffs, USA.

Shoesmith, D.W, and Dmitrij Zagidulin. 2010. The corrosion of zirconium under deep geological repository conditions. Nuclear Waste Management Organization Technical Report NWMO TR-2010-19. Toronto, Canada.

Shoesmith, D.W. 2008. The role of dissolved hydrogen on the corrosion/dissolution of spent nuclear fuel. Nuclear Waste Management Organization Technical Report NWMO TR-2008-19. Toronto, Canada.

Shoesmith, D.W. 2007. Used fuel and uranium dioxide dissolution studies – A review. Nuclear Waste Management Organization Technical Report NWMO TR-2007-03. Toronto, Canada.

Shoesmith, D.W., S. Sunder and J.C. Tait. 1997. Validation of the oxidative dissolution model for used CANDU fuel. Atomic Energy of Canada Limited Report AECL-11798.

3. VAULT MODEL

3.1 MODEL OVERVIEW

In a deep geologic repository, the containers are emplaced in rooms excavated from the rock, and surrounded by a layer of dense clay buffer that controls both groundwater flow and the chemical environment near the container. Beyond the buffer, other engineered materials may be present, notably other clay- or cement-based backfill. The emplacement room will also have an excavation-damaged zone (EDZ) in the adjacent rock wall. This EDZ is included here as part of the repository or “vault” model.

After each room is filled and sealed, groundwater will start to move back into the residual porosity, and will eventually saturate the buffer and contact the container. This saturation process may take hundreds of years in sparsely fractured rock. However, release of contaminants through and from the repository cannot occur until this process is substantively complete. The CC4 vault model does not directly model this saturation time, but accounts for it by an input delay time t_F , the time needed to form a continuous groundwater pathway from the waste in the defective container to the outside of the container. At this time, the repository is assumed to be saturated. The delay time also accounts for any time required for container failure, for water to enter the container, and for fuel cladding to have been breached.

The model then simulates the following processes:

- diffusive transport of nuclides released from a container defect through the surrounding buffer, and
- dispersive and convective transport of nuclides through the backfill and EDZ into the surrounding rock.

A few emplacement room layouts are under consideration, as illustrated in Figure 3.1. The CC4 model represents each room by concentric cylinders of materials, as shown in Figure 3.2. This model is a simplification of the geometry, but is intended to include the key processes and features. The main model result is the total (integrated) flow rate of nuclides out of each room. This simpler model has been compared with more detailed calculations, and found to be a sufficient or conservative representation of the total release (Johnson et al. 1996; Garisto et al. 2004, 2005).

3.2 VAULT SECTOR PROPERTIES

Since the repository extends over a few km^2 , the surrounding rock will likely vary in its properties and in the groundwater flow. To account for these variations, as well as possible variations in room lengths in different locations, the vault is divided into sectors and contaminant releases are calculated for each sector. Within each sector, the properties of the rock, vault (e.g., room length), and failed container characteristics (e.g., time of failure, size of defect) are assumed to be the same.

The vault transport model requires as input a number of parameters that are related to the average properties of the rock zone surrounding each sector. The rock zone parameters are the Darcy velocity resolved into its components, (V_x, V_y, V_z) , in the Cartesian coordinate directions of the geosphere transport model, and the near-field rock porosity, ε_R , tortuosity, τ_R , permeability, k_R , and dispersion length, α_R . In addition, the free water diffusion coefficient, $D_{0,i}$,

and the retardation factor, R_i , used in the geosphere transport model calculations are also adopted in the vault transport model for consistency.

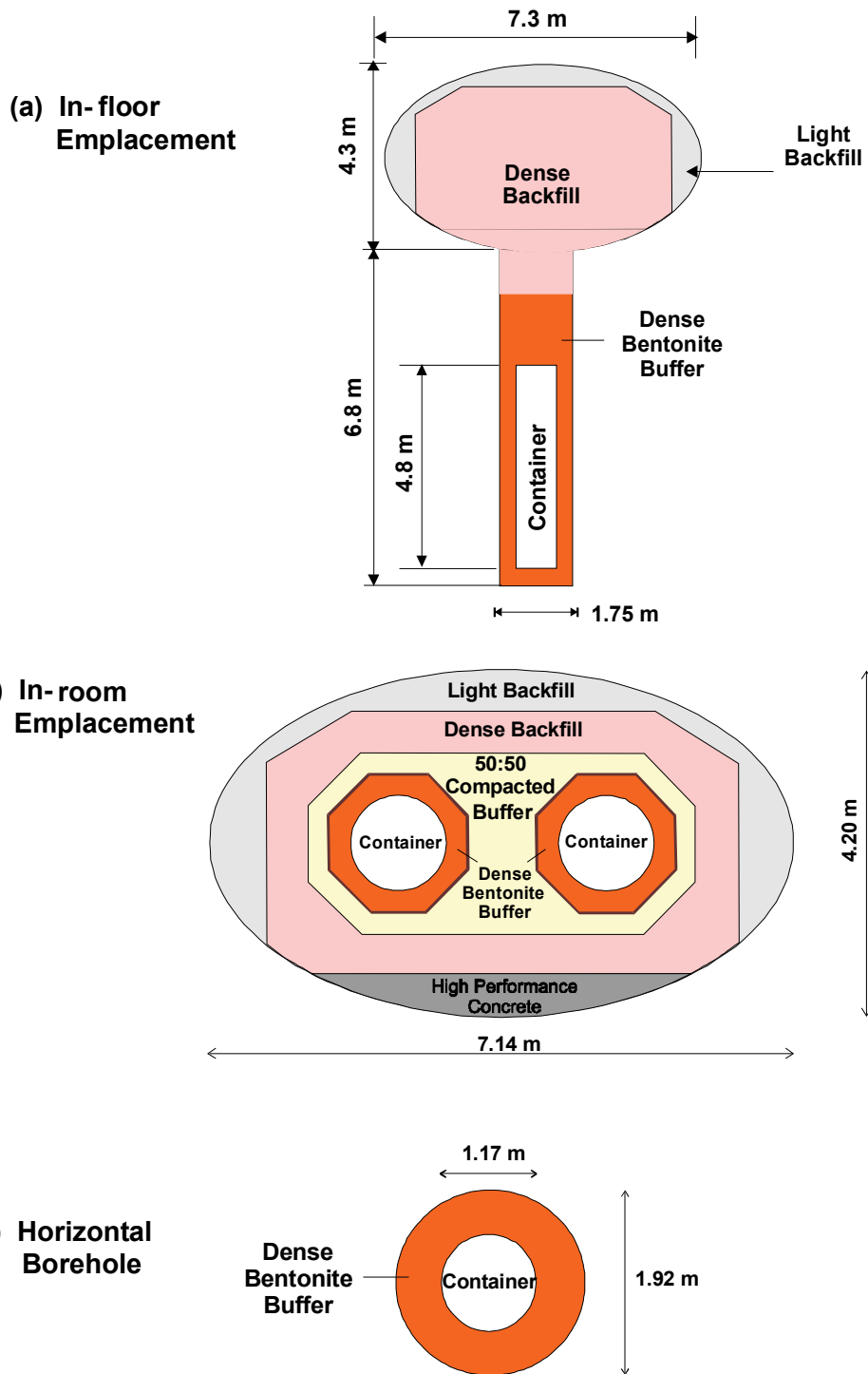


Figure 3.1: Cross-sectional view of three candidate emplacement room layouts, showing the main material components

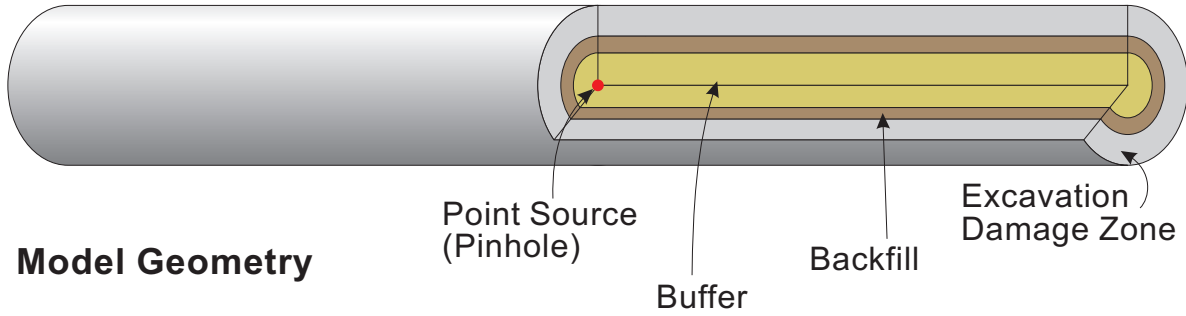


Figure 3.2: Emplacement room geometry used in the CC4 vault model

The axis of the emplacement rooms is in general aligned to some angle θ counter-clockwise from the x-coordinate direction of the geosphere model. Hence, the axial (parallel to the room long axis), V_R^A , and transverse (orthogonal to the room long axis), V_R^T , components of the Darcy velocity of the groundwater in the rock (as used in the vault model) are given by:

$$\begin{aligned} V_R^A &= V_x \cos\theta + V_y \sin\theta \\ V_R^T &= \sqrt{(-V_x \sin\theta + V_y \cos\theta)^2 + V_z^2} \end{aligned} \quad (3.1)$$

The Darcy velocities of the groundwater in the backfill and EDZ are proportional to the velocities in the surrounding rock, V_R^T (transverse to the room axis), and V_R^A (parallel to the room axis). The equations describing this proportionality were obtained using simplified concepts of the distribution of groundwater flow among the different media based on water mass balance, the resistances (permeabilities) of each medium to the water flow, and the relative cross-sectional areas occupied by each medium. The following two subsections describe how these transverse and axial Darcy velocities are obtained for the EDZ and the backfill. The buffer is considered to have very low permeability, so the groundwater velocity in this medium is set to zero.

3.2.1 Excavation Damaged Zone Physical Properties

The porosity of the EDZ, the permeability of the EDZ, and the nuclide sorption capacity factors for the EDZ are all related to the corresponding properties in the surrounding rock.

The porosity in the EDZ, ϵ_Z , is larger than the porosity in the rock, ϵ_R , because the damage caused by the excavation can only increase the porosity.

$$\epsilon_Z \geq \epsilon_R \quad (3.2)$$

The EDZ may have anisotropic permeability (more permeable parallel to the room axis than transverse to the room). The axial EDZ permeability is set to a multiple f_{ZR} of the rock

permeability ($f_{ZR} \geq 1$), while the transverse EDZ permeability is taken to be a fraction, f_{TA} , of the axial permeability ($f_{TA} \leq 1$). The axial permeability should not be less than the permeability of the surrounding rock; that is, the damage caused by the excavation can only increase the permeability, not make the rock tighter. Hence

$$k_Z^A = f_{ZR} k_R \quad (3.3a)$$

$$k_Z^T = \max(f_{TA} k_Z^A, k_R) \quad (3.3b)$$

The retardation factor for a nuclide in the rock, R_R , is converted into a capacity factor for the species in the rock, K_R , by multiplying by the rock porosity.

$$K_R = \varepsilon_R R_R \quad (3.4)$$

The retardation factor for a nuclide in the EDZ, since it is composed of the same suite of sorbing materials, is set equal to the retardation factor in the rock and converted to capacity factor for the nuclide in the EDZ, K_Z , by multiplying by the porosity of the EDZ.

$$K_Z = \varepsilon_Z R_R \quad (3.5)$$

3.2.2 Transverse Darcy Velocities

The magnitude of the transverse velocity in the EDZ and backfill is estimated from the transverse velocity in the host rock by an equivalent resistor model. It is assumed that the transverse host rock flow is primarily vertical since this would generally be a more unfavorable groundwater flow. In this direction, the repository has a large horizontal extent.

The Darcy velocity for the EDZ, V_Z^T , is then:

$$V_Z^T = \frac{k_Z^T V_R^T}{fA_F k_F + fA_Z k_Z^T + (1 - fA_F - fA_Z - fA_B) k_R} \quad (3.6)$$

where k_R and k_F are the permeabilities of the surrounding rock and of the backfill, and k_Z^T is the permeability in the EDZ transverse to the room axis.

The area factors fA_Z , fA_F and fA_B are related to the extents of the EDZ, backfill and buffer as

$$fA_j = \frac{2T_j}{S} \quad (3.7)$$

where the T_j are the radial thicknesses of the EDZ, backfill, and buffer and S is the centre-to-centre spacing of the emplacement rooms.

Similarly, the transverse Darcy velocity in the backfill, V_F^T , is

$$V_F^T = \frac{k_F V_R^T}{fA_F k_F + fA_Z k_Z^T + (1 - fA_F - fA_Z - fA_B) k_R} \quad (3.8)$$

The transverse Darcy velocity in the buffer, V_B^T is zero because of its low permeability.

$$V_B^T = 0 \quad (3.9)$$

3.2.3 Axial Darcy Velocities

In the axial direction, the vault has a small cross-section to the host rock groundwater flow. However, higher permeability within the vault may result in a distortion of the groundwater flow towards the vault. The axial Darcy velocities in the EDZ and the backfill are estimated from relative permeabilities and proportionality to the Darcy velocities in the surrounding rock.

In the EDZ, the axial velocity, V_{DZ}^A , is given by

$$V_{DZ}^A = \frac{k_Z^A}{k_R} V_R^A \quad (3.10)$$

and in the backfill the axial Darcy velocity, V_{DF}^A , is given by

$$V_{DF}^A = \frac{k_F}{k_R} V_R^A \quad (3.11)$$

The axial Darcy velocity in the buffer, V_B^A , is effectively zero because of its low permeability

$$V_B^A = 0 \quad (3.12)$$

3.3 TRANSPORT THROUGH BUFFER, BACKFILL AND EDZ

Transport through the barriers of the engineered part of the repository (buffer, backfill and excavation damaged zone (EDZ) surrounding an emplacement room) is calculated with the response function approach (see Appendix A.1). For the transport of a decay chain member nuclide i ,

$$F_i(t) = \sum_j \int_0^t J_j(\tau) \cdot G_{ij}(t - \tau) \cdot d\tau \quad (3.13)$$

The input flow rate, $J_j(t)$, is the flow rate of precursor nuclide j out of the container defect, $F_j^{OUT}(t)$, as determined in Section 2, and the summation is over all decay chain precursors of nuclide i , plus nuclide i .

The response functions are derived from a Boundary Integral Model for mass transport (Kolar and LeNeveu 1995, LeNeveu and Kolar 1996). In this report, the response functions $G_{ij}(t)$ used are identified below and the details of their origin are given by LeNeveu and Kolar (1996).

The response functions are developed for the case of a point defect in a container emplaced in an excavated room of an underground repository with "in-room" emplacement design; that is, the containers are placed along the axis of the emplacement room.

In the model geometry, the cross-section of an emplacement room is approximated by three coaxial cylinders of finite extent surrounded by the rock of the geosphere, assumed for modelling purposes to be a fourth cylinder of infinite extent in the radial direction. The innermost cylinder is used to model the buffer, the next cylinder models the backfill, and the outermost cylinder models the EDZ. The effective radial dimensions of the cylinders are inputs to the model. Since actual emplacement geometries are unlikely to have this cylindrical symmetry, approximate or bounding values for the effective radii must be chosen as inputs. The dimensions of the containers themselves are disregarded; the containers become point sources located along the central axis of the nested cylindrical array. All properties are assumed to be symmetric about the cylindrical axis. Thus the transport model is two-dimensional, using only the axial (z) and radial (r) coordinates of the cylinder and not using the angular (θ) coordinate of rotation about the cylindrical axis.

The transport model determines the outward nuclide flow rate integrated over the entire surface of the EDZ from a single failed container within the room. Should more than one container fail in a room (or in a sector), the integrated flow rate for a single container is multiplied by the number of failed containers. This multiplication can be done because the integrated flow rates are independent of the position of the failed container, as discussed later. This final flow rate out of the EDZ, $F_i(t)$, is the final output from the vault model and this flow rate is then used as the input flow rate for the geosphere transport model to which the model is connected.

Transport through the buffer, backfill and EDZ is determined with the response function approach using a boundary integral model and convolution integrals. A detailed description of the determination of these response functions has been published (LeNeveu and Kolar 1996) and some of the relevant equations are indicated here.

The response function itself cannot be solved analytically. However, because of the cylindrical symmetry, analytical expressions are obtained for the Laplace transform of the response function, which then can be inverted using numerical techniques (Talbot 1979, LeNeveu and O'Connor 1994) to give the required response function for use in Equation (3.13), which also must be evaluated using numerical techniques, as discussed in Appendix B.

3.3.1 Mass Balance Equation and Parameters

In cylindrical (r, z) co-ordinates, the advection-dispersion mass balance equation for a single decaying nuclide in a cylindrically symmetric system is written:

$$\frac{\partial C}{\partial t} - \frac{D_r}{K} \frac{\partial^2 C}{\partial r^2} - \frac{D_r}{Kr} \frac{\partial C}{\partial r} - \frac{D_z}{K} \frac{\partial^2 C}{\partial z^2} + \frac{V_z}{K} \frac{\partial C}{\partial z} + \frac{\phi}{Kr} \frac{\partial C}{\partial r} + \lambda C = 0 \quad (3.14)$$

A similar equation, with an additional term for the source from a decaying parent, is used for decay chains. In Equation (3.14) (cf. LeNeveu and Kolar, 1996, Equation 1), the nuclide subscripts i have been dropped. The equation applies in each medium i.e., in each of the nested cylinders representing buffer, backfill, EDZ and the surrounding rock zone. Within each medium, C is the concentration of nuclide in the pore water, D_r is the radial intrinsic dispersion coefficient, D_z is the axial intrinsic dispersion coefficient, V_z is the axial Darcy velocity, ϕ is the product of the radial Darcy velocity and the radius; i.e., rV_r , which must be a constant to preserve water mass balance within the medium, K is the capacity factor for the nuclide, and λ is the radionuclide decay constant.

The axial Darcy velocities, V_z , in the rock, EDZ, and backfill are taken to be those determined in the previous Section 3.2. The axial Darcy velocity in the buffer is zero.

As an approximation, the radial Darcy velocities, V_r , in the rock, EDZ and backfill are taken to be the transverse Darcy velocities determined in the previous Section 3.2.2. (The radial Darcy velocity in the buffer is zero.) In a cylindrical system, the preservation of water mass balance requires that the radial water velocity decrease as $1/r$ making the quantity ϕ in Equation (3.14) a constant. In determining a constant value for $\phi = rV_r$ for a medium, the radial Darcy velocity for the medium, V_r , assigned above is multiplied by the radius, r_{max} , of the maximum extent of the medium in the cylindrical geometry approximation.

In this cylindrical approximation, the apparent source of water for the radial component of the groundwater flow is along the common axis of the cylinders and the flow is radially outward everywhere in the backfill and the EDZ. This situation with radially outward flow does not correspond to the physical situation, which has a component of the flow transverse to the emplacement room. However, the restriction of this approximation is not significant for the buffer layer where the groundwater velocity is zero and works reasonably well for the other layers as long as the ratio of the outer radius and the inner radius of each cylinder does not become too large. Johnson et al. (1996) document the results of some tests of this approximation against the finite-element code MOTIF.

In the buffer, the dispersion coefficients, both axial and radial, are given simply by the intrinsic diffusion coefficients for the contaminants in the buffer because the groundwater velocity is zero.

$$D_z = D_r = D_i \quad (3.15)$$

The intrinsic diffusion coefficients in buffer are inputs to the vault model.

In the backfill, the axial and radial dispersion coefficients are found by multiplying the Darcy velocities of the groundwater by longitudinal and transverse dispersion lengths, α_L and α_T , for both the axial and transverse directions, summing the two velocity component contributions and adding on the intrinsic diffusion coefficient, D_i , for the contaminants in the backfill.

$$\begin{aligned} D_z &= \alpha_L V_z + \alpha_T V_r + D_i \\ D_r &= \alpha_T V_z + \alpha_L V_r + D_i \end{aligned} \quad (3.16)$$

The longitudinal and transverse dispersion lengths and the intrinsic diffusivities in backfill are input to the vault model.

In the EDZ, the dispersion coefficients are calculated from other properties of the EDZ.

$$\begin{cases} D_z = \alpha_{zz}V_z + \alpha_{rT}V_r + \tau_z D_0 \epsilon_z \\ D_r = \alpha_{zT}V_z + \alpha_{rr}V_r + \tau_z D_0 \epsilon_z \end{cases} \quad (3.17)$$

where D_0 is the free water diffusivity used in the geosphere transport model, τ_z is the tortuosity of the EDZ and, because of the anisotropy of the EDZ, there are four different dispersion lengths. Here, α_{zz} and α_{zT} are the longitudinal and transverse dispersion lengths associated with the axial Darcy velocity component of the groundwater flow, and α_{rr} and α_{rT} are the longitudinal and transverse dispersion lengths associated with the radial Darcy velocity component of the groundwater flow. The dispersion lengths associated with the radial flow component are in turn calculated as fractions, $f_{\alpha L}$ and $f_{\alpha T}$ of the dispersion lengths associated with the axial flow component.

$$\begin{cases} \alpha_{rr} = f_{\alpha L} \alpha_{zz} \\ \alpha_{rT} = f_{\alpha T} \alpha_{zT} \end{cases} \quad (3.18)$$

D_0 , α_{zz} , α_{zT} , $f_{\alpha L}$, $f_{\alpha T}$ and τ_z are all inputs to the model.

The dispersion coefficients, D_z and D_r , for the rock zone surrounding the EDZ are determined from the rock properties of Darcy velocity V_R , dispersion length α_R , porosity ϵ_R , and tortuosity τ_R . A factor, f_{ω} is used to determine the dispersivity orthogonal to the groundwater flow direction as a fraction of the longitudinal dispersivity in the rock, α_R . The projection of the dispersion coefficient onto the axial and transverse directions of the emplacement room is done using the same algorithm as that used in the MOTIF groundwater modelling code (Chan et al. 1999, Equation 18). The dispersion coefficients in the axial and transverse directions are given by

$$\begin{cases} D_z = \alpha_R (V_R^A)^2 / V_R + f_{\omega} \alpha_R (V_R^T)^2 / V_R + \tau_R D_0 \epsilon_R \\ D_r = \alpha_R (V_R^T)^2 / V_R + f_{\omega} \alpha_R (V_R^A)^2 / V_R + \tau_R D_0 \epsilon_R \end{cases} \quad (3.19)$$

Capacity factors for the buffer and backfill are inputs to the vault model. Capacity factors for the rock zone and capacity factors for the EDZ are determined from the rock zone values, as described in Section 3.2.1.

3.3.2 Boundary Conditions and Solution

The radial boundary conditions used in the model are those of continuity of flux and concentration integrated over the interfacial area separating any two media (two cylindrical surfaces), rather than continuity at every point on the interface. The boundary conditions at the ends of the rooms (cylinders in the model) are that the contaminant flux is proportional to the axial Darcy velocity of the groundwater. The result of interest is the integrated total contaminant flow rate out of each of the three media - buffer, backfill, and EDZ.

The use of integrated radial continuity and flux axial boundary conditions results in a solution for the integrated release rate that is independent of the location of the source (the failed container) (LeNeveu and Kolar 1996). The point source can be at any position along the room axis with the same result for the integrated release rate across each interface.

The final result for the Laplace transform of the response function giving the total integrated contaminant flow rate out of the EDZ is given by Equation (25) of LeNeveu and Kolar (1996) for single nuclides and by Equation (38) of the reference for a nuclide that is a member of a decay chain. These equations are not reproduced here because of their complexity. In the reference, equations are also given for the Laplace transform of the response functions giving the contaminant flow rates out of the buffer and out of the backfill.

Because of the cylindrical symmetry of the modelled system, these solutions involve modified Bessel functions of the first and second kind. The order of the modified Bessel functions used in the evaluation of the response function is controlled by the values of the constant parameters ϕ and D_r appearing in Equation (3.13).

3.4 INTERFACE WITH SURROUNDING GEOSPHERE

The vault transport model requires as input a number of parameters that are related to the properties of the rock zone surrounding each emplacement room. The rock zone properties used are the Darcy velocity resolved into its components, (V_x , V_y , V_z), in the Cartesian coordinate directions of the geosphere transport model, and the near-field rock porosity, ϵ_R , tortuosity, τ_R permeability, k_R , and dispersion length, α_R . In addition, the free water diffusivities for each contaminant, D_{0i} , and the retardation factors, R , for each contaminant used in the geosphere transport model calculations are also adopted in the vault transport model for consistency. The axes of the emplacement rooms are aligned to some angle θ from the x-coordinate direction of the geosphere model.

Releases of contaminants are integrated over the entire surface of the outermost EDZ region to provide the contaminant flux into the geosphere transport model from a given sector, where the total flow rate depends on the number of failed containers in that sector.

3.5 REFERENCES

- Chan, T., N.W. Scheier and V. Guvanase. 1999. MOTIF code version 3.2 theory manual. Ontario Hydro Report 06819-REP-01200-0091-R00. Toronto, Canada.
- Garisto, F., J. Avis, N. Calder, A. D'Andrea, P. Gierszewski, C. Kitson, T. Melnyk, K. Wei and L. Wojciechowski. 2004. Third case study - Defective container scenario. Ontario Power Generation Report 06819-REP-01200-10126-R00. Toronto, Canada.
- Garisto, F., J. Avis, N. Calder, P. Gierszewski, C. Kitson, T. Melnyk, K. Wei and L. Wojciechowski. 2005. Horizontal borehole concept case study. Ontario Power Generation Report 06819-REP-01200-10139-R00. Toronto, Canada.
- Johnson, L.H., D.M. LeNeveu, F. King, D.W. Shoesmith, M. Kolar, D.W. Oscarson, S. Sunder, C. Onofrei and J.L. Crosthwaite. 1996. The disposal of Canada's nuclear fuel waste: A study of postclosure safety of in-room emplacement of used CANDU fuel in

copper containers in permeable pluton rock, Volume 2: Vault Model. Atomic Energy of Canada Limited Report, AECL-11494-2, COG-95-552-2. Pinawa, Canada.

Kolar, M. and D.M. LeNeveu. 1995. Near-field mass transport from a point source (instantaneously failed container) located in a disposal room. Atomic Energy of Canada Limited Report, AECL-11172, COG-I-94-444. Pinawa, Canada.

LeNeveu, D.M. and M. Kolar. 1996. Radionuclide response function to the convection-dispersion equation for a point source along the axis of nested cylindrical media. Atomic Energy of Canada Limited Report, AECL-11549, COG-96-90. Pinawa, Canada.

LeNeveu, D.M. and P.A. O'Connor. 1994. Numerical inversion of Laplace transforms applied to the boundary integral method. Proc. 1994 Symposium on Applied Mathematics, 22-26.

Talbot, A. 1979. The accurate numerical inversion of Laplace transforms. Jrnl. Inst. Maths. Applics. 23, 97-120.

4. GEOSPHERE MODEL

4.1 INTRODUCTION

The geosphere model accounts for contaminant transport along a simplified set of pathways leading from a source to groundwater discharge locations at ground surface. It calculates the transport rate of contaminants along these pathways, but it does not determine the groundwater flow field that is the basis for these pathways. Instead, the model depends on the groundwater flow field being provided from an external source, in the form of either a set of reference hydraulic heads or a set of groundwater velocities.

This flow field is approximated by a set of one-dimensional (1-D) transport elements or flow tubes called segments that are connected together in three-dimensional (3-D) space to form a transport network. The transport network represents the pathways through the rock that contaminants would follow. An example is shown in Figure 4.1.

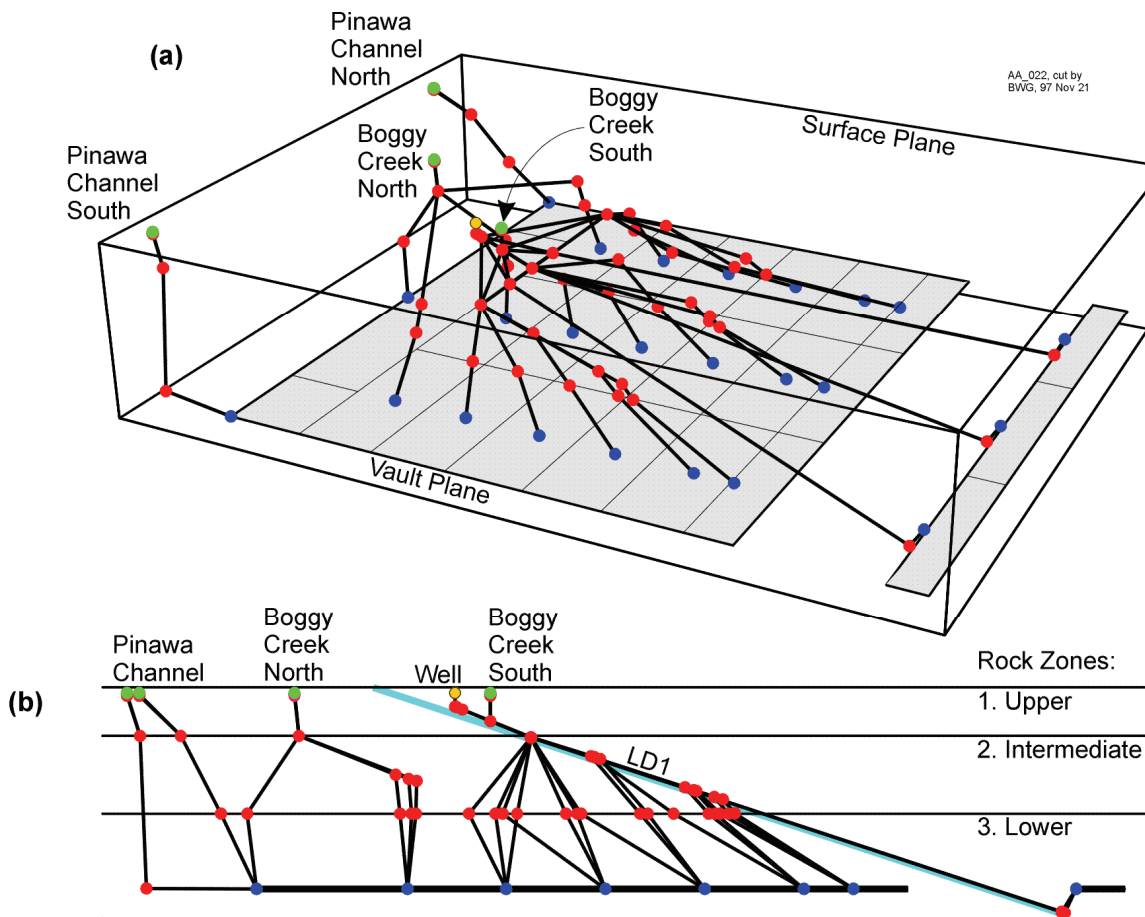


Figure 4.1: (a) 3-D and (b) 2-D views of the geosphere network used to model a hypothetical repository placed within the Whiteshell Research Area (Davison et al. 1994)

The state of the geosphere can evolve with time. For example, its properties can vary because of the effects of climate change, and repeated glaciations may lead to cycles of state changes. The geosphere (versions CC4.07 and CC4.08) submodel can simulate multiple state changes, including multiple cycles of glaciation, with two main presumptions.

1. The transformation from one state to the next can be adequately approximated as a step change in time, as implied in Equation (1.1).
2. The changes affect only the properties of the network transport segments used to describe the movement of groundwater and contaminants throughout the geosphere.

The properties affected are principally groundwater velocities (rate and direction) and the potential convergence and divergence of transport pathways. For example, when a temperate climate state is altered to a permafrost state, groundwater velocities near the ground surface might become very small or vanish, and groundwater flow at depth might be diverted to or away from different pathways. Groundwater discharge areas might change radically, affecting flows into the biosphere.

In implementing such a transport network for a specific site, we closely represent the detailed field information available for the site. The network is derived from 3-D groundwater modelling of the geosphere at the site. The 3-D modelling of groundwater flow is performed externally to the geosphere model using, for example, the finite-element groundwater flow code FRAC3DVS-OPG (Therrien et al. 2010, Therrien and Sudicky 1996). Typically the 3-D modelling is performed for each possible geosphere state, and a rationalization process ensures that the resulting network for CC4 permits a coherent and consistent transformation between states. That is, the network must be sufficiently accommodating that it can represent groundwater flow for each state to be simulated.

One-dimensional transport segments are used for computational efficiency so that analytical solutions to the transport equations for radionuclide decay chains can be used. The output from one segment of the network is calculated and used as the input to the next segment of the network. The transport network may converge and diverge. Convergence occurs, for example, at a well inlet.

The geosphere model was implemented in the CC4/GEONET model. This model is formulated generally and can be applied to many different sites since most of the site-specific information is incorporated into the model using input data files.

Section 4.2 describes general features of the transport model. Section 4.3 describes the transport equations and their application, and also describes the parameters in the transport equation. Section 4.4 describes the model for contaminant transport to a groundwater supply well that penetrates the geosphere. Section 4.5 describes the options available to include matrix diffusion and Section 4.6 describes colloid effects in the model. Sections 4.7 and 4.8 describe the interfaces between the geosphere and the vault and biosphere models.

4.2 MODEL OVERVIEW

In CC4/GEONET, the contaminant pathways are approximated by a 3-D network of nodes, connected in pairs by one-dimensional transport segments. A schematic example of such a transport network is shown in Figure 4.2.

In this example, the (two-dimensional) geosphere is approximated by a network of 13 nodes (N1 to N13) connected by 10 one-dimensional transport segments (S1 to S10). A set of 5 nodes (N1, N2, N4, N9, and N11) are source nodes connected to the repository, which is divided into 5 sectors (M1 to M5). The total flow rate of each contaminant out of each vault sector is calculated by the vault model (Section 3) and is transferred to the source nodes in the geosphere model.

A set of 4 nodes (N3, N6, N8, and N13) represents the locations where transport pathways from the repository through the geosphere emerge at groundwater discharge areas in the biosphere. The node N7 is the location where a well intersects the low-dipping fracture zone and the well discharges through node N8. Discharges may be to an aquatic body such as a stream or a lake, to a groundwater supply well, to the base of the unsaturated zone of a terrestrial area, to a wetland area such as a marsh or bog, or directly as a gas to the atmosphere. The flow rates of contaminants that reach these different discharge areas are transferred to the biosphere model (see Section 5).

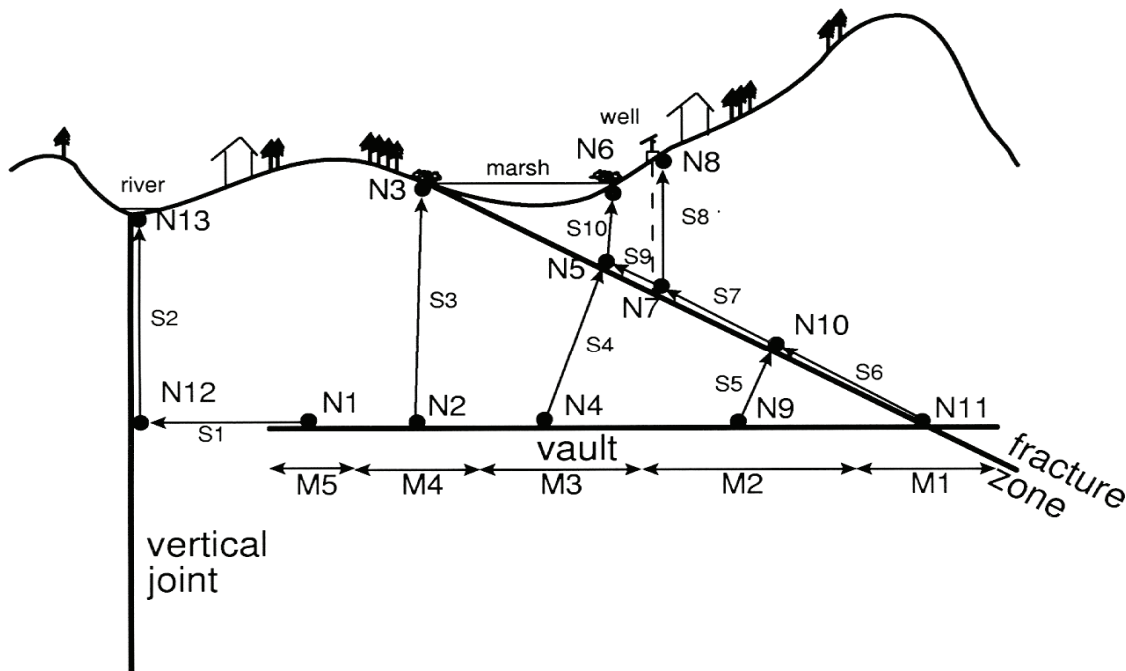


Figure 4.2: A schematic example of a CC4/GEONET representation of a two-dimensional geosphere model (surface relief exaggerated)

The transport segments of the model network are placed to coincide with the main pathways that contaminants would follow if released from the repository. These would be identified from groundwater flow and transport simulations with other more detailed geosphere models. If only groundwater flow simulations are used, then care must be taken with regions with very low groundwater flow velocities. In these regions, contaminant transport is dominated by diffusion rather than by advection, and the transport network segments should reflect the direction of maximum concentration gradient, representing the shortest diffusion pathways to regions where the permeability and groundwater flow are significantly higher.

The transport network is defined by a set of Cartesian nodal coordinates and a table of connectivities defining which segments connect which pair of nodes. Transport segments can either converge or diverge at nodes. If segments converge, their output is summed before being used as input to the succeeding segment. If segments diverge, the output of a segment is fractionated, and a portion is used as input to each succeeding segment.

Each segment of the network has specific physical, chemical and hydraulic properties that reflect the conditions determined by site evaluation studies. The principal segment properties used in the model are depicted in Figure 4.3. Each segment of the transport network is assigned constant physical and chemical properties, so that analytical solutions can be used to simulate the transport of contaminants along the transport segment. However, properties can vary from segment to segment along the transport pathway, and they can also be different for different geosphere states, e.g., the permafrost and ice sheet states of a glacial cycle (Garisto et al. 2010).

The physical properties of the segments are the porosity, tortuosity, and several parameters used to simulate fracture flow with diffusion into the rock matrix. The latter parameters are used only if matrix diffusion is invoked as a transport process (otherwise an equivalent porous medium model is assumed). The chemical properties of the segments are the mineral composition, groundwater salinity, colloid concentration, and geosphere retardation coefficient for each element. The hydraulic properties of the segment include the longitudinal dispersivity, and either the axial permeability, hydraulic conductivity or groundwater velocity.

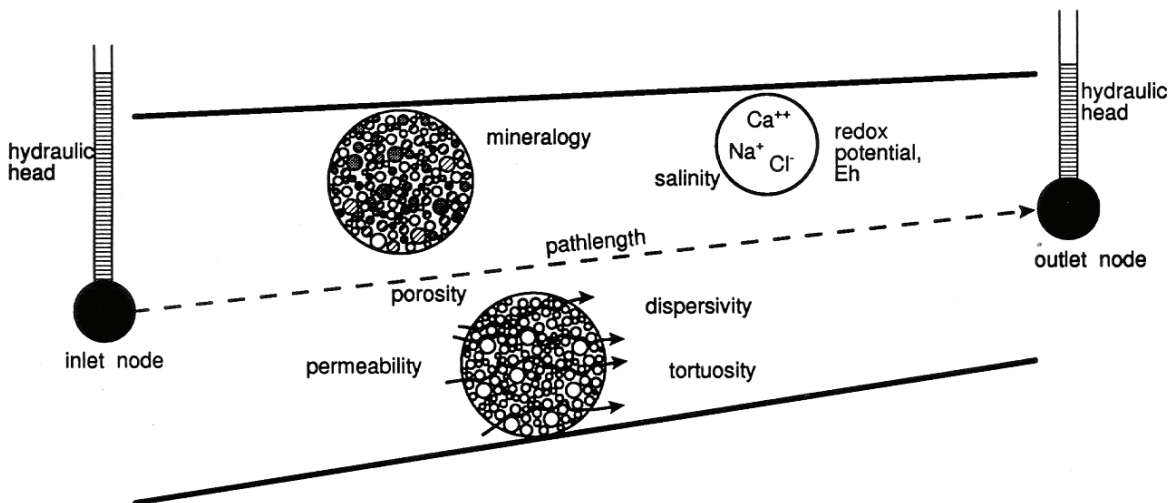


Figure 4.3: Illustration of the principal properties of a transport segment

In the geosphere model, three nodes are required to represent a pathway that could emerge at an aqueous, terrestrial or wetland discharge area. The three nodes are illustrated in Figure 4.4. One node is the actual discharge point and two other nodes define the positions of the lowest extents of the compacted sediment layer and the overburden layer that might exist at these discharge areas. These two nodes are located directly under the discharge node. The two extra layers have specified thicknesses and replace a portion of the last transport segment leading to the discharge area. These layers of surface deposits may not have been included in the detailed groundwater model, since they are relatively thin and do not affect the overall flow of groundwater from the repository to the discharge area. However, they are explicitly added to the geosphere network model since they have chemical and sorption properties very different from the rest of the geosphere pathways through the rock, and they do affect the transfer of contaminants to the biosphere.

The biosphere model (Section 5) discusses two layers of sediment - "mixed" or "bioturbated" sediment and "compacted" sediment. The interface between the geosphere and biosphere models is at the interface of these two sediment layers. The compacted sediment layer is considered to be part of the geosphere model. All references to "sediment" or "the sediment layer" in this section on the geosphere model are to the layer referred to as "compacted sediment" in the biosphere model. Other details of these two layers are described later in Section 4.8 describing the interface between the geosphere and biosphere models.

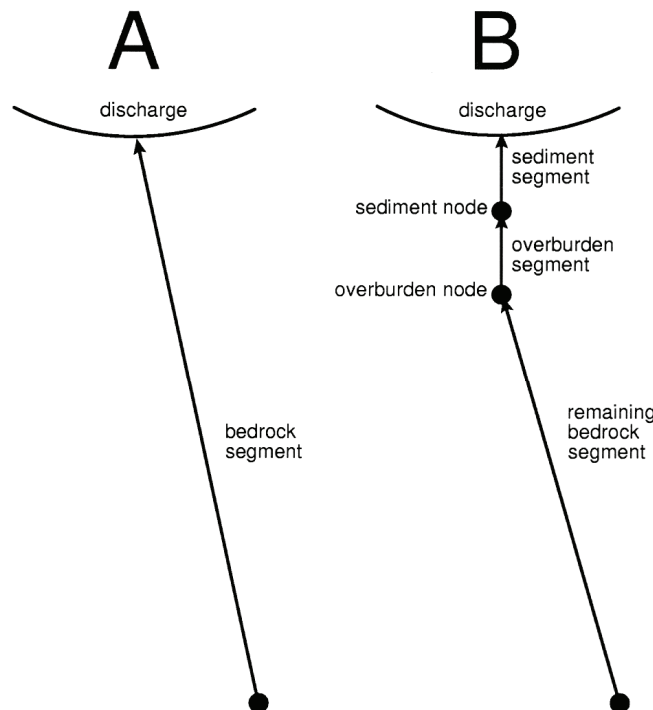


Figure 4.4: Illustration of the insertion of sediment and overburden layers. Figure (A) shows a transport segment passing through a layer of bedrock leading to a discharge. Figure (B) shows the introduction of nodes added to define sediment and overburden layers in the geosphere transport network

A groundwater supply well is defined in the geosphere transport network by a set of six nodes, as shown in Figure 4.5. Two of the nodes are reference nodes, which may or may not be a part of the transport network; these define the orientation and position of the central groundwater flow line to the well. The other four nodes are part of the transport network. One node, the well discharge node, is located at the ground surface and the other three nodes are located in the aquifer from which the well draws its water. One of these three nodes is the actual well node in the aquifer; the other two, called drawdown nodes, define two short segments leading to the well and are placed at specified distances from the well node in the aquifer. These two drawdown nodes are used to represent the shape of the hydraulic head drawdown created near the well by pumping. These two reference nodes define the central groundwater flow line passing through the well.

This set of well nodes is connected to the rest of the transport network through one or more well capture nodes that collect the contaminants moving from other parts of the network and lead them to the well. The positions of four nodes (the well discharge node, the well node in the aquifer, and the two drawdown nodes) are adjusted to give the required depth for the well that is the required vertical distance between the well node at the surface and the node representing the intersection of the well with the aquifer. The well node in the aquifer is moved along the central flow line and the well discharge node is located at the ground surface vertically above. Transport up the well segment is assumed to be instantaneous. The well model is described in more detail in Section 4.4, and by Chan and Nakka (1994).

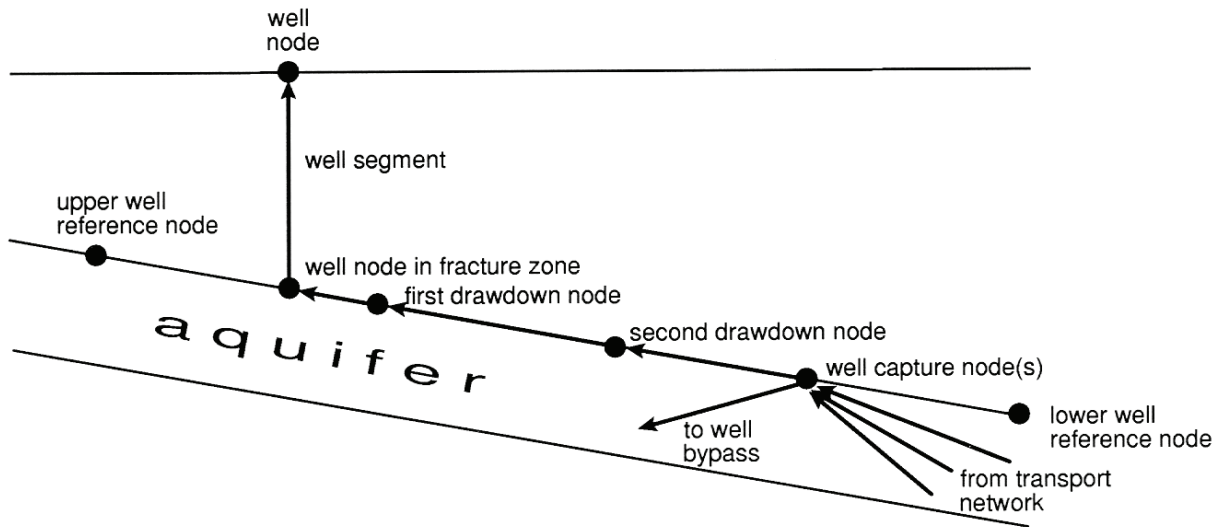


Figure 4.5: Schematic illustration of a vertical cross-section through the well reference nodes

4.3 TRANSPORT MODEL

4.3.1 Transport Equation

The mathematical equations describing radionuclide transport in the segments of the transport network are a set of 1-D mass-balance partial differential equations for a decay chain of length n (von Wicke 1939, Lapidus and Amundson 1952, Lester et al. 1975, Heinrich and Andres 1985, LeNeveu 1987). These equations include the processes of advection, dispersion, linear sorption (retardation), and radioactive decay. The equation for one nuclide of a decay chain is

$$R_q \frac{\partial C_q}{\partial t} = D \frac{\partial^2 C_q}{\partial \zeta^2} - U \frac{\partial C_q}{\partial \zeta} - R_q \lambda_q C_q + R_{q-1} \lambda_{q-1} C_{q-1}, \quad \text{for } q = 1, n \quad (4.1a)$$

where:

- U = average linear groundwater flow velocity [m/a],
- D = dispersion coefficient [m²/a],
- R_q = retardation factor for nuclide q [-],
- λ_q = radioactive decay constant for nuclide q [a⁻¹], and,
- C_q = concentration in groundwater of nuclide q [mol/m³].

The independent variables are time, $t > 0$, and a single linear spatial coordinate, ζ , measured along the axis of the transport segment. The term on the left-hand side is an accumulation term, in which the retardation factor R_q accounts for equilibrium linear sorption of the nuclide with the adjacent solid rock matrix. The successive terms on the right-hand side of Equation (4.1a) represent dispersive transport, advective transport, radioactive decay of nuclide q , and ingrowth of nuclide q from decay of its chain precursor nuclide $q-1$.

In order to obtain a simple analytical solution to Equation (4.1a), all other parameters are assumed to be constant (i.e., independent of time and spatial coordinate) throughout each transport segment. However, the parameters may take on different values in different segments to represent the spatial variation in the site.

4.3.2 Transport Calculation Using Response Functions

The expression for the contaminant flow rate out of a transport segment in response to an impulse input of contaminant into the segment is called a response function. The response function, $G_{pq}(t)$, is defined as the mass flow rate of a nuclide q out of the segment that corresponds to an impulse source of a chain precursor nuclide p at the inlet of the segment at $t=0$. The nuclide p is not necessarily the immediate parent of nuclide q ; it can be any of the chain precursors or even the nuclide q itself.

Analytical solutions exist for the response function for certain cases of interest. For semi-infinite domains with impulse sources, Equation (4.1a) and its boundary conditions can be transformed so that it uses flux or mass flow rate of contaminant, J_q , instead of concentration of contaminant, C_q , as a dependent variable (Davison et al. 1994, Heinrich and Andres 1985).

The mass flow of contaminant is carried in the water phase only and so the mass flow across a boundary b of cross sectional area S orthogonal to the groundwater flow direction and having porosity ϵ , is given by:

$$J_q = S\varepsilon \left(UC_q - D \frac{\partial C_q}{\partial \zeta} \right)_b \quad (4.1b)$$

The first term in Equation (4.1b) is the flow due to advection of the water and the second term is due to diffusion/dispersion. The negative sign indicates the positive dispersion flow rate is in the direction of negative concentration gradient; that is, from higher to lower concentration.

To calculate the time-dependent mass flow rate of nuclide q exiting from a segment of the geosphere network as a result of a general time-varying input of nuclide precursor p , $I_p(t)$, the response function for the segment, $G_{pq}(t)$, is convoluted with the input mass flow rate. The contributions from all decay chain precursors are summed to give the total mass flow rate out of the segment of nuclide q , $O_q(t)$, where

$$O_q(t) = \sum_p \int_0^t I_p(t') G_{pq}(t-t') dt' \quad (4.2)$$

t' is the time of integration, and p takes values from 1 to q .

4.3.3 Boundary Conditions

The form of the response function solution to Equation (4.1), $G_{pq}(t)$, depends on the boundary and initial conditions. Three different analytical response functions have been developed for use in the CC4 geosphere model. These response functions can be chosen independently for each transport segment of the network:

1. semi-infinite medium response function (Heinrich and Andres 1985),
2. mass transfer coefficient response function (LeNeveu 1987), and
3. zero concentration boundary condition response function (Garisto and LeNeveu 1991, Johnson et al. 1994).

The differences in the boundary conditions for these three cases are illustrated in Figure 4.6.

In some places in the geosphere network, contaminant flow is passed unchanged from the inlet to the outlet of a segment. This transfer is formally counted as a fourth response function:

4. dirac delta function response where contaminant flow is passed unchanged from inlet to outlet, that is, $O_q(t) = I_q(t)$.

Two other solutions to Equation (4.1), described in Section 4.3.4, are called response functions 5 and 6 and are used when simulating changes in a geosphere state. Strictly speaking, these two extra solutions are not response functions but it is convenient to label them as such.

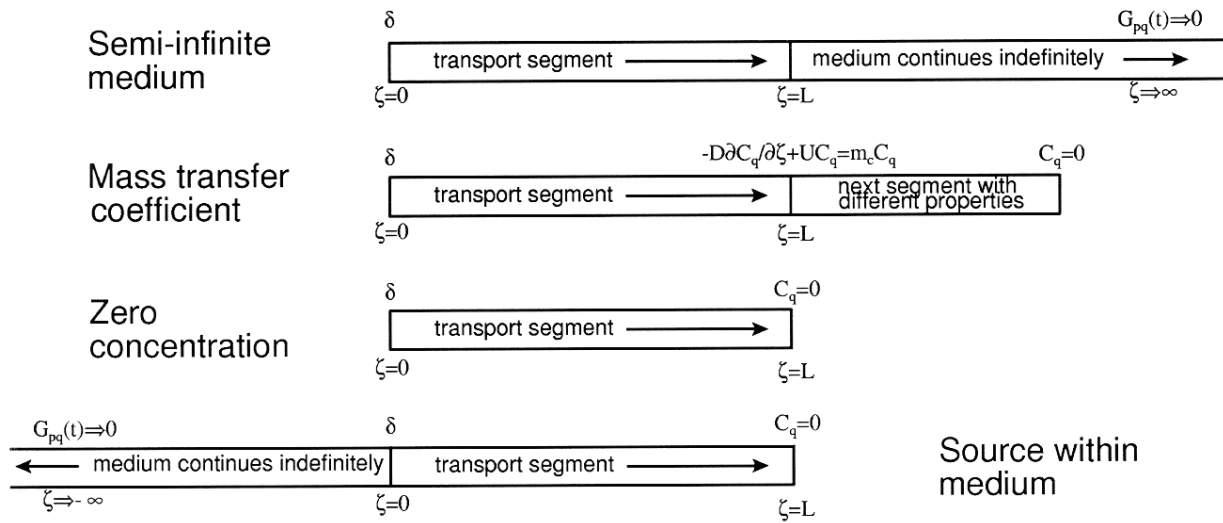


Figure 4.6: Illustration of the boundary conditions for which response functions have been developed for use in transport of contaminants across 1-D segments

The choice of which response function to use for any particular transport segment depends on the boundary conditions for that particular segment. These boundary conditions differ at the segment outlet, but all are based (by definition of “response function”) on the same unit impulse boundary condition at the segment inlet, $\zeta = 0$, expressed here with flow of contaminant as the dependent variable:

$$J_q(t) = \begin{cases} 0 & \zeta = 0, q \neq p \\ \delta(t - t_o) & \zeta = 0, q = p \end{cases} \quad (4.3)$$

where $\delta(t - t_o)$ is the Dirac delta function and t_o is the time of the impulse of a parent nuclide p (not necessarily the immediate precursor of nuclide q), usually taken to be $t_o = 0$.

For those segments of the network where advective transport dominates, the semi-infinite medium response function is recommended. This response function is based on the assumption that the transport segment extends infinitely far from the inlet boundary, with the outlet boundary condition

$$J_q(t) = 0, \quad \text{for all } t, \quad \zeta \rightarrow \infty \quad (4.4)$$

Since we have a finite segment, the response function is evaluated at $\zeta = L$, giving the mass flow rate of nuclide q passing a plane within this semi-infinite transport segment at distance L from the inlet boundary.

Response functions based on mass transfer coefficients are appropriate choices for those transport segments in which the transport is not advection dominated, and which do not originate at the contaminant source location at the repository. The mass transfer coefficient

response functions apply to a finite transport segment with outlet boundary at distance L from the inlet boundary. At the outlet boundary, the condition

$$-D \frac{dC_q}{d\zeta} + UC_q = m_c C_q, \text{ where } \zeta = L \quad (4.5)$$

applies where m_c is the mass transfer coefficient. In this case, Equation (4.1) is solved with the contaminant concentration as the dependent variable and the mass flow rate of contaminant at the outlet boundary is obtained from $J_q = m_c C_q$.

The mass transfer coefficient m_c used in Equation (4.5) depends on the properties of the media on both sides of this boundary and is determined from a formula based on one developed and described in the vault model report (Johnson et al. 1994). If m_c approaches zero, the medium on the other side of the outlet boundary becomes very resistant to the passage of nuclides, and the contaminant flow rate out of the transport segment approaches zero. If m_c becomes large, the contaminant flow rate out of the transport segment approaches an asymptotic maximum where mass flow across the outlet boundary is limited only by the transport properties of the segment itself and is not affected by the properties of the medium on the other side of the boundary. This condition is equivalent to having a zero concentration (i.e., a large sink for nuclides) on the other side of the boundary, and is used for the third response function.

For the transport segments originating at the repository, a third physical situation must be considered. This situation has an impulse source term at $\zeta = 0$, not at a boundary of the transport medium, but within the transport medium itself. The transport medium is assumed to extend to infinity on one side of the source and to a finite distance L on the other side. At the outlet boundary of the transport segment, at distance L from the source, a zero concentration boundary condition applies. The complete solution to the transport equation for this case is different from the solution for the other cases. However, the analytical expression for the response function for nuclide mass flow rate crossing the outlet boundary at $\zeta = L$ is the same as that for the response function for nuclide mass flow rate crossing a plane at $\zeta = L$ in the semi-infinite transport segment case described above (Davison et al. 1994). Hence, for this physical situation, the semi-infinite medium response function can also be used. This case applies to all transport segments originating at the repository and having an outlet at a location where there is increased permeability and groundwater flow, such as at a fracture zone.

In all cases the response function gives the mass flow rate of a contaminant at position $\zeta = L$ in response to an impulse source of contaminant at $\zeta = 0$. The impulse source is denoted by the symbol δ in Figure 4.6. The response function for the fourth case "Source within medium" can be shown to be mathematically equivalent to the first case "Semi-infinite medium".

4.3.4 Response Functions for Time Dependent Parameters

Some properties of the geosphere could change with time. For example, a permafrost and ice sheet state in a glacial cycle could have profound effects on transport pathways within the geosphere. The geosphere transport calculation methodology described above using response functions requires that parameter values be held constant (i.e., independent of time) and that the transport path have zero inventory of contaminant at the start of the calculation. An approach that permits time-dependent parameter values is to implement the transport calculations using a linearly coupled set of compartment models. This approach is similar to

that employed by some other transport codes, such as AMBER (Quintessa 2009), which handle time dependent parameter values through time stepping. Using transport modelling with a series of well-mixed compartments is an approximation that increases numerical dispersion, but some multi compartment modelling documentation (Quintessa 2009) suggests that using 5 to 10 linearly coupled compartments is sufficient for adequate representation of transport.

The introduction of a coupled set of compartments for geosphere transport is done as an additional “response function” implemented in a general way and available for use in any segment of the geosphere transport network, similar to the use of the four response functions described in the previous section. A loop over states is handled internal to the response function transport calculation over each segment. At the end of each state, the contents of each compartment are saved and used as the initial amounts in the compartment for the next state, where the transport calculation is done with a different set of values for the transport parameters. In each state the transport parameters have constant values for the duration of the state. This loop allows for time dependent changes to parameter values in a stepwise constant way.

4.3.4.1 Inter-Compartment Transfers

For this compartment model based response function, the inter-compartment behaviour is driven by the fractional loss rate, Λ_q , from the donor compartment,

$$\Lambda_q = J_q/A_q \quad (4.6)$$

where A_q is the total amount of contaminant in the donor compartment and, as before, J_q is the flow rate of contaminant, in this case from the donor compartment to the next compartment in the linearly coupled set. From Equation (4.1b), advective transport is governed by the forward rate of water flow between compartments and dispersive transport depends on the difference in amount/concentration in neighbouring compartments. Hence, the dispersive transport is divided into a forward portion and a backward portion, each donor driven by its corresponding compartment (this is analogous to the way of treating dispersive transport in AMBER). Consequently the transport between the neighbouring compartments has both an advective and a dispersive portion in the forward direction and a dispersive portion in the backward direction.

Consider each compartment to have volume V ; that is, a finite well-mixed volume of a rectangular shape with cross-sectional area S orthogonal to the water flow direction ζ and length $\ell = L/m$ in the direction of water flow where m is the number of linearly coupled compartments used in the representation of the segment. The contaminant flow rate from the compartment due to advective flow of the groundwater, whose well-mixed average concentration is C_q , is given by the first term in Equation (4.1b):

$$J_q^{adv} = S\varepsilon UC_q \quad (4.7)$$

Since the total amount of contaminant in the compartment is

$$A_q = R_q\varepsilon VC_q \quad (4.8)$$

then, the fraction loss rate from the compartment due to advection is

$$\Lambda_q^{adv} = U/R_q\ell \quad (4.9)$$

Considering the diffusion contribution from Equation (4.1b)

$$J_q^{disp} = -S\varepsilon D \frac{\partial C_q}{\partial \zeta} \quad (4.10)$$

For the compartment model approach, the derivative is calculated using the finite difference approximation

$$\frac{\partial C_q}{\partial \zeta} = \frac{\Delta C_q}{\Delta \zeta} = \frac{(C_q - C_{q+1})}{d} \quad (4.11)$$

where C_q is the mean concentration in the compartment under consideration and C_{q+1} is the mean concentration in the adjacent downstream compartment and d is the distance over which this concentration difference applies, generally taken as the distance between the mid-points of the two compartments.

The flow rate due to diffusion expressed by these two equations is a net diffusion flow rate, the result of two competing processes: the flow rate out of compartment q into compartment $q+1$ and a return flow rate from compartment $q+1$ back to compartment q . In a compartment model, the net diffusive flow is separated into its two competing processes. The flow from compartment q to $q+1$ is expressed as

$$J_{q \rightarrow q+1}^{disp} = S\varepsilon D \frac{C_q}{d} \quad (4.12)$$

and similarly the return flow rate from compartment $q+1$ to q is

$$J_{q+1 \rightarrow q}^{disp} = S\varepsilon D \frac{C_{q+1}}{d} \quad (4.13)$$

Hence, from Equations (4.6), (4.8), and (4.12) the fractional diffusive loss rate from the compartment q is

$$\Lambda_q^{disp} = \frac{SD}{R_q V d} = \frac{D}{R_q \ell d} \quad (4.14)$$

Equation (4.14) is also applied to compartment $q+1$, which has a mean concentration C_{q+1} , to determine the corresponding fractional loss from compartment $q+1$ back to compartment q and the net diffusive flow rate results from the difference between the two.

4.3.4.2 Boundary Conditions and Segment Release

Boundary conditions affect dispersive/diffusive transport, since it depends on the properties of two adjacent compartments. The advective transfer rates are always given by Equation (4.9). If the adjacent compartments are the same size and have the same properties, as in the CC4

representation, then there is no inherent boundary condition approximation (only the inherent approximation due to the discretization) and, in addition, in Equation (4.14)

$$d = \ell \text{ (same size compartments)} \quad (4.15)$$

The breakup of the net flow rate, Equation (4.10), into two portions: forward and back rates given by Equations (4.12) and (4.13), gives two parts that are intended to represent parts of the same physical process and in these two equations only the concentration terms C_q and C_{q+1} are different.

In the multi-compartment model for a transport segment, an extra boundary compartment is added. The flow rate out of the segment is taken to be the flow rate into the boundary compartment. One option implemented is to consider the boundary compartment to have the same size and properties of its adjacent segment and Equation (4.14) with (4.15) is applied unchanged. In this case, the transport medium is assumed to continue unchanged, analogous to the analytical boundary condition where the medium is considered to be semi-infinite in extent. Another approach is to consider there to be a zero concentration boundary, so that Equations (4.10) and (4.11) are exactly equivalent to Equation (4.12) (C_{q+1} is zero) and can be directly applied. However, since the zero concentration is at the compartment boundary, the distance to the zero concentration boundary is taken to be $\frac{1}{2}$ the size of the compartment so that

$$d = \ell/2 \text{ (zero concentration boundary)} \quad (4.16)$$

If a compartment is directly coupled to an adjacent compartment with different properties, then the properties of the two media need to be averaged in some way so that the coefficients in Equations (4.12) (4.13) and (4.14) are the same for both the forward and the reverse transport rates. The only difference in these two rates is the difference in the concentration driving force.

4.3.4.3 Zones of impermeability and their effects on transport

Water movement and contaminant transport can be significantly smaller in areas associated with limited permeability. Zones of low permeability can occur, for example, in areas with permafrost or frozen ground, desert environments associated with the effects of drying out, and as a result of an engineered impermeable cover. There also can be open pathways through such areas, such as an open talik (an unfrozen zone in a permafrost layer) and an oasis.

A segment is considered to be within a zone of impermeability if the majority of its length lies within the zone. If a transport segment becomes impermeable, then all water and contaminant movement ceases. Both the advective and diffusive transfer rates are set to zero. Hence, there is no release from the final compartment to the boundary compartment. Segments that are part of an open pathway passing through the impermeability zone retain their normal advective and diffusive transfer rates.

If a transport segment terminates at an impermeability zone, where the next transport segment is impermeable, then the releases from the last compartment to the boundary compartment are set to zero. In addition, the advective transport rates in the segment are set to zero, regardless of the groundwater velocity determined as described in Section 4.3.5.1, but normal diffusion processes take place, redistributing the contaminants within the segment.

In some instances a flow path can be split into two segments, one of which is associated with a talik, i.e., an open pathway, and the other segment might lie within an impermeable zone. In this case, a normal transport segment would lead through the open pathway and, hence, does not have zero releases assigned to its boundary and the next segment. The impermeable segment will accept contaminant releases into its first compartment; however, the contaminants will remain within this compartment for the duration of the condition of impermeability.

4.3.4.4 Compartment Sink

In the multi-compartment model for a transport segment, another extra compartment is added as a sink (which has no return flow to the other compartments) to the end of each set of segment compartments to keep the accumulated amount in the boundary compartment from increasing without end. The transport with the sink has NO backward component; hence the forward portion of the dispersive transport (i.e., into the sink) is also dropped for consistency. Hence the sink compartment has only a forward advective transport component into the sink. However, if there was zero advective flow rate, then there would be no transport into the sink compartment at all. In this rare case, the forward dispersion rate is applied to provide a slow transport into the sink.

4.3.4.5 Multi-Compartment Model Summary

In summary, the multi-compartment geosphere model represents a section of the flowpath as a series of linear linked compartments. The model includes an extra compartment to act as the boundary for the segment, at which the boundary condition can be applied. Two response functions, #5 and #6, are implemented using the multi-compartment model. The boundary compartment for response function #5 is given the same properties as the other sub-compartments, thus acting as if the current segment extends further, analogous to the semi-infinite medium response function #1. Response function #6 is similar but implements a zero concentration boundary, analogous to response function #3. Additional multi-compartment model based response functions could be added; for example, a condition that more completely couples the transport to the properties of the next transport segment, analogous to response function #2, could be made for the boundary compartment.

4.3.5 Parameters in the Transport Equation

4.3.5.1 Groundwater Velocity

The groundwater flow field is not determined in CC4/GEONET itself. Rather, the groundwater flow information is obtained from results calculated externally. Values for parameters such as porosity and permeability, on which these results depend, are also used by CC4/GEONET, and hence the groundwater flow continuity and mass balance conditions inherent in these results are preserved in this geosphere transport model. A scaling factor, which modifies all velocities in the flow field, may be applied to the determined velocities. The state-dependant scaling factor is used to apply variability to the overall flow field or segment by segment to give modified flow fields for different time dependent states.

Average linear groundwater velocities, U , one for each segment, are determined by one of six possible methods. In the cases where constant groundwater properties are assumed for the entire transport network, a fixed density and viscosity for the water, corresponding to fixed reference values for the temperature and pressure, are used. For example, at a reference

temperature of $T_r = 6^\circ\text{C}$ and pressure of 0 MPa (gauge), the density of water is $\rho_r = 1000 \text{ kg/m}^3$, and the viscosity of water is $\mu_r = 0.001472 \text{ kg/m}\cdot\text{s}$. The six methods are as follows.

1. Average linear velocities, U , are supplied directly for each segment.
2. Specific discharges (Darcy velocities), q , are supplied for each segment. Average linear groundwater velocities, U , are then calculated from

$$U = q/\varepsilon \quad (4.17)$$

where ε is the porosity of the segment.

3. Reference hydraulic heads, h , are supplied for each node and hydraulic conductivities, K , are supplied for each segment. Average linear groundwater velocities for each segment are then calculated from Darcy's law, and from Equation (4.17)

$$q = K\Delta h/L \quad (4.18)$$

where Δh is the difference in hydraulic head between the inlet and outlet nodes of the segment; L is the geometric length of the segment; and K the hydraulic conductivity is assumed to be constant within the segment.

4. Reference hydraulic heads, h , are supplied for each node, and intrinsic permeabilities, k_ζ , are supplied for each segment. Average linear groundwater velocities for each segment are calculated as above, Equations (4.17) and (4.18), where the hydraulic conductivities for each segment are calculated using a reference viscosity, μ_{ref} and reference density ρ_{ref} , for the groundwater consistent with the reference heads:

$$K = k_\zeta \rho_{ref} g / \mu_{ref} \quad (4.19a)$$

where g is the acceleration due to gravity.

5. Reference hydraulic heads, h , and temperatures, T , are supplied for each node, and intrinsic permeabilities, k_ζ , are supplied for each segment. Average linear groundwater velocities for each segment are calculated as above, Equations (4.17) and (4.18), where the hydraulic conductivities for each segment are calculated using the viscosity μ and density ρ of the groundwater in each segment.

The viscosity and density of the groundwater in the segment is calculated from the equations of state for water using the temperature, T , and excess pressure, ΔP , calculated from the elevation of the midpoint of each segment. The viscosity as a function of temperature is given by an empirical equation (Davison et al. 1994)

$$\mu = \mu_A \exp [\mu_B/(273+T)] \quad (4.19b)$$

where μ_A and μ_B are constants, and the density as a function of temperature and pressure is also given by an empirical equation (Davison et al. 1994)

$$\rho = \rho_0 [1 + \beta_w \Delta P + \rho_A(T - T_0) + \rho_B(T - T_0)^2] \quad (4.19c)$$

where ρ_0 is the density of water at a reference temperature T_0 and pressure $p_0 = 0$ MPa (gauge); β_w is the compressibility of the groundwater, ρ_A and ρ_B are empirical constants, and the pressure excess is given by

$$\Delta P = p - p_0 = (h - z) \rho_{ref} g - p_0 = (h - z) \rho_{ref} g \quad (4.19d)$$

where z is the elevation.

6. Reference hydraulic heads, h , and temperatures, T , supplied for each node, and intrinsic permeabilities, k_{ζ} , supplied for each segment. Average linear groundwater velocities for each segment are determined in this case with the gravitational buoyancy effects implemented. The hydraulic conductivities for each segment are calculated using the viscosity, μ , obtained from Equation (4.19b) and the same reference density, $\rho = \rho_{ref}$, of the groundwater as in the definition of the reference hydraulic head using Equation (4.19a). The specific discharge or Darcy velocity is determined from:

$$q = K[\Delta h/L + (\Delta\rho/\rho_{ref})\Delta z/L] \quad (4.19e)$$

where Δz is the change of elevation from inlet to outlet of the segment and $\Delta\rho = (\rho - \rho_{ref})$;

In cases 1 and 2, the well drawdown nodes, described in Section 4.2, are not inserted into the transport network and the well is defined by only 2 nodes. In cases 3 to 6, the heads are modified by the groundwater pressure drawdowns caused by the presence of the well before the velocities are calculated (see Section 4.4).

The hydrogeological data and the resulting calculated hydraulic heads are obtained from the detailed groundwater flow modelling, and they cannot be varied randomly in the network model. They must have exactly the same values as those used in the external calculations. If they had different values, the connection with these detailed groundwater flow calculations, from which the heads and velocities were obtained, would be lost, and mass balance of the groundwater flow within the entire groundwater flow system would not necessarily be maintained.

4.3.5.2 Dispersion Coefficient

A longitudinal dispersion coefficient, D , for each nuclide in each transport segment is determined from the sum of a mechanical dispersion term and an effective diffusion term:

$$D = a_L U + D_0 \tau \quad (4.20a)$$

where τ is the tortuosity factor of the diffusive transport path along the axis of the segment, D_0 is the molecular diffusion coefficient in free water for the nuclide, and the longitudinal dispersivity or dispersion length a_L is given as a multiple of the segment length

$$a_L = f_{aL} L \quad (4.20b)$$

However, if U is negative; that is, the direction of the groundwater velocity is opposite to the direction of transport under consideration, then no mechanical dispersion term contributes to the transport in this direction. Under this condition, the hydrodynamic dispersion is composed of diffusion against the direction of the groundwater flow only:

$$D = D_0 \tau \quad (4.20c)$$

The analytical solution to the coupled equations for nuclides in decay chains requires a single dispersion coefficient for each segment that applies to all nuclides in the chain. In this model, the value determined for the first member of the chain is used for all chain members. When the mechanical dispersion term, $a_L U$, dominates the dispersion, the dispersion coefficient has the same value for all chain members anyway. When the diffusion term dominates, the diffusion coefficients for the actinide elements in decay chains, Am, Np, Pa, Pu, Ra, Th, and U, with similar atomic masses, have about the same value. Hence, using a single value for dispersion coefficient for all members of a decay chain is a good approximation.

4.3.5.3 Retardation Factors

Retardation factors due to sorption are calculated using empirical equations, depending on mineralogical properties and chemical state of each transport segment. More details of the sorption model are given by Davison et al. (1994) and Vandergraaf et al. (1993). Only the final equations of the model are summarized here. Retardation effects are determined for each element in each transport segment.

The distribution coefficient K_d for each element is calculated from a general equation

$$K_d = [b_0 + b_1 X_1 + b_2 X_2 + b_{11} X_1^2 + b_{22} X_2^2 + b_{12} X_1 X_2] \Omega(r_1, b_3) \quad (4.21)$$

where the coefficients b_i are dependent on element, mineral and chemical state. (This variable is frequently written as K_D^i below to more clearly show its dependence on contaminant or nuclide i . More precisely, distribution coefficients are actually dependent on chemical elements, so if two contaminants i and j are isotopes of the same element, $K_D^i = K_D^j$.) The chemical state is treated as either oxidizing or reducing. The location along the flow path where the redox potential Eh switches over from reducing to oxidizing is determined by the elevation of a redox divide within the geosphere. Transport segments below the redox divide are considered to be reducing; segments above the divide (i.e. closer to surface) are oxidizing.

The possible effect of salinity on sorption is treated explicitly through variable X_1 , the logarithm of the groundwater salinity in the transport segment. The salinity is expressed as total dissolved solids (TDS) in units of g/L,

$$X_1 = \log_{10}(TDS) \quad (4.22)$$

The possible effect of nuclide concentration is treated explicitly through variable X_2 , the logarithm of the nuclide concentration, C_q , in the groundwater of the transport segment solution in units of mole/L,

$$X_2 = \log_{10}(C_q) \quad (4.23)$$

The uncertainty in the distribution coefficient is represented through the function

$$\Omega(r_1, b_3) = (r_1)^{b_3} \quad (4.24)$$

where r_1 is a loguniform distributed random number which lies in the range [0.1, 10.]. With this choice of r_1 , the coefficient b_3 is the number of orders of magnitude over which K_d is allowed to vary, with the bracketed expression in Equation (4.21) giving the geometric mean value for K_d .

The distribution coefficient can depend on nuclide concentration, notably at high concentrations. However, at the low concentrations relevant to a deep geologic repository, it is normally independent of concentration. Since the semi-analytic solution used for transport across segments requires retardation factors that are constant in space and time, the generally small dependence of sorption on nuclide concentration is treated as an additional source of uncertainty in the sorption model by pre-defining a nominal range in nuclide concentration, C_q . This is expressed in a similar manner to Equation (4.24).

$$C_q(r_2, b_4, b_5) = b_4(r_2)^{b_5} \quad (4.25)$$

where r_2 is a random number, similar to r_1 , from a loguniform distribution over the range [0.1, 10]. Coefficient b_4 gives the geometric mean value about which the nuclide concentration is varied, and coefficient b_5 , similar to b_3 , is the number of orders of magnitude over which the nuclide concentration is varied about this mean.

For a given media, the retardation factor is then related to its distribution coefficient by

$$R = 1 + b_6 K_d \quad (4.26)$$

where b_6 is a normalization factor [m^3/kg] that represents the effective volume for sorption per unit mass. For a porous medium with solid density ρ_s and porosity ε , $b_6 = \rho_s(1 - \varepsilon)/\varepsilon$.

Typically, K_d values are obtained from laboratory experiments with crushed rock, which resembles a porous medium. However, for use in fractured rock transport, a different normalization factor b_6 may be appropriate - Vandergraaf et al. (1993) recommend $b_6 = \rho_s$ if K_d values are from crushed rock tests. For generality, the model requires the user to specify an appropriate value of b_6 .

For a segment containing several minerals, the overall retardation factor is obtained using the weighted fractional abundance, f^m , of each mineral, m , to give an overall retardation factor, R_q , for nuclide q in the segment

$$R = 1 + \sum_m f^m b_6^m K_d^m \quad (4.27)$$

Hence each sorption equation has ten coefficients: the six coefficients in the sorption equation, the order of magnitude for variation of K_d , the geometric mean and order of magnitude for variation of nuclide concentration, and the normalization factor b_6 used to give a retardation factor that is appropriate for the in-situ conditions of the transport segment.

There are some nuclide/mineral combinations for which a detailed sorption equation is unavailable and only a single constant K_d is supplied. In these situations a minimum set of three coefficients is used: the geometric mean value for K_d (coefficient b_0), the order of magnitude for

variation of this value (coefficient b_3), and the normalization factor (coefficient b_6). Equations (4.21) through (4.26) then reduce to

$$R = 1 + b_6 b_0 (r_1)^{b_3} \quad (4.28)$$

4.4 WELL MODEL

4.4.1 Overview

The geosphere network can include a well intersecting a more permeable fracture zone or aquifer.

After the nodes defining the groundwater supply well in the transport network are repositioned to give the required well depth (described in Section 4.2), and the well demand is determined (described in Section 5.2.1), a set of analytical equations is used to determine the effects of pumping the well on the transport of contaminants in the geosphere network.

Wells whose depth is less than the depth to the bottom of the overburden layer are classed as overburden wells. An overburden well is assumed to obtain its groundwater entirely from the overburden layer (described in Section 4.8), although we estimate the capacity of these relatively shallow wells is still given approximately by Equation (4.29) below. We further assume that these wells draw no water from the reference model aquifer, do not affect the groundwater flow field in the bedrock, and do not directly capture any contaminants coming from the repository. The water in these wells is assumed to be contaminated at the same level as lake water.

Wells whose depth places them into the bedrock are of most interest in this model. These are assumed to penetrate a more permeable fracture zone or aquifer in order to be able to extract sufficient water from the typically low permeability rock. The behaviour of these wells is described below.

The analytical equations describing the groundwater supply well model were derived (Chan and Nakka 1994) using complex potential theory and the method of images. The well model assumes that pumping is from a confined aquifer with constant and uniform hydraulic properties. The well is also assumed to be near a constant hydraulic head boundary (for example, a lake) located where the aquifer comes to surface. Initially (i.e., with no well pumping) we assume there is a uniform and symmetric groundwater flow field in the aquifer in the vicinity of the well.

Depending on the well pumping rate, the groundwater flow in the vicinity of the well will be affected. The well model is used to calculate the following four quantities:

1. the maximum well capacity;
2. the drawdowns at nodes in the aquifer, from which new hydraulic heads in the aquifer are determined;
3. the quantity of surface water captured into the well by induced infiltration; and

4. the contaminant capture fractions reaching the well, which determine the quantities of contaminants entering the well water.

The groundwater flow field in the aquifer is assumed to be adequately represented by an idealized, symmetrical flow field. Close to the well, the effect of drawdown on the flow field is greatest and the importance of the model assumption is larger. In regions far from the pumping well, the drawdowns are small and the errors in drawdown due to this approximation are small.

In the geosphere model, the location of the constant head boundary (i.e., where the aquifer plane intersects the surface) is determined approximately from the extrapolation of the central groundwater flow line passing through the well, defined by the upper and lower well reference nodes, to the elevation of the well discharge node located at the ground surface. Figure 4.6 shows a schematic illustration of the location of these nodes.

In the CC4/GEONET well model, the well demand can be scaled by a constant factor to calibrate the behaviour of the analytic well model to that of available detailed models.

4.4.2 Maximum Well Capacity

The well capacity, Q_{cap} , is defined from the analytical well model equations by (Chan and Nakka 1994):

$$Q_{cap} = -2\pi K_f \cdot \beta_f \left[\frac{d_w + q_f L_w / K_f}{\ln(r_w / 2L_w \cos(\alpha))} \right] \quad (4.29)$$

where K_f and β_f are the hydraulic conductivity and thickness of the aquifer, and q_f is the initial specific discharge of the groundwater in the aquifer (i.e., with zero well pumping). In addition, as illustrated in Figure 4.7, d_w is the depth of the well from ground surface, L_w is the distance of the well from the constant head boundary at the ground surface measured along the central flow line of the well, r_w is the radius of the well casing, and α is the angle between the aquifer plane (i.e., following the lower to upper well nodes) and the horizontal plane.

The value determined for well capacity Q_{cap} is passed to the biosphere model. The biosphere model then determines the actual demand, Q_{well} , placed on the well, ensuring that it is less than or equal to this well capacity.

At high pumping rates, in addition to groundwater from within the aquifer, the well can also capture groundwater from the rock mass adjacent to the aquifer in which the well is located. This additional capture is described further in a site-specific context in Section 4.4.6. The amount of groundwater captured from the rock adjacent to the aquifer is assumed to be relatively small in this model, and so it does not affect the well capacity calculated from Equation (4.29).

4.4.3 Drawdowns in the Aquifer

Drawdown in hydraulic head, Δh_d , at the position of each node in the aquifer containing the well, illustrated in Figure 4.7, is calculated from the well position and the node position using the analytical well model as follows (Chan and Nakka 1994):

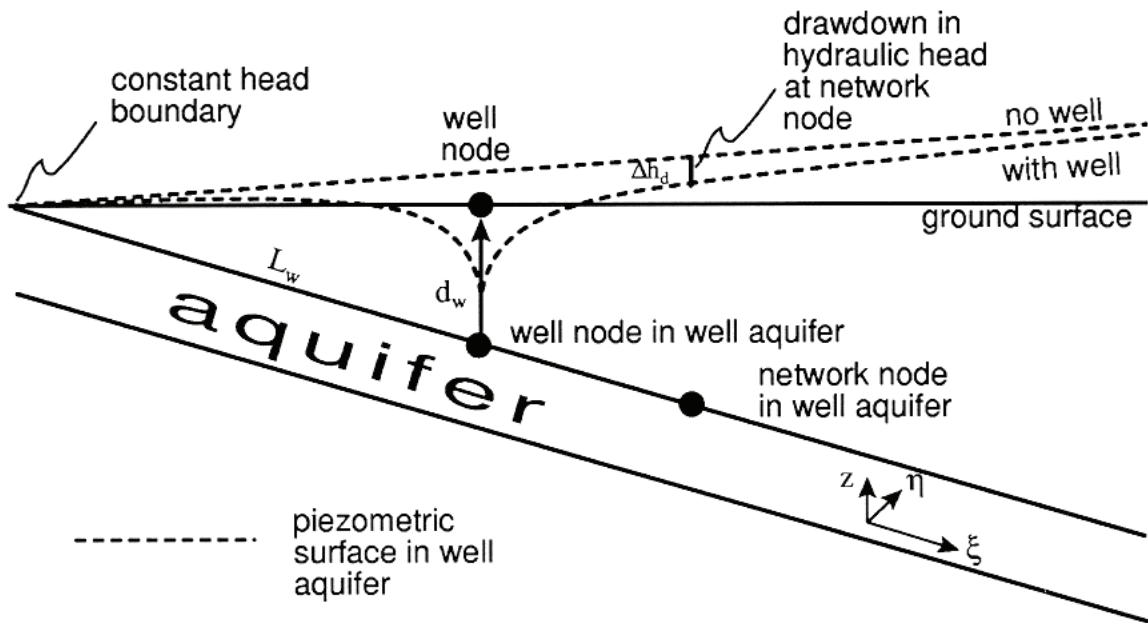


Figure 4.7: Schematic illustration in cross-section of piezometric surfaces in the well aquifer with and without a well present

$$\Delta h_d = \frac{-Q_{well}}{4\pi K_f \beta_f} \ln \left[\frac{(\xi - L_w)^2 + \eta^2}{(\xi + L_w)^2 + \eta^2} \right] \quad (4.30)$$

where Q_{well} is the demand on the well. The coordinates ξ and η are the coordinates of the node position in the Cartesian coordinate system of the analytical well model, illustrated in Figure 4.7. Coordinate ξ is the distance of the node from the constant head boundary at the surface in direction parallel to the central flow line of the well. Coordinate η is the distance of the node from the central flow line of the well in a direction perpendicular to the central flow line.

Equation (4.30) gives positive values for drawdowns, which are then subtracted from the initial reference hydraulic heads to give final reference hydraulic heads used in the groundwater velocity calculations. The initial heads at the three well nodes in the aquifer that were repositioned (Section 4.2) to give the required well depth are obtained by linear interpolation between the initial heads at the upper and lower well reference nodes. Equation (4.30) would give an infinitely large drawdown at the geometric centre of the well where $\xi = L_w$ and $\eta = 0$. For the node defining the intersection of the well with the aquifer, the drawdown is determined at the edge of the well casing, where $\eta = r_w$.

4.4.4 Surface Water Captured

The rate of surface water inflow to the well, Q_{sur} , is determined from the analytic well model based on the well drawdown and on the distance to the constant head boundary at the surface discharge of the aquifer.

No water is captured from the surface if the well demand is less than a critical value, Q_{crt}

$$Q_{crt} = \pi\beta_f q_f L_w \quad (4.31)$$

If Q_{well} is greater than Q_{crt} , then the rate of surface water capture is given by

$$Q_{sur} = \frac{2Q_{well}}{\pi} \tan^{-1} \left[\frac{\eta_c}{L_w} \right] - 2\beta_f q_f \eta_c \quad (4.32)$$

where η_c is the critical distance from the central flow line of the well, measured at the ground surface along the constant head boundary to the dividing streamline, and is given by

$$\eta_c = L_w [Q_{well}/Q_{crt} - 1]^{1/2} \quad (4.33)$$

This pathway from surface to well is not a transport segment of the geosphere transport network, and the model assumes that only diluting (surface) water and not contaminants are captured by the well by this mechanism.

If the aquifer velocity is very small, then Equation (4.32) would imply that all the well water came from uncontaminated surface waters. In fact, the equation does not strictly apply in this case, and so in the model the surface water inflow is set to 50% of the well demand. This is a somewhat arbitrary division, but gives equal weight to the possibility that both surface water and contaminated groundwater can supply the well.

4.4.5 Plume Capture Fractions

The details of the derivations described in this section are given in Chan and Nakka (1994). One or more nodes of the transport network are considered to be well capture nodes. These nodes are placed on a capture line oriented orthogonal to the central flow line passing through the well. This line is located at a distance farther down the dipping aquifer than the deepest well nodes, as illustrated in Figure 4.4. The segments leading from these capture nodes to the first well drawdown node (the well collection node) are assigned widths that represent the widths at the capture line. The envelope of these widths represents the total width of the contaminant plume at this point.

The fraction of contaminants from the repository, moving along pathways in the aquifer, that is captured by the well, is determined from the stream function expression given by the analytic well model. The stream function expression (Equation 4.37 below) is illustrated in Figure 4.8.

It is used to determine the equation of the dividing streamline, i.e., the streamline that passes through the stagnation point resulting from the pumping of the well. Groundwater flow inside this divide travels to the well in the aquifer; groundwater flow outside this divide bypasses the

well and discharges from the aquifer to the surface. The fraction captured at each of the capture nodes is obtained by calculating, from simple geometry, the proportion of the width associated with the segment leading from that node that lies within the groundwater divide, as illustrated in Figure 4.8.

The fraction of the contaminants captured by the well is transported to the well drawdown nodes and then to the well itself. The drawdown nodes are used to give better definition to the drawdown cone in the aquifer in the region near the well. The fraction of the contaminants not captured by the well is transported along well bypass segments to other network nodes for eventual discharge at the ground surface, as illustrated in Figure 4.4.

The stagnation points are locations in the groundwater flow field of the aquifer where the groundwater velocity becomes zero as a result of the well pumping. There are two cases. If $Q_{well} \leq Q_{crt}$, then there exists one stagnation point on the central flow line of the well between the well and the constant head boundary. It has coordinates, (ξ_s, η_s) , in the coordinate system of the analytic well model (described above) given by

$$\begin{aligned} \xi_s &= L_w (1 - Q_{well}/Q_{crt})^{1/2} \quad \text{and} \\ \eta_s &= 0 \end{aligned} \tag{4.34}$$

If $Q_{well} > Q_{crt}$, then there are two stagnation points on the constant head boundary, symmetrically placed about the central flow line. In this case surface water is captured by the well, as described in Section 4.4.4. The coordinates of the stagnation points are

$$\left. \begin{aligned} \xi_s &= 0 \\ \eta_s &= \pm \eta_c \end{aligned} \right\} \tag{4.35}$$

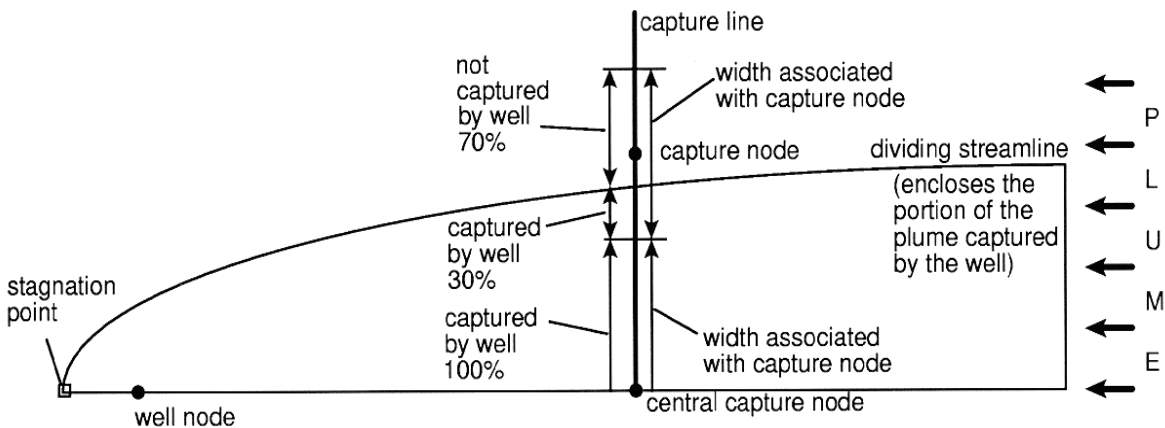


Figure 4.8: Schematic plan view showing capture line, capture nodes and dividing streamline in the aquifer

where η_c is given by Equation (4.33). The dividing streamline is the streamline that passes through the stagnation point(s). The stream function is constant along a streamline, so the equation of the dividing streamline is

$$\psi(\xi, \eta) = \psi(\xi_s, \eta_s) \quad (4.36)$$

where the stream function $\psi(\xi, \eta)$ is given by

$$\psi(\xi, \eta) = c + q_f \eta + \frac{Q_{well}}{2\pi\beta_f} \tan^{-1} \left[\frac{2\eta L_w}{\xi^2 + \eta^2 - L_w^2} \right] \quad (4.37)$$

and where c is an arbitrary constant that determines a particular streamline. The width of the groundwater divide at the well capture nodes is obtained by first finding the value of $\xi = \xi_r$, the distance of the line of well capture nodes from the constant head boundary in the coordinate system of the analytic well model, and then finding $\eta = \eta_r$, to give the point on the groundwater divide streamline with this value of $\xi = \xi_r$. Hence, the transcendental equation

$$\psi(\xi_r, \eta_r) = \psi(\xi_s, \eta_s) \quad (4.38)$$

must be solved for η_r . Having found η_r , the total width of the groundwater divide at $\xi = \xi_r$ is $2\eta_r$.

The contaminant capture is determined separately for each segment leading to the well. For each segment leading from a capture node towards the well, a width is assigned. The capture fraction for each segment is obtained by a geometrical calculation, illustrated in Figure 4.8, of how much of the width assigned to the segment lies inside the $2\eta_r$ width of the groundwater divide streamlines at $\xi = \xi_r$. Each individual capture fraction and the overall capture fraction cannot exceed unity.

Figure 4.9 shows streamlines calculated from the analytic well model, in plan view, for two situations:

- One with a well demand only slightly smaller than Q_{crit} , in which case there is a single stagnation point and an overall capture of about 75% of the contaminant flow paths within the aquifer, and
- One with a well demand greater than Q_{crit} , in which case there are two stagnation points located on the constant head boundary. The entire width of the contaminant plume is captured together with diluting water from outside of the plume and diluting surface water infiltrated from the constant head boundary.

Only the upper half plane is shown in each case in Figure 4.9, since there is a line of symmetry along the well centre line. Hence, the well itself is shown by "o" on the lower axis at $\eta = 0$. The ξ -coordinate depicted is measured along the aquifer from the constant head boundary (at the ground surface). The η -coordinate is measured orthogonal to the central flow line of the well. The dotted line shows the width of the contaminant plume at this location and is the line at which plume capture fraction is determined. The upper figure shows one stagnation point on the well centre line with about 75% plume capture. The lower figure shows two stagnation points (one depicted and a matching one by symmetry). In this case, the well captures 100% of

the contaminant plume, together with diluting water from outside the plume and diluting surface water infiltrated from the constant head boundary.

As in Figure 4.8, there is a line of symmetry at the bottom of the figure. The plume width associated with the central capture node lies completely inside the dividing streamline and this portion of the plume is 100% captured by the well. The plume width associated with the other capture node shown in the figure lies partially within the dividing streamline. In this case, 30% of this portion of the plume is captured by the well and the other 70% of this portion of the plume bypasses the well and discharges elsewhere at the ground surface.

In some cases, there may be capture of contaminants from the repository moving in flow paths outside of the aquifer. The analytic well model does not apply to these cases and, if required, capture fractions must be calculated from site-specific empirical equations. This capture is further discussed in a site-specific context in Sections 4.4.6.

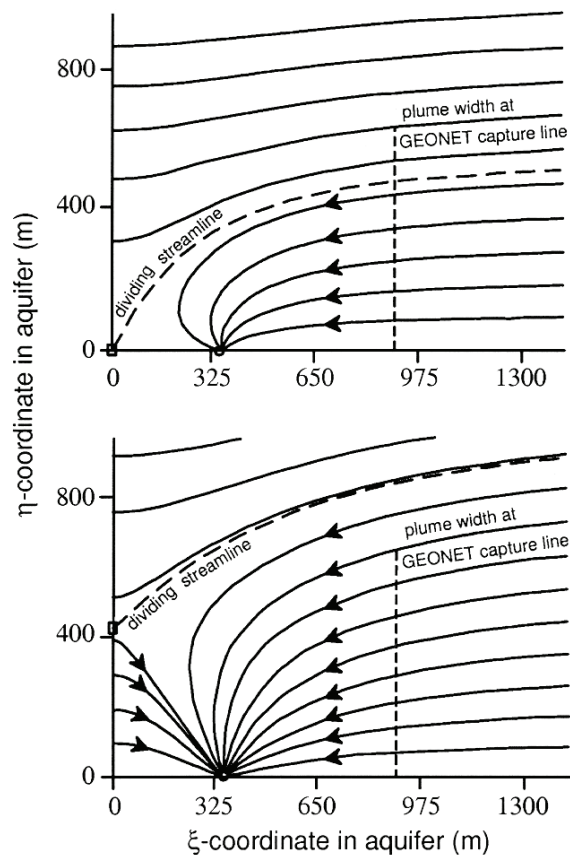


Figure 4.9: Plan view of groundwater streamlines in the aquifer supplying the well with moderate well demand (upper figure) and higher well demand (lower figure). The stagnation points are shown by the symbol □

4.4.6 Site-Specific Effects of the Well

The well may affect three additional quantities:

1. Hydraulic head drawdowns outside the well aquifer.
2. Capture fractions for segments leading to the well from outside the well aquifer.
3. Discharge rates from surface discharges affected by the operation of the well.

The effect of the well on these three quantities is specific to the hydrogeological conditions of the site being modelled.

The derivation of empirical equations applicable to these quantities for use in the geosphere model of the Whiteshell Research Area (WRA) is described in Stanchell et al. (1996), and the derivation for the Third Case Study geosphere is described in Garisto et al. (2004). In the former study, well depths up to 100 m were considered, while in the latter study, a fixed well depth of 100 m was used. The latter model is described below as an example.

Drawdowns Outside the Well Aquifer

Pumping groundwater from the well causes a drawdown that reduces the hydraulic head in the geosphere. The drawdown within the aquifer (fracture zone) is calculated by the well model described in Section 4.4.3. However, pumping on the well may also draw down the heads in other portions of the geosphere.

The approach used is to determine an empirical equation for the hydraulic head change for each node outside the aquifer that could be potentially affected by the well drawdown. This drawdown must be determined from separate modelling with a hydrogeological code.

For the WRA model and the Third Case Study model, the head drawdown for the affected nodes could be expressed by an equation of the form:

$$\Delta h^n = a^n (d_w/100 \text{ m})^2 Q_{well} \quad (4.39)$$

where

Δh^n is the head drawdown at non-aquifer node n [m],
 a^n is the drawdown constant for node n [a/m^2],
 d_w is the well depth [m] (fixed at 100 m in the Third Case Study), and
 Q_{well} is the well demand [m^3/a].

Contaminant Capture from Outside Aquifer

In the Third Case Study hypothetical site, the discharges from the vault Sectors 3 and 4, which normally go to the River, may be captured by the well. This is modelled by diverting a fraction of the contaminant flow from Sectors 3 and 4 to the well:

$$f_{divert} = 1 - \exp(-C \cdot Q_{well}) \quad (4.40a)$$

where $C = 9.55287 \times 10^{-5}$ for Sector 3 and 1.34068×10^{-4} for vault Sector 4, based on results from hydrogeological modelling with FRAC3DVS as a function of well demand from 0 to 4000 m³/a.

Effects on Discharge Areas

The diversion of groundwater due to capture by the well could reduce the volumetric groundwater discharge rate and, therefore, the discharge area relative to natural conditions (Chan et al. 1991). This can affect the availability of contaminated field area. In order to represent this effect, we define a discharge area reduction factor, f_{site}^d , where

$$A^d = f_{site}^d A_0^d \quad (4.40b)$$

and for the Third Case Study (Garisto et al. 2004):

$$f_{site}^d = \begin{cases} 1 & d = \text{well} \\ 1 - f_{capture} & d = \text{lake (aquatic and terrestrial)} \\ \exp(-C_1 \cdot Q_{well}) & d = \text{river (aquatic and terrestrial)} \\ 1 & d = \text{stream} \end{cases} \quad (4.40c)$$

where

A_0^d is the initial discharge area (without effects of the well),
 $f_{capture}$ is the well plume capture fraction, see Section 4.4.6 [-],
 Q_{well} is the well demand [m³/a], and
 $C_1 = 5.04 \times 10^{-5}$ [a/m³].

4.5 MATRIX DIFFUSION

4.5.1 Requirements for Application

Matrix diffusion effects apply when the groundwater can be conceptually divided into a flowing portion in flow channels or fractures and a stagnant portion in the rock matrix. In the present model, if matrix diffusion is specified, then the following approximations are applied.

The equations approximating the effects of diffusion into the rock matrix are based upon modelling the flow channels by a set of plane parallel fractures with constant aperture and constant spacing (Lever et al. 1982). Under this conceptual model, if the effective aperture of these fractures that carry the flowing groundwater is β and the effective spacing between them is H , the effective transport porosity of the fractures, ε_f , is given by

$$\varepsilon_f = \beta / H \quad (4.41)$$

The transport porosity ε_f is less than the bulk rock porosity ε_h . The porosity of the matrix surrounding the fractures, ε_m , is given by

$$\varepsilon_m = \varepsilon_h - \varepsilon_f \quad (4.42)$$

The groundwater velocity in the fractures will be larger than the groundwater velocity in a homogenous medium with the same bulk porosity. Hence, the groundwater velocity under the homogenous flow concept, U , must be rescaled by the ratio of the total porosity to the fracture transport porosity to give the groundwater velocity in the fractures, V :

$$V = U \varepsilon_h / \varepsilon_f \quad (4.43)$$

This rescaling preserves the same volumetric groundwater flow rate or specific discharge in the two concepts and hence remains consistent, assuming the permeabilities are also preserved, with the results of the detailed numerical modelling of the groundwater flow and the head distributions. Modified retardation factors and enhanced dispersion coefficients, due to the diffusion of nuclides out of the flowing water zones into the stagnant water zones, can then be applied to the transport of the nuclides.

The equations developed in the Harwell reports (Lever et al. 1982, Lever and Bradbury 1983) for asymptotic solutions of matrix diffusion transport equations are summarized here. These equations are used to define approximate modified dispersion coefficients and retardation factors for use in the transport equations described in Section 4.3. Sorption of contaminants in both the flowing water zones and in the stagnant water zones of the rock matrix is incorporated through the use of constant retardation factors, R_f and R_m respectively, arising from assumed linear sorption isotherms.

In the equations developed at Harwell, matrix diffusion is assumed to take place orthogonal to the fracture plane and this approximation is shown to be good if

$$\frac{2\tau_m D_o \varepsilon_m}{V\beta} \ll 1 \quad (4.44)$$

where D_o is the free water diffusion constant of the contaminant and τ_m is the tortuosity of the rock matrix surrounding the fractures. In most cases this condition is fulfilled, but for the purposes of the approximations used here, the orthogonal diffusion approximation is accepted even if this condition is poorly fulfilled.

However, matrix diffusion effects are not applied if the Peclet number in the fractures is less than unity. In this case, diffusion is the dominant transport mechanism and orthogonal matrix diffusion from flowing water is a meaningless concept. It would also be inconsistent to consider, for a segment, the fracture flow concept and a rescaled velocity for some nuclides, but a homogeneous medium concept for other nuclides. In order to keep the concept the same for all nuclides and to ensure that every nuclide meets the minimum conditions for the application of matrix diffusion, the minimum value for the Peclet number over all the nuclides is used to decide whether the matrix diffusion concept can be applied. The minimum Peclet number occurs for the maximum value of the diffusion coefficient.

Thus, matrix diffusion effects are not applied if

$$P_e \equiv V L / D_f^{max} \leq 1 \quad (4.45)$$

where D_f^{max} , the maximum dispersion coefficient in the fractures, is given by

$$D_f^{max} = a_L |V| + \tau_\zeta D_0^{max} \quad (4.46)$$

and

a_L is the dispersion length of the transport segment,

τ_ζ is the tortuosity in the fractures in the axial or principal transport direction of the segment, and

D_0^{max} is the maximum free water diffusion constant for all the nuclides in the simulation.

Contaminant transport is divided into three regimes: i) the hydrodynamic regime where dispersion is dominated by hydrodynamic dispersion, ii) the thick-rock regime where the effects of neighbouring fractures are not felt and matrix diffusion can be considered to take place into semi-infinite medium, and iii) the quasi-equilibrium regime where the rock surrounding the fracture is equilibrated by the matrix diffusion. These regimes are shown schematically in Figure 4.10.

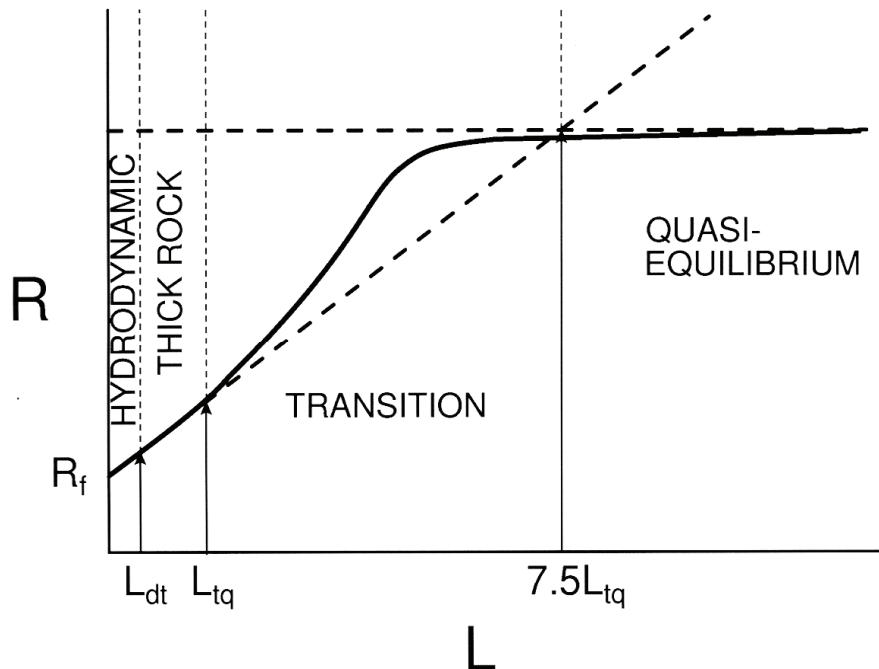


Figure 4.10: Illustration of the magnitude of the effective retardation factor, R , as a result of matrix diffusion effects as a function of travel distance, L , showing the three regimes: hydrodynamic, thick rock and quasi-equilibrium. There is a long transition region between the thick rock and the quasi-equilibrium regimes (after Lever et al. 1982)

4.5.2 Quasi-Equilibrium Regime

In the quasi-equilibrium regime, migration of contaminant is governed by an enhanced constant retardation factor, R , and an enhanced constant Fickian dispersion coefficient, D . The enhanced retardation factor is given by

$$R = R_f + R_m \theta_m / \theta_f \quad (4.47)$$

where R_f is the retardation factor due to sorption in the fractures and R_m is the retardation factor due to sorption in the surrounding rock matrix, The enhanced dispersion coefficient, D , given by

$$D = D_f + \frac{H^3 V^2 \theta_m R_m^2}{12 \beta \tau_m D_0 R^2} \quad (4.48)$$

4.5.3 Thick-Rock Regime

In the thick-rock regime, the solution to the transport equations depends on a characteristic diffusion time constant, $T(\zeta)$, given by

$$T(\zeta) = \frac{\tau_m D_0 R_m \theta_m^2 \zeta^2}{V^2 \beta^2} \quad (4.49)$$

The retardation factors, breakthrough times and spreading of fronts are related to $T(\zeta)$. For example, the point where $C/C_o = 0.5$ from a continuous injection of concentration C_o of non-sorbing water tracer occurs at distance ζ at time, $t_{0.5}$, given by

$$t_{0.5} = R_f \zeta / V + 4.3 \cdot T(\zeta) \quad (4.50)$$

Alternatively, the peak of a pulse input reaches distance ζ at time t_p given by

$$t_p = R_f \zeta / V + 0.67 \cdot T(\zeta) \quad (4.51)$$

Equations (4.49) and (4.51) give an expression for the effective retardation of the peak of a pulse input, $R(\zeta)$, as a function of distance travelled

$$R(\zeta) = R_f + \frac{2 \tau_m D_0 R_m \theta_m^2 \zeta}{3 V \beta^2} \quad (4.52)$$

A similar retardation factor expression can be written, for retardation of the $C/C_o = 0.5$ point in a continuous input case, from Equations (4.49) and (4.50).

The first and third quartiles of a pulse input arrive at distance ζ at t_1 and t_3 given by

$$\left. \begin{aligned} t_1 &= R_f \zeta / V + 0.22 \cdot T(\zeta) \\ t_3 &= R_f \zeta / V + 3.84 \cdot T(\zeta) \end{aligned} \right\} \quad (4.53)$$

The fronts where $C/C_o = 0.1$ and 0.9 in a continuous input case arrive at $t_{0.1}$ and $t_{0.9}$ given by

$$\left. \begin{aligned} t_{0.1} &= R_f \zeta / V + 0.74 \cdot T(\zeta) \\ t_{0.9} &= R_f \zeta / V + 120 \cdot T(\zeta) \end{aligned} \right\} \quad (4.54)$$

These widths of pulses and fronts, proportional to $T(\zeta)$, can be approximately related to effective dispersion coefficients, but the large values of $t_{0.1}$ and $t_{0.9}$ clearly show the asymmetric nature of the dispersion caused by matrix diffusion. This asymmetric dispersion cannot be accurately described by a Fickian dispersion coefficient. However, for the purposes of the approximations used here, an interpolation is made between the enhanced value of the Fickian dispersion coefficient in the quasi-equilibrium regime, and the value for the Fickian dispersion coefficient in the hydrodynamic regime, $D = D_f$. The true dispersion in the thick-rock regime is larger and asymmetric.

4.5.4 Hydrodynamic Regime

In the hydrodynamic regime, dispersion is dominated by hydrodynamic dispersion so that $D = D_f$. The retardation factor, R , is given by Equation (4.52) since the diffusion is into thick rock where the presence of neighbouring fractures is not felt.

4.5.5 Transitions Between the Regimes

Close to the source, the contaminant transport is in the hydrodynamic regime. The transition between the hydrodynamic regime and the thick-rock regime occurs at a distance L_{dt} from the source given by

$$L_{dt} = 3 \left[\frac{VD_f \beta^4 R^2 (L_{dt})}{16\tau_m^2 D_o^2 \theta_m^4} \right]^{1/3} \quad (4.55)$$

where $R(L_{dt})$ is taken as the smaller of the two values given by Equations (4.52) and (4.47). Thus, in general, Equation (4.55) is a cubic equation in L_{dt} . If the second term in Equation (4.52), the retardation factor due to the matrix diffusion, is much greater than R_f , Equation (4.55) simplifies to

$$L_{dt} = \frac{3D_f R_m^2}{4V} \sim \frac{3a_L R_m^2}{4} \quad (4.56)$$

The influence of neighbouring fractures is felt, and the thick-rock regime equations are no longer strictly valid, at a distance L_{tq} from the source given by

$$L_{dt} = \frac{HbV}{5\tau_m D_o q_m} \quad (4.57)$$

There is a fairly long transition between the thick-rock and quasi-equilibrium regimes. The thick-rock retardation factor asymptote does not intersect the quasi-equilibrium asymptote until $\sim 7.5L_{tq}$ and quasi-equilibrium is not fully observed until $\sim 10L_{tq}$ from the source. For the approximations used here, the thick-rock retardation factor from Equation (4.52) is used for $L \leq 7.5L_{tq}$ and the quasi-equilibrium retardation factor from Equation (4.47) is used for $L \geq 7.5L_{tq}$. Similarly, the quasi-equilibrium dispersion coefficient from Equation (4.48) is used for $L \geq 7.5L_{tq}$. The hydrodynamic dispersion coefficient, D_f , is used for $L \leq L_{dt}$ and, as an approximation giving a continuous transition, linear interpolation is used for $L_{dt} < L < 7.5L_{tq}$.

These retardation factor asymptotes and the different migration regimes are shown schematically in Figure 4.10. Also shown is a curve showing a typical behaviour in the transition between these regimes. Note that in the thick-rock regime, the retardation factor is larger than the thick-rock asymptote.

In some cases $L_{tq} < L_{dt}$ and there is a transition directly from the hydrodynamic regime to the quasi-equilibrium regime. These cases often occur when L_{tq} is small and, for most transport calculations, quasi-equilibrium can be assumed throughout most of the migration path. This condition can occur, for example, with a closely spaced network of fine fractures. In this case the hydrodynamic dispersion coefficient, D_f , is used for $L \leq L_{tq}$; the diffusion into the rock matrix begins to enhance the dispersion coefficient beyond this point. The quasi-equilibrium dispersion coefficient from Equation (4.48) is used for $L \geq L_{dt}$, with linear interpolation, as an approximation giving a continuous transition, used for $L_{tq} < L < L_{dt}$. The transition for the retardation factor remains unchanged at $7.5L_{tq}$.

4.6 COLLOIDS

Although colloids are generally not expected to be a significant factor affecting transport of contaminants through groundwater around a deep geologic repository in the Canadian Shield (Vilks 1996), a simple model is included to provide an indication of their importance. This model assumes a reference colloid material and reversible sorption of the contaminant onto the colloids. The colloid itself may move either with the groundwater or at a different rate characterized by its own retardation factor, R_{coll} .

In this case, the retardation factor R arising from sorption on minerals, Equation (4.27), is adjusted to give a new retardation factor R_{eff} for use in the transport equations. This adjustment is done for each element in each transport segment as follows:

$$R_{eff} = [R + C_{coll} K_{d,coll}] / [1 + C_{coll} K_{d,coll} / R_{coll}] \quad (4.58)$$

where

C_{coll} is the concentration of colloid material in the groundwater of the segment [kg/L],
 $K_{d,coll}$ is the sorption coefficient for sorption of the element on the colloid material [L/kg],
 R_{coll} is the retardation factor for the movement of the colloids themselves through the transport segment relative to the movement of the groundwater [-],

If there are no colloids or no sorption on colloids, then Equation (4.58) reverts to $R_{eff} = R$. If the colloids are immobile and do not move with the groundwater, (R_{coll} is very large), then Equation (4.58) becomes $R_{eff} = R + C_{coll} K_{d,coll}$ and the net effect is an increase in contaminant

retardation due to the sorption on immobile colloids. In contrast, if the colloids move at the rate of the groundwater, (R_{coll} is unity), then Equation (4.58) becomes

$$R_{eff} = [R + C_{coll} K_{d,coll}] / [1 + C_{coll} K_{d,coll}], \quad (R_{coll} = 1) \quad (4.59)$$

and the net effect is always a reduction in contaminant retardation, $R_{eff} < R$, and more rapid migration of the contaminant.

4.7 INTERFACE WITH VAULT MODEL

The principal interface between the geosphere and vault models is the passing of the time-dependent contaminant flow rates from each of the repository sectors to the geosphere transport network. These time-dependent flow rates are determined in the vault model and passed to the inlet nodes of the network, which are located at the repository.

The geosphere model passes some data characterizing the rock near the repository to the vault model for use in the vault model mass transport calculations. This repository-geosphere connection ensures that the nuclide mass flow coming from each vault sector can be absorbed into the geosphere, taking into account the porosity, specific discharge and other parameters characterizing the solute transport properties of the adjacent geosphere layer.

The quantities passed for each repository sector are obtained from the properties for the adjacent geosphere transport segment, and include the following:

1. The porosity, ϵ_R , and permeability, k_R of the rock.
2. The capacity factor in the segment for each chemical element, obtained as the product of the retardation factor and the porosity of the segment.
3. The retardation factor for each chemical element in the excavation damaged zone (EDZ), which is set to the same value as the retardation factor in the rock of the segment since the EDZ is composed of the same suite of sorbing minerals.
4. The magnitudes of the specific discharge (Darcy velocity) in the segment projected on the Cartesian coordinate directions.
5. The dispersion length of the segment, α_R , the tortuosity of the rock, τ_ζ , and the free water diffusivity, D_0 .

Geosphere network inlet nodes starting at the repository have input Cartesian coordinates placing the node along the central plane of the disposal repository, not at the boundary between the vault system and the geosphere. The transport across the buffer, backfill and EDZ is accounted for in the vault model. Hence, the length of the first geosphere segment is automatically adjusted to remove the repository barrier thicknesses.

4.8 INTERFACE WITH BIOSPHERE MODEL

The principal interface between the geosphere and biosphere models is the passing of the time-dependent flow rates of contaminants from the geosphere at each of the discharges to the biosphere.

Groundwater discharge from the geosphere to the biosphere can occur at a surface water body such as a stream or a lake, to the unsaturated zone of a low-lying terrestrial area, or to a wetland area such as a marsh. The area of each discharge at the ground surface is determined from the characteristics of the groundwater flow field and is an input to the geosphere model. Aquatic, terrestrial and wetland discharge zones may be associated together as illustrated in Figure 4.11. The discharge area determined for such an associated group is initially assigned to the aquatic discharge. The nuclide contaminant flow migrating towards such a group of discharges and the discharge area is fractionated among the associated discharges by parameters of the biosphere model. Each of these discharge zones is assigned layers of compacted sediment and overburden associated with it. These thin surface layers may not be included in the external detailed groundwater flow calculation since they may not affect the overall flow of groundwater from the repository to the biosphere. However, these layers are included in the CC4 geosphere network model because they have chemical and sorption properties very different from the rest of the geosphere bedrock layers, and therefore they affect the transfer of nuclides from the geosphere to the biosphere.

Specifically, each of the surface water, terrestrial and wetland discharge nodes has two extra nodes associated with it - a sediment node and an overburden node, as shown schematically in Figure 4.11. These two nodes define the positions of the bottom of the sediment and overburden layers at these discharge locations. The positions of these nodes are adjusted automatically such that they are placed directly under the discharge node giving layers of the specified thicknesses (which may be zero if the layer is absent). These additional layers replace a small portion of the last bedrock segment leading to the groundwater discharge areas.

A group of closely associated discharges has diverging transport pathways that branch at the beginning of the last bedrock segment as illustrated in Figure 4.11. The fractionation of the nuclide flow migrating towards the group of discharges is done at the beginning of the last bedrock segment of the geosphere transport network.

Reference hydraulic heads for the sediment node, h_{ss} , and for the overburden node, h_{ov} , are determined by interpolation between the fixed head at the groundwater discharge location, h_{ds} , and the fixed head at the bottom of the last bedrock segment, h_{rk} . This interpolation is based on both the thicknesses and permeabilities of the sediment, overburden and bedrock layers. In the interpolation, it is assumed that the three layers are in series and that no additional groundwater enters the flow system (so that groundwater mass balance is maintained between all three layers). A common specific discharge is maintained in each of these segments across the discharge zones. However, these interpolated heads define a new specific discharge that is slightly different from the original specific discharge calculated in the bedrock by the detailed groundwater flow model in the absence of these layers. The interpolation yields the following:

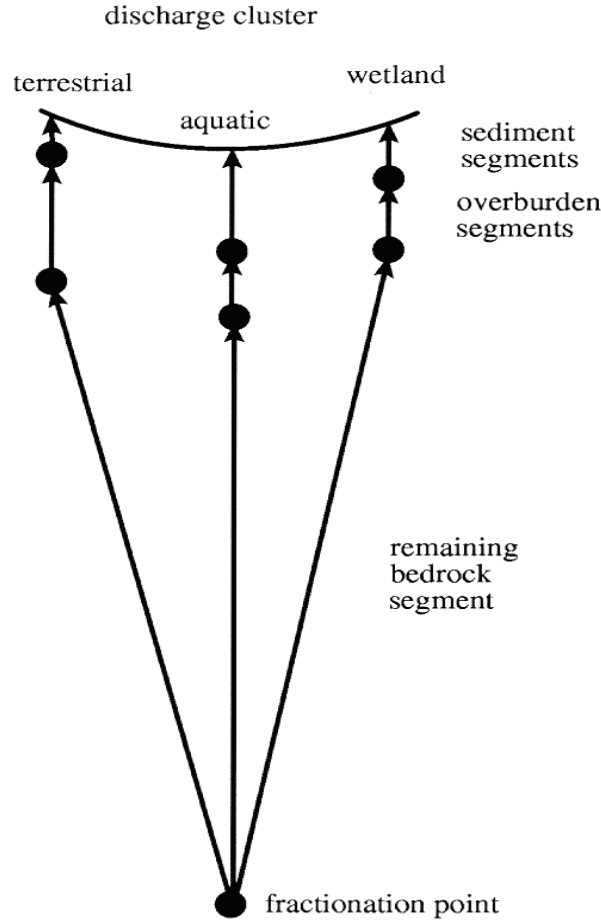


Figure 4.11: Illustration of a cluster of associated discharges - aquatic, terrestrial and wetland

$$\left\{ \begin{array}{l} h_{ss} = \frac{h_{rk} L_{ss} k_{rk} k_{ov} + h_{ds} \cdot (L_{ov} k_{rk} k_{ss} + L_{rk} k_{ov} k_{ss})}{L_{ss} k_{rk} k_{ov} + L_{ov} k_{rk} k_{ss} + L_{rk} k_{ov} k_{ss}} \\ h_{ov} = \frac{h_{rk} \cdot (L_{ss} k_{rk} k_{ov} + L_{ov} k_{rk} k_{ss}) + h_{ds} L_{rk} k_{ov} k_{ss}}{L_{ss} k_{rk} k_{ov} + L_{ov} k_{rk} k_{ss} + L_{rk} k_{ov} k_{ss}} \end{array} \right. \quad (4.60)$$

where L_{ss} , L_{ov} , and L_{rk} are the lengths, and k_{ss} , k_{ov} , and k_{rk} are the permeabilities of the sediment, overburden and last bedrock segments respectively.

Overburden wells, as described in Section 4.4.1, obtain their water entirely from the surface layers, and we assume the capacity of these relatively shallow wells is still given approximately by Equation (4.29).

The geosphere model passes porosities, θ , and distribution coefficients, K_d , for the sediment layers, and also passes the retardation factors, R_q , for the last segment of the pathway leading to each groundwater discharge area to the biosphere model. For most aquatic discharge

locations this last segment will be the segment passing through the sediment layer; for the situation describing discharge from a groundwater supply well, this segment is the last segment in the aquifer from which the well water is drawn; for terrestrial discharges, this last segment is generally the segment passing through the overburden layer. These retardation factors are used for calculations of nuclide mass flow rates of daughters in secular equilibrium with their parent nuclides. The details of these calculations are described in Section 5.

The maximum well capacity obtained from the analytical well model (Section 4.4.2) is passed to the biosphere model for use in determining the possible well uses. Subsequently, the actual pumping demand placed on the well is determined by the biosphere model, and the well demand is passed back to the geosphere model for use in the analytic well model, as described in Section 4.4. The principal biosphere parameters used in determining the well demand are: (a) the size of the critical group, and (b) whether or not the irrigation of their garden is done using well water. The determination of the well demand is described in Section 5. In addition, the quantity of any surface water infiltrated to the well is passed to the biosphere model.

Empirical equations associated with the well model (Sections 4.4.6) may also be used to reduce the areas where the transport pathways emerge at the ground surface, depending upon the effects of groundwater capture by the pumping well. These reduced discharge areas and the resulting rate of discharge of groundwater are also passed to the biosphere model.

4.9 REFERENCES

- Chan, T. and B.W. Nakka. 1994. A two-dimensional analytical well model with applications to groundwater flow and convective transport modeling in the geosphere. Atomic Energy of Canada Limited, AECL-10880, COG-93-215. Pinawa, Canada.
- Chan T., D. Ophori and F. Stanchell. 1991. Sensitivity of advective contaminant movement to possible pumping near a hypothetical nuclear fuel waste disposal vault. Proc. World Environment, An IASTED International Symposium (Calgary, Canada). ACTA Press, Calgary, Canada. 125-129.
- Davison, C.C., T. Chan, A. Brown, M. Gascoyne, D.C. Kamineni, G.S. Lodha, T.W. Melnyk, B.W. Nakka, P.A. O'Connor, D.U. Ophori, N.W. Scheier, N.M. Soonawala, F.W. Stanchell, D.R. Stevenson, G.A. Thorne, T.T. Vandergraaf, P. Vilks and S.H. Whitaker. 1994. The disposal of Canada's nuclear fuel waste: The geosphere model for postclosure assessment. Atomic Energy of Canada Limited Report, AECL-10719, COG-93-9. Pinawa, Canada.
- Garisto, N. and D.M. LeNeveu. 1991. A radionuclide mass-transport model for the performance assessment of engineered barriers in a used nuclear fuel disposal vault. Atomic Energy of Canada Limited Report, AECL-10277. Pinawa, Canada.
- Garisto, F., J. Avis, N. Calder, A. D'Andrea, P. Gierszewski, C. Kitson, T. Melnyk, K. Wei and L. Wojciechowski. 2004. Third case study - Defective container scenario. Ontario Power Generation Report 06819-REP-01200-10126-R00. Toronto, Canada.
- Garisto, F., J. Avis, T. Chshyolkova, P. Gierszewski, M. Gobien, C. Kitson, T. Melnyk, J. Miller, R. Walsh and L. Wojciechowski. 2010. Glaciation scenario: Safety assessment for a

- deep geological repository for used fuel. Nuclear Waste Management Organization Technical Report NWMO TR-2010-10. Toronto, Canada.
- Heinrich, W.F. and T.H. Andres. 1985. Response functions of the convection-dispersion equations describing radionuclide migration in a semi-infinite medium. *Annals of Nuclear Energy* 12, 685-691.
- Johnson, L.H., D.M. LeNeveu, D.W. Shoesmith, D.W. Oscarson, M.N. Gray, R.J. Lemire and N. Garisto. 1994. The disposal of Canada's nuclear fuel waste: The vault model for postclosure assessment. Atomic Energy of Canada Limited Report, AECL-10714, COG-93-4. Pinawa, Canada.
- Lapidus, L. and N.R. Amundson. 1952. Mathematics of adsorption in beds. VI. The effect of longitudinal diffusion in ion-exchange and chromatographic columns. *J. Physical Chemistry* 56, 984-988.
- LeNeveu, D.M. 1987. Response function of the convection-dispersion equations describing radionuclide migration in a finite medium. *Annals of Nuclear Energy*, 14, 77-82.
- Lester, D.H., G. Jansen and H.C. Burkholder. 1975. Migration of radionuclide chains through an adsorbing medium. *AIChE Symposium Series No. 152 – Adsorption and Ion Exchange* 71, 202.
- Lever D.A. and M.H. Bradbury. 1983. Rock matrix diffusion and its implications for radionuclide migration. U.K. Atomic Energy Authority Report AERE-TP-1004. Harwell, UK.
- Lever, D.A., M.H. Bradbury and S.J. Hemingway. 1982. Modelling the effect of diffusion into the rock matrix on radionuclide migration. U.K. Atomic Energy Authority Report, AERE-R-10614. Harwell, UK.
- Quintessa. 2009a. AMBER 5.3 Reference Guide. Quintessa Ltd. report QE-AMBER-1, Version 5.3. Henley-on-Thames, UK.
- Quintessa. 2009b. AMBER 5.3 Getting Started. Quintessa Ltd. report QE-AMBER-2, Version 5.3. Henley-on-Thames, UK.
- Stanchell, F.W., C.C. Davison, T. Melnyk, N.W. Scheier and T. Chan. 1996. The disposal of Canada's nuclear fuel waste: A study of postclosure safety of in-room emplacement of used CANDU fuel in copper containers in permeable plutonic rock; Volume 3: Geosphere model. Atomic Energy of Canada Limited Report, AECL-11494-3, COG-552-3. Pinawa, Canada.
- Therrien, R. and Sudicky, E.A. 1996. Three-dimensional analysis of variably-saturated flow and solute transport in discretely-fractured porous media. *J. Contaminant Hydrology* 23, 1-44.
- Therrien, R., R. G. McLaren, E. A. Sudicky, S.M. Panday, and, V. Guvanasen. 2010. FRAC3DVS-OPG: A three-dimensional numerical model describing subsurface flow and solute transport. User's guide. Groundwater Simulations Group, University of Waterloo. Waterloo, Canada.

Vandergraaf, T.T., K.V. Ticknor and T.W. Melnyk. 1993. Generation of a sorption database for the Canadian Nuclear Fuel Waste Management Program. *J. Contaminant Hydrology* 13, 327-345.

Vilks, P. 1996. The role of colloids and suspended particles in radionuclide transport in the Canadian concept for nuclear fuel waste disposal. Atomic Energy of Canada Limited Report, AECL-10280, COG-92-26. Pinawa, Canada.

von Wicke, E. 1939. *Kolloid Z.* 86, 289.

5. BIOSPHERE MODEL

5.1 MODEL OVERVIEW

The biosphere model describes the movement of radioactive and stable contaminants in the surface environment after release from the geosphere as gas or in groundwater, and the consequent radiological dose to a reference human individual or representative non-human biota.

The biosphere model, CC4/BIOTRAC, was developed specifically to evaluate the long-term postclosure environmental and health impacts of a deep geologic repository. It was not intended as a preclosure model, e.g., it does not contain a sufficiently detailed representation of the site and nearest communities as would exist at the time of repository construction and operation. Rather, it calculates the consequences to a hypothetical reference human group and to biota that might live at the site in the future, as an indicator of the health and environmental consequences of any release of contaminant from the geosphere.

The state of the biosphere can evolve with time and may undergo profound changes in response to changes in climate. For example, in many locations across southern Canada, the current state of the biosphere can be characterized as temperate. The duration of this state might be significantly affected by global warming, or it might be shortened with the onset of a permafrost state which might precede other glacial states. The CC4 biosphere submodel can simulate multiple state changes, including multiple cycles of glaciation, with two main presumptions.

1. The transformation from one state to the next can be adequately approximated as a step change in time.
2. The changes affect only the parameters used to characterize the different components of the biosphere. That is, there is no need to modify the equations currently used in the biosphere submodel to describe processes and interactions.

The submodel for the biosphere uses a large set of parameters to characterize its properties and behaviour. Some parameters focus on specific components of the biosphere, such as bodies of surface water, terrestrial soil and the atmosphere, while other parameters describe how these components interact with one another and with the geosphere. Another important component of the biosphere model typifies the properties of humans and non-humans who might be subject to impacts from a deep geologic disposal facility.

Many, but not all, of the parameters in the biosphere will be affected by changes in the biosphere state. For example, if the biosphere state changes from temperate to permafrost, it would likely be important to modify the data for parameters describing lake surface area, irrigation rates of gardens and the number of humans who inhabit the area (Garisto et al. 2010). It is also reasonable to assume that other parameters would not be affected by some changes in state, such as the porosity of deep lake sediment, the bulk dry density of soil and the sensitivity of humans to ingested radionuclides. Finally, some possible states may correspond to a biosphere that is uninhabitable. This would be the case for an “ice sheet” state when a vast area around the repository is overlain with a thick layer of ice.

Appendix C lists all parameters in the CC4 biosphere submodel segregated into two tables: one identifying state-dependent parameters, and the second identifying state-independent

parameters. Appendix C also identifies potential sources of data for biosphere states corresponding to different potential states occurring during a glacial cycle.

The remainder of this section describes the equations used to describe a single biosphere state. Although originally developed for a temperate biosphere, the governing equations are meant to be independent of any particular state, and a state change is simulated by adjustments to the set of data for state-dependent parameters. Nevertheless, we have included a few pertinent suggestions for some states. For example we recommend setting occupancy factors to zero to deal with states when humans and other biota are not present, as might be the case for an ice sheet state. A related topic in Section 7, on complementary safety indicators, examines indicators that are potentially less dependent upon different biosphere states.

Human radiation doses are calculated for individuals belonging to a group of people receiving the greatest exposure because of its location and lifestyle. This "critical" group is composed of a sequence of self-sufficient families living near where nuclides would discharge to the biosphere. The lifestyle of this exposed group is based on present human behaviour using conservative, yet reasonable, assumptions. For example, members of the critical group are assumed to live their entire lives at the discharge zone, having access to all those parts of the biosphere that are potentially contaminated. They are assumed to be entirely self-sufficient, drawing all their resources, including food, water, air, heating fuels and building materials, from the local environment. For dose estimation purposes, the group is represented by the reference human defined by the International Commission on Radiological Protection (ICRP 1975). Note that some of their characteristics, such as food sources, could differ for different biosphere states. Also the size of the critical group could change, and possibly vanish as might occur, for example, during an ice-sheet state.

Non-human radiation doses are predicted for a generic plant, mammal, bird and fish. Some properties of these biota are state dependent (see Appendix C).

Concentrations in various environmental media can also be tracked with the models described here, and then compared with relevant criteria for chemical toxicity.

The basic biosphere model considers several discharge points from the geosphere, each characterized by the relevant groundwater flow conditions and a surface discharge area. These can be contaminated by groundwater discharges. These in turn can provide a path for contaminants to enter biota and humans, through such pathways as plants grown on these contaminated lands. Ultimately, the local watershed - and any contaminants - is assumed to collect at a lake. Contaminants are lost from the local region by burial into deep sediments, by release with the lake water discharge and by loss to the atmosphere.

Areas downstream of the local watershed are not modelled because calculated impacts would be smaller than those for the reference human group living near the repository site due to the conservative exposure model for the reference human group, and the large dilution and decay that will occur as contaminants move downstream.

The biosphere code is composed of four submodels:

- surface water submodel (Bird et al. 1992);
- soil submodel for a garden (vegetable patch) and forage field;
- local atmosphere submodel (Amiro 1992); and
- foodchain submodel (Zach and Sheppard 1992).

The pathways modelled are illustrated in Figure 5.1.

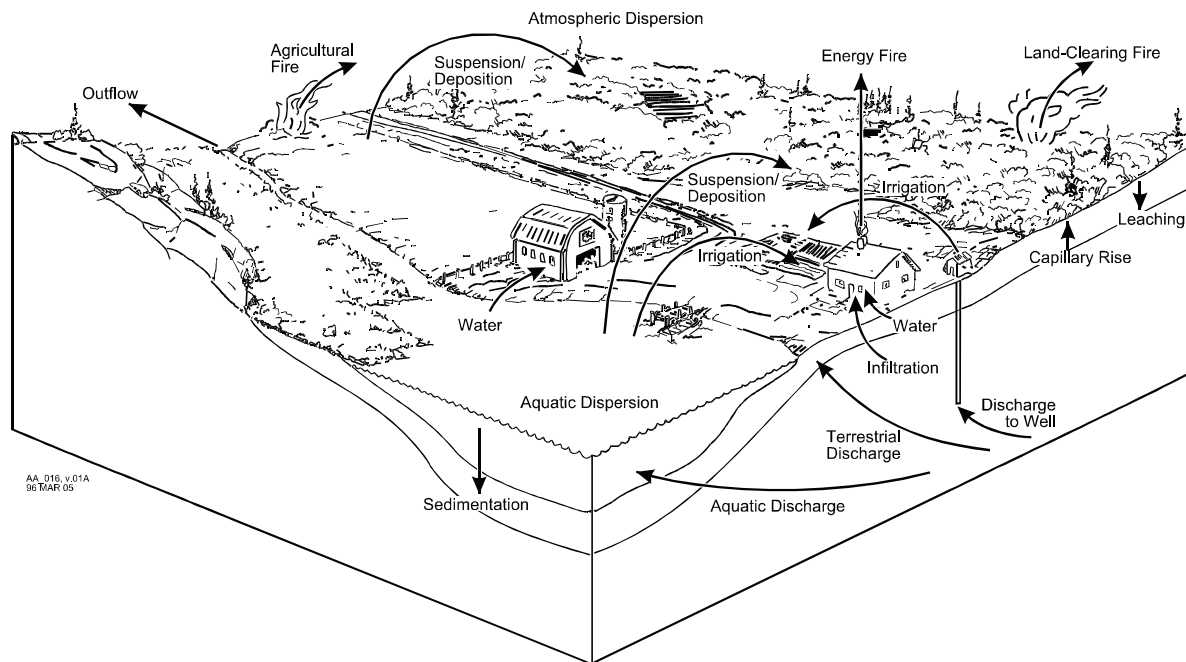


Figure 5.1: Conceptual view of biosphere model (Davis et al. 1993)

5.2 GEOSPHERE-BIOSPHERE INTERFACE

The biosphere model connects with a geosphere model. The biosphere affects the geosphere through the well water withdrawal rate, and acts as a recipient for nuclides released from the geosphere.

Given an assumed well location and depth (defined as part of the geosphere model), the geosphere model determines the well's maximum capacity to supply water, Q_{cap} based on the local geosphere properties. Independently, the biosphere model calculates the demand on the well, Q_{well} , based on water needed by the reference human group for domestic use and irrigation of fields, which in turn is based on the size of the human group and other factors such as number of livestock. Based on the balance between these parameters, the models decide how much of the well water is drawn from the geosphere and how much is drawn from surface waters, Q_{sur} (Section 4.4.4), which dilutes the nuclide concentration in the well water.

The geosphere model also sends to the biosphere the areas of the discharges modified for the effect of the well, A^d for discharge d , as well as the deep-sediment porosity, $\epsilon_{d_{sed}}$, the sediment partition coefficients, K_d^{sed} , and retardation factors, for each contaminant nuclide, for the last geosphere layer preceding discharge to the biosphere, K_d^d . The biosphere model uses the discharge areas to calculate the part of each discharge area assumed to be terrestrial, A_t^d .

5.2.1 Modelling Well Usage

Humans use water for drinking, domestic needs (such as cooking, bathing, laundry), watering livestock, irrigating a garden, and irrigating a forage field.

The possible sources of this water are a surface water body (e.g., a lake) and a well. An input parameter determines the source of water for the human group.

If a well is the preferred water source, its capacity is compared to the water demand in order to determine if it can be used as the source. If not, then the "lake" is used. It is assumed that the "lake" is large enough to supply all water demands.

Domestic Water Demand

The human group's domestic water needs, Q_{dom} , consist of direct personal requirements for drinking, cooking, bathing and laundry, and the requirements of the group's livestock, i.e. the terrestrial animal-food types meat, milk and bird. The direct human requirement is described by an annual demand per person supplied by the water source, and the number of persons in the critical group.

The water requirement for domestic animals is described by a consumption rate per animal Q_{dw} , and the number of animals N_{an}^j of each type j (meat, milk, bird) supplying the critical group.

The number of animals of each type is calculated from:

$$N_{an}^j = N_{crit} \cdot U^j / Y_{an}^j \quad (5.1)$$

where

N_{an}^j is the number of animals of each type j (meat, milk, bird) supplying the critical group [-],

N_{crit} is the number of persons in the critical group [-],

U^j is the annual ingestion rate per person of animal food type $j = \text{milk, meat or bird}$ [$\text{kg}_{\text{wetbio}} \cdot \text{a}^{-1}$, or $\text{L}_{\text{milk}} \cdot \text{a}^{-1}$], and

Y_{an}^j is the average dressed yield of that type of animal j [$\text{kg}_{\text{wetbio}} \cdot \text{a}^{-1}$ or $\text{L}_{\text{milk}} \cdot \text{a}^{-1}$].

The numerical value of N_{an}^j is rounded to the next higher integer.

The (total) domestic water demand Q_{dom} is then given by:

$$Q_{dom} = N_{crit} \cdot Q_{pc} + \sum_j (N_{an}^j \cdot Q_{dw}^j) \cdot cda \cdot clm \quad (5.2)$$

where

Q_{dom} is the annual domestic water demand [$\text{m}^3_{\text{water}} \cdot \text{a}^{-1}$],

Q_{pc} is the annual water demand per person for drinking and domestic (bathing, laundry, etc.) use [$\text{m}^3_{\text{water}} \cdot (\text{person} \cdot \text{a})^{-1}$],

Q_{dw}^j is the water consumption rate per animal that corresponds to food type j (meat, milk or bird) [$\text{L}_{\text{water}} \cdot \text{d}^{-1}$],

cda is the number of days per tropical year 365.2422 [$\text{d} \cdot \text{a}^{-1}$], and

clm is the conversion factor from m^3 to L [$0.001 \text{ m}^3 \cdot \text{L}^{-1}$].

Irrigation Demand and Areas of Fields

The model considers four field types f (garden, forage field, woodlot and peat bog). Only the garden and the forage field would be irrigated. Water for the garden may come from the lake or the well, if there is one. Water for the forage field comes only from the lake. The rate of irrigation per square metre of soil, I_{irr} , is defined as an input parameter for each field type f .

For any given simulation, it is assumed that all fields have the same soil type and experience the same annual precipitation. The irrigation demand per square metre of irrigated soil is then considered to be the same for all gardens and for all forage fields. Each field has a different area, so the annual volume of water required to irrigate the respective fields will vary.

Garden field area

The garden is assumed to be just large enough to supply the reference human group with fruit or leafy vegetables, root plants and grains¹. Its area is calculated from the food-crop-plant yield, Y_p^{garden} , a person's annual ingestion rate of plants, U^{plant} , and the number of persons in the critical group, N_{crit} :

$$A^{garden} = N_{crit} U^{plant} / (Y_p^{garden} \cdot ff_{crop}) \quad (5.3)$$

where

- A^{garden} is the area of the garden field [m²],
- N_{crit} is the number of persons in the critical group,
- U^{plant} is a person's annual ingestion rate of plant produce (fruit, leafs, roots and grain) [kg_{wetbio}·a⁻¹],
- Y_p^{garden} is the garden plant biomass density (yield) [kg_{wetbio}·m⁻²],
- ff_{crop} is the cropping frequency of garden and forage fields [a⁻¹].

Forage field area

The forage field is made large enough to support the household's domestic animals with forage crops. Its area is calculated from:

$$A^{forage} = \sum_j N_{an}^j Q_{f,an}^j / (Y_p^{forage} \cdot ff_{crop}) \quad (5.4)$$

where

- A^{forage} is the area of the forage field [m²],
- N_{an}^j is number of animals of food type j ,
- $Q_{f,an}^j$ is the forage consumption rate of animal food type j [kg_{wetbio}·a⁻¹],

¹ "Gardens" do not normally include grains, but this title is used here for convenience rather than the more general food-crop field. Note also that only one 'plant' is modelled, and this hypothetical plant supplies fruit, leafy vegetables, roots and grains to the critical group.

Y_p^{forage} is the forage plant biomass density (yield) for animal food type j (i.e. *meat, milk, bird*)
 $[kg_{wetbio} \cdot m^{-2}]$, , and
 ff_{crop} is the cropping frequency of garden and forage fields $[a^{-1}]$.

Woodlot and peat bog field areas

The areas of the woodlot and peat bog, which may be the source of heating fuel, are calculated as follows:

$$A^{woodlot} = Q_{fuel} \cdot t_{for} / (E_{wood} \cdot Y_w), \quad (5.5)$$

where

$A^{woodlot}$ is the area of the field for field type = woodlot $[m^2]$,
 Q_{fuel} is the energy required to heat the critical group's dwelling for a year $[MJ \cdot a^{-1}]$,
 t_{for} is the forest renewal time $[a]$,
 E_{wood} is the convertible energy content of fuel wood $[MJ \cdot kg_{wetbio}^{-1}]$,
 Y_w is the plant yield for wood (for building or fuel) $[kg_{wetbio} \cdot m^{-2}_{soil}]$;

and

$$A^{peatbog} = Q_{fuel} \cdot t_{peat} / (E_{peat} \cdot \rho_{soil}^{organic} \cdot Z_{ss}), \quad (5.6)$$

where

$A^{peatbog}$ is the area of the field for field type = peatbog $[m^2]$,
 t_{peat} is the duration of fuel peat use $[a]$,
 E_{peat} is the convertible energy content of dry fuel peat $[MJ \cdot kg_{drypeat}^{-1}]$,
 $\rho_{soil}^{organic}$ is the soil bulk density for organic (peat) soil $[kg_{drysoil} \cdot m^{-3}_{drysoil}]$,
 Z_{ss} is the depth of the surface soil $[m]$.

It is assumed that the forest renews itself every t_{for} years, and that at all times sufficient peat is available to heat the critical group's dwelling for a period of t_{peat} years, no matter what the choice of fuel source was at previous times.

Choice of Water Source

As noted above, water is required for domestic purposes, and possibly to irrigate a garden or a forage field. In addition to the conditions noted above, four further constraints have been applied to the use of water sources.

1. It is assumed that if a well is used to supply water for domestic purposes, it will also be used to water the garden (if its capacity permits - see below).
2. It is assumed that if the forage field is irrigated, it will be irrigated using lake water. This assumption is based upon economic considerations and current practice.
3. A source must be capable of meeting the total demand placed upon it. In most cases, it is expected that the well will be able to meet domestic needs (this is tested in the model). If

the well is to be used also as a source of water to irrigate the garden, its annual capacity to supply water, Q_{cap} must be greater than the combined demand for domestic and irrigation needs. It is assumed that the lake is large enough to meet any water demand on it.

4. The model allows for the situation where the garden is irrigated with well water and the forage field is irrigated with lake water.

Selection of Water Source

Taken together, the above considerations could require different choices to be made when specifying the water source(s) needed to meet domestic needs and garden and forage field irrigation. In each simulation, the volumetric demand on the well, Q_{well} , is calculated as follows:

- i) If the domestic water source is the well, and the garden is also irrigated using well water, then

$$Q_{well} = Q_{dom} + I_{irr}^{garden,stype} \cdot A^{garden} \quad (5.7)$$

where:

- Q_{well} is the annual capacity of the well to supply water [$m^3_{water} \cdot a^{-1}$],
- Q_{dom} is the annual domestic water demand [$m^3_{water} \cdot a^{-1}$],
- $I_{irr}^{garden,stype}$ is the garden irrigation rate for the soil type *stype* [$m^3_{water} m^{-2}_{soil} a^{-1}$],
- A^{garden} is the area of the garden field [m^2].

- ii) If the domestic water source is the well, but the garden is not irrigated using well water, then

$$Q_{well} = Q_{dom} \quad (5.8)$$

- iii) If the well is not used at all,

$$Q_{well} = 0. \quad (5.9)$$

5.2.2 Nuclide Concentrations in the Discharges to the Biosphere

Nuclides escaping the geosphere may enter the biosphere via

- a) the well,
- b) the lakebed, and
- c) the soils at the top of the saturated unconsolidated overburden (water table).

Nuclides discharged at all of these locations may flow to and contaminate other parts of the biosphere. The geosphere model does not generate discharge flow rates, $X_{gw}(t)$, for daughter radionuclides that are in secular equilibrium with their parent radionuclide in the geosphere. Therefore, the biosphere model must evaluate these daughter inflows. This is given by:

$$X_{gw}^{i,d}(t) = X_{gw}^{p,d}(t) \cdot (\lambda^p / \lambda^i) \cdot (R_{fac}^{p,d} / R_{fac}^{i,d}) \quad (5.10)$$

where:

$X_{gw}^{i,d}(t), X_{gw}^{p,d}(t)$ are the discharge flow rates of a nuclide i and its parent p from discharge location d at time t [mol·a⁻¹],
 λ^p, λ^i are the decay constants for nuclide i and its parent p [a⁻¹],
 $R_{fac}^{i,d}, R_{fac}^{p,d}$ are the retardation factors for nuclide i and p in the last geosphere layer preceding discharge to the biosphere at discharge location d [-]; and
 d is the discharge location.

a) Concentration in the Well

The concentration of nuclide i in water withdrawn from the well, $C_{well}^i(t)$, is a function of the fraction of the aquifer's flow that is captured by the well.

The model distinguishes between two broad classifications of wells: overburden wells and bedrock wells. An overburden well is relatively shallow, and extends only into the overburden above the rock of the geosphere. A bedrock well is generally deeper and it is conservatively assumed that it always intersects a fracture zone in the centre of the contaminant plume.

For the bedrock well, the capture rate of nuclide i , $X_{gw}^{i,well}$, is calculated in the geosphere model. It is assumed that the captured nuclides are dispersed and diluted uniformly throughout the total volume of water withdrawn from the well, Q_{well} . A volume, Q_{sur} , of lake water containing a concentration of contaminant nuclide, C_L , may also be drawn back down into the well. The well water concentration is thus

$$C_{well}^i(t) = [X_{gw}^{i,well}(t) + C_L^i(t) \cdot Q_{sur}] / Q_{well} \quad (5.11)$$

where:

$C_{well}^i(t)$ is the concentration of nuclide i in the well at time t [mol·m⁻³_{water}],
 $X_{gw}^{i,well}(t)$ is the flow of nuclide i captured by the well at time t [mol·a⁻¹],
 $C_L^i(t)$ is the concentration of nuclide i in the lake water at time t [mol·m⁻³_{water}],
 Q_{sur} is the quantity of well water drawn from surface waters (Section 4.4.4) [m³_{water}·a⁻¹],
 Q_{well} is the total annual volume of water drawn from the well [m³_{water}·a⁻¹].

For overburden (i.e., shallow) wells that do not penetrate into the bedrock (i.e., if the depth of the well, Z_{well} , is less than overburden depth, Z_o), then the well water concentration is set equal to the lake water concentration.

b) Concentration in the Lakebed

It is conservatively assumed that all water-borne nuclides reach the lake quickly, whether they enter the biosphere via the well, the lakebed or the soils of the fields. Sorption of nuclides dissolved in the water rising through compacted sediment is modelled in the geosphere model. Transfer of nuclides on particles settling out of the lake to form a well-mixed surface layer of sediment is modelled in the biosphere lake submodel.

It is assumed that used well water and groundwater from the fields both run off into the lake. They contaminate some quantity of soil en route to the lake, but it is conservatively assumed that this process does not diminish the amount of nuclides entering the lake. Therefore the amount of nuclide i flowing to the lake is simply the sum of all geosphere discharges, $X_{gw}^{i,d}(t)$ over all the discharge locations d , including the well.

c) Concentration in the Groundwater Under Fields

The concentration of nuclide i in surface soil may be affected by the groundwater concentration of nuclide i , $C_{gw}^{i,d}(t)$, at each discharge location. $C_{gw}^{i,d}(t)$ is calculated from

$$C_{gw}^{i,d}(t) = X_{gw}^{i,d}(t) / Q_{gw}^d \quad (5.12)$$

where

$C_{gw}^{i,d}(t)$ is the groundwater discharge concentration of nuclide i at each location d [$\text{mol} \cdot \text{m}^{-3}_{\text{water}}$],

$X_{gw}^{i,d}(t)$ is the flow of nuclide i from location d at time t [$\text{mol} \cdot \text{a}^{-1}$],

Q_{gw}^d is the volumetric water discharge rate to the biosphere from location d [$\text{m}^3 \cdot \text{a}^{-1}$], and

d is the geosphere discharge location.

5.3 THE SURFACE WATER SUBMODEL

5.3.1 General

Nuclides would be discharged from the geosphere to one or more topological low points. For modelling purposes, it is assumed that the entire discharge ends up in a lake. This allows complex processes such as runoff, recycling and atmospheric suspension and deposition to be treated very simply (Davis et al. 1993, p.38). The transport processes included in the model are illustrated in Figure 5.2. We assume that these processes endure during all biosphere states, but the extent to which they occur is controlled by state-dependent parameter values. For instance, sedimentation and runoff will continue, but might be reduced during permafrost periods and most activities in the biosphere would be strongly attenuated during an ice sheet state. We also suggest that the use of lake sediment in fields (Section 5.3.6) would only occur during a temperate state. Finally, we note that there may be a substantial change in lake size accompanying a change in state. The biosphere model (CC4.07 and CC4.08) assumes that a decrease in lake volume is accompanied by a decrease in radionuclide mass in the lake through downstream 'flushing', such that radionuclide concentrations in the lake do not change during the state change. See Appendix C for the identity of state-dependent parameters.

Small fractions of the discharges may contact the water table under fields near the lake shore and contaminate the overlying soil zone and plants. It is assumed that these fractions of the nuclide flows eventually reach the lake in runoff. The amounts thus temporarily diverted from entering the lake are not subtracted from the discharge flows to the lake.

Similarly, it is assumed that the nuclides in water drawn from the well for domestic and irrigation purposes also reach the lake. Consequently the total input flow of nuclide i to the lake, $X_L^i(t)$, is:

$$X_L^i(t) = \sum_d X_{gw}^{i,d}(t) \quad (5.13)$$

where

$X_L^i(t)$ is the total input flow of nuclide i to the lake at time t [$\text{mol}\cdot\text{a}^{-1}$], and

$X_{gw}^{i,d}(t)$ is the annual flow of nuclide i from the geosphere to the biosphere at discharge location d [$\text{mol}\cdot\text{a}^{-1}$].

The volume of the lake is assumed to be constant for the duration of each biosphere state, so the water flow into the lake, Q_{lake} , equals the flow out of the lake. This flow is calculated from the annual average watershed surface runoff and watershed area:

$$Q_{lake} = A_{watershed}(R_t + R_{melt}) \quad (5.14)$$

where:

Q_{lake} is the water flow into and out of the lake [$\text{m}^3\cdot\text{a}^{-1}$],

R_{melt} is the total meltwater from glaciers [$\text{m}^3_{\text{water}}\cdot\text{m}^{-2}_{\text{watershed}}\cdot\text{a}^{-1}$],

R_t is the total watershed runoff [$\text{m}^3_{\text{water}}\cdot\text{m}^{-2}_{\text{watershed}}\cdot\text{a}^{-1}$],

$A_{watershed}$ is the watershed or catchment area of the lake [$\text{m}^2_{\text{watershed}}$].

R_t is measured as the annual flow of water leaving the watershed divided by watershed area and includes water that has percolated through the soil and then drained into the surface water body.

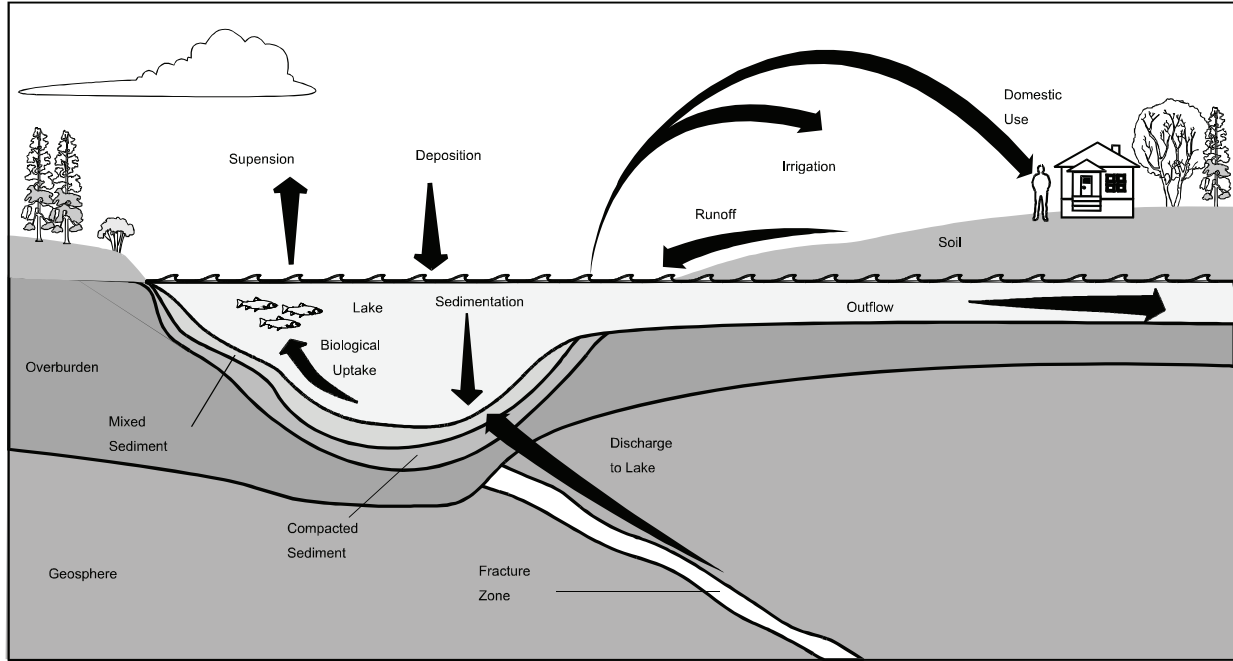


Figure 5.2: Transport processes considered in the lake (surface water) submodel (Goodwin et al. 1994)

5.3.2 Lake Water

The rate of change of the total amount of nuclide i in the lake water and lake sediments may be written as the sum of the inflows, plus ingrowth from parent nuclides, p , minus losses due to outflow, decay within the lake, and gaseous evasion from the surface of the lake:

$$\frac{dM_{Lt}^i(t)}{dt} = X_L^i(t) - Q_{lake} \cdot C_L^i(t) + \lambda^p M_{Lt}^p(t) - \lambda^i M_{Lt}^i(t) - \lambda_{ivol}^i C_L^i(t) V_L \quad (5.15)$$

$$= \frac{dM_L^i(t)}{dt} + \frac{dM_{sed}^i(t)}{dt} \quad (5.16)$$

where:

$M_{Lt}^i(t)$ and $M_{Lt}^p(t)$ are the total amounts of nuclide i and its parent p in lake water [mol],

Q_{lake} is the lake water throughput [$m^3 \cdot a^{-1}$],

λ_{ivol}^i is the rate constant at which volatile or gaseous isotope i is released from the lake's surface and enters the atmosphere [a^{-1}],

V_L is the volume of lake [m^3],

$C_L^i(t)$ is the concentration of nuclide i in lake water at time t [$mol \cdot m^{-3}$],

λ^p and λ^i are the radiological decay constants for nuclide i and its parent p [a^{-1}],

$M_L^i(t)$ is the amount of nuclide i in lake water [mol], and

$M_{sed}^i(t)$ is the amount of nuclide i in lake sediments [mol].

Note that the lake volume is given by

$$V_L = A_L Z_L \quad (5.17)$$

where

A_L is the lake surface area [m²], and
 Z_L is the mean depth of the lake [m].

Nuclides in the lake water may adhere to suspended particles and be deposited in lake sediments. In the long term, this transfer can be described by a net rate of transfer. The quantity of nuclide i in the lake sediments is:

$$\frac{dM_{sed}^i(t)}{dt} = \alpha_{sed}^i V_L C_L^i(t) + \lambda^p M_{sed}^p(t) - \lambda^i M_{sed}^i(t) \quad (5.18)$$

where α_{sed}^i is the rate constant for net transfer of nuclide i from the lake water to the lake sediments [a⁻¹].

For the lake water, it follows from Equations (5.15), (5.16) and (5.18) that

$$\frac{dC_L^i(t)}{dt} + C_L^i(t) \left(\alpha_{sed}^i + \lambda_{vol}^i + \frac{Q_{lake}}{V_L} + \lambda^i \right) = \frac{X_L^i(t)}{V_L} + \frac{\lambda^p M_L^p(t)}{V_L} \quad (5.19)$$

Solving Equation (5.19) using Laplace transforms results in the following expression for the lake water concentration:

$$C_L^i(t) = \int_0^t [X_L^i(t')/V_L + \lambda^p C_L^p(t')] e^{-\beta(t-t')} dt' \quad (5.20)$$

where

$$\beta = \alpha_{sed}^i + \lambda_{vol}^i + \frac{Q_{lake}}{V_L} + \lambda^i \quad (5.21)$$

$$C_L^p(t) = M_L^p(t)/V_L \quad (5.22)$$

5.3.3 Lake Sediment

The aquatic discharge zones are covered by a layer of bioturbated sediment lying on a compacted sediment layer. The two layers together constitute sediment considered accessible to humans, and the depth-weighted average concentration of a contaminant in the two layers is used in assessment calculations.

The amount of nuclide in the sediment is obtained by solving Equation (5.18) by use of Laplace transforms. This relationship (assuming the area of the sediment A_{sed} equals the area of the lake A_L) is as follows:

$$M_{sed}^i(t) = \int_0^t [\alpha_{sed}^i V_L C_L^i(t') + \lambda^p M_{sed}^p(t')] e^{-\lambda^i(t-t')} dt' \quad (5.23)$$

The concentration of nuclide in the sediment is given by:

$$C_{sed}^i(t) = \frac{M_{sed}^i(t)}{A_L W_{sed}(t)} \quad (5.24)$$

where

$C_{sed}^i(t)$ is the concentration of nuclide i in the sediment at time t [$\text{mol} \cdot \text{kg}_{\text{dry}}^{-1}$],

A_L is the lake surface area [m^2], and

$W_{sed}(t)$ is the dry mass of sediment per unit area of lake at time t [$\text{kg}_{\text{dry}} \cdot \text{m}^{-2}$].

Combining Equations (5.23) and (5.24), we arrive at the convolution integral for the concentration of nuclide in the sediment:

$$C_{sed}^i(t) = \int_0^t \left\{ \frac{\alpha_{sed}^i Z_L C_L^i(t')}{W_{sed}(t)} + \frac{\lambda^p M_{sed}^p(t')}{A_L W_{sed}(t)} \right\} e^{-\lambda^i(t-t')} dt' \quad (5.25)$$

5.3.4 Concentration in Bioturbated Sediment Layer

In the lake submodel, it is assumed that sedimentation occurs continuously and contributes to the sediment bulk at the bottom of the lake. The rate of accumulation of sediment is assumed to be constant. This means that the mass of sediment per unit area at any time is given by:

$$W_{sed}(t) = Q_{sed} \cdot t + W_{sed}^0 \quad (5.26)$$

where

Q_{sed} is the rate of accumulation of (dry) sediment per unit area of lake [$\text{kg}_{\text{dry}} \cdot \text{m}^{-2} \cdot \text{a}^{-1}$],

t is time [a],

W_{sed}^0 is the initial mass of (dry) sediment per unit area of sediments [$\text{kg}_{\text{dry}} \cdot \text{m}^{-2}$].

It is assumed the bioturbated sediment is the sediment that was deposited in the last 50 years. Beyond this time, the sediment becomes part of the deeper compacted sediment layer. For a time period 50 years, the amount of sediment deposited per unit area is

$$W_{sed}^{50} = Q_{sed} \cdot (50 \text{ a}) \quad (5.27)$$

Hence, the accumulated contaminant mass in the bioturbated sediment over the last 50 years becomes

$$M_{sed}^{i,50} = \int_{t-50}^t [\alpha_{sed}^i \cdot V_L \cdot C_L^i(t') + \lambda^p M_{sed}^{p,50}(t')] e^{-\lambda^i(t-t')} dt' \quad (5.28)$$

and substituting W_{sed}^{50} for $W_{sed}(t)$ gives the concentration in the bioturbated layer:

$$C_{sed}^{i,50}(t) = \int_{t-50}^t [\alpha_{sed}^i Z_L C_L^i(t') + \frac{\lambda^p}{A_L} M_{sed}^{p,50}(t')] R_{sed}^i(t-t') dt' \quad (5.29)$$

where

$$R_{sed}^i(t-t') = e^{-\lambda_i(t-t')} / W_{sed}^{50} \quad (5.30)$$

The lower limit of the integral is set equal to 0 for times t less than 50 years.

5.3.5 Concentration in Sediment over a Discharge

The aquatic discharge zones are covered by a sediment layer of thickness Z_{sed} , comprised of thickness Z_{biosed} of bioturbated sediment lying on a compacted layer of thickness $(Z_{sed} - Z_{biosed})$. The two layers together constitute sediment considered accessible to humans.

The nuclide concentration in the compacted layer over each discharge location is calculated from the groundwater concentration at the upper boundary of the compacted sediment layer, $C_{gw}^{i,d}$, the sediment distribution coefficient for this nuclide, $K_{d,sed}$, the deep sediment bulk density, ρ_{dsed} , and the deep sediment porosity, ϵ_{dsed} . The effective sediment concentration for the discharge location, $C_{sed,e}^{i,d}$, is calculated by depth-weighting the concentrations of bioturbated, $C_{sed}^{i,50}$, and compacted sediment layers for all aquatic discharges:

$$C_{sed,e}^{i,d} = \frac{Z_{biosed} \cdot C_{sed}^{i,50}}{Z_{sed}} + \frac{Z_{sed} - Z_{biosed}}{Z_{sed}} \cdot \left\{ \frac{\epsilon_{dsed}}{\rho_{dsed}} + K_{d,sed} \right\} \cdot C_{gw}^{i,d} \quad (5.31)$$

where

- $C_{sed,e}^{i,d}$ is the effective sediment concentration of nuclide i at discharge location d [$\text{mol} \cdot \text{kg}^{-1}_{\text{dry sed}}$],
- Z_{biosed} is the bioturbated sediment thickness (i.e., the amount accumulated over a 50 year period) [m],
- $C_{sed}^{i,50}$ is the nuclide concentration in bioturbated sediment (i.e. Equation 5.29) [$\text{mol} \cdot \text{kg}^{-1}_{\text{dry sed}}$],
- Z_{sed} is thickness of sediment that can be accessed [m] (generally, this is the same as Z_s),
- ϵ_{dsed} is the deep sediment porosity [-],
- ρ_{dsed} is the deep sediment bulk density [$\text{kg}_{\text{dry sed}} \cdot \text{m}^{-3}$],
- $K_{d,sed}$ is the sediment solid/liquid distribution coefficient for nuclide i [$\text{m}^3 \cdot \text{kg}^{-1}_{\text{dry sed}}$], and
- $C_{gw}^{i,d}$ is the groundwater concentration of nuclide i [$\text{mol} \cdot \text{m}^{-3}_{\text{water}}$].

5.3.6 Use of Sediments in Fields

The model also considers the case where the agricultural fields are contaminated by lake sediments, either because the lake was recently drained for farming, or the sediments were dredged for use on the fields. In this case, the field areas are assigned to the lake portion of the discharge zones (the terrestrial portions are ignored). That is, the fields (possibly distributed into several portions if the fields are larger than the discharge areas) are assumed to lie over the

aquatic discharge areas (which have contaminated sediment). The average soil concentration in each field consists of an area-weighted average of the contributions from each discharge zone on which a given field is distributed (see also Section 5.4.6).

$$C_{seds}^{i,f} = \sum_d f_{ss}^{f,d} C_{sed,e}^{i,d} \quad (5.32)$$

where

$C_{seds}^{i,f}$ is the average concentration of nuclide i on field f from sediment-used-as-soil, and $f_{ss}^{f,d}$ is the fractional area of field f that is on aquatic discharge location d [-].

Fields are assumed to lie over discharges such that the average contaminant concentration of each field, $C_{seds}^{i,f}$, will decrease in the order $f =$ garden, forage field, woodlot and peat bog, corresponding to their general importance as human dose pathways.

If the total area of all the fields is larger than all the aquatic discharges, then an area of bioturbated lakebed sediment is used to complete the total field area. Any areas of the lakebed that are not over a discharge are assumed to be covered by sediments with the same nuclide concentration as bioturbated sediment (Equation 5.29). This area (i.e., no contribution from direct discharge) is calculated as follows:

$$A_{ss} = A_L - \sum_d A^d \quad (5.33)$$

where

A_L is the area of the lake [m^2],

A^d is the area of the discharge for location d [m^2], and

A_{ss} is the area of the lakebed covered by bioturbated sediments [m^2].

If still more area is needed to complete the total field area, then the additional area is assumed to have a concentration determined by the soil submodel for the conditions applied to the type of field whose area is being made up.

See also Davis et al. (1993, p.141) for further discussion of how field areas are assigned to sediments

5.4 THE SOIL SUBMODEL

5.4.1 Overview of the Soil Model

The soil model calculates the concentration of contaminants in the surface (rooting or cultivated) soil layer. This layer is assumed to be well-mixed. Figure 5.3 illustrates the general processes treated in the soil submodel. We assume that these processes endure during all states, but the extent to which they occur is controlled by state-dependent parameter values (see Appendix C). For instance, different states would likely have different precipitation rates, but the underlying processes would still persist. Many of these processes might be strongly attenuated during some states. For example, irrigation would likely be practised only during temperate states.

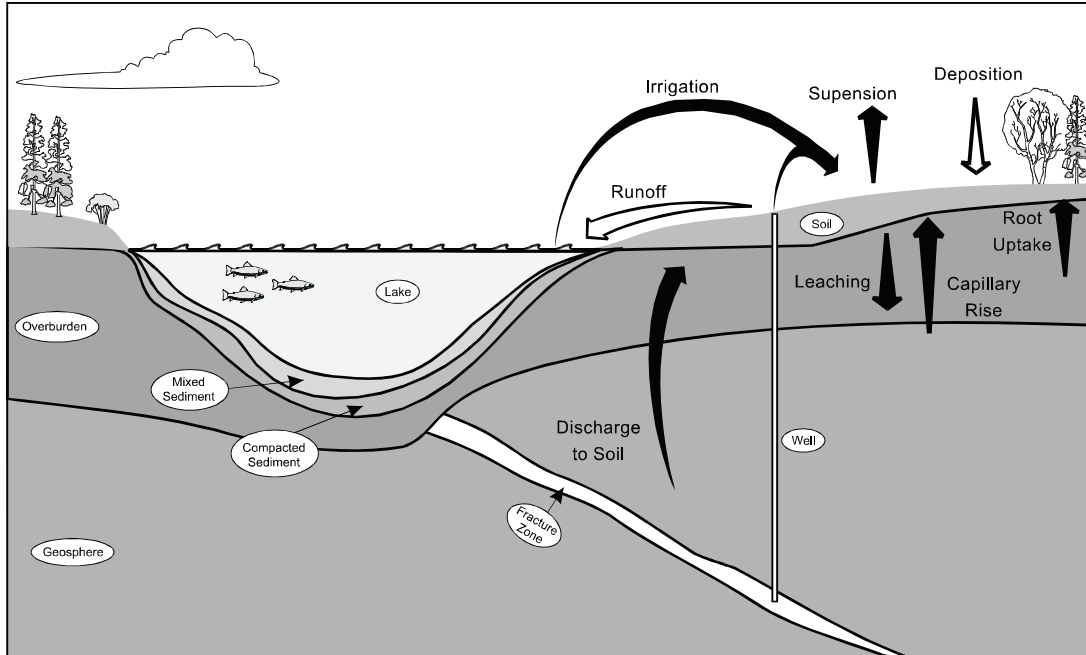


Figure 5.3: Transport processes considered in the soil submodel (Goodwin et al. 1994)

The soil model includes the possibility that contaminants could be introduced by irrigation water, and the source of that water could be a lake (shown in Figure 5.3) or a well. However, since irrigation is uncommon on the present Canadian Shield, the biosphere model was developed specifically to incorporate capillary rise as a possible contaminant source. Capillary rise only occurs in specific circumstances where the water table is close to the soil surface and the soil texture is appropriate to draw water. In comparison to irrigation, the flux of contaminants from capillary rise is usually quite smaller, especially if contaminated well water is used for irrigation (Sheppard 1992, Grogan et al. 1991, Grogan 1989, Jones 1990, BIOMOVSI 1996).

Upland and Shallow soils

Two soil cases are considered: an upland soil and a shallow soil. Upland soil is the usual case, with the water table somewhat below the surface soil layer. In the shallow soil case, the water table extends into the surface soil on a regular and extended basis. The distinction between these two cases is important in how readily contaminated groundwater can reach the surface. In an upland soil case, it must be transported by processes such as capillary action. In the shallow soil case, the groundwater is directly discharged into the surface soil.

The two cases are distinguished using an input parameter called the depth to the water table, Z_d [m],

$$Z_d \geq Z_{ssi} \text{ signifies the upland soil case applies and} \quad (5.34a)$$

$$Z_d < Z_{ssi} \text{ specifies the shallow soil case applies,} \quad (5.34b)$$

where Z_{ssl} is the shallow soil limit [m] with a recommended value of 0.5 m because capillary rise decreases strongly with depth.

For both upland and shallow soil, the thickness of the active surface soil layer, Z_{ss} , is:

$$Z_{ss} = \min\{Z_s, Z_d\} \quad (5.35)$$

where

Z_s is the depth of soil normally accessed by plant roots [m], and

Z_d is the depth to the annual average water table [m].

Z_s is mandated by the empirical data used for the soil-to-plant transfer parameter. It represents the soil root zone compartment of most importance for contaminant-to-plant transfer, and its depth is based in part on plant behaviour and on the practical depth of a well-mixed plough layer in agricultural or garden settings.

Soil Type and Properties

The CC408 soil model can deal with four types of soil: sand, loam, clay, and organic. In each simulation, the soil type is an input parameter and is identified in the following equations and parameters using the variable name *stype*. For example, the input parameter $I_{irr}^{f,stype}$ represents the rate of irrigation of the field *f*, and is dependent on soil type found in the field. Other soil parameters also depend on soil type, such as bulk density, moisture content and soil/water partition coefficients.

It is assumed that all field types have the same soil type. It is also assumed that peat bog fields are exclusively associated with organic soil. That is, a peat bog can occur in a simulation if and only if the soil type is organic.

Field Types

The CC408 soil model simulates four different types of fields and their soils in the surface environment: a garden, forage field, woodlot and peatbog. The garden is used to supply vegetable produce (fruits, leafy vegetables, roots and grain) to members of the critical group and the forage field is used to supply footstuff for the animals used by the critical group for animal produce (milk, meat and bird products). The woodlot is used as a source of heating fuel and building materials. The peatbog is an alternate source of heating fuel.

Siting of the Fields

To maximize potential exposures to the critical group, the model assumes that the four fields are sited in areas that are most contaminated. These areas are the terrestrial discharge locations, where deep groundwaters reach the surface environment after having passed through the repository. (Section 5.3.6 describes another possibility where fields are sited in lake sediment.)

The various discharge locations are expected to be contaminated to varying extents, and it is desirable to site the fields in such a way that estimated impacts will be maximized. The following algorithm is used to that end; it sites the various fields *f* amongst the various discharge locations *d* (cf. Davis et al. 1993, p. 139-143) in a pessimistic fashion. The algorithm has two steps.

1. Discharge area importance. As discussed in Sections 4.8 and 5.2, each terrestrial discharge location is associated with a finite area, A_t^d and together they define the set, $\{A_t^d\}_d$, of discharge locations. This set may have just one member but typically several terrestrial discharge locations may exist. The first step in the algorithm is to order all members of the set according to their potential importance. The importance could be based on factors such as time of contaminant arrival, contaminant concentrations and total mass discharged. In CC408, the importance is specified by the user and corresponds to the order in which discharge locations appear in the input file.
2. Field importance. The various fields need not be located contiguously. For example, the vegetable garden can be spread among several discharge locations. The second step in the algorithm is to apportion the fields into the discharge areas. The area of each discharge location, starting from the most important location, is assigned to a field based on the field assignment priority. The field assignment priority is as follows:

- (i) peat, if peat is used as fuel, otherwise it is not assigned;
- (ii) garden;
- (iii) forage; and
- (iv) woodlot.

That is, the discharge location with the highest priority is first allotted to the highest priority field. If the area of the discharge location is large enough to contain that field, then its remaining area is allotted to the next highest priority field. If the area of the discharge location is insufficient to contain that field, then the discharge location with the next highest priority is also employed. The process continues until the entire area of all discharge locations is used, or the areas of all fields have been assigned. If the discharge locations have insufficient area for all fields, it is assumed that any additional needed area is free of groundwater contamination.

It is possible that all fields could be sited within one large discharge location, or that one large field spans several discharge locations. These possibilities are covered by the following specification:

$$A^f = \sum_d A_t^{f \in d} + A^{f \in 0} \quad (5.36)$$

where the summation is over all discharge locations d ,

A^f denotes the area [m²] of fields f (f =garden, forage field, woodlot or peatbog) which are defined in Equations (5.3) to (5.6),

$A_t^{f \in d}$ is the area of terrestrial field f which is located within discharge area d (i.e. $f \in d$) [m²], and

$A^{f \in 0}$ represents any extra area which might be needed for field f because the total available discharge areas have already been taken into consideration; this extra area is assumed to be free of groundwater contamination [m²].

In earlier versions of the soil model, the importance of discharge locations was based on the calculated contaminant concentrations, with the highest priority assigned to the location with the highest concentration. This approach necessitated the prior calculation of concentrations in all possible combinations of fields and discharge zones. The following description provides the equations needed for the all-combinations method to maintain continuity with the previous theory manual (and associated code) (Gierszewski et al. 2004). That is, the following equations first describe the calculation of a matrix of contaminant mass in soils for all possible combinations of fields and discharge locations, where any field is wholly or in part sited in each discharge location. In Section 5.4.4, the terrestrial areas $A_t^{f \in d}$ and the corresponding concentrations are then combined to arrive at the average contaminant concentrations in the fields as required for the current, simpler definition of discharge location importance.

Mathematical formulation

The equation describing the soil model is based on conservation of mass within a well-mixed compartment and is solved using the compartment model described in Appendix A. The equation is

$$\frac{dM_s^{i,(f \in d)}(t)}{dt} = X_{inflow}^{i,(f \in d)}(t) - \lambda_{loss}^{i,(f \in d)} M_s^{i,(f \in d)}(t) \quad (5.37)$$

where

$M_s^{i,(f \in d)}(t)$ represents the mass of contaminant i at time t within a soil compartment, $X_{inflow}^{i,(f \in d)}(t)$ is the total input flow of contaminant i to the compartment at time t [$\text{mol} \cdot \text{a}^{-1}$], and $\lambda_{loss}^{i,(f \in d)}$ is the total fractional loss rate of nuclide i from the soil compartment [a^{-1}].

In each of these variables, the superscripted acronym $f \in d$ signifies one of the possible combinations of field type f and discharge locations d . As noted earlier, the equation is solved for all such combinations.

The next two sections describe the components that contribute to the inflow and loss terms, $X_{inflow}^{i,(f \in d)}(t)$ and $\lambda_{loss}^{i,(f \in d)}$, and include a discussion of their dependence on factors such as field type and discharge location, soil type and whether the soil is categorized as upland or shallow.

5.4.2 Soil Inflow Terms

Figures 5.4 and 5.5 illustrate water and contaminant inflows for shallow and upland soil cases. The total input flow of contaminant i into the soil compartment, $X_{inflow}^{i,(f \in d)}(t)$, for any combination of field and discharge location, $f \in d$, can be expanded as follows:

$$X_{inflow}^{i,(f \in d)}(t) = X_{irrigation}^{i,(f \in d)}(t) + X_{deposition}^{i,(f \in d)}(t) + X_{discharge}^{i,(f \in d)}(t) + \lambda^p M_s^{i,(f \in d)}(t) \quad (5.38)$$

where

$\lambda^p M_s^{i,(f \in d)}(t)$ represents the ingrowth of radionuclide i from its parent nuclide, p , given as the product of the decay rate and mass of the parent, λ^p [a^{-1}] and $M_s^{i,(f \in d)}(t)$ [mol] for every field type f and discharge location d [$\text{mol} \cdot \text{a}^{-1}$];

$X_{deposition}^{i,(f \in d)}(t)$ is the inflow rate of contaminant i from atmospheric deposition into the soil of field type f in discharge location d [$\text{mol} \cdot \text{a}^{-1}$];

$X_{irrigation}^{i,(f \in d)}(t)$ is the inflow rate of contaminant i from irrigation into the soil of field type f in discharge location d [$\text{mol} \cdot \text{a}^{-1}$]; and

$X_{discharge}^{i,(f \in d)}(t)$ is the inflow rate from discharge (i.e. from upward movement of groundwater) of contaminant i into the soil of field type f in discharge location d [$\text{mol} \cdot \text{a}^{-1}$].

Each of these terms is discussed further below.

Ingrowth

The ingrowth term, $\lambda^p M_s^{i,(f \in d)}(t)$, is linearly dependent on the amount of the precursor or parent nuclide in the compartment, and on the decay constant of the parent.

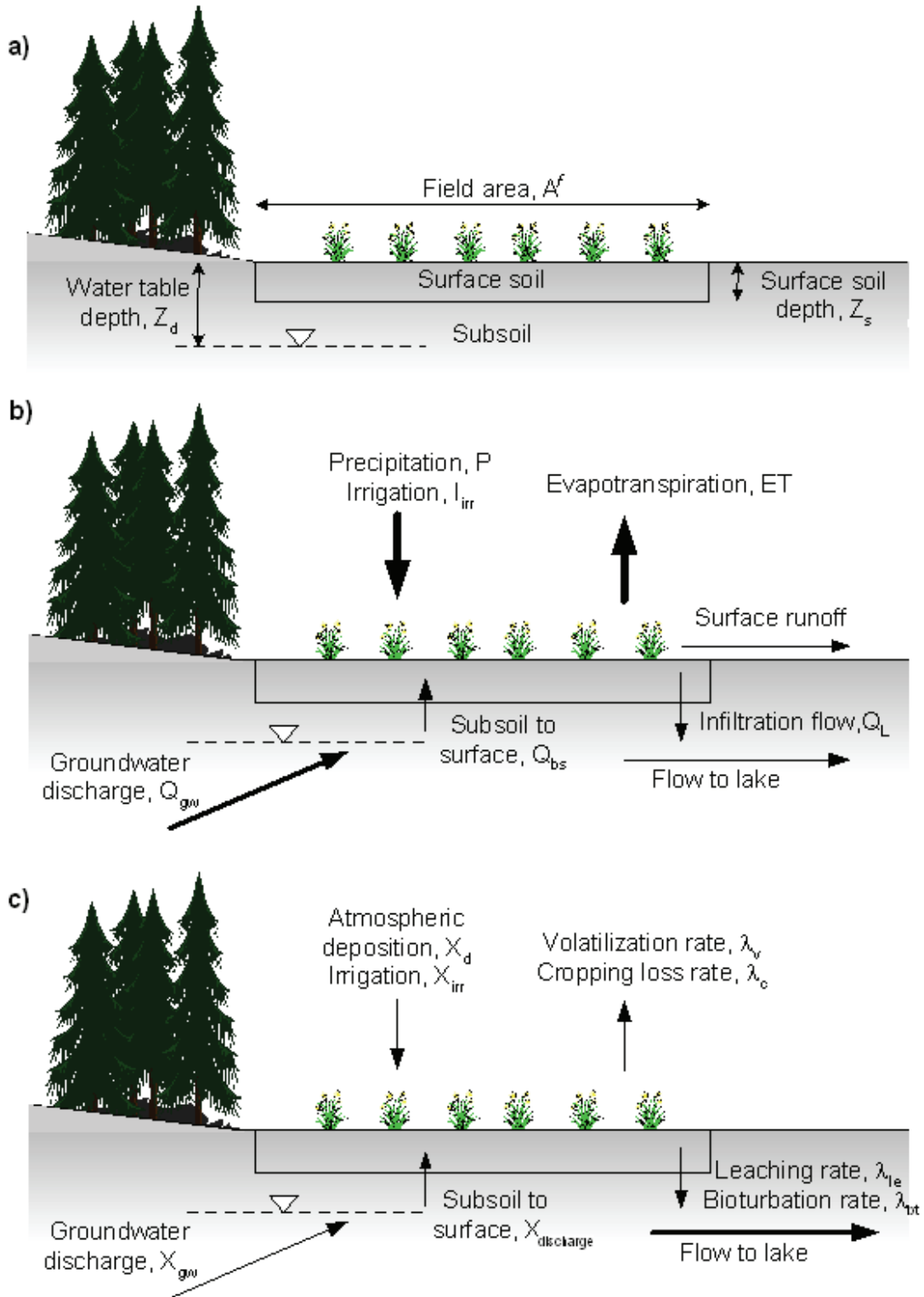


Figure 5.4: Illustration of the upland surface soil model: (a) dimensions, (b) water flow, and (c) contaminant flow

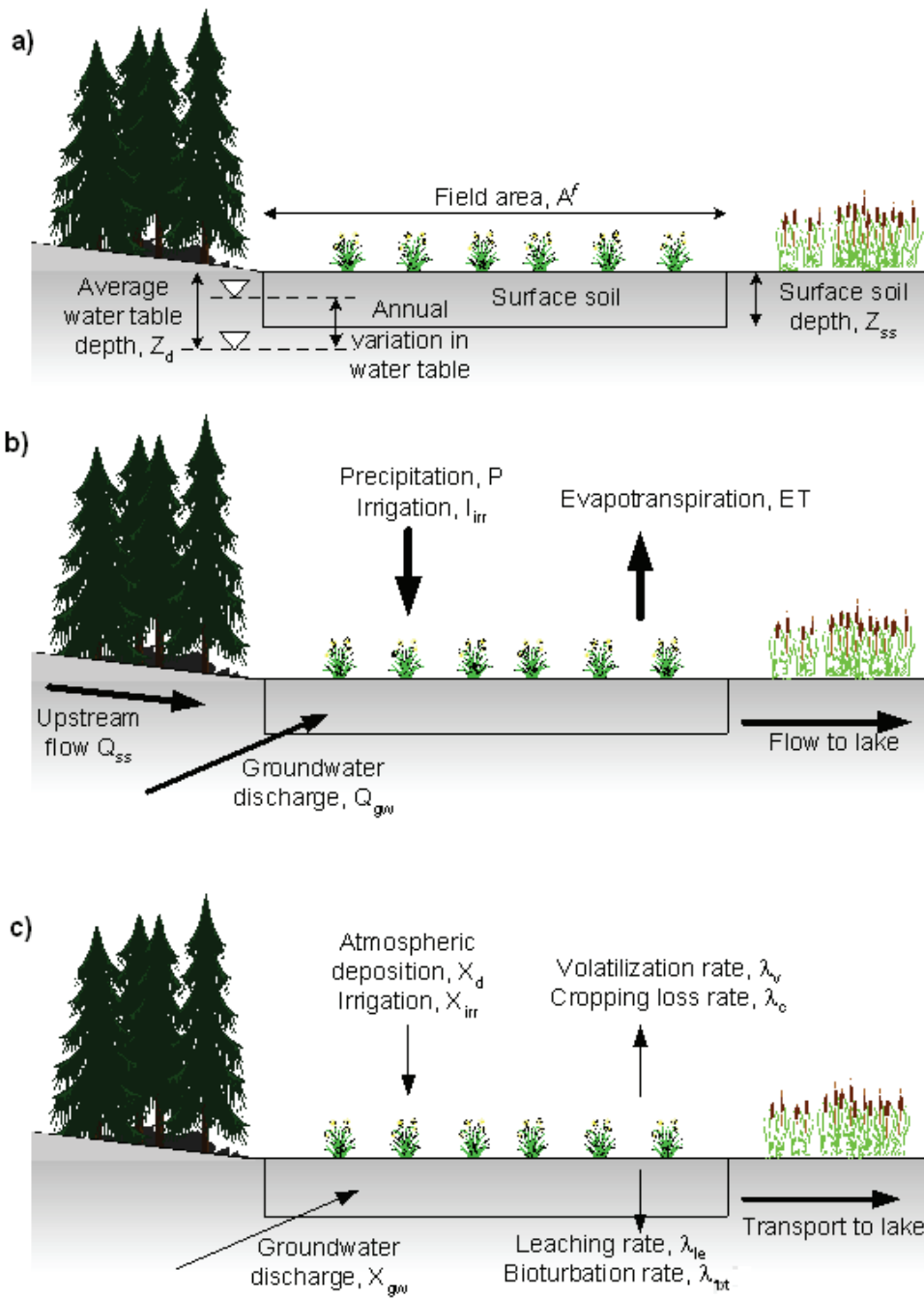


Figure 5.5: Illustration of the shallow soil model: (a) dimensions, (b) water flow, and (c) contaminant flow. In this model, the water table fluctuates seasonally into the surface soil region, so the groundwater discharge is assumed to go directly into the surface soil

In this model, ingrowth is calculated in the surface soil compartment only - not in the subsoil or in any of the input flow terms. Ingrowth is computed for both the upland and shallow soil model. Ingrowth during transit is most likely to be of importance in the transfer from the groundwater to the surface soil in the upland soil model, where the time scales of the process may be long enough.

Atmospheric Deposition

Atmospheric deposition contributes to both the upland soil and the shallow soil. The inflow rate from atmospheric deposition of contaminant i into the soil of field type f in discharge location d [mol a^{-1}], $X_{deposition}^{i,(f \in d)}(t)$ is given by

$$X_{deposition}^{i,(f \in d)}(t) = D_{soil}^i(t) \cdot \min\{A^f, A^d\} \quad (5.39)$$

where

$D_{soil}^i(t)$ is the atmospheric deposition rate of contaminant i onto the soil of at time t [$\text{mol m}^{-2} \text{a}^{-1}$] (see Sec. 5.5.10) and
 $\min\{A^f, A^d\}$ is the smaller of the areas of the field f and discharge location d for the combination of $f \in d$ under consideration [m^2].

The rate of atmospheric deposition rate of nuclides to soil, D_{soil} , is described in Section 5.5.10. In general, it is the sum of washout processes with precipitation, and dry deposition without precipitation. In either instance, the source of contaminants is taken to be the emissions from the surface of the lake.

The area factor, $\min\{A^f, A^d\}$, is required so that the airborne deposits are limited to the area of the field that is located in the discharge location. If the field is smaller than the discharge location, then its area defines the area available for deposition. If the field is larger than the deposition zone, then the available area is the entire discharge location area (and the part of the field in another discharge location is covered by a different $f \in d$ combination).

Irrigation

The inflow rate of contaminant i from irrigation is given by

$$X_{irrigation}^{i,(f \in d)}(t) = I_{irr}^{f,stype} \cdot C_{irr}^i(t) \cdot \min\{A^f, A^d\} \quad (5.40)$$

where

$I_{irr}^{f,stype}$ is the irrigation rate for each field f with soil type $stype$ [$\text{m}^3_{\text{water}} \cdot \text{m}^{-2}_{\text{soil}} \cdot \text{a}^{-1}$],
 $C_{irr}^i(t)$ is the concentration of contaminant i in the irrigation water at time t [$\text{mol} \cdot \text{m}^{-3}$], and
 $\min\{A^f, A^d\}$ is the smaller of the areas of the field f and discharge location d for the combination of $f \in d$ under consideration [m^2].

The CC408 model includes an input irrigation option which specifies whether irrigation is practised, and whether it includes the garden. The irrigation rate is another input parameter and it is dependent on the field and soil type. Finally, the source of irrigation water is also an input

parameter. The CC408 model assumes that a well, if it exists, is first used to supply domestic water. If irrigation of the garden is specified, then the irrigation water is obtained from the well, provided that the well has sufficient capacity. If the well is not able to supply the necessary water, then the CC408 model assumes that irrigation water is drawn from the lake. Finally, the CC408 model includes an option for irrigation of the forage field, but in this case the source of irrigation water is the lake. The concentration $C_{irr}^i(t)$ represents the concentration of contaminant i in the source of the irrigation water, which could be either the well or the lake.

Irrigation is included here for shallow soils because irrigation may be seasonally used regardless of the annual average water table depth.

Subsoil to surface soil nuclide transport

The surface soil is the layer that forms the substrate for food-chain pathways such as plant uptake, soil ingestion, inorganic building material, and external exposure. The subsoil is defined as the layer of soil subject to direct groundwater discharge from the geosphere.

Contaminants can move to the upland surface soil from subsoil contamination because of:

- capillary rise of water in response to evaporation at the soil surface,
- root uptake by deep-rooted plants,
- bioturbation (movement of soil by activities such as animal burrowing and tree-ploughing),
- biological transport (movement of contaminated organisms), and
- diffusion.

All of these processes are depth-limited - the deeper the contamination, the less effectively these processes can bring it to the surface.

Shallow soil is directly contaminated by groundwater, and the subsoil-to-surface-soil processes do not pertain to the shallow soil model. For shallow soil, the contaminant inflow is based directly on the discharge rate of contaminant i associated with groundwater discharge, $X_{gw}^{i,d}$.

The inflow of contaminant i for a shallow-soil field f located in discharge zone d is

$$X_{discharge}^{i,(f \in d)}(t) = X_{gw}^{i,d}(t) \cdot \frac{\min\{A^f, A^d\}}{A^d} \quad (\text{shallow soil}) \quad (5.41)$$

where

$X_{gw}^{i,d}(t)$ is the flow rate of contaminant i flow rate associated with groundwater discharge at discharge location d [mol a^{-1}] (see equation (5.12)); and

$\min\{A^f, A^d\}$ is the smaller of the areas of the field f and discharge location d for the combination of $f \in d$ under consideration (it is divided by the discharge area to yield the fraction of total discharge into d that reaches field f) [m^2].

For upland soils (i.e., surface soils above the water table), the net effect of these processes is modelled by defining a flow of water, Q_{bs}^d , from the subsoil to the surface soil. Plant uptake from the subsoil has an implied flow of water, but the concentration of nuclide in the water is modified (usually decreased) by the transfer across the cell membranes of the root. Bioturbation and diffusion may not directly involve a physical movement of water. Nonetheless, the transfer can be simulated by specifying a water flow that results in nuclide transfer

consistent with the underlying processes. The nuclide flow $X_{discharge}^{i,(f \in d)}$ for upland soils is defined by:

$$X_{discharge}^{i,(f \in d)} = C_{pw}^{i,d} \cdot Q_{bs} \cdot \min\{A^f, A^d\} \quad (\text{upland soil}) \quad (5.42)$$

where

$C_{pw}^{i,d}$ is the groundwater pore water nuclide concentration at location d [$\text{mol} \cdot \text{m}^{-3}$ water],
 Q_{bs} is the water flux from the subsoil to the surface soil [m^3 water $\cdot \text{m}^{-2}$ soil $\cdot \text{a}^{-1}$], and
 $\min\{A^f, A^d\}$ is the smaller of the areas of the field f and discharge location d for the combination of $f \in d$ under consideration [m^2].

In general, the groundwater pore water concentration $C_{pw}^{i,d}(t)$ for each discharge location could be calculated using a compartment model with input and output flows similar to the surface soil submodel. This was the approach used in CC3 (Davis et al. 1993, p.78). However, since the groundwater contribution to the surface soil is expected to be small for most upland soils, a simple approximation is used here (see Equation (5.12)):

$$C_{pw}^{i,d}(t) \approx C_{gw}^{i,d}(t) = X_{gw}^{i,d}(t) / Q_{gw}^d \quad (5.43)$$

where, from Equation (5.12),

$C_{gw}^{i,d}(t)$ is the concentration of contaminant i in the groundwater discharging at location d [mol m^{-3}],
 $X_{gw}^{i,d}(t)$ is the flow of contaminant i from the geosphere into discharge zone d at time t [$\text{mol} \cdot \text{a}^{-1}$], and
 Q_{gw}^d is the volumetric water discharge rate from the geosphere into this subsoil (discharge) zone d [$\text{m}^3 \cdot \text{a}^{-1}$].

The assumption that subsoil porewater and geosphere concentrations are equal means that Equations (5.41) and (5.42) are almost identical (when allowance is made for the differences between Q_{bs} and Q_{gw}^d). It also means that the soil between the geosphere (i.e., the overburden layer) and the surface soil does not affect the concentration of the water entering the surface soil compartment. This situation would be true when nuclide concentrations in the soil profile are at steady state, which could occur in a few years for a shallow intervening layer of soil and a mobile nuclide. For a thicker intervening soil and a less mobile nuclide, steady state might not occur for thousands of years. This assumption is therefore conservative because nuclide movement from groundwater into the surface soil compartment would otherwise be lower.

Deriving the value of Q_{bs} is not straightforward. The approach adopted here is to acknowledge that upward flow probably only occurs in summer. The upper limit for Q_{bs} can then be set equal to the summer water deficit, Q_{swd} ; that is, capillary rise of water from the water table is able to meet the evaporative demand that causes the summer water deficit. The value of Q_{swd} would be based on meteorological information and is not dependent on soil properties. For example, long-term records of rainfall and potential evaporation for the summer water deficit in the

Northern Ontario portion of the Shield indicate that the amount of water needed to eliminate the deficit is about 0.2 m a^{-1} .

When the depth to the water table, Z_d , is equal to the shallow soil limit, Z_{ssl} , the flow of water from the subsoil to the surface soil, Q_{gw}^d , will be able to meet the summer water deficit, Q_{swd} .

When the water table is further from the surface, soil properties will limit the upward flow of water. In this case, the flow will be less than Q_{swd} . Hillel (1980) provides an overview of the theory to estimate water flow from a water table to the soil surface. The effect of depth is very pronounced; flow varies as a function of $(Z_d)^{-b}$ where b is about 3 for a fine sandy loam (where capillary rise is probably most effective). This relationship can be summarized as:

$$Q_{bs} = Q_{swd} \left(\frac{Z_{ssl}}{Z_d} \right)^b, \text{ if } Z_d \geq Z_{ssl} \quad (5.44)$$

where:

- Q_{bs} is the flow of water from the subsoil to the surface soil [$\text{m}^3_{\text{water}} \cdot \text{m}^{-2}_{\text{soil}} \cdot \text{a}^{-1}$],
- Q_{swd} is the summer water deficit [$\text{m}^3_{\text{water}} \cdot \text{m}^{-2}_{\text{soil}} \cdot \text{a}^{-1}$],
- Z_{ssl} is the shallow soil limit [m],
- Z_d is the depth to the water table [m], and
- b is about 3 for a fine sandy loam.

When $Z_d < Z_{ssl}$, the water table is close to the surface and Equation (5.44) does not apply and the shallow soil model should be used.

Irrigation affects the relationship in Equation (5.44). If the field corresponding to this discharge area is irrigated, then the irrigation water will remove some portion of the water deficit. In this case, there will be less capillary rise because there is a decreased soil water-pressure gradient to draw the water upward. Thus, if irrigation is practiced, the value of Q_{bs} is revised as follows:

$$\text{If } Q_{bs} > Q_{swd} - I_{irr}^{f,stype}, \text{ then } Q_{bs} = \max \begin{cases} Q_{swd} - I_{irr}^{f,stype} \\ 0 \end{cases} \quad (5.45)$$

Note also that conservation of nuclide mass requires that:

$$Q_{bs} \leq (Q_{gw}^d / A^d) \quad (5.46)$$

where A^d is the area [m^2] of discharge location d .

5.4.3 Loss Terms

The total loss rate of contaminant i , $\lambda_{loss}^{i,(f \in d)}$, is the sum of all the fractional loss rate terms for the nuclide loss mechanisms included in the soil submodel:

$$\lambda_{loss}^{i,(f \in d)} = \lambda^i + \lambda_v^i + \lambda_c^i + \lambda_e^{i,(f \in d)} + \lambda_{bt}^i \quad (5.47)$$

where several terms are not dependent on field f or discharge location d and where

λ^i is the loss due to radioactive decay of nuclide i [a^{-1}],

- λ_v^i is the loss of contaminant i due to volatilization [a^{-1}],
 $\lambda_c^{i,f}$ is the loss of contaminant i due to crop removal (cropping) [a^{-1}],
 $\lambda_{le}^{i,(f=d)}$ is the loss of contaminant i due to leaching [a^{-1}], and
 λ_{bt}^i is the loss of contaminant i due to bioturbation by flora and fauna [a^{-1}].

The loss of nuclides through the loss of surface soil particles by erosion has been reviewed (Sheppard 1995). Erosion models tend to be site-specific (e.g., dependent on slope). These loss rates also tend to be small on the Canadian Shield with its relatively flat topology, and may be compensated for on long time scales by soil formation (possibly from deposition from flooding). In the present soil model, erosion and soil formation are not further considered.

Most of the loss terms are simple input parameters that are not dependent on other parameters in the model. However, the leaching loss is dependent on precipitation and soil properties such as dry bulk density and the soil/water partition coefficient. Thus the leaching loss, $\lambda_{le}^{i,(f=d)}$, is both soil (texture) and nuclide specific. Similarly, $\lambda_c^{i,f}$, the loss due to crop removal, is crop (yield and uptake), soil type and nuclide specific as noted in Section 5.6.2.

Radioactive decay and volatilization

Radioactive decay is the simplest type of loss, where λ^i is a physical constant for each nuclide i . Other simple loss terms arise from degassing or volatilisation for each nuclide, λ_v^i , and are described in Davis et al. (1993) and Zach et al. (1996). They are also input parameters.

Volatilization losses are treated the same in shallow soil and upland soil. There are very few data on volatilisation of the important nuclides; certainly not enough to differentiate rates based on soil moisture. Despite higher moisture contents, shallow soils still support plants, and plants especially in wetland settings mediate gas exchange between the soil and the atmosphere. Many plants adapted to wetlands have air tubes (aerenchyma) from the shoot to the root, and these are known to transport gases both up and down.

Cropping loss

Loss of nuclide by removal of plant material, $\lambda_c^{i,f}$ (nuclide cropping loss), was also described in Davis et al. (1993) for the upland soil. It is based on an assumption that recycling of nuclides (and nutrients) is less than perfect, so that biological processes such as loss of plant material and animal migration (agricultural or natural) will result in some loss of nuclide from a specific assessment location. The cropping loss $\lambda_c^{i,f}$ for each field type f and nuclide i is defined as:

$$\lambda_c^{i,f} = (f_{cl} CR^{i,f} Y_{p,min}^f) / (Z_{ss} \rho_{soil}) \quad (5.48)$$

where

- f_{cl} is the fraction of crop elemental composition lost each year [-];
 $CR^{i,f}$ is the plant/soil concentration ratio for nuclide i and field f [$kg_{wetbio} \cdot kg^{-1}_{wetsoil}$];
 Z_{ss} is the depth of rooting zone soil [m];
 ρ_{soil} is dry soil bulk density [$kg \cdot m^{-3}_{drysoil}$]; and

$Y_{p,min}^f$ is the minimum plant biomass yield for field f [$\text{kg}_{\text{wetbio}} \cdot \text{m}^{-2} \cdot \text{a}^{-1}$]:

$$Y_{p,min}^f = Y_p^{\text{garden}} ff_{\text{crop}} \quad \text{for } f = \text{garden} \quad (5.49a)$$

$$Y_{p,min}^f = \min^j (Y_p^{\text{forage}}) ff_{\text{crop}}, \quad j = \text{meat, milk, bird} \quad \text{for } f = \text{forage, and} \quad (5.49b)$$

$$Y_{p,min}^f = Y_w ff_{\text{woodlot}} \quad \text{for } f = \text{woodlot} \quad (5.49c)$$

for which

Y_p^{garden} is the garden plant yield for human food [$\text{kg}_{\text{wetbio}} \cdot \text{m}^{-2}$],

Y_p^{forage} is the forage plant yield for animal food type j [$\text{kg}_{\text{wetbio}} \cdot \text{m}^{-2}$],

Y_w is the plant yield for wood (for building or fuel) [$\text{kg}_{\text{wetbio}} \cdot \text{m}^{-2}_{\text{soil}}$],

ff_{crop} is the cropping frequency of garden or forage fields [a^{-1}], and

ff_{woodlot} is the cutting frequency of woodlot field [a^{-1}].

Humans must occupy the site and use it for farming for cropping to occur. Therefore, assuming that a field that is irrigated will be cropped, cropping losses are allowed only over the irrigation period, I_p . In cases when there is no irrigation, the cropping loss is applied over a 50-year period (Davis et al. 1993). As a result of this restriction $\lambda_c^{i,f}$ is set to the value estimated by Equation (5.48) in the period defined by I_p (or 50 years), and to zero for times outside the period.

Leaching loss

Loss by leaching, $\lambda_{le}^{i,(f \in d)}$ deals with downward migration through the soil in solution or on colloidal particles. It is usually considered that the flow is through a porous medium, but it can also be used to reflect flow in soil cracks. The nuclides are lost from the surface soil, but are assumed to quickly move down to the water table and from there to the lake.

The mobile phase is usually thought of as the nuclide in soil porewater, so that $\lambda_{le}^{i,(f \in d)}$ can be based on the fraction of soil pore water that leaves the soil per unit time. The amount of contamination in the pore water can be computed using the solid/liquid partition coefficient, K_d^i (which is element-dependent), and parameters for soil bulk density and moisture content. Values of K_d^i , and hence $\lambda_{le}^{i,(f \in d)}$ are strongly dependent on nuclide and soil type, and can also include sorption on mobile colloidal particles. Bulk density and moisture content vary with soil type. Clearly, moisture content varies on a much shorter time scale (days to weeks) than intended for the model (years to centuries), but water movement only occurs when the soil reaches field capacity (field capacity is the amount of water a soil can hold against gravity, because of capillarity in soil pores). Field capacity is essentially a constant property for a given soil.

For the upland soil, the simplest formula for the leaching rate, $\lambda_{le}^{i,(f \in d)}$, for nuclide i is (Baes and Sharp 1981):

$$\lambda_{le}^{i,(f \in d)} = \frac{Q_L^{(f \in d)}}{(\theta_s + K_d^i \rho_{\text{soil}}) \cdot Z_{ss}} \quad (5.50)$$

where

- $Q_L^{(f \in d)}$ is the net infiltration rate of water through the soil [$m \cdot a^{-1}$],
 θ_s is the volumetric water-content of the surface soil [$m^3_{\text{water}} \cdot m^{-3}_{\text{soil}}$],
 Z_{ss} is the depth of the surface soil layer [m],
 K_d^i is the sorption coefficient of nuclide i in the surface soil [$m^3 \cdot kg^{-1}$], and
 ρ_{soil} is the dry bulk density of the surface soil [$kg \cdot m^{-3}_{\text{drysoil}}$].

The net infiltration rate of water into the soil for field type f is:

$$Q_L^{(f \in d)} = f_{le} \cdot (Q_{bs}^{(f \in d)} + I_{irr}^{f,stype} + R_T) \quad (5.51)$$

where

- f_{le} is an input leaching rate fraction for upland soils (i.e., fraction leaching relative to total input minus evapotranspiration [-]),
 $Q_{bs}^{(f \in d)}$ is the water flow from the subsoil to surface soil for field type f and discharge location d [$m \cdot a^{-1}$],
 $I_{irr}^{f,stype}$ is the irrigation rate for field f and soil type $stype$ [$m \cdot a^{-1}$], and
 R_T is the average watershed runoff rate [$m^3_{\text{water}} \cdot m^{-2}_{\text{soil}} \cdot a^{-1}$].

The watershed runoff rate is the difference between the total precipitation, P_{tot} , and the evapotranspiration rate, ET,

$$R_T = P_{tot} - ET. \quad (5.52)$$

This water either runs off the surface of the soil or penetrates into the soil down to the water table. It ultimately shows up with the total watershed outflow.

For the shallow soil model, the expression for $\lambda_{le}^{i,(f \in d)}$ is computed from a similar water mass balance:

$$\lambda_{le}^{i,(f \in d)} = \frac{(Q_{ss} + Q_{gw}^d) / A^d + I_{irr}^{f,stype} + R_T}{(\theta_s + \rho_{soil} \cdot K_d^i) \cdot Z_{ss}} \quad (5.53)$$

where

- Q_{ss} is the flow of uncontaminated water from other areas of the catchment [$m^3 \cdot a^{-1}$],
 Q_{gw}^d is the flow of water from the geosphere overburden at location d as calculated in the geosphere model [$m^3 \cdot a^{-1}$], and
 A^d is area of a discharge location d [m^2].

For a specific site, Q_{ss} would refer to the uncontaminated flow from the area of the catchment upslope to the discharge area.

Biologically Mediated Loss

Loss by flora or fauna-relatedurbation (bioturbation) processes, λ_{bt}^i , is not a single concept. In Section 5.4.1, bioturbation was considered based on the concept that earthworms and plant roots could bring nuclides up from the subsoil. Similarly, the mixing of contaminated surface soil into the subsoil could occur by biologically mediated transport, thus removing it from the most active root zone. Stated another way, this process is the dilution of the contaminated surface soil with clean subsoil materials.

This loss mechanism is not applicable to a shallow soil because the shallow soil is very close to or extends down to the water table. Biota do not operate effectively below the water table, and so there is little biologically mediated movement across the water table plane. Some plant roots can extend into the water table, because they can transport some oxygen internally from the surface into the water-saturated soil. However, the amount of root penetration supported in this way is minor.

This parameter is included for completeness, but is likely not important in Canadian Shield settings. Affected nuclides are removed from the surface soil, but assumed to quickly reach the water table and from there move to the lake.

5.4.4 Contaminant Concentrations in the Field Soils

The final result required from the soil model are concentrations of contaminant i in the soils of different fields. The total contaminant concentration (both surface-sorbed and porewater) in the surface soil, on a dry weight basis, is computed for every combination of field f and discharge location d :

$$C_{soil}^{i,(f \in d)}(t) = \frac{M_s^{i,(f \in d)}(t)}{\min\{A^f, A^d\} \cdot Z_{ss} \cdot \rho_{soil}} \quad (5.54)$$

where

$C_{soil}^{i,(f \in d)}(t)$ is the total concentration of contaminant t in the surface soil for the combination of field f and discharge location d [$\text{mol} \cdot \text{kg}^{-1}_{\text{drysoil}}$];

$M_s^{i,(f \in d)}(t)$ is the mass of contaminant i in field f and discharge location d , resulting from the solution of Equation (5.37) [mol];

$\min\{A^f, A^d\}$ is the smaller of the areas of the field f and discharge location d for the combination of $(f \in d)$ under consideration [m^2];

Z_{ss} is the depth of the surface soil compartment in field f [m]; and

ρ_{soil} is the dry bulk density of the surface soil in field f [$\text{kg} \cdot \text{m}^{-3}_{\text{drysoil}}$].

For the use of peat as heating fuel, Szekely et al. (1994) indicated that an average concentration with depth was used. To do this with the present model requires estimation of K_d and related parameters for the subsoil. There are few data to support this, and the effect on total dose is not likely to be significant. Instead, the assumption is made that all the peat used for fuel has the concentration of the surface (peat) soil.

To estimate the total mass in the soil, only the surface soil to depth Z_{ss} is considered, because this is the only compartment that receives nuclide flow from the geosphere. In a real setting, there would be nuclide in the intervening subsoil, but this contaminant is assumed here to reach the surface soil instantaneously.

Equation (5.54) provides the concentration of contaminant i in different combinations of fields and discharge locations. In accordance with the field location algorithm described in Section 5.4.1,

$$C_{soil}^{i,f}(t) = \frac{\sum_d C_{soil}^{i,(f \in d)}(t) \cdot A_t^{f \in d}}{A^f} \quad (5.55)$$

where the summation runs over all discharge locations d ,

$C_{soil}^{i,f}(t)$ is the concentration [mol m^{-3}] of contaminant i in the soil of field f , considering all discharge locations that may include all or a portion of the field;

$A_t^{f \in d}$ is the area [m^2] of field f that is within discharge location d , as established by the importance algorithm; and

A^f is the area [m^2] of field f , calculated in Equations (5.3) to (5.6).

The extra area term $A^{f \in 0}$, which was defined in Equation (5.36), is not required here because the concentration of contaminant i is zero in this extra area.

5.5 THE ATMOSPHERE SUBMODEL

5.5.1 General

The purpose of the atmosphere submodel is to calculate nuclide concentrations in air due to suspension of particulates and gases from soils, vegetation and water bodies. The processes considered in the atmosphere submodel are shown in Figure 5.6. We assume that these processes endure during all states, but the extent to which they occur is controlled by state-dependent parameter values (see Appendix C). For instance, suspension arising from fuel fires could increase during permafrost and proglacial lake states, but this and most other processes occurring in the biosphere could be strongly attenuated during an ice sheet state.

The inputs to the atmosphere submodel are (dropping their time-dependence for clarity):

- $C_{soil}^{i,f}$ - the concentration of nuclide i in the soil root zone for a field f (garden, forage, woodlot, peatbog), from Equation (5.55) of the soil model [$\text{mol} \cdot \text{kg}^{-1}_{\text{drysoil}}$];
- $C_{seeds}^{i,f}$ - the concentration of nuclide i in sediments used as soil for each field f – available from Equation (5.32) of the surface water submodel, [$\text{mol} \cdot \text{kg}^{-1}_{\text{drysoil}}$];
- C_L^i - the concentration of nuclide i in surface water body from Equation (5.20) of the surface water model [$\text{mol} \cdot \text{m}^{-3}_{\text{water}}$];
- C_{well}^i - the concentration of nuclide i in well water, from Equation (5.11) using discharges calculated in the geosphere model [$\text{mol} \cdot \text{m}^{-3}_{\text{water}}$]; and

$X_{gw}^{i,d}$ and $X_{gw}^{p,d}$ - the flow of nuclides i and p from the geosphere to the biosphere, from Equation (5.10) for parent nuclide p and calculated in the geosphere model for nuclide i [mol/a].

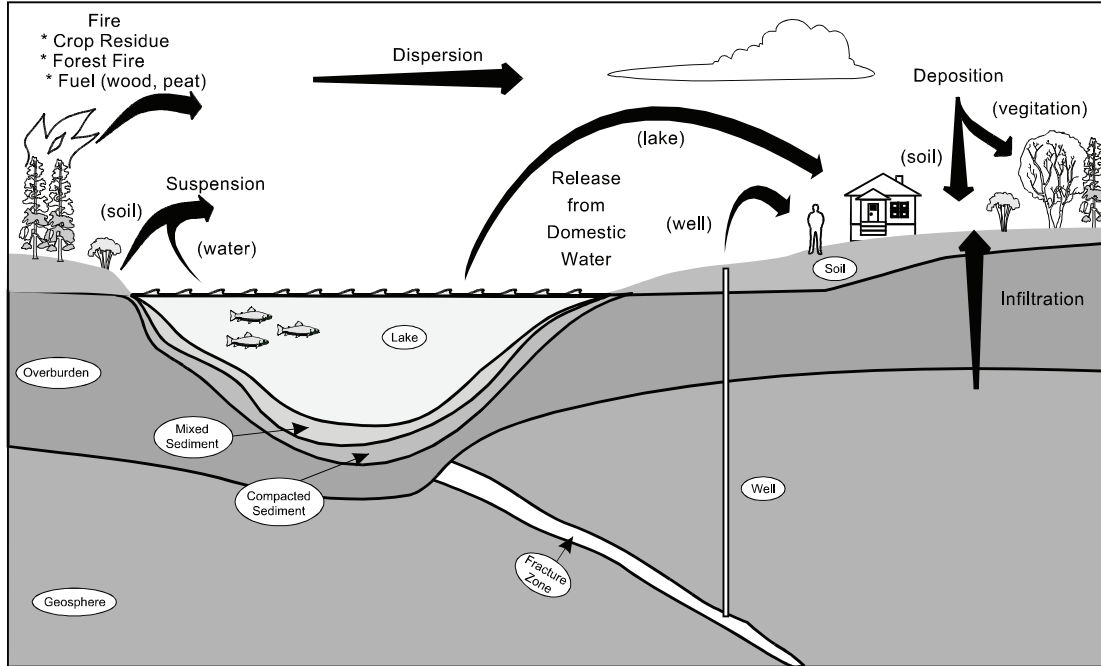


Figure 5.6: Transport processes considered in the atmosphere submodel (Goodwin et al. 1994)

The primary output of the atmosphere model is the concentration of nuclide i in air C_{air} (indoor and outdoor concentrations may differ).

The normal surface soil substrate is used for the terrestrial air contaminant source unless lake sediments are used for farming. That is:

$$C_{se}^{i,f} = C_{soil}^{i,f} \quad \text{if soil is the substrate, or} \quad (5.56a)$$

$$C_{se}^{i,f} = C_{segs}^{i,f} \quad \text{if lake sediment is used as soil} \quad (5.56b)$$

where $C_{se}^{i,f}$ is the concentration of nuclide i in the soil for field f (garden, forage, woodlot, peatbog) used as substrate for exposure pathways [$\text{mol} \cdot \text{kg}^{-1}_{\text{soil}}$].

Most elements reaching the surface through the groundwater will be in a relatively non-volatile form. Other than the noble gases, there are three pathways by which nuclides could be dispersed into the atmosphere:

1. as particulates (dust) from terrestrial sources – TP ;
2. as particulates (aerosols) from aquatic sources – AP ; and

3. as particulates from the burning of biomass, through agricultural fires (*AF*), burning peat or wood for energy (*EF*) or land fires (*LF*).

The noble gases argon, krypton and xenon are inert, and move rapidly through the biosphere without accumulating in the food chain. They do not cause appreciable internal dose because they are not retained in the body. Since the dominant dose pathway is air immersion (ICRP 1979), only air concentrations are needed. These are estimated conservatively by assuming these nuclides are released instantaneously from the geosphere groundwater discharging through the lake, *GWR*. Radon is also a noble gas, but because ^{222}Rn quickly decays into particulate daughters that can cause inhalation dose, it is treated separately.

Tritium (^3H) concentrations in air are not calculated because of a special specific activity relationship used in the food-chain submodel (discussed in Section 5.6).

Some important nuclides - notably ^{14}C , ^{36}Cl , ^{129}I and ^{222}Rn - can also be in a gaseous or volatile form. For these nuclides, we include four additional pathways:

1. gaseous emissions from terrestrial sources – *TG*,
2. gaseous emissions from aquatic sources – *AG*,
3. indoor radon emissions from soil – *IRN*, and
4. indoor suspension from water - *ISW*.

The above ten pathways are represented in the following discussion using the acronyms *TP*, *AP*, *TG*, *AG*, *AF*, *EF*, *LF*, *IRN*, *ISW* and *GWR*.

The total indoor or outdoor air concentration C_{air}^i for nuclide *i* is just the sum of all the appropriate contributions for the nuclide.

Note that this model assumes that the atmospheric particulates are all contaminated to the same extent as the contaminating source. That is, there is no separate ingrowth or decay for the air concentration.

5.5.2 Particulates

Terrestrial (*TP*):

$$C_{air,TP}^{i,f} = A_{DLT} \cdot C_{se}^{i,f} \quad i \neq \text{Ar, Kr, Xe} \quad (5.57)$$

where

$C_{air,TP}^{i,f}$ is the indoor or outdoor air concentration of nuclide *i* from terrestrial sources for field type *f* (garden, forage, woodlot, peatbog) [$\text{mol} \cdot \text{m}^{-3}_{\text{air}}$],
 A_{DLT} is the atmospheric dust load from soil [$\text{kg}_{\text{drysoil}} \cdot \text{m}^{-3}_{\text{air}}$], and
 $C_{se}^{i,f}$ is the concentration of nuclide *i* in the soil for field *f* (garden, forage, woodlot, peatbog) used as substrate for exposure pathways [$\text{mol} \cdot \text{kg}^{-1}_{\text{soil}}$].

Aquatic (*AP*):

$$C_{air,AP}^i = A_{DLA} \cdot C_L^i \quad i \neq \text{Ar, Kr, Xe} \quad (5.58)$$

where

- $C_{air,AP}^i$ is the indoor or outdoor air concentration of nuclide i from aquatic sources [mol·m⁻³_{air}],
 A_{ADL} is the atmospheric particle (aerosol) load from aquatic sources [m³_{water}·m⁻³_{air}],
 C_L^i is the concentration of nuclide i in the lakewater [mol·m⁻³_{water}].

5.5.3 Indoor suspension from water (ISW)

The indoor air concentration due to suspension from domestic water usage is:

$$C_{air,ISW}^i = \frac{N_{crit} fr_{iw}^i Q_{pc}}{V_{bldg} I_{bldg} csa} \cdot \begin{cases} C_{well}^i & \text{if well} \\ C_L^i & \text{if lake} \end{cases} \quad (5.59)$$

for whichever is the domestic water source (lake or well), where

- $C_{air,ISW}^i$ is the indoor air concentration of nuclide i from indoor water usage [mol·m⁻³_{air}],
 C_{well}^i is the concentration of nuclide i in the well water [mol·m⁻³_{water}],
 C_L^i is the concentration of nuclide i in the lakewater [mol·m⁻³_{water}],
 N_{crit} is the number of persons in the critical group [persons],
 fr_{iw}^i is the fraction of nuclide i released to indoor air from the water [-],
 Q_{pc} is the annual domestic water demand per person for drinking and domestic use (bathing, laundry, etc.) [m³_{water}·(person·a)⁻¹],
 I_{bldg} is the building infiltration rate [s⁻¹], and
 csa is the number of seconds per tropical year 31,556,926 [s a⁻¹].

The building volume V_{bldg} is estimated from the nominal height H_{bldg} and width W_{bldg} , assuming an square footprint

$$V_{bldg} = H_{bldg} \cdot W_{bldg}^2 \quad (5.60)$$

5.5.4 Terrestrial Degassing (TG)

The air concentration due to degassing of volatile nuclides from soil is $C_{air,TG}^i$ [mol·m⁻³_{air}],

$$C_{air,TG}^{Rn} = q_{Rn} \cdot \max[C_{se}^{Ra,f}] \cdot D_T^{all} \quad i = {}^{222}Rn \quad (5.61)$$

$$C_{air,TG}^i = \frac{\lambda_V^i}{csa} \cdot \max[C_{se}^{i,f}] \cdot Z_{ss} \cdot \rho_{soil} \cdot D_T^{all} \quad i \neq {}^{222}Rn \quad (5.62)$$

where

- q_{Rn} is the radon emission rate per unit ²²⁶Ra concentration in the soil [mol_{222Rn} m⁻²_{soil} s⁻¹ mol⁻¹_{226Ra} kg_{drysoil}],

$\max[C_{se}^{Ra,f}]$ is the maximum concentration among field types f (garden, forage, woodlot, peatbog) of ^{226}Ra in soil (or sediment as soil) [$\text{mol}_{^{226}\text{Ra}} \cdot \text{kg}_{\text{drysoil}}^{-1}$],
 λ_{ν}^i is the volatilization rate constant for nuclide i degassing from soil [a^{-1}],
 $\max[C_{se}^{i,f}]$ is the maximum concentration among field types f (garden, forage, woodlot, peatbog) of nuclide i in soil (or sediment as soil) [$\text{mol} \cdot \text{kg}_{\text{drysoil}}^{-1}$],
 Z_{ss} is the surface soil depth [m],
 ρ_{soil} is the surface soil dry bulk density, depending on soil type [$\text{kg}_{\text{drysoil}} \cdot \text{m}^{-3}$], and
 c_{sa} is the number of seconds per tropical year 31,556,926 [s a^{-1}].

The annual average atmospheric dispersion factor for a ground-level terrestrial area source is D_T^{all} [$\text{s} \cdot \text{m}^2_{\text{soil}} \cdot \text{m}^{-3}_{\text{air}}$]. A semi-empirical dispersion model, based on the average wind speed across the Canadian Shield and suitable for use with a ground-level area source and a receptor height of 1.5 m, was developed by Davis et al. (1993, p.170):

$$D_T^{\text{all}} = \left[4.87 \cdot \left(\frac{A_{\text{total}}}{\text{m}^2} \right)^{1/8} - 3.56 \right] \cdot \left(\frac{U_{w,\text{ref}}}{U_w} \right) \frac{s}{m} \quad (5.63)$$

where

$A_{\text{total}} = \sum_f A^f$ is the total field area [m^2],

A^f is the area of field f (forage field, woodlot, garden, peatbog) [m^2],

$U_{w,\text{ref}} = 2.36$ m/s, is the annual average wind speed across the Canadian Shield, and

U_w is the annual average wind speed at the repository site [m/s].

5.5.5 Aquatic Degassing (AG)

The air concentration due to degassing of volatile nuclides from the lake water is $C_{\text{air,AG}}^i$ [$\text{mol} \cdot \text{m}^{-3}_{\text{air}}$]:

$$C_{\text{air,AG}}^i = \frac{\lambda_{\text{vol}}^i}{c_{sa}} C_L^i Z_L D_L \quad (5.64)$$

where

$C_{\text{air,AG}}^i$ is the indoor or outdoor air concentration of nuclide i from aquatic degassing [$\text{mol} \cdot \text{m}^{-3}_{\text{air}}$],

λ_{vol}^i is the water-to-air loss rate constant for nuclide i for surface water [a^{-1}],

c_{sa} is the number of seconds per tropical year 31,556,926 [s a^{-1}],

C_L^i is the concentration of nuclide i in lake water [$\text{mol} \cdot \text{m}^{-3}$],

Z_L is the lake depth [m], and

D_L is a semi-empirical dispersion function over water [$\text{s} \cdot \text{m}^2_{\text{water}} \cdot \text{m}^{-3}_{\text{air}}$], defined for the average Canadian Shield wind speed by Davis et al. (1993, p.170):

$$D_L = \exp(5 \cdot \ln(\ln A_L) - 9) \cdot \left(\frac{U_{w,ref}}{U_w} \right) \frac{s}{m} \quad (5.65)$$

where

A_L is the surface area of the water body [m²],
 $U_{w,ref}$ = 2.36 m/s, is the annual average wind speed across the Canadian Shield, and
 U_w is the annual average wind speed at the repository site [m/s].

5.5.6 Indoor Radon Gas Sources (IRN)

$$C_{air,IRN}^{Rn} = \max[C_{se}^{Ra,f}] \cdot Ki_{Rn} \quad (5.66)$$

where

$C_{air,IRN}^{Rn}$ is the indoor air concentration of ²²²Rn from gaseous emission from soil sources f , (garden, forage, woodlot, peatbog) [mol·m⁻³_{air}],
 $\max[C_{se}^{Ra,f}]$ is the maximum concentration among field types f (garden, forage, woodlot, peatbog) of ²²⁶Ra in soil (or sediment as soil) [mol²²⁶Ra·kg⁻¹_{drysoil}], and
 Ki_{Rn} is the indoor radon transfer coefficient from ²²⁶Ra [(mol²²²Rn·m⁻³_{air})/(mol²²⁶Ra·kg⁻¹_{drysoil})].

5.5.7 Noble Gas Groundwater Release (GWR)

The noble gases are assumed to discharge through the lake to the air.

$$C_{air,GWR}^i = \left(\sum_d X_{gw}^{i,d} \right) / (A_L \cdot csa) D_L \quad i = Ar, Kr, Xe \quad (5.67)$$

where

$C_{air,GWR}^i$ is the total indoor or outdoor air concentration of nuclide i [mol·m⁻³_{air}],
 $\sum_d X_{gw}^{i,d}$ is the sum of all geosphere discharge flows for the nuclide i [mol a⁻¹],
 csa is the number of seconds per tropical year 31,556,926 [s a⁻¹],
 D_L is the dispersion function over water, Equation (5.65),
 d is discharge location, and
 A_L is the area of the lake [m²].

5.5.8 Fires

Agricultural Fires (AF):

Although not common, sometimes crop residues such as straw are burned. The intent here is to estimate this potential contribution to the atmosphere by assuming that the forage field was representative of the size of field that could be burned and the available biomass and contamination:

$$C_{air,AF}^i = C_{se}^{i,forage} CR^{i,forage} Y_{p,max} ff_{Afire} fr_{Afire}^i D_T^f / csa \quad i \neq Ar, Kr, Xe \quad (5.68)$$

where

$C_{air,AF}^i$ is the indoor or outdoor air concentration of nuclide i from agricultural fires [$\text{mol} \cdot \text{m}^{-3}_{air}$],

$CR^{i,forage}$ is the plant/soil concentration ratio for forage fields for nuclide i [$\text{kg}_{drysoil} \cdot \text{kg}^{-1}_{wetbio}$],

$C_{se}^{i,forage}$ is the soil concentration or sediment-as-soil concentration of nuclide i for the forage field [$\text{mol} \cdot \text{kg}^{-1}_{drysoil}$],

$Y_{p,max}$ is the maximum plant biomass density (yield) among the garden and the forage fields for all food types [$\text{kg}_{wetbio} \cdot \text{m}^{-2}_{soil}$],

ff_{Afire} is the frequency of agricultural fires [a^{-1}],

fr_{Afire}^i is the emission fraction from agricultural fires [-],

csa is the number of seconds per tropical year 31,556,926 [s a^{-1}], and

D_T^f is the dispersion over the field area given by (see Equation (5.63))

$$D_T^f = \left[4.87 \cdot \left(\frac{A^f}{m^2} \right)^{1/8} - 3.56 \right] \cdot \left(\frac{U_{w,ref}}{U_w} \right) \frac{s}{m} \quad \text{for } f = \text{forage} \quad (5.69)$$

Here A^f is the area of field f (forage field, woodlot, garden, peatbog) [m^2].

Energy Fires (EF):

Nuclides would be released to the atmosphere if wood or peat were burnt as fuel. It is assumed that the house has a chimney that exhausts the air, and so the primary exposure to energy fire exhaust is outside and downstream from the chimney (i.e., not indoors).

If wood is burned as fuel (excludes Ar, Xe, and Kr):

$$C_{air,EF}^i = CR^{i,forage} \cdot C_{se}^{i,woodlot} \cdot fr_{Efire}^i \cdot D_{chimney} \cdot Q_{fuel} / E_{wood} \quad (5.70a)$$

or if peat is burned as fuel (excludes Ar, Xe, and Kr):

$$C_{air,EF}^i = C_{se}^{i,peat} \cdot fr_{Efire}^i \cdot D_{chimney} \cdot Q_{fuel} / E_{peat} \quad (5.70b)$$

where

$C_{se}^{i,peat}$ and $C_{se}^{i,woodlot}$ are the soil concentration and sediment-as-soil concentration for the peatbog or woodlot [$\text{mol} \cdot \text{kg}^{-1}_{drysoil}$],

$CR^{i,forage}$ is the forage plant/soil concentration ratio of nuclide i [$\text{kg}_{drysoil} \cdot \text{kg}^{-1}_{wetbio}$],

fr_{Efire}^i is the emission fraction from energy fires [-],

Q_{fuel} is the energy requirement from the fuel [$\text{MJ} \cdot \text{a}^{-1}$],

E_{peat} is the amount of energy in peat fuel [$\text{MJ} \cdot \text{kg}^{-1}_{drysoil}$],

E_{wood} is the amount of energy in wood fuel [$\text{MJ} \cdot \text{kg}^{-1}_{wetbio}$],

$D_{chimney}$ is a semi-empirical chimney dispersion term [a/m^3], defined as

$$D_{chimney} = \frac{f_{downwind} K_k}{W_{bldg} H_{bldg} U_w csa} \quad (5.71)$$

where

$f_{downwind}$ is the fraction of time spent downwind from energy fires [-],
 K_k is the plume wake entrainment parameter [-],
 W_{bldg} is the building width [m],
 H_{bldg} is the building height [m],
 U_w is the annual average wind speed [m/s], and
 csa is the number of seconds per tropical year 31,556,926 [s a⁻¹].

Land Fires (LF)

Natural forest fires (or peat fires), or those caused by humans to clear land, could release contaminants into the atmosphere. This is unlikely to be a significant dose pathway. However, a simple estimate is provided by considering a local fire consuming an area of forest or peat bog equivalent to that required for household heating use, and sited on contaminated soil.

The air concentration (excluding Ar, Xe, and Kr) within this area is then given by

$$C_{air,LF}^i = \frac{ff_{Lfire} fr_{Lfire}^i}{csa} \cdot \begin{cases} C_{se}^{i,woodlot} CR^{i,forage} Y_{for} D_T^{woodlot} & \text{if wood burned as fuel} \\ C_{se}^{i,peat} \rho_{soil}^{organic} Z_{ss} D_T^{peat} & \text{if peat burned as fuel} \end{cases} \quad (5.72)$$

where

$C_{se}^{i,f}$ is the soil concentration or sediment-as-soil concentration of nuclide i for field f (woodlot or peatbog) [mol·kg⁻¹_{drysoil}],
 ff_{Lfire} is the frequency of land fires [a⁻¹],
 fr_{Lfire}^i is the emission fraction of nuclide i from land fires [-],
 csa is the number of seconds per tropical year 31,556,926 [s a⁻¹],
 $CR^{i,forage}$ is the forage plant/soil concentration ratio of nuclide i [kg_{drysoil}·kg⁻¹_{wetbio}],
 Y_{for} is the forest yield [kg_{biomass}·m⁻²],
 $\rho_{soil}^{organic}$ the organic (peat) soil density [kg_{drysoil}·m⁻³_{drysoil}],
 Z_{ss} is the depth of the surface soil zone [m], and
 D_T^f is the dispersion source term given by (see Equation (5.63)):

$$D_T^f = \left[4.87 \cdot \left(\frac{A^f}{m^2} \right)^{1/8} - 3.56 \right] \cdot \left(\frac{U_{w,ref}}{U_w} \right) \frac{s}{m} \quad \text{for } f = \text{peat or woodlot.} \quad (5.73)$$

5.5.9 Total

The outdoor and indoor air concentrations from the above pathway contributions are calculated as described below, depending on the element.

All nuclides i except ^{222}Rn , ^3H , Ar, Kr and Xe:

$$C_{air,out}^{i,f} = C_{air,TP}^{i,f} + C_{air,AP}^i + C_{air,AF}^i + C_{air,EF}^i + C_{air,LF}^i + C_{air,TG}^i + C_{air,AG}^i \quad (5.74)$$

$$C_{air,in}^{i,f} = C_{air,TP}^{i,f} + C_{air,AP}^i + C_{air,AF}^i + C_{air,LF}^i + C_{air,ISW}^i + C_{air,TG}^i + C_{air,AG}^i \quad (5.75)$$

^{222}Rn

$$C_{air,out}^{Rn,f} = C_{air,TP}^{Rn,f} + C_{air,AP}^{Rn} + C_{air,AF}^{Rn} + C_{air,EF}^{Rn} + C_{air,LF}^{Rn} + C_{air,TG}^{Rn} + C_{air,AG}^{Rn} \quad (5.76)$$

$$C_{air,in}^{Rn,f} = C_{air,TP}^{Rn,f} + C_{air,AP}^{Rn} + C_{air,AF}^{Rn} + C_{air,LF}^{Rn} + C_{air,IRN}^{Rn} + C_{air,ISW}^{Rn} + C_{air,TG}^{Rn} + C_{air,AG}^{Rn} \quad (5.77)$$

For Ar, Kr and Xe

$$C_{air,out}^{i,f} = C_{air,in}^{i,f} = C_{air,GWR}^i \quad (5.78)$$

^3H :

$$C_{air,out}^{i,f} = C_{air,in}^{i,f} = 0 \quad (\text{Specific activity model is used}) \quad (5.79)$$

5.5.10 Deposition Flows

Nuclides in the atmosphere can settle onto surfaces such as soil and vegetation, and lead to contamination at points distant from the contamination source. Typically, the deposition processes are categorized as either wet or dry deposition (i.e., occurring with or without precipitation). Wet and dry depositions are about equally effective over the long term for North American climates in removing contaminants from the atmosphere (Davis et al. 1993, p.186).

For most nuclides, the deposition model simulates dry deposition using a deposition velocity, V_d (Davis et al. 1993, Beak 2002). Wet deposition is treated using a washout ratio, W_r and the total precipitation rate (Davis et al. 1993, Beak 2002). For the noble gases, the deposition rate is zero. For tritium, dose exposures are calculated through a specific activity model and the deposition rate is not required.

Deposition to Soil (Used in Soil submodel, Section 5.4.2)

The soil can receive atmospheric nuclides from the lake through deposition:

$$D_{soil}^i = [C_{air,AG}^i + C_{air,AP}^i] \cdot (V_d + P_{tot} \cdot W_r) \cdot csa \quad i \neq ^3\text{H}, \text{Ar}, \text{Kr}, \text{Xe}, ^{222}\text{Rn} \quad (5.80)$$

where

D_{soil}^i is the deposition flux to the soil [$\text{mol} \cdot \text{m}^{-2} \cdot \text{a}^{-1}$],

V_d is the dry deposition velocity [$\text{m} \cdot \text{s}^{-1}$],

P_{tot} is the total annual precipitation rate [$\text{m} \cdot \text{s}^{-1}$],

W_r is the washout ratio [-], and

csa is the number of seconds per tropical year 31,556,926 [$\text{s} \cdot \text{a}^{-1}$].

Deposition to Vegetation (Used in Food-chain Submodel, Section 5.6.4):

Vegetation can receive nuclides from the atmosphere that have originated from a variety of sources. This includes the possibility of having a forest fire or agricultural fire next to a vegetated area. The model is conservative in the case of fires where the vegetation is burned, but then a portion of the nuclide inventory is redeposited; the model simplification bypasses the need to calculate nuclide flows between fields.

For volatile and biologically active elements such as ^{14}C , ^{36}Cl and ^{129}I , the plant/soil concentration factors already take into account the contribution through the leaves since the plant is immersed in the released gases (Davis et al. 1993). (The effective plant/soil concentration factor for ^{14}C is dominated by the atmospheric absorption path.) Therefore, the atmospheric deposition from terrestrial gas sources is not included as a separate plant contamination route.

Therefore, for all nuclides except ^3H , Ar, Kr, Xe and ^{222}Rn , the total deposition rate is [$\text{mol m}^{-2} \text{s}^{-1}$]:

$$D_{plant}^{i,f} = [C_{air,TP}^{i,f} + C_{air,AP}^i + C_{air,AF}^i + C_{air,EF}^i + C_{air,LF}^i + C_{air,AG}^i] \cdot (V_d + P_{tot} \cdot W_r) \quad (5.81)$$

The interception fraction by the plants that contributes to dose is discussed further in Section 5.6.4. The deposition of nuclides on vegetation from irrigation water is treated separately.

5.6 THE FOOD-CHAIN AND DOSE SUBMODEL

5.6.1 General

The purpose of the foodchain and dose model is to calculate the dose to humans from all important exposure pathways, given the nuclide concentration in the various environmental compartments. We assume that the different exposure pathways could exist during all states, but their significance is controlled by state-dependent parameter values. Some characteristics of the food ingestion pathways are expected to be strongly dependent on the state because sources of food could be significantly different. Many of these processes could be strongly attenuated (and essentially vanish) during an ice sheet state, for example, when the site is not occupied. To simulate an uninhabitable biosphere state (such as an ice sheet state), we recommend setting the 'overall' occupancy factors Oh and Onh to zero for human and non-human biota respectively. See Appendix C for the identity of state-dependent parameters.

The inputs to the foodchain and dose model are:

$Ca_{se}^{i,f}$ The concentration (activity) of nuclide i in the root zone of the soil for a field f (garden, forage, woodlot) [$\text{Bq} \cdot \text{kg}^{-1}_{\text{drysoil}}$],

$Ca_{sed}^{i,f}$ The concentration (activity) of nuclide i in the bottom sediments of the surface water body [$\text{Bq} \cdot \text{kg}^{-1}_{\text{drysoil}}$],

$Ca_{air,out}^{i,f}$ and $Ca_{air,in}^{i,f}$ The concentrations (activities) of nuclide i in outdoor and indoor air for field f (garden or forage) [$\text{Bq} \cdot \text{m}^{-3}_{\text{air}}$],

- $Ca_{air,out}^i$ and $Ca_{air,in}^i$ The maximum concentrations (activities) among field types f of nuclide i in outdoor or indoor air [$Bq \cdot m^{-3}_{air}$],
- Ca_L^i The concentration (activity) of nuclide i in the surface water body [$Bq \cdot m^{-3}_{water}$],
- Ca_{well}^i The concentration (activity) of nuclide i in well water [$Bq \cdot m^{-3}_{water}$],
- Ca_{gw}^i The concentration (activity) of nuclide i in groundwater [$Bq \cdot m^{-3}_{water}$],
- Ca_{dw}^i The concentration (activity) of nuclide i in drinking water, which will be equal to C_L or C_{well} depending on the source of domestic water [$Bq \cdot m^{-3}_{water}$],
- Ca_{geo}^i The concentration (activity) of nuclide i in the overburden of the last geosphere segment in the terrestrial discharge pathway [$Bq \cdot kg^{-1}_{drysoil}$].

Note that all of the activity concentrations used in the foodchain and dose submodel, Ca , have units of Bq, and are converted from the corresponding molar concentrations by using the $Bq \cdot mol^{-1}$ conversion appropriate for each nuclide.

The main outputs from the foodchain and dose model are:

- De^{ijk} Internal dose from nuclide i due to ingestion of food type j along pathway k [$Sv \cdot a^{-1}$],
- Dw^i Internal dose from nuclide i due to ingestion of drinking water [$Sv \cdot a^{-1}$],
- Ds^i Internal dose from nuclide i due to ingestion of soil [$Sv \cdot a^{-1}$],
- Di^i Internal dose from nuclide i due to inhalation [$Sv \cdot a^{-1}$],
- Da^i External dose from nuclide i due to immersion in air [$Sv \cdot a^{-1}$],
- Dh^i External dose from nuclide i due to immersion in water [$Sv \cdot a^{-1}$],
- Dg^i External dose from nuclide i due to standing on contaminated ground [$Sv \cdot a^{-1}$],
- Db^i External dose from nuclide i due to exposure to contaminated building material [$Sv \cdot a^{-1}$].

Notation: i = nuclide
 j = food type (plant, meat, milk, bird, or fish)
 k = food ingestion pathway

There are 9 food ingestion pathways considered:

- | | | | |
|--------|-------|----------------------------------|---------|
| (i) | soil | → plant roots (garden) | → human |
| (ii) | soil | → plant roots(forage) → animals | → human |
| (iii) | air | → plant leaves(garden) | → human |
| (iv) | air | → plant leaves(forage) → animals | → human |
| (v) | water | → animals | → human |
| (vi) | soil | → animals | → human |
| (vii) | water | → fish | → human |
| (viii) | air | → animals | → human |
| (ix) | soil | → human | |

Pathways (ii), (iv), (v), (vi), and (viii) each involve three branches corresponding to the three terrestrial animal types: meat, milk, and bird.

Soil or lake sediments may act as sources of contamination in all of the above food ingestion pathways except (v) and (vii), depending on whether or not lake sediment is used as farming soil. Soil or sediment may also be used in the soil ingestion and external exposure pathways.

As noted in the soil submodel, we model four different fields: a garden, a forage field, a woodlot and a peat bog. The main difference between the treatment of the fields is with respect to irrigation. The garden (or "vegetable patch") has a much higher probability of irrigation and may be irrigated with either lake water or well water. The forage field, if irrigated, will be irrigated only with lake water. If lake sediments form the substrate for plants in the garden or forage field, then either no field is irrigated or they are irrigated with clean water (i.e. no irrigation contamination). Furthermore, a difference in the types of plants is modelled through the use of different soil-to-plant transfer factors for the garden plants versus those grown in the other fields.

The food-chain submodel and related dose pathways can be expressed as a series of equations. Each equation starts with a nuclide concentration in water, soil or atmosphere, or an atmospheric deposition rate, which is then translated into a radiological dose to a person. The water, soil and air concentrations, and the atmospheric deposition rates, are supplied by the other three submodels of the biosphere model.

5.6.2 Ingrowth

Ingrowth from decay of a parent nuclide is modelled explicitly within the water and soil compartments. Ingrowth within the biosphere food chains (e.g., while in a plant) is treated approximately as one of two limiting cases. Specifically, for long-lived parents, their ingrowth contribution within the food chain is small and can be ignored. For short-lived parents, their ingrowth contribution is given by assuming that the daughter is in secular equilibrium within the food chain for purposes of daughter dose calculations. In the present model, only these two limiting cases are considered, with the distinction based on half-life. If the parent half-life is longer than an input $t_{1/2,fc}$, (e.g., conservatively set to 20 years), then the total dose from the daughter nuclide i is modelled by adding a second ingrowth contribution from the decay of the parent, assuming that this second source has reached its maximum (secular equilibrium) value.

Therefore, for the food chain pathways except soil and fish ingestion, the dose rates are modified as follows:

$$De^{ijk} = [De^{ijk}]_{ni} + De^{pj k} \frac{DFe^i}{DFe^p} \quad (5.82)$$

where

De^{ijk} and $De^{pj k}$ are the human ingestion doses from nuclide i or its parent p through foodchain pathway k involving food type j =plant, meat, milk or bird, including ingrowth [$Sv \cdot a^{-1}$],

$[De^{ijk}]_{ni}$ is the human ingestion dose from nuclide i or its parent p through foodchain pathway k involving food type j =plant, meat, milk or bird, without foodchain ingrowth [$Sv \cdot a^{-1}$],

DFe^i and DFe^p are the ingestion dose conversion factors for nuclide i and its parent p [$Sv \cdot Bq^{-1}$].

The first term in Equation (5.82) accounts for direct uptake of the nuclide i or parent p , and the second term for ingrowth based on secular equilibrium with the parent. Equation (5.82) is very general and it applies to seven of the food ingestion pathways. It is not included for soil and fish because ingrowth in the soil and water is already included.

5.6.3 Human Ingestion and Inhalation Rate

The reference human ingestion rate, drinking water rate (U_{dw}) and inhalation (I_i) rate are inputs to the model. However, the various food ingestion rates are scaled to correspond to an input total energy intake.

Food Ingestion Rates

The human ingestion rates are provided as input for plant and animal food types, based on survey data for example. The total energy available from a given set of ingestion rates U_{in}^j is

$$Eu = \sum_j U_{in}^j [(Cym^j \cdot Cec) + (Fym^j \cdot Fec) + (Pym^j \cdot Pec)] (0.001 \frac{kg}{g}) \quad (5.83)$$

where

Eu is the total food energy intake based on the ingestion rates U^j [$kJ \cdot d^{-1}$];

U_{in}^j is the human ingestion rate of food type j [$g_{wetbio} \cdot d^{-1}$] in which j refers to plant products (from a hypothetical plant which provides fruits, vegetables, roots and grains) and the four animal products: milk, meat, bird and fish;

Cym^j is the carbohydrate content (concentration) of food type j [$g \cdot kg^{-1}_{wetbio}$];

Cec is the carbohydrate fuel value [$kJ \cdot g^{-1}$];

Fym^j is the fat content of food type j [$g \cdot kg^{-1}_{wetbio}$];

Fec is the fat fuel value [$kJ \cdot g^{-1}$];

Pym^j is the protein content of food type j [$g \cdot kg^{-1}_{wetbio}$]; and

Pec is the protein fuel value [$kJ \cdot g^{-1}$].

In order to provide a specified total energy need En [$kJ \cdot d^{-1}$], the food ingestion rates are scaled

$$U^j = \frac{En}{Eu} U_{in}^j \quad (5.84)$$

where U^j ($[kg_{wetbio} a^{-1}]$ or $[L_{milk} a^{-1}]$) is the scaled food ingestion rate for food type j , in which j refers to plant products and the four animal products.

5.6.4 Terrestrial Plant/Animal Pathways

The plant pathways include root uptake and atmospheric deposition of nuclides on leaves. The plants, or plant products, may then be directly consumed by humans, or be eaten by animals that are subsequently consumed by humans.

Nuclide Concentration in Plants

Nuclides are incorporated into plants from the soil through the roots and through atmospheric deposition on the leaves. Leaf deposition can occur through deposition of nuclides from the air, or through aerial sprinkler irrigation.

The plant concentration of nuclide i due to uptake from the soil is calculated assuming equilibrium using a concentration ratio, CR^i ,

$$C_{plant}^{i,f} = C_{se}^{i,f} \cdot CR^{i,f} \quad (5.85)$$

The plant-to-soil concentration ratio depends on a number of factors, such as plant type. Note that the concentration ratio is actually element-dependent, meaning that values of CR^i would be identical for isotopes of the same chemical element. In the present model, we distinguish between plants that are generally consumed directly by humans, such as garden crops (CR_{hfood}^i), and plants that are generally consumed by non-human biota, such as forage field grasses (CR_{nhfood}^i).

Since the amount of nuclide from the surface soil that is bound up in plants is typically small, we conservatively neglect to decrease the amount of nuclide in the soil by the amount transferred to plants. However, under certain combinations of parameter values, this simplification might imply that more nuclide was transferred to plants than was present in the soil. To ensure that this does not happen, the plant/soil concentration ratio for nuclide i in field f is constrained as follows:

$$CR^{i,f=garden} = \begin{cases} CR_{hfood}^i & \text{if } MR^{ft=plant,i} \leq 1 \\ \frac{CR_{hfood}^i}{MR^{ft=plant,i}} & \text{if } MR^{ft=plant,i} > 1 \end{cases} \quad (5.86a)$$

and

$$CR^{i,f=(forage, woodlot, peatbog)} = \begin{cases} CR_{nhfood}^i & \text{if } MR_{max}^i \leq 1 \\ \frac{CR_{nhfood}^i}{MR_{max}^i} & \text{if } MR_{max}^i > 1 \end{cases} \quad (5.86b)$$

where

$MR^{j,i}$ is the total plant-to-soil mass ratio of nuclide i for food type j , where $j = \text{plant, meat, milk or bird (poultry/eggs)}$ $[(\text{mol} \cdot \text{m}^{-2}_{\text{plant}})/(\text{mol} \cdot \text{m}^{-2}_{\text{soil}})]$;

$$MR^{j,i} = \begin{cases} \frac{CR_{hfood}^i \cdot Y_p^{garden}}{Z_{ss} \cdot \rho_{soil}} & j = \text{plant} \\ \frac{CR_{nhfood}^i \cdot Y_j^{forage}}{Z_{ss} \cdot \rho_{soil}} & j = \text{meat, milk, bird} \end{cases} \quad (5.87a)$$

and

$$MR_{max}^i = \max(MR^{meat,i}, MR^{milk,i}, MR^{bird,i}) \quad ; \quad (5.87b)$$

Y_p^{garden} is the garden plant biomass density (yield) $[\text{kg}_{\text{wetbio}} \cdot \text{m}^{-2}]$;

Y_j^{forage} is the forage plant biomass density (yield) for food type j $[\text{kg}_{\text{wetbio}} \cdot \text{m}^{-2}]$;

Z_{ss} is the depth [m] of the surface soil compartment; and

ρ_{soil} is the surface soil dry bulk density $[\text{kg} \cdot \text{m}^{-3}_{\text{dry soil}}]$.

Plant Root - Human Pathway

The dose to humans from ingesting plants (food type $j = \text{plant}$) contaminated by root uptake of nuclides is given by

$$De^{ijk} = [Ca_{se}^{i,garden} \cdot CR^{i,garden} \cdot e^{-\lambda^{i,th/cda}}] \cdot U^{plant} \cdot DFe^i \cdot Oh \quad (5.88)$$

where

- De^{ijk} is the human ingestion dose from nuclide i and food type j , and k is the plant root - human pathway k [$Sv \cdot a^{-1}$],
- $Ca_{se}^{i,garden}$ is the annual average garden soil concentration (activity) of nuclide i [$Bq \cdot kg^{-1}_{drysoil}$],
- $CR^{i,garden}$ is the garden plant/soil concentration ratio for nuclide i [$(Bq \cdot kg^{-1}_{wetbio}) / (Bq \cdot kg^{-1}_{drysoil})$],
- λ^i is the radiological decay constant of nuclide i [a^{-1}],
- th is the holdup time between harvest and consumption of plants [d],
- U^{plant} is the human ingestion rate of plant food types [$kg_{wetbio} \cdot a^{-1}$],
- DFe^i is the ingestion dose conversion factor for nuclide i [$Sv \cdot Bq^{-1}$], and
- Oh is the overall human occupancy factor [-], i.e., the fraction of the year the human group resides near the repository site and is exposed to contaminants.

Plant Root - Animal - Human Pathway

The dose to humans from ingestion of animal food types ($j = \text{milk, meat and bird}$) that have eaten plants contaminated by root uptake of nuclides is given by the following:

$$De^{ijk} = [Ca_{se}^{i,forage} \cdot CR^{i,forage} \cdot F^{ij} \cdot Q_{f,an}^j \cdot e^{-\lambda^{i,thf^j/cda}}] \cdot U^j \cdot DFe^i \cdot Oh \quad (5.89)$$

where

- De^{ijk} is the dose to humans for nuclide i , from ingestion of animal food types j , for plant root - animal - human pathway k [$Sv \cdot a^{-1}$],
- $Ca_{se}^{i,forage}$ is the annual average forage soil concentration (activity) of nuclide i [$Bq \cdot kg^{-1}_{drysoil}$],
- $CR^{i,forage}$ is the forage plant/soil concentration ratio for nuclide i [$(Bq \cdot kg^{-1}_{wetbio}) / (Bq \cdot kg^{-1}_{drysoil})$],
- F^{ij} is the terrestrial transfer coefficient for nuclide i and food type j [$d \cdot kg^{-1}_{wetbio}$],
- $Q_{f,an}^j$ is the feed or forage consumption rate for food type j [$kg_{wetbio} \cdot d^{-1}$],
- thf^j is the terrestrial animal feed or forage holdup time between harvest and consumption for food type j [d],
- cda is the number of days per tropical year 365.2422 [$d \cdot a^{-1}$], and
- U^j is the ingestion rate by humans of animal food types in which j which refers to meat, milk and bird [$kg_{wetbio} \cdot a^{-1}$] or [$L_{milk} \cdot a^{-1}$].

Plant Leaf - Human Pathway

The dose to humans from ingesting plants contaminated by irrigation and by atmospheric deposition of nuclides on the surface of plants is given by

$$De^{ijk} = \left[\frac{(Ad_{air}^{i,garden} r_{air}^j + Ad_{irr}^i r_{irr}^j)}{Y_j^{garden} \cdot \lambda_E^{i,tp}} \cdot e^{-\lambda^i th/cda} \cdot (1 - e^{-\lambda_E^{i,tp} te^{jk}}) \right] \cdot U^{plant} \cdot DFe^i \cdot Oh \quad (5.90)$$

where

- De^{ijk} is the dose to humans for nuclide i , from ingestion of plant produce (in this instance leafy vegetables) via the plant leaf - human pathway k [Sv·a⁻¹],
- $Ad_{air}^{i,garden}$ is the atmospheric deposition rate of nuclide i to surface of plants [Bq·m⁻²·soil·d⁻¹],
- Ad_{irr}^i is the irrigation deposition rate of nuclide i to surface of plants [Bq·m⁻²·soil·d⁻¹],
- r_{air}^j is the atmospheric plant interception fraction for food type j [-],
- r_{irr}^j is the irrigation plant interception fraction for food type j [-],
- th is the holdup time between harvest and consumption of plants [d],
- $\lambda_E^{i,tp}$ is the effective removal constant of nuclide i from garden vegetation [d⁻¹],
- te^{jk} is the time of above-ground exposure for food type j during the growing season, or return time for pasture [d],
- cda is the number of days per tropical year 365.2422 [d a⁻¹], and
- Y_p^{garden} is the garden plant biomass density (yield) [kg_{wetbio}·m⁻²].

The model conservatively does not account for any translocation factor from the exposed surface (foliage) to the consumed product. For example, Beak (2002, p.44) suggests values ranging from 0.01 to 1.

The effective removal constant, $\lambda_E^{i,tp}$ [d⁻¹], defines the loss of atmospheric deposits from vegetation due to radiological decay and weathering of the plant and is given by:

$$\lambda_E^{i,tp} = (\lambda^i / cda) + (\ln 2 / tp) \quad (5.91)$$

where

- λ^i is the radiological decay constant of nuclide i [a⁻¹], and
- tp represents one of the following:
- tpb is the plant environmental half time for non-human biota [d],
- tpf is the forage plant environmental half time [d], and
- tpg is the garden plant environmental half time [d].

The deposition rate of nuclides from the atmosphere is described in Section 5.5.10 as the sum of the dry and wet deposition processes, and the atmospheric concentration

$$Ad_{air}^{i,f} = D_{plant}^{i,f} \cdot \lambda^i \cdot N_{av} / cda \quad (5.92)$$

where

- $D_{plant}^{i,f}$ is the nuclide atmospheric deposition rate on plants in field f (garden or forage) [mol·m⁻²·s⁻¹],
- N_{av} is Avogadro's number [6.023x10²³ atoms/mole], and
- cda is the number of days per tropical year 365.2422 [d a⁻¹].

The deposition rate from aerial irrigation is:

$$Ad_{irr}^i = Ca_{irr}^i I_{irr} / cda \quad (5.93)$$

where

Ca_{irr}^i is the irrigation source (well or lake) concentration (activity) of nuclide i [$Bq \cdot m^{-3}$],

I_{irr} is the annual irrigation rate [$m^3_{water} \cdot m^{-2}_{soil} \cdot a^{-1}$], and

cda is the number of days per tropical year 365.2422 [$d \cdot a^{-1}$].

Plant Leaf - Animal - Human - Pathway

The dose to humans from ingesting animal food types j ($j =$ milk, meat and birds) from animals that have consumed plants contaminated by irrigation and atmospheric deposition of nuclides is given by the following:

$$De^{ijk} = \left[\frac{(Ad_{air}^{i,forage} r_{air}^j + Ad_{irr}^i r_{irr}^j)}{Y_j^{forage} \cdot \lambda_E^{i,tp}} \cdot e^{-\lambda^{i,thf^j}/cda} \cdot (1 - e^{-\lambda_E^{i,tp} te^{jk}}) \cdot F^{ij} \cdot Q_{f,an}^j \right] \cdot U^j \cdot DFe^i \cdot Oh \quad (5.94)$$

where

F^{ij} is the terrestrial transfer coefficient for nuclide i and food type j [$d \cdot kg^{-1}_{wetbio}$],

$Q_{f,an}^j$ is the feed or forage consumption rate for food type j [$kg_{wetbio} \cdot d^{-1}$],

thf^j is the terrestrial animal feed or forage holdup time between harvest and consumption for food type j [d],

te^{jk} is the time of above-ground exposure for food type j during the growing season, or return time for pasture [d],

Y_j^{forage} is the forage plant biomass density (yield) for food type j [$kg_{wetbio} \cdot m^{-2}_{soil}$],

$\lambda_E^{i,tp}$ is the effective removal constant of nuclide i from forage field vegetation [d^{-1}], and

k is the plant leaf - animal - human pathway.

Note that Equations (5.88) and (5.93) apply to both deposition from the air (Amiro 1992), and to deposition from aerial sprinkler irrigation only if the field is irrigated.

Water - Animal - Human Pathway

This pathway involves ingestion of nuclides by animals via drinking water and nuclide transfer to animal food types. The dose to humans from ingesting contaminated animal food type j ($j =$ milk, meat and bird) is given by

$$De^{ijk} = [Ca_{dw}^i \cdot F^{ij} \cdot Q_{dw}^j \cdot cIm \cdot e^{-\lambda^{i,thw^j}/cda}] \cdot U^j \cdot DFe^i \cdot Oh \quad (5.95)$$

where

Ca_{dw}^i is the annual average concentration of nuclide i , in the drinking water (domestic) source, and may equal Ca_L (lake) or Ca_{well} (well) [$Bq \cdot m^{-3}_{water}$],

Q_{dw}^j is the animal drinking water ingestion rate for food type j (as defined in Equation (5.2))
 $[L_{\text{water}} \cdot d^{-1}]$,
 clm is a conversion factor from m^3 to L [$0.001 m^3 \cdot L^{-1}$],
 thw^j is the terrestrial animal drinking water holdup time for food type j [d], and
 k is the water - animal - human pathway.

Note that nuclide transfers via drinking water and ingestion of feed or forage are treated in an equivalent manner. It is assumed that the contaminant ingested with water is transferred from the gut to the animal tissue to that same extent as the contaminant ingested with feed or forage.

Air - Animal - Human Pathway

This pathway involves inhalation of nuclides by animals and nuclide transfer to animal food types consumed by humans. The dose to humans from ingesting contaminated animal food type j (j = milk, meat and bird) is given by:

$$De^{ijk} = [Ca_{air,out}^i \cdot Fl^{ij} \cdot Q_a^j \cdot e^{-\lambda^i th_a^j / cda}] \cdot U^j \cdot DFe^i \cdot Oh \quad (5.96)$$

where

$Ca_{air,out}^i$ is the maximum outdoor air concentration (activity) among fields f of nuclide i [$Bq \cdot m^{-3}$],
 Fl^{ij} is the terrestrial animal inhalation transfer coefficient for nuclide i and food type j
 $[d \cdot L^{-1}$ or $d \cdot kg^{-1}]$,
 Q_a^j is the animal inhalation rate for food type j [$m^3 \cdot d^{-1}$],
 th_a^j is the terrestrial animal inhalation holdup time for food type j [d],
 cda is the number of days per tropical year 365.2422 [$d a^{-1}$], and
 k is the air - animal - human pathway.

Soil - Animal - Human Pathway

This pathway defines animals' ingestion of nuclides in soil, and their transfer to animal food types consumed by humans. The dose to humans from ingesting contaminated animal food type j (j = milk, meat and bird) is given by

$$De^{ijk} = [Ca_{se}^{i,forage} \cdot F_s^{ij} \cdot Q_s^j \cdot e^{-\lambda^i th_s^j / cda}] \cdot U^j \cdot DFe^i \cdot Oh \quad (5.97)$$

where

$Ca_{se}^{i,forage}$ is the average forage soil concentration (activity) of nuclide i [$Bq \cdot kg^{-1}_{drysoil}$],
 Q_s^j is the animal soil ingestion rate for food type j [$kg_{drysoil} \cdot d^{-1}$],
 th_s^j is the terrestrial animal soil ingestion holdup time for food type j [d],
 k is the soil - animal - human pathway.

Water - Fish - Human Pathway

This pathway deals with the transfer of nuclides from freshwater to fish consumed by humans. The dose to humans from ingesting contaminated fish (j = fish) is given by:

$$De^{ijk} = [Ca_L^i \cdot clm \cdot B^{ij} \cdot e^{-\lambda^i thp^j / cda}] \cdot U^j \cdot DFe^i \cdot Oh \quad (5.98)$$

where

- Ca_L^i is the concentration (activity) of nuclide i in the lake [$Bq \cdot m^{-3}_{water}$],
 clm is a conversion factor from m^3 to L [$0.001 m^3 \cdot L^{-1}$],
 B^{ij} is the aquatic concentration ratio for nuclide i and food type j [$L_{water} \cdot kg^{-1}_{wetbio}$],
 thp is the holdup time for j =fish [d],
 cda is the number of days per tropical year 365.2422 [$d a^{-1}$],
 k is the water - fish - human pathway, and
 U^j is the ingestion rate by humans of animal food type j in which j refers to fish [$kg_{wetbio} a^{-1}$].

5.6.5 Human Drinking Water Pathway

The dose to humans from ingesting contaminated drinking water is given by the following:

$$Dw^i = [Ca_{dw}^i \cdot clm \cdot e^{-\lambda^i thdw / cda}] \cdot U_{dw} \cdot DFe^i \cdot Oh \quad (5.99)$$

where

- Dw^i is the human ingestion dose from nuclide i in drinking water [$Sv \cdot a^{-1}$],
 Ca_{dw}^i is the annual average concentration of nuclide i , in the drinking water (domestic) source, and may equal Ca_L (lake) or Ca_{well} (well) [$Bq \cdot m^{-3}_{water}$],
 $thdw$ is the holdup time for human drinking water [d],
 U_{dw} is the human ingestion rate of drinking water [$L_{water} a^{-1}$].

5.6.6 Human Soil Ingestion Pathway

The dose to humans from coincidental ingestion of soil on plants and dirty hands is given by

$$Ds^i = Ca_{se}^{i,garden} \cdot Us \cdot DFe^i \cdot Oh \quad (5.100)$$

and

$$Us = Hs + (Ps \cdot U^{plant}) \quad (5.101)$$

where

- Ds^i is the human soil ingestion dose from nuclide i [$Sv \cdot a^{-1}$],
 $Ca_{se}^{i,garden}$ is the annual average soil concentration (activity) of nuclide i [$Bq \cdot kg^{-1}_{drysoil}$],
 Us is the human soil ingestion rate [$kg_{drysoil} a^{-1}$],
 DFe^i is the ingestion dose conversion factor for nuclide i [$Sv \cdot Bq^{-1}$],
 Hs is the soil ingestion rate from hands [$kg_{drysoil} a^{-1}$],
 Ps is the amount of soil on plants [$kg_{drysoil} \cdot kg^{-1}_{wetbio}$],
 U^{plant} is the human ingestion rate of plant produce (from Equation (5.84)).

5.6.7 Human Inhalation Pathway

The dose to humans from inhaling nuclides in air is given by:

$$D_i^i = [Ca_{air,in}^i \cdot Ob + Ca_{air,out}^i \cdot Og] \cdot li \cdot DFi^i \cdot Oh \quad (5.102)$$

where

D_i^i is the human inhalation dose from nuclide i [$Sv \cdot a^{-1}$],
 $Ca_{air,in}^i$ and $Ca_{air,out}^i$ are the indoor and outdoor air concentrations (activity) of nuclide i [$Bq \cdot m^{-3}$],
 Ob is the building occupancy factor [-],
 Og is the ground occupancy factor [-],
 li is the human inhalation rate [$m^3_{air} \cdot a^{-1}$], and
 DFi^i is the inhalation dose conversion factor for nuclide i [$Sv \cdot Bq^{-1}$].

5.6.8 Human External Doses

People may be exposed to external doses from being immersed in contaminated air and contaminated water, standing on contaminated ground and being exposed to contaminated building materials. These pathways do not involve nuclide transfer to humans.

Immersion in Air

The external dose to humans from immersion in air contaminated by nuclides is given by:

$$Da^i = [Ca_{air,in}^i \cdot Ob + Ca_{air,out}^i \cdot Og] \cdot DFa^i \cdot Oh \quad (5.103)$$

where

Da^i is the human immersion dose in air from nuclide i [$Sv \cdot a^{-1}$],
 $Ca_{air,in}^i$ and $Ca_{air,out}^i$ are the indoor and outdoor air concentrations of nuclide i [$Bq \cdot m^{-3}$], and
 DFa^i is the air immersion dose conversion factor for nuclide i [$Sv \cdot a^{-1} / (Bq \cdot m^{-3}_{air})$].

Immersion in Water

The external dose to humans from swimming and bathing in water contaminated by nuclides is given by:

$$Dh^i = Ca_{dw}^i \cdot Oe \cdot DFh^i \cdot Oh \quad (5.104)$$

where

Dh^i is the human immersion dose in water from nuclide i [$Sv \cdot a^{-1}$],
 Ca_{dw}^i is the annual average concentration of nuclide i , in the drinking water (domestic) source, and may equal Ca_L (lake) or Ca_{well} (well) [$Bq \cdot m^{-3}_{water}$],
 Oe is the water immersion occupancy factor [-], and
 DFh^i is the water immersion dose conversion factor for nuclide i [$Sv \cdot a^{-1} / (Bq \cdot m^{-3}_{water})$].

Ground Exposure

The external dose to humans from standing on contaminated ground is given by:

$$Dg^i = \max^f [Ca_{se}^{if}] \cdot cdws \cdot Og \cdot DFg^i \cdot Oh \quad (5.105)$$

where it is conservatively assumed that the exposure occurs on the most contaminated field, and

Dg^i is the human ground exposure dose from nuclide i [$Sv \cdot a^{-1}$],
 $\max^f [Ca_{se}^{if}]$ is the maximum concentration (activity) of nuclide i in soil, $f =$ garden, forage, woodlot, peat [$Bq \cdot kg^{-1}_{drysoil}$],
 $cdws$ is the dry/wet soil conversion factor [$kg_{drysoil} \cdot kg^{-1}_{wetsoil}$],
 Og is the ground exposure occupancy factor [-], and
 DFg^i is the ground exposure dose conversion factor for nuclide i [$Sv \cdot a^{-1} / (Bq \cdot kg^{-1}_{wetsoil})$].

Exposure to Building Material

The external dose to humans from exposure to contaminated building material is given by:

$$Db^i = Ca_b^i \cdot Ob \cdot DFb^i \cdot Oh \quad (5.106)$$

where

Db^i is the human exposure dose from nuclide i in building materials [$Sv \cdot a^{-1}$],
 Ca_b^i is the average concentration of nuclide i in building material, taken as the maximum of the organic (wood) or inorganic (geosphere) material concentrations [$Bq \cdot kg^{-1}_{dry}$] (see Equations (5.107) and (5.108) below),
 Ob is the building occupancy factor [-],
 DFb^i is the building material exposure dose conversion factor for nuclide i [$Sv \cdot a^{-1} / (Bq \cdot kg^{-1}_{dry})$].

For wooden building materials, the nuclide concentration based on root uptake and leaf deposition is given by (except 3H)

$$Ca_{wbm}^i = f_{wdw} \cdot e^{-\lambda^i \cdot t_{hwbm} / cda} \cdot \left\{ Ca_{se}^{i,woodlot} \cdot CR^{forage,i} + Ad_{air}^i \cdot \frac{r_{pb}}{Y_w \cdot \lambda_E^{i,tpg}} \cdot (1 - e^{-\lambda_E^{i,tpg} \cdot t_{eb}}) \right\} \quad (5.107a)$$

where

Ca_{wbm}^i is the nuclide concentration in wooden (organic) building material [$Bq \cdot kg^{-1}_{dry}$],
 $Ca_{se}^{i,woodlot}$ is the concentration (activity) of nuclide i in soil in the field $f=woodlot$ [$Bq \cdot kg^{-1}_{drysoil}$],
 $CR^{i,forage}$ is the forage plant/soil concentration ratio for nuclide i [$(Bq \cdot kg^{-1}_{wetbio}) / (Bq \cdot kg^{-1}_{drysoil})$],
 t_{hwbm} is the holdup time for wooden building material [d],
 cda is the number of days per tropical year 365.2422 [$d \cdot a^{-1}$],
 Ad_{air}^i is the deposition rate of nuclide i , to surface of plants [$Bq \cdot m^{-2}_{soil} \cdot d^{-1}$] (Equation (5.92)),
 r_{pb} is the plant interception fraction for wooden building material [-],
 $\lambda_E^{i,tpg}$ is the effective removal constant of nuclide i from vegetation [d^{-1}] (Equation (5.91)),
 t_{eb} is the time of above-ground exposure for wooden building material [d],
 Y_w is the plant yield for wood [$kg_{wetbio} \cdot m^{-2}_{soil}$], and
 f_{wdw} is the wet/dry wood conversion factor [$kg_{wetbio} \cdot kg^{-1}_{dryveg}$].

Nuclide transfer from soil to wood is assumed to be the same as to forage field plants.

In the case of tritium (^3H), the activity in the wooden building material is determined as follows:

$$Ca_{w\text{b}m}^{H3} = Ca_L^{H3} \cdot \frac{C_{\text{wood}}^H}{C_{\text{water}}^H} \quad (5.107b)$$

where

Ca_L^{H3} is the activity of tritium in the lake water [Bq/m^3],

C_{wood}^H is the average concentration of hydrogen in wood [$\text{g}/\text{kg}_{\text{dry wood}}$], and

C_{water}^H is the concentration of hydrogen in water [$\text{g}\cdot\text{m}^{-3}$].

For inorganic building materials, such as brick, nuclide concentrations are derived from the concentration in the overburden of the last geosphere segment assuming clay properties:

$$Ca_{i\text{b}m}^i = Ca_{g,\text{max}}^i \cdot f_{\text{sbc}} \cdot e^{-\lambda^i \cdot t_{\text{hibm}}/cda} \quad (5.108)$$

where

$Ca_{i\text{b}m}^i$ is the nuclide concentration (activity) in inorganic building material [$\text{Bq}\cdot\text{kg}^{-1}_{\text{dry}}$],

f_{sbc} is the soil/inorganic building material conversion factor [-],

t_{hibm} is the holdup time for inorganic building material [d],

cda is the number of days per tropical year 365.2422 [d a^{-1}], and

$Ca_{g,\text{max}}^i$ is the maximum concentration (activity) of nuclide i in the overburden [$\text{Bq}\cdot\text{kg}^{-1}_{\text{dry}}$] over all discharge zones d :

$$Ca_{g,\text{max}}^i = \max \left[C_{\text{pw}}^{i,d} \cdot \left(\frac{\theta_{\text{clay}}}{\rho_{\text{clay}}} + Kd_{\text{clay}}^i \right) \right] \cdot \frac{\lambda^i N_{\text{Av}}}{c\text{sa}}, \quad (5.109)$$

where

$C_{\text{pw}}^{i,d}$ is the nuclide i porewater concentration in discharge zone d [$\text{mol}\cdot\text{m}^{-3}_{\text{water}}$],

θ_{clay} water-content of the clay [$\text{m}^3_{\text{water}}\cdot\text{m}^{-3}_{\text{soil}}$],

ρ_{clay} is the surface soil dry bulk density for clay [$\text{kg}_{\text{drysoil}}\cdot\text{m}^{-3}$],

Kd_{clay}^i distribution coefficient in clay for the nuclide i [$\text{m}^3\cdot\text{kg}^{-1}_{\text{drysed}}$],

λ^i is the radioactive decay constant [a^{-1}],

N_{Av} is Avogadro's number [mol^{-1}], and

$c\text{sa}$ is the number of seconds per tropical year 31,556,926 [s a^{-1}].

5.6.9 Mass/Radioactivity Conversion Factor

Calculation of the mass/radioactivity conversion factor, gb^i , is given by:

$$gb^i = c\text{sa} \cdot M_w^i / (N_{\text{AV}} \cdot \lambda^i) \quad (5.110)$$

where

- M_w^i is the molecular weight [$\text{kg}\cdot\text{mol}^{-1}$],
 N_{AV} is Avogadro's number [mol^{-1}],
 λ^i is the radioactive decay constant [a^{-1}], and
 csa is the number of seconds per tropical year 31,556,926 [$\text{s}\cdot\text{a}^{-1}$].

5.6.10 Internal Dose Arising from ^{129}I

The total internal dose for ^{129}I may be estimated by the usual pathway equation:

$$Dit^{129}(\text{pathways model}) = \sum_{k,i} De^{129,k,i} + Dw^{129} + Ds^{129} + Dj^{129} \quad (5.111)$$

However, iodine is a trace element that is required for the functioning of the thyroid gland, and therefore the human body regulates the amount of iodine. Since the body does not distinguish between stable and radioactive iodine, the concentration of radio-iodine in the thyroid is limited by the relative amounts of radio-iodine and stable iodine in food and drinking water. The intake of stable iodine is essentially the normal human intake of iodine, which is a measured quantity that can be input directly into the model for current critical groups. However, for a self-sufficient critical group living at the site, the relative intake of radioactive and stable iodine can be related to the local environmental (water) concentrations of radioactive and stable iodine (i.e., neglecting any external sources of stable iodine). In this case, the internal dose from exposure to ^{129}I can be estimated by a specific activity model:

$$Dit^{129}(\text{gw limit model}) = DF^{129} \cdot \left[\frac{Ca_{max}^{129}}{C^i/clm + Ca_{max}^{129} \cdot gb^{129}} \right] \cdot \frac{Thi}{Thm} \cdot Oh \quad (5.112)$$

where

- Dit^{129} is the human internal dose from ^{129}I [$\text{Sv}\cdot\text{a}^{-1}$],
 DF^{129} is the internal dose conversion factor for ^{129}I in the thyroid [$(\text{Sv}\cdot\text{a}^{-1})/(\text{Bq}\cdot\text{kg}^{-1})$],
 Ca_{max}^{129} is conservatively taken as the maximum of the well water activity and the groundwater activity at the different discharges [$\text{Bq}\cdot\text{m}^{-3}_{\text{water}}$], $Ca_{max}^{129} = \max(Ca_{well}^{129}, Ca_{gw}^{129,d})$,
 C^i is the annual average groundwater concentration of stable iodine [$\text{kg}\cdot\text{L}^{-1}_{\text{water}}$],
 clm is the conversion factor from m^3 to L [$0.001\text{ m}^3\cdot\text{L}^{-1}$],
 gb^{129} is the mass/radioactivity conversion factor for ^{129}I [$\text{kg}\cdot\text{Bq}^{-1}$],
 Thi is the iodine content of thyroid [kg],
 Thm is the mass of thyroid [kg], and
 Oh is the overall human occupancy factor [-].

The total internal dose from ^{129}I is the minimum of these two dose estimates

$$D_{int}^{129} = \min(D_{pathways}^{129}, D_{gw\ limit}^{129}) \quad (5.113)$$

5.6.11 Internal Dose Arising from ¹⁴C

A total internal dose for ¹⁴C is first estimated by the usual pathway equations. This estimated dose is compared with the maximum possible internal dose, which is calculated using a ¹⁴C specific activity model and the average annual concentration of stable carbon in groundwater. The minimum of these two ¹⁴C dose rates is taken to be the ¹⁴C internal dose:

$$Dit^{C14} (\text{pathways model}) = \sum_{k,i} De^{C14,k,i} + Dw^{C14} + Ds^{C14} + Di^{C14} \quad (5.114)$$

and

$$Dit^{C14} = \min \left(\frac{Dit^{C14} (\text{pathways model})}{DF^{C14} \left[Ca_{max}^{C14} / (C_{C12} / clm + Ca_{max}^{C14} \cdot gb^{C14}) \right] (B_{C12} / bm) \cdot Oh} \right) \quad (5.115)$$

where

Dit^{C14} is the human total internal dose from ¹⁴C [Sv·a⁻¹],

DF^{C14} is the internal dose conversion factor for ¹⁴C [Sv·a⁻¹/(Bq·kg⁻¹)],

Ca_{max}^{C14} is the maximum ¹⁴C activity in the water (either well water or groundwater at discharge zones) [Bq·m⁻³_{water}],

C_{C12} is the average stable carbon concentration in the surrounding water [kg_C · L⁻¹_{water}],

gb^i is the mass/radioactivity conversion factor for nuclide $i = ^{14}\text{C}$ [kg·Bq⁻¹],

B_{C12} is the carbon content of soft tissues in a human [kg], and

Bm is the soft tissue mass in a human [kg].

5.6.12 Internal Dose Arising from ³⁶Cl

A total internal dose for ³⁶Cl is first estimated by the usual pathway equations. This estimated dose is compared with the maximum possible internal dose, which is calculated using a ³⁶Cl specific activity model and the average annual concentration of stable chlorine in groundwater. The minimum of these two ³⁶Cl dose rates is taken to be the ³⁶Cl internal dose:

$$Dit^{Cl36} (\text{pathways model}) = \sum_{k,i} De^{Cl36,k,i} + Dw^{Cl36} + Ds^{Cl36} + Di^{Cl36} \quad (5.116)$$

and

$$Dit^{Cl36} = \min \left(\frac{Dit^{Cl36} (\text{pathways model})}{DF^{Cl36} \cdot [Ca_{max}^{Cl36} / (C_{Cl} / clm + Ca_{max}^{Cl36} \cdot gb^i)] \cdot B_{Cl} / Bm \cdot Oh} \right) \quad (5.117)$$

where

Dit^{Cl36} is the human total internal dose from ³⁶Cl [Sv·a⁻¹],

DF^{Cl36} is the internal dose conversion factor for ³⁶Cl [Sv·a⁻¹/(Bq·kg⁻¹)],

Ca_{max}^{Cl36} is the maximum ³⁶Cl activity in the water (either well water or groundwater at discharge zones) [Bq·m⁻³_{water}],

C_{Cl} is the average stable chlorine concentration in the surrounding water [kg_{Cl}·L⁻¹_{water}],

gb^i is the mass/radioactivity conversion factor for nuclide $i = ^{36}\text{Cl}$ [kg·Bq⁻¹],

B_{Cl} is the chlorine content of soft tissues in a human [kg],

B_m is the soft tissues mass in a human [kg].

5.6.13 Internal Dose Arising from ^3H

The human total internal dose from ^3H is given by:

$$Dit^{H3} (\text{specific activity model}) = DF^{H3} \cdot (Ca_{dw}^{H3} / C_H) \cdot B_H \cdot Oh \quad (5.118)$$

where

Dit^{H3} is the human total internal dose from ^3H [$\text{Sv}\cdot\text{a}^{-1}$],
 DF^{H3} is the internal dose conversion factor for ^3H [$\text{Sv}\cdot\text{a}^{-1}/(\text{Bq}\cdot\text{kg}^{-1})$],
 Ca_{dw}^{H3} is the average drinking water concentration of ^3H [$\text{Bq}\cdot\text{m}^{-3}$],
 C_H is the concentration of hydrogen in water [$\text{g}\cdot\text{m}^{-3}$], and
 B_H is the average hydrogen concentration in humans [$\text{g}\cdot\text{kg}^{-1}$].

5.6.14 Total Doses to Humans

Total Dose from Food Ingestion

The total food ingestion dose to humans from nuclide i (except ^3H) is given in general as:

$$Det^i = \sum_j \sum_k De^{ijk} \quad (5.119)$$

where

Det^i is the human total food ingestion dose from nuclide i [$\text{Sv}\cdot\text{a}^{-1}$],
 j is the food type j = plant, meat, milk, bird or fish,
 k is the food ingestion pathway k .

This summation is limited to the appropriate combinations of j and k in the internal exposure pathways:

- | | | | |
|--------|-------|----------------------------------|---------|
| (i) | soil | → plant roots (garden) | → human |
| (ii) | soil | → plant roots(forage) → animals | → human |
| (iii) | air | → plant leaves(garden) | → human |
| (iv) | air | → plant leaves(forage) → animals | → human |
| (v) | water | → animals | → human |
| (vi) | soil | → animals | → human |
| (vii) | water | → fish | → human |
| (viii) | air | → animals | → human |
| (ix) | soil | | → human |

Pathways (ii), (iv), (v), (vi), and (viii) each involve branches corresponding to the 3 domestic terrestrial animal types: meat, milk, and bird. Therefore, a more specific statement of the total food ingestion dose rate is:

$$Det^i = \left\{ \begin{array}{l} De^{ik=(i)} + De^{ik=(iii)} + De^{ik=(vii)} \\ + \sum_{j=1}^3 [De^{ijk=(ii)} + De^{ijk=(iv)} + De^{ijk=(v)} + De^{ijk=(vi)} + De^{ijk=(ix)}] \end{array} \right\} \quad (5.120)$$

where $j = 1-3$ refers to the animal food types: meat, milk and bird.

Total Internal Dose

The human total internal dose from nuclide i from ingestion of food, water and soil and inhalation of air is given by Dit^i [$Sv \cdot a^{-1}$]:

$$Dit^i = Det^i + Dw^i + Ds^i + Di^i \quad (5.121)$$

However, for the special nuclides 3H , ^{14}C , ^{36}Cl and ^{129}I , the internal dose is calculated separately as described in Sections 5.6.10 to 5.6.13.

The total internal dose from all nuclides Dit [$Sv \cdot a^{-1}$] is then

$$Dit = \sum_i Dit^i \quad (5.122)$$

Total External Dose

The human total external dose from air and water immersion, ground exposure and exposure to building materials is given by:

$$Dot = \sum_i (Da^i + Dh^i + Dg^i + Db^i) \quad (5.123)$$

where Dot is the human total external dose [$Sv \cdot a^{-1}$].

Note that the more conservative building material is chosen for calculating Db^i .

Total Dose

The human total dose Dtt [$Sv \cdot a^{-1}$] from all sources (food ingestion, drinking water consumption, inhalation and external dose) is given by:

$$Dtt = Dit + Dot \quad (5.124)$$

5.7 CHEMICAL TOXICITY

The concentrations of contaminant i in well water, $C_{well}^i(t)$, lake water, $C_L^i(t)$, lake sediment used as soil, $C_{seeds}^{i,f}(t)$, surface soil, $C_{soil}^{i,f}(t)$, outdoor air, $C_{air,out}^{i,f}(t)$ and indoor air $C_{air,in}^{i,f}(t)$ are calculated in Equations (5.11), (5.20), (5.32), (5.55), and (5.74) through (5.79), respectively.

These concentrations are summed for all modelled isotopes of an element, including stable and radioactive, to give the concentration of the element in these compartments.

For well water, lake water, outdoor air and indoor air:

$$CT_{comp}^e(t) = \sum_{i=e} C_{comp}^i(t) \quad (5.125)$$

where the summation is over all nuclides i that are isotopes of an element e , $comp$ signifies the compartments L (lake), $well$, $air\ out$ and $air\ in$,

$C_{well}^i(t)$ is the concentration of nuclide i in the well at time t [$\text{mol}\cdot\text{m}^{-3}_{\text{water}}$],

$C_L^i(t)$ is the concentration of nuclide i in lake water at time t [$\text{mol}\cdot\text{m}^{-3}_{\text{water}}$],

$C_{air,out}^{i,f}(t)$ is the concentration of nuclide i in outdoor air [$\text{mol}\cdot\text{m}^{-3}_{\text{air}}$], and

$C_{air,in}^{i,f}(t)$ is the concentration of nuclide i in indoor air [$\text{mol}\cdot\text{m}^{-3}_{\text{air}}$].

For soil and lake sediment compartments:

$$CT_{comp}^e(t) = \max^f \left[\sum_{i=e} C_{comp}^{f,i}(t) \right] \quad (5.126)$$

where

f is the field type, $f = \text{garden, forage field, woodlot or peat bog}$,

$comp$ signifies either sediment used as soil (seds) or surface soil (soil),

$C_{seds}^{i,f}(t)$ is the concentration of nuclide i in sediment used as soil for field f [$\text{mol}\cdot\text{kg}^{-1}_{\text{dry sed}}$],

$C_{soil}^{i,f}(t)$ is the concentration of nuclide i in the surface soil for field f [$\text{mol}\cdot\text{kg}^{-1}_{\text{dry soil}}$].

The maximum element concentration may then be determined and compared to standards for chemical toxicity in soil, water and air. This comparison is not done in the model.

5.8 RADIOLOGICAL IMPACTS ON NON-HUMAN BIOTA

5.8.1 Reference Biota

Non-human biota include plants, animals, invertebrates and microorganisms living in water, sediment, soil and air as part of aquatic and terrestrial ecosystems. As an indication of the potential impact of a repository on non-human biota, we consider a small set of reference generic biota that represents a broad range of species and habitats. These are generic biota in the sense that their characteristics are not species specific, but represent a range. For example, we examine the dose for a biota as if fully immersed in water as well as if fully immersed in air. We assume that these different biota could exist during all states, but some of their characteristics are controlled by state-dependent parameter values. For example, their occupancy factor will change from state to state. See Appendix C for more details.

The reference biota considered are as follows:

1. A plant with nuclide uptake characteristics similar to a broad range of terrestrial vascular plants. This would include many grasses, herbs and trees. The plant can be immersed in contaminated soil, air and water, so it reflects the external exposures received by both terrestrial and aquatic species.
2. A mammal most similar to a herbivore in its eating habits. Typical species would include moose, beaver and meadow vole. The mammal can be immersed in contaminated air, soil and water, thereby reflecting external exposures received by terrestrial land, soil-burrowing and aquatic mammals. To a large extent, most mammalian predators are also included here.
3. A bird most similar to a terrestrial species that eats seeds and fruit. Typical species would include the ruffed grouse, song sparrow, and evening grosbeak. The bird can be immersed in air, soil and water, corresponding to a wide range of terrestrial and aquatic species. Thus, waterfowl would also be included to some extent.
4. A fish representing a wide range of free-swimming (pelagic) and bottom-feeding (benthic) species. This would include characteristics of diverse species such as lake trout, smallmouth bass, northern pike, lake whitefish and white sucker. The fish can be immersed in either water or sediment.

The model is analogous to the human food-chain and dose submodel. Nuclide concentrations in lake water, soil and air are calculated as described previously. These concentrations are used to calculate doses from external radiation and through food-chain transfer. Our model calculates whole-body doses, except for internal exposure of animals to ^{129}I . This nuclide is exceptional because iodine tends to accumulate in the thyroid gland; hence we consider the dose to that gland. As with human dose, groundwater limits are considered for ^{14}C , ^{36}Cl and ^{129}I , and a specific activity model is used for ^3H .

5.8.2 Mathematical Formulation

As for the human food-chain model, all the nuclide concentrations are expressed in Bequerels [Bq]. The use of Bq simplifies the application of the DCFs, which conventionally are expressed in radioactivity units. The radiological dose for the target organisms is calculated in units of Grays per year [$\text{Gy}\cdot\text{a}^{-1}$]. This differs from the units used for humans [$\text{Sv}\cdot\text{a}^{-1}$] because of a radiation quality factor and a tissue weighting factor.

Many of the human food-chain equations include an exponential term for radiological decay during a holdup time. This term is not included in the equations for calculating dose to non-human organisms because these organisms usually consume food and water directly without delay. This is conservative for some animals that store food, such as beavers, squirrels and blue jays.

Several equations involve water, for which the nuclide concentration is designated by C_{dw}^i .

Water may be derived from the well, C_{well}^i , or the lake, C_L^i . The transfer factors and concentration ratios for the non-human biota are the same as those used for plants and animals in the human food-chain pathways. This is also true for ancillary data such as plant yields, feed and water intakes, etc.

Plants are assumed to be located in fields with the greatest nuclide concentration, which may be enhanced through contaminated well or lake water from irrigation.

The forage field soil is used to reflect the habitat of animals. Since the model places forage fields on more contaminated soils than forests, the selection of the forage field for wild animals is likely conservative.

5.8.3 Internal Exposure of Plants

Plants can accumulate nuclides from the soil via root uptake and from aerial deposition. We conservatively assume that the plant is located in the garden, which has the greatest soil nuclide concentration and also receives irrigation water, often from a potentially contaminated well. The plant/soil concentration factor for forage type plants is assumed.

The activity concentration in plant biota from nuclide i , $CBa^{i,plant}$ is given by:

$$CBa^{i,plant} = Ca_{se}^{i,garden} \cdot CR^{i,forage} + \left[Ad_{air}^i \cdot (r_{air}^{plant} / Y_p^{garden}) \cdot \left(1 - e^{-\lambda_E^{i,tpb} \cdot te^{plant,k}} \right) / \lambda_E^{i,tpb} \right] \quad (5.127)$$

and the internal dose to plant biota, including the contribution due to ingrowth from the parent nuclide, is given by:

$$DBa^{i,plant} = (CBa^{i,plant} + CBa^{p,plant}) \cdot DFB_{int}^i \cdot Onh \quad (5.128)$$

where

$CBa^{i,plant}$, $CBa^{p,plant}$ is the concentration (activity) of nuclide i or parent p in plants [$Bq \cdot kg^{-1}_{wetbio}$],

$Ca_{se}^{i,garden}$ is the average garden soil concentration (activity) of nuclide i [$Bq \cdot kg^{-1}_{drysoil}$],

$CR^{i,forage}$ is the forage plant/soil concentration ratio for nuclide i [$Bq \cdot kg^{-1}_{wetbio} / (Bq \cdot kg^{-1}_{drysoil})$],

Ad_{air}^i is the atmospheric deposition rate of nuclide i to surface of plants [$Bq \cdot m^{-2}_{soil} \cdot d^{-1}$],

r_{air}^{plant} is the atmospheric plant interception fraction for plant biota [-],

Y_p^{garden} is the garden plant biomass density (yield) [$kg_{wetbio} \cdot m^{-2}_{soil}$],

$\lambda_E^{i,tpb}$ is the effective removal rate constant of nuclide i from vegetation [d^{-1}],
Equation (5.91)

$te^{plant,k}$ is the time of above-ground exposure for the plant during the growing season, or return time for pasture [d],

k is the plant leaf - human pathway,

$DFB_{int}^{i,plant}$ is the internal dose to plant biota from nuclide i [$Gy \cdot a^{-1}$],

DFB_{int}^i is the internal dose conversion factor for nuclide i [$(Gy \cdot a^{-1}) / (Bq \cdot kg^{-1}_{wetbio})$],
and

Onh is the overall non-human occupancy factor [-].

5.8.4 Internal Exposure of Terrestrial Animals

Terrestrial animals can accumulate nuclides internally through ingestion of contaminated food, water and soil and inhalation of contaminated air. The activity concentration of nuclide i in animal $m =$ bird or mammal is given by

$$CBA^{i,m} = (CBA^{i,plant} \cdot F^{im} \cdot Q_{f,an}^m) + (Ca_{se}^{i,forage} \cdot F^{im} \cdot Q_s^m) + (Ca_{dw}^i \cdot F^{im} \cdot Q_{dw}^m \cdot clm) + (Ca_{air,out}^i \cdot FI^{im} \cdot Q_a^m) \quad \text{for } i \neq {}^3\text{H and } {}^{222}\text{Rn} \quad (5.129)$$

$$CBA^{i,m} = Ca_{air,out}^i \cdot FI^{i,m} \cdot Q_a^m \quad \text{for } i = {}^{222}\text{Rn}$$

where

$CBA^{i,m}$ is the concentration (activity) of nuclide i in $m =$ bird or mammal [$\text{Bq} \cdot \text{kg}^{-1}_{\text{wetbio}}$],

$CBA^{i,plant}$ is the concentration (activity) of nuclide i in plant biota [$\text{Bq} \cdot \text{kg}^{-1}_{\text{wetbio}}$],

F^{im} is the ingestion transfer coefficient for nuclide i for biota $m =$ mammal and bird [$\text{d} \cdot \text{kg}^{-1}_{\text{wetbio}}$],

$Q_{f,an}^m$ is the feed or forage consumption rate for biota m [$\text{kg}_{\text{wetbio}} \cdot \text{d}^{-1}$],

$Ca_{se}^{i,forage}$ is the average forage soil concentration (activity) of nuclide i [$\text{Bq} \cdot \text{kg}^{-1}_{\text{drysoil}}$],

Q_s^m is the animal soil ingestion rate for biota m [$\text{kg}_{\text{drysoil}} \cdot \text{d}^{-1}$],

Ca_{dw}^i is the average concentration of nuclide i in the water source, and may equal C_L (lake) or C_{well} (well) [$\text{Bq} \cdot \text{m}^{-3}_{\text{water}}$],

Q_{dw}^m is the animal drinking water ingestion rate for biota m [$\text{L}_{\text{water}} \cdot \text{d}^{-1}$]

clm is the conversion factor from m^3 to L [$0.001 \text{ m}^3 \cdot \text{L}^{-1}$],

$Ca_{air,out}^i$ is the concentration (activity) of nuclide i in outdoor air [$\text{Bq} \cdot \text{m}^{-3}$],

FI^{im} is the terrestrial animal inhalation transfer coefficient for nuclide i and biota m [$\text{d} \cdot \text{L}^{-1}$ or $\text{d} \cdot \text{kg}^{-1}$], and

Q_a^m is the animal inhalation rate for biota m [$\text{m}^3 \cdot \text{d}^{-1}$].

The ${}^3\text{H}$ non-human biota doses are calculated in Section 5.8.13.

Equation (5.129) accounts for nuclide intake through eating plants (contaminated by root uptake and deposition onto leaves), water ingestion, soil ingestion, and inhalation. The animals considered are the reference generic mammal and bird. In the present CC4/BIOTRAC model, the characteristics of these generic biota are considered to be the same as the human food animals $j =$ meat and bird.

The internal ${}^{129}\text{I}$ dose conversion factor for the mammal, bird and fish must be increased by a factor of ten over that for the plant to account for accumulation of iodine in the thyroid gland. This accumulation is not taken into account in food-chain transfer through the transfer coefficients or through the aquatic concentration ratio for these animals (Amiro 1992).

For radon, with its short-lived daughter nuclides, only the last term of Equation (5.129) concerned with inhalation applies. Radon is an inert gas and so is not itself subject to food-chain transfer.

The internal dose to a generic animal DB_{int} is given by:

$$DB_{int}^{i,m} = (CBa^{i,m} + CBa^{p,m}) \cdot DFB_{int}^i \cdot Onh \quad (5.130)$$

where

$DB_{int}^{i,m}$ is the internal dose to biota m from nuclide i [$Gy \cdot a^{-1}$],
 $CBa^{i,m}$, $CBa^{p,m}$ is the concentration (activity) of nuclide i or parent p for biota $m =$ bird or mammal [$Bq \cdot kg^{-1}_{wetbio}$], and
 DFB_{int}^i is the internal dose conversion factor for nuclide i [$(Gy \cdot a^{-1}) / (Bq \cdot kg^{-1}_{wetbio})$].

5.8.5 Internal Exposure of Fish

Fish inhabiting the discharge lake may become contaminated through ingestion of food and sediment, and through osmotic exchange of fluids. The dose to fish from internal exposure, DB_{int} is given by:

$$DB_{int}^{i,fish} = (Ca_L^i + Ca_L^p) \cdot B^{i,fish} \cdot DFB_{int}^{i,fish} \cdot clm \cdot Onh \quad (5.131)$$

where

$DB_{int}^{i,fish}$ is the internal dose to fish from nuclide i [$Gy \cdot a^{-1}$],
 Ca_L^i , Ca_L^p is the concentration (activity) of nuclide i or parent p in the lake [$Bq \cdot m^{-3}_{water}$],
 $B^{i,fish}$ is the aquatic concentration ratio for nuclide i and biota $m =$ fish [$L_{water} \cdot kg^{-1}_{wetbio}$], and,
 $DFB_{int}^{i,fish}$ is the dose conversion factor for internal exposure of fish to nuclide i [$(Gy \cdot a^{-1}) / (Bq \cdot kg^{-1}_{wetbio})$].

5.8.6 Immersion in Water

To evaluate the impact of aquatic habitats, all the generic biota are assumed to be immersed in water. For example, fish spend their whole lives in water; plants can be aquatic or have their roots submerged in soil pore-water; and many animals can spend a portion of their time swimming, wading or lying in water.

The dose to biota from immersion in water from the well or lake, $DB_{w,ext}$ is given by:

$$DB_{w,ext}^{i,m} = Ca_{dw}^i \cdot DFB_{w,ext}^{i,m} \cdot Onh \quad (5.132)$$

where

$DB_{w,ext}^{i,m}$ is the external dose to biota in water from nuclide i for $m =$ bird, plant or mammal, [$Gy a^{-1}$],
 Ca_{dw}^i is the average concentration (activity) of nuclide i in the water, and may equal Ca_L^i (lake) or Ca_{well}^i (well) [$Bq \cdot m^{-3}_{water}$], and
 $DFB_{w,ext}^{i,m}$ is the water immersion dose conversion factor for $m =$ bird, plant or mammal for nuclide i [$(Gy \cdot a^{-1}) / (Bq \cdot m^{-3}_{water})$].

For $m = \text{fish}$, Ca_{dw}^i is equal to Ca_L^i .

5.8.7 Immersion in Soil or Sediment

To evaluate the impact of ground-dwelling habitats, all the generic biota are also assumed to be immersed in soil. For example, plants are rooted in soil and they may also accumulate soil particles on foliage from aerial deposition; terrestrial animals may lie or burrow in soil or be covered with contaminated soil particles; and bottom-feeding fish can be essentially immersed in sediments.

The external dose to biota from immersion in soil, $DB_{s,ext}$ is given by:

$$DB_{s,ext}^{i,m} = Ca_{se}^{i,forage} \cdot DFB_{s,ext}^{i,m} \cdot Onh \quad (5.133)$$

where

$DB_{s,ext}^{i,m}$ is the external dose from nuclide i for immersion in soil or sediment for $m = \text{bird, plant or mammal}$ [$\text{Gy} \cdot \text{a}^{-1}$],

$Ca_{se}^{i,forage}$ is the average forage soil concentration (activity) of nuclide i , which in some cases will be a sediment concentration [$\text{Bq} \cdot \text{kg}^{-1}_{\text{drysoil}}$], and

$DFB_{s,ext}^{i,m}$ is the soil or sediment immersion dose conversion factor for $m = \text{bird, plant or mammal}$ for nuclide i , [$(\text{Gy} \cdot \text{a}^{-1}) / (\text{Bq} \cdot \text{m}^{-1}_{\text{drysoil}})$].

For $m = \text{fish}$,

$$DB_{s,ext}^{i,m} = Ca_{sed}^i \cdot DFB_{s,ext}^{i,fish} \cdot Onh \quad (5.134)$$

where

Ca_{sed}^i is the concentration (activity) of nuclide i in the bottom sediments of the surface water body [$\text{Bq} \cdot \text{kg}^{-1}_{\text{drysoil}}$],

5.8.8 Immersion in Air

We assume that plants, mammals and birds can be immersed in air, but fish cannot. In all cases, the organisms are exposed to outdoor air concentrations and all the concentrations of nuclide i in air, C_{air} , refer to the sum from all the outdoor contributions.

The dose to biota from nuclide i from immersion in air, $DB_{a,ext}$, for $m = \text{bird, plant or mammal}$ is given by:

$$DB_{a,ext}^{i,m} = Ca_{air,out}^i \cdot DFB_{a,ext}^{i,m} \cdot Onh \quad (5.135)$$

where

- $DB_{a,ext}^{i,m}$ is the dose to biota from nuclide i from immersion in air for $m = \text{bird, plant or mammal}$ [$\text{Gy}\cdot\text{a}^{-1}$],
- $Ca_{air,out}^i$ is the concentration (activity) of nuclide i in outdoor air [$\text{Bq}\cdot\text{m}^{-3}$], and
- $DFB_{a,ext}^{i,m}$ is the air immersion dose conversion factor for $m = \text{bird, plant or mammal}$ for nuclide i [$(\text{Gy}\cdot\text{a}^{-1})/(\text{Bq}\cdot\text{m}^{-3}_{air})$].

5.8.9 Immersion in Vegetation

Terrestrial animals can be surrounded or immersed in vegetation during much of their lives. For example, many birds nest and roost in vegetation, many small mammals burrow and feed in vegetation, domestic animals may bed on straw, and forest dwellers are surrounded by trees and other plants. We assess the dose from external exposure to vegetation that has been contaminated from a variety of sources. We assume that exposure to contaminated vegetation is unimportant for fish because most of their external dose should come directly from water and sediment, and water forms an efficient shield against radiation penetration from remote sources.

We do not calculate external exposure to a plant from other plants. This situation is implicitly included in our internal dose conversion factors, which conservatively assume that all the radiation is absorbed by the plant (Amiro 1992). Therefore, we only calculate external exposure for mammals and birds from vegetation.

Plant concentrations are calculated using the same methods as for the human food chain. Vegetation can receive nuclides from the soil through root uptake and through aerial deposition. We assume that the animals inhabit the forage field. This field is rarely irrigated, and if so, only by lake water, so its plant concentrations tend to be lower than those in the garden. The forage-field plant concentrations are similar or greater than those in the woodlot (according to how fields are assigned to contaminated soils in the CC4/BIOTRAC model), so the use of the forage field is reasonable and likely conservative. The forage field is also used for soil immersion of animals.

The concentrations in vegetation are calculated using both soil and air pathways, and the resulting dose is given by:

$$DB_{v,ext}^{i,m} = CBa^{i,plant} \cdot DFB_{v,ext}^{i,m} \cdot Onh \quad (5.136)$$

where

- $DB_{v,ext}^{i,m}$ is the dose to biota from nuclide i from immersion in vegetation for $m = \text{bird or mammal}$ [$\text{Gy}\cdot\text{a}^{-1}$],
- $CBa^{i,plant}$ is the activity concentration of nuclide i for plants from Equation (5.127) [$\text{Bq}\cdot\text{kg}^{-1}_{wetbio}$],
- $DFB_{v,ext}^{i,m}$ is the dose conversion factor for nuclide i , for $m = \text{bird or mammal}$, for external exposure to vegetation [$(\text{Gy}\cdot\text{a}^{-1})/(\text{Bq}\cdot\text{m}^{-3}_{wetbio})$].

5.8.10 Determination of Total External Doses

The contribution of these pathways to the biota total dose will vary with biota. No biota would be exposed to 100% of all these pathways. Therefore, the total external doses, DB_{ext} [$\text{Gy}\cdot\text{a}^{-1}$], for

each of the four reference biota are estimated as the maximum of the contributions from each relevant source.

Therefore the external dose for nuclide i for fish is given by:

$$DB_{ext}^{i, fish} = \max\{DB_{w,ext}^{i, fish}, DB_{s,ext}^{i, fish}\} \quad (5.137)$$

The external dose for nuclide i for plants is given by:

$$DB_{ext}^{i, plant} = \max\{DB_{w,ext}^{i, plant}, DB_{s,ext}^{i, plant}, DB_{a,ext}^{i, plant}\} \quad (5.138)$$

The external dose for nuclide i for $m =$ bird or mammal is given by:

$$DB_{ext}^{i, m} = \max\{DB_{w,ext}^{i, m}, DB_{s,ext}^{i, m}, DB_{a,ext}^{i, m}, DB_{v,ext}^{i, m}\} \quad (5.139)$$

5.8.11 Calculation of Total Radiological Doses

The total dose, DB_{tot} [$\text{Gy} \cdot \text{a}^{-1}$], for each reference biota is simply the sum of all external and internal doses from all nuclides.

The total dose for $m =$ bird, plant, mammal and fish, is given by:

$$DB_{tot}^{i, m} = DB_{ext}^{i, m} + DB_{int}^{i, m} \quad (5.140)$$

5.8.12 Groundwater Limits to ^{14}C , ^{36}Cl and ^{129}I Internal Doses for Non-Human Biota

The presence of stable carbon, chlorine and iodine in groundwater sets an upper dose limit for non-human biota from ^{14}C , ^{36}Cl and ^{129}I since the nuclide/stable element ratio will not exceed that of the natural background. The models applicable for non-human biota are essentially the same as those for humans. Furthermore, the models for non-human biota for ^{14}C , ^{36}Cl and ^{129}I are all essentially the same.

The upper dose limit to the internal dose for non-human biota from ^{14}C for biota m is given by:

$$DB_{lim}^{C14} = CB_{C12}^m \cdot [Ca_{gw,max}^{C14} / (C_{C12} / clm)] \cdot DFB_{int}^{C14} \cdot Onh \quad (5.141)$$

where

DB_{lim}^{C14} is the upper dose limit to internal dose from ^{14}C for non-human biota for $m =$ bird, plant, mammal or fish [$\text{Gy} \cdot \text{a}^{-1}$],

CB_{C12}^m is the concentration of carbon in biota m [$\text{kg}_C \cdot \text{kg}^{-1}_{\text{wetbio}}$],

$Ca_{gw,max}^{C14}$ is the maximum concentration (activity) of ^{14}C in groundwater among all the discharge locations [$\text{Bq} \cdot \text{m}^{-3}_{\text{water}}$],

C_{C12} is the annual average groundwater concentration of stable carbon [$\text{kg}_C \cdot \text{L}^{-1}_{\text{water}}$],

DFB_{int}^{C14} is the internal dose conversion factor for ^{14}C [$(\text{Gy} \cdot \text{a}^{-1}) / (\text{Bq} \cdot \text{kg}^{-1})$], and

Onh overall non-human occupancy factor [-].

Similar equations apply for ^{36}Cl and ^{129}I .

Unlike the groundwater dose limits for humans, the limits for non-human biota are always based on water discharging from the geosphere to the lake at the most contaminated discharge zone. Thus, Ca_{gw}^i (for $i = ^{14}\text{C}$, ^{36}Cl and ^{129}I) is never based on water from the bedrock well, regardless of the source of domestic water for the critical group.

In the dose analysis, the total internal dose estimated from the transport model, DB_{tot} is compared with the appropriate groundwater dose limit, DB_{lim} , and the smaller dose is adopted as the total internal dose.

5.8.13 Model for Tritium

The model to estimate internal doses from tritium for non-human biota is essentially the same as our specific-activity model for humans (Davis et al. 1993). The model assumes the specific activity of tritium in these biota is the same as the specific activity in surface water. For humans, surface water can be represented by either well or lake water, but for non-human biota it is always lake water because we are mainly concerned with natural plants and animals. The internal dose to biota m from tritium, DB_{H3} , is given by:

$$DB_{H3}^m = CB_H^m \cdot [Ca_L^{H3}/C_H] \cdot DFB_{int}^{H3} \cdot Onh \quad (5.142)$$

where

DB_{H3}^m is the internal dose to biota m from ^3H [$\text{Gy} \cdot \text{a}^{-1}$],

CB_H^m is the concentration of hydrogen in $m = \text{plant, mammal, bird and fish}$ [$\text{g}_\text{H} \cdot \text{kg}^{-1}_{\text{wetbio}}$].

Ca_L^{H3} is the average ^3H concentration in lake water [$\text{Bq} \cdot \text{m}^{-3}_{\text{water}}$]

C_H is the concentration of hydrogen in water [$\text{g}_\text{H} \cdot \text{m}^{-3}_{\text{water}}$], and

DFB_{int}^{H3} is the internal dose conversion factor for ^3H [$(\text{Gy} \cdot \text{a}^{-1})/(\text{Bq} \cdot \text{kg}^{-1})$].

This model accounts for all the pathways and mechanisms whereby non-human biota can become internally contaminated with tritium. Thus, there is no need to consider any other exposure pathways. For external exposure, tritium is treated in the same way as all the other nuclides.

5.9 REFERENCES

Amiro, B.D. 1992. The atmosphere submodel for the assessment of Canada's nuclear fuel waste management concept. Atomic Energy of Canada Limited Report, AECL-9889, COG-91-199. Pinawa, Canada.

Baes, III, C.F. and R.D. Sharp. 1981. Predicting radionuclide leaching from root zone soil for assessment applications. Transactions of the American Nuclear Society 38, 111-112.

- BEAK International. 2002. Guidance for calculation of Derived Release Limits for radionuclides in airborne and liquid effluents from Ontario Power Generation nuclear facilities. Ontario Power Generation Report OPG N-REP-03482-10000-R00. Toronto, Canada.
- BIOMOVSII. 1996. Uncertainty and Validation: Effect of Model Complexity on Uncertainty Estimates. Swedish National Institute of Radiological Protection (SKI), BIOMOVSII Technical Report No. 16. Stockholm, Sweden.
- Bird, G.A., M. Stephenson and R.J. Cornett. 1992. The surface water submodel for the assessment of Canada's nuclear fuel waste management concept. Atomic Energy of Canada Limited Report, AECL-10290, COG-91-193. Pinawa, Canada.
- Davis, P.A., R. Zach, M.E. Stephens, B.D. Amiro, G.A. Bird, J.A.K. Reid, M.I. Sheppard, S.C. Sheppard and M. Stephenson. 1993. The disposal of Canada's nuclear fuel waste: The biosphere model, BIOTRAC, for postclosure assessment. Atomic Energy of Canada Limited Report, AECL-10720, COG-93-10. Pinawa, Canada.
- Garisto, F., J. Avis., T. Chshyolkova, P. Gierszewski, M. Gobien, C. Kitson, T. Melnyk, J. Miller, R. Walsh and L. Wojciechowski. 2010. Glaciation scenario: Safety assessment for a deep geological repository for used fuel. Nuclear Waste Management Organization Technical Report NWMO TR-2010-10. Toronto, Canada.
- Gierszewski, P., T.W. Melnyk, S.C. Sheppard and J. Tait. 2004. SYVAC3-CC4 theory manual. Ontario Power Generation Report 06819-REP-01300-10072. Toronto, Canada.
- Goodwin, B.W., D.B. McConnell, T.H. Andres, W.C. Hajas, D.M. LeNeveu, T.W. Melnyk, G.R. Sherman, M.E. Stephens, J.G. Szekely, P.C. Bera, C.M. Cosgrove, K.D. Dougan, S.B. Keeling, C.I. Kitson, B.C. Kummen, S.E. Oliver, K. Witzke, L. Wojciechowski and A.G. Wikjord. 1994. The disposal of Canada's nuclear fuel waste: Postclosure assessment of a reference system. Atomic Energy of Canada Limited Report, AECL-10717, COG-93-7. Pinawa, Canada.
- Grogan, H.A. 1989. Scenario B2: Irrigation with contaminated groundwater. Swedish National Institute of Radiological Protection (SKI), BIOMOVS Technical Report No. 6. Stockholm, Sweden.
- Grogan, H., B. Baeyens, H. Müller-Lemans and F. van Dorp. 1991. Biosphere modelling for a deep radioactive waste repository: Transport of groundwater to soil in a small valley, NAGRA Technical Report NTB 89-21. Wettingen, Switzerland.
- Hillel, D. 1980. Applications of Soil Physics. Academic Press, Toronto, Canada.
- ICRP (Internal Commission of Radiological Protection.) 1975. Reference man: anatomical, physiological and metabolic characteristics. ICRP Publication 23. Pergamon Press, Oxford, UK.
- ICRP (Internal Commission of Radiological Protection.) 1979. Limits on intakes of radionuclides by workers. Annals of the ICRP 2(3/4) (ICRP Publication 30).

- Jones, C.H. 1990. Scenario B6: Transport of contaminated groundwater to the soil surface. Swedish National Institute of Radiological Protection (SKI), BIOMOVs Technical Report B6. Stockholm, Sweden.
- Sheppard, M.I. 1992. The soil submodel, SCEMR1, for the assessment of Canada's nuclear fuel waste management concept. Atomic Energy of Canada Limited Report, AECL-9577, COG-91-194. Pinawa, Canada.
- Sheppard, M.I. 1995. Strategy for modelling soil erosion and soil profile development in a landscape for environmental impact assessments. Atomic Energy of Canada Limited Technical Record TR-679, COG-95-72. Pinawa, Canada.
- Szekely, J.G., L.C. Wojciechowski, M.E. Stephens and H.A. Halliday. 1994. Analysis specification for the CC3 biosphere model BIOTRAC. Atomic Energy of Canada Limited Report AECL-11078, COG-94-102. Pinawa, Canada.
- Zach, R. and S.C. Sheppard. 1992. The food-chain and dose submodel, CALDOS, for the assessment of Canada's nuclear fuel waste management concept. Atomic Energy of Canada Limited Report AECL-10165, COG-91-195. Pinawa, Canada.
- Zach, R., B.D. Amiro, G.A. Bird, C.R. Macdonald, M.I. Sheppard, S.C. Sheppard and J.G. Szekely. 1996. The disposal of Canada's nuclear fuel waste: A study of postclosure safety of in-room emplacement of used CANDU fuel in copper containers in permeable plutonic rock; Volume 4: Biosphere Model. Atomic Energy of Canada Limited Report, AECL-11494-4, COG-95-552-4. Pinawa, Canada.

6. MASS ACCUMULATION AND DISTRIBUTION

6.1 MASS IN CONTAINER

The amount of nuclide i in the containers is determined in both intact and failed containers.

Amount in intact containers:

The distribution of mass for intact containers consists of three parameters defined at the end of the simulation, t_{end} :

$$(1) N_{ICtr} \cdot I_{ICtr}^i(t_{end}) \quad (6.1a)$$

- is the remaining amount of nuclide i in intact containers at t_{end} [mol];

$$(2) N_{ICtr} \cdot \int_0^{t_{end}} \lambda_r^i \cdot I_{ICtr}^i(t) \cdot dt \quad (6.1b)$$

- is the amount of nuclide i lost to decay in intact containers [mol];

$$(3) N_{ICtr} \cdot \int_0^{t_{end}} \lambda_r^p \cdot I_{ICtr}^p(t) \cdot dt \quad (6.1c)$$

- is the amount of nuclide i formed by ingrowth in intact containers [mol];

where

$$\frac{\partial I_{ICtr}^i}{\partial t} = \left[-\lambda_r^i \cdot I_{ICtr}^i(t) + \lambda_r^p \cdot I_{ICtr}^p(t) \right] \quad (6.2)$$

$$N_{ICtr} = \left(\sum_{sectors} N_{ICtr}^s \right) \quad (6.3)$$

$I_{ICtr}^i(t)$ is the amount of nuclide i in one intact container at time t [mol],

$I_{ICtr}^p(t)$ is the amount of the parent p of nuclide i in one intact container at time t [mol],

λ_r^i, λ_r^p are the decay constants for nuclides i and p [1/a], and

N_{ICtr}^s is the number of intact containers in sector s [-].

Note: There is zero release from the intact containers.

Amount in failed containers:

The distribution of mass for failed containers consists of four parameters defined at the end of the simulation, t_{end} :

$$(1) \sum_{sectors} N_{Fctr}^s \cdot I_{Fctr}^{i,s}(t_{end}) \quad (6.4a)$$

- is the remaining amount of nuclide i in failed containers at t_{end} [mol];

$$(2) \sum_{sectors} N_{Fctr}^s \cdot \int_0^{t_{end}} \lambda_r^i \cdot I_{Fctr}^{i,s}(t) \cdot dt \quad (6.4b)$$

- is the amount of nuclide i lost to decay in failed containers [mol];

$$(3) \sum_{sectors} N_{Fctr}^s \cdot \int_0^{t_{end}} \lambda_r^p \cdot I_{Fctr}^{p,s}(t) \cdot dt \quad (6.4c)$$

- is the amount of nuclide i formed by ingrowth from parent p in failed containers [mol];

$$(4) \sum_{sectors} N_{Fctr}^s \cdot \int_0^{t_{end}} F_{OutFctr}^{i,s}(t) \cdot dt \quad (6.4d)$$

- is the amount of nuclide i that flows out from failed containers [mol].

where

$$\frac{\partial I_{Fctr}^{i,s}}{\partial t} = \left[-\lambda_r^i \cdot I_{Fctr}^{i,s}(t) + \lambda_r^p \cdot I_{Fctr}^{p,s}(t) - F_{OutFctr}^{i,s}(t) \right] \quad \text{and} \quad (6.5)$$

$F_{OutFctr}^{i,s}(t)$ is the flow of nuclide i out of a failed container in sector s at time t [mol/a].

6.2 MASS IN ENGINEERED BARRIERS

The amount of nuclide i in the repository rooms is determined from the inventory in the buffer, backfill and EDZ, but not that in the containers, since that is calculated separately. The distribution of mass consists of four parameters defined at the end of the simulation, t_{end} :

$$(1) \sum_{sectors} N_{Fctr}^s \cdot I_{Vit}^{i,s}(t_{end}) \quad (6.6a)$$

- is the remaining amount of nuclide i in rooms at t_{end} [mol];

$$(2) \sum_{sectors} N_{Fctr}^s \cdot \int_0^{t_{end}} \lambda_r^i \cdot I_{Vit}^{i,s}(t) \cdot dt \quad (6.6b)$$

- is the amount of nuclide i lost to decay in rooms [mol];

$$(3) \sum_{sectors} N_{Fctr}^s \cdot \int_0^{t_{end}} \lambda_r^p \cdot I_{Vit}^{p,s}(t) \cdot dt \quad (6.6c)$$

- is the amount of nuclide i formed by ingrowth in rooms [mol];

$$(4) \sum_{sectors} N_{Fctr}^s \cdot \int_0^{t_{end}} F_{OutEDZ}^{i,s}(t) \cdot dt \quad (6.6d)$$

- is the amount of nuclide i that flows out from repository rooms [mol];

where

$$\frac{\partial I_{VIt}^{i,s}}{\partial t} = \left[-\lambda_r^i \cdot I_{VIt}^{i,s}(t) + \lambda_r^p \cdot I_{VIt}^{p,s}(t) + F_{OutCtr}^{i,s}(t) - F_{OutEDZ}^{i,s}(t) \right] \quad (6.7)$$

- $I_{VIt}^{i,s}(t)$ is the amount of nuclide i in a repository room in sector s at time t [mol],
 $I_{VIt}^{p,s}(t)$ is the amount of parent p of nuclide i in a repository room in sector s at time t [mol],
 λ_r^i, λ_r^p are the decay constants for nuclides i and p [1/a],
 N_{FCtr}^s is the number of failed containers in sector s [-],
 $F_{OutCtr}^{i,s}(t)$ is the flow of nuclide i out of a failed container in sector s at time t [mol/a], and
 $F_{OutEDZ}^{i,s}(t)$ is the flow of nuclide i out of the EDZ in sector s at time t due to one failed container [mol/a].

6.3 MASS IN GEOSPHERE

The amount of nuclide i in the geosphere is determined from the inventory in all segments between (but excluding) the EDZ and the biosphere surface soil. The distribution of mass consists of four parameters defined at the end of the simulation, t_{end} :

$$(1) I_{Geo}^i(t_{end}) \quad (6.8a)$$

- is the remaining amount of nuclide i in geosphere at t_{end} [mol];

$$(2) \int_0^{t_{end}} \lambda_r^i \cdot I_{Geo}^i(t) \cdot dt \quad (6.8b)$$

- is the amount of nuclide i lost to decay in geosphere [mol];

$$(3) \int_0^{t_{end}} \lambda_r^p \cdot I_{Geo}^p(t) \cdot dt \quad (6.8c)$$

- is the amount of nuclide i formed by ingrowth from parent p in geosphere [mol];

$$(4) \sum_d \int_0^{t_{end}} F_{OutGeo}^{i,d}(t) \cdot dt \quad (6.8d)$$

- is the amount of nuclide i that flows out from geosphere through discharges d [mol],

where

$$\frac{\partial I_{Geo}^i}{\partial t} = \left[-\lambda_r^i \cdot I_{Geo}^i(t) + \lambda_r^p \cdot I_{Geo}^p(t) + \sum_{s=sectors} F_{OutEDZ}^{i,s}(t) - \sum_{d=discharges} F_{OutGeo}^{i,d}(t) \right] \quad (6.9)$$

- $I_{Geo}^i(t)$ is the amount of nuclide i in the geosphere at time t [mol],
 $I_{Geo}^p(t)$ is the amount of parent p of nuclide i in the geosphere at time t [mol],

λ_r^i, λ_r^p are the decay constants for nuclides i and p [1/a],

$F_{OutEDZ}^{i,s}(t)$ is the flow of nuclide i out of the EDZ into the geosphere in sector s at time t [mol/a], and

$F_{OutGeo}^{i,d}(t)$ is the flow of nuclide i out of the geosphere at discharge location d at time t [mol/a].

When simulating a change in state, the geosphere submodel (CC4.07 and CC4.08) ensures that the mass of radionuclide in each segment is the same at the end of one state and the beginning of the succeeding state.

6.4 MASS IN BIOSPHERE

The biosphere can be divided conceptually into a local biosphere representing the watershed around the repository, and a downstream biosphere. The local biosphere is centered on a surface water body (referred to here as a "lake", although it could also be a river) in which the surface and groundwaters collect. Within this local biosphere, we are interested in a detailed distribution of the nuclide mass between waters, soils, air and biomass. Nuclides leave the local biosphere with the flow of water and air and enter the downstream biosphere. The details of this are not modelled, but the total downstream mass is tracked.

When simulating a change in state, the CC4 biosphere submodel ensures the mass of radionuclide in each component of the biosphere is the same at the end of one state and the beginning of the succeeding state, with one exception. That exception involves radionuclide mass in the surface water, nominally a lake, during a transition from one state to another with different lake volume. The CC4 biosphere model assumes that any decrease in lake volume is accompanied by a decrease in radionuclide mass in the lake such that radionuclide concentrations in the lake are invariant. The radionuclide mass that is 'flushed' out of the local biosphere is included in the total downstream mass.

Local biosphere overall distribution

The distribution of mass consists of four parameters defined at the end of the simulation, t_{end} :

$$(1) I_{Bio}^i(t_{end}) \quad (6.10a)$$

- is the remaining amount of nuclide i in local biosphere at t_{end} [mol];

$$(2) \int_0^{t_{end}} \lambda_r^i \cdot I_{Bio}^i(t) \cdot dt \quad (6.10b)$$

- is the amount of nuclide i lost to decay in local biosphere [mol];

$$(3) \int_0^{t_{end}} \lambda_r^p \cdot I_{Bio}^p(t) \cdot dt \quad (6.10c)$$

- is the amount of nuclide i formed by ingrowth in local biosphere [mol];

$$(4) \int_0^{t_{end}} F_{OutLake}^i(t) \cdot dt + \int_0^{t_{end}} F_{DegasSoil}^i(t) \cdot dt + \int_0^{t_{end}} F_{DegasLake}^i(t) \cdot dt \quad (6.10d)$$

- is the amount of nuclide i that flows out of the local biosphere [mol] via the lake and atmosphere;

where

$$\frac{\partial I_{Bio}^i}{\partial t} = \left[-\lambda_r^i \cdot I_{Bio}^i(t) + \lambda_r^p \cdot I_{Bio}^p(t) + \sum_{discharges} F_{OutGeo}^{i,d}(t) - F_{OutLake}^i(t) - F_{DegasSoil}^i(t) - F_{DegasLake}^i(t) \right] \quad (6.11)$$

$$F_{OutLake}^i = C_L^i \cdot R_t \cdot A_{watershed} \quad (6.12)$$

$$F_{DegasSoil}^i = Ms_{Total}^i \cdot \lambda_{DegasSoil} \quad (6.13)$$

$$F_{DegasLake}^i = C_L^i \cdot V_{Lake} \cdot \lambda_{DegasLake} \quad (6.14)$$

- $I_{Bio}^i(t)$ is the amount of nuclide i in the local biosphere at time t [mol],
 $I_{Bio}^p(t)$ is the amount of parent p of nuclide i in the local biosphere at time t [mol],
 λ_r^i, λ_r^p are the decay constants for nuclides i and p [1/a],
 $F_{OutGeo}^{i,d}(t)$ is the flow of nuclide i out of the geosphere at discharge location d at time t [mol/a],
 R_t is the watershed average runoff into the lake (after evapotranspiration, R=P-ET) [m/a],
 $A_{watershed}$ is the watershed area that feeds into the lake [m²],
 V_{Lake} is the lake volume [m³],
 $\lambda_{DegasSoil}, \lambda_{DegasLake}$ are the degassing rate constants from soil and lakewater [1/a],
 Ms_{Total}^i is the total amount of nuclide i in terrestrial field surface soils [mol], and
 C_L^i is the concentration of nuclide i in the lake [mol/m³].

(Note that cropping losses are assumed to be retained within the local biosphere.)

Accumulated amount in local biosphere:

The total amount in the biosphere should be the sum of several biosphere subcompartments:

$$I_{Bio}^i \approx Ms_{Total}^i + M_{Lake}^i + M_{sed}^i, \quad (6.15)$$

where the summation includes the surface soil in all fields, the lake water and lake sediment. This estimate does not include the surface biomass (the surface soil microbial biomass should be implicitly included with the soil), mass in air, or mass in subsoils. However, these are all expected to be much smaller than the soil and lake water content (and in the present model, the nuclide holdup in the subsoil region is neglected).

The total amount of nuclide i in the field surface soils [mol] is

$$Ms_{Total}^i = \sum_{f=fields} Ms^{f,i} \quad (6.16)$$

where

$Ms^{f,i} = C_{st}^{i,f} \cdot A^f \cdot Z_{ss} \cdot \rho_{soil}$ is the total amount of nuclide i in the surface soil in field f [mol],

$C_{st}^{i,f}$ is the total (porewater and solid) concentration of nuclide i in field f [mol/kg_{drysoil}],

A^f is the area of field f [m²],

Z_{ss} is the depth of the surface soil compartment, taken to be the minimum of Z_s or Z_d [m],

and

ρ_{soil} is the dry bulk density of the soil [kg/m³].

The total amount of nuclide i in the lake water [mol] is

$$M_{Lake}^i = C_L^i \cdot V_{Lake} \quad (6.17)$$

The total amount of nuclide i in the lake sediment [mol] is

$$\frac{\partial M_{sed}^i}{\partial t} = \left[V_{Lake} \alpha_{sed}^i C_L^i(t) - \lambda_r^i M_{sed}^i(t) + \lambda_r^p M_{sed}^p(t) \right] \quad (6.18)$$

where

α_{sed}^i is the rate constant for net transfer of nuclide n from the lake water to the lake sediments [a⁻¹].

Mass balance ratio for local biosphere:

The mass balance ratio for the local biosphere is a ratio of the flow out to the flow in:

$$MR_{bio}^n = \frac{\left(\int_0^{t_{end}} F_{OutLake}^n(t) \cdot dt + \int_0^{t_{end}} F_{DegasSoil}^n(t) \cdot dt + \int_0^{t_{end}} F_{DegasLake}^n(t) \cdot dt \right) + \left(\int_0^{t_{end}} \lambda_r^n \cdot I_{bio}^n(t) \cdot dt \right) + I_{bio}^n(t_{end})}{\left(\int_0^{t_{end}} \lambda_r^p \cdot I_{bio}^p(t) \cdot dt \right) + \left(\sum_{discharges} \int_0^{t_{end}} F_{outgeo}^{n,d}(t) \cdot dt \right)} \quad (6.19)$$

Accumulated amount in downstream biosphere:

The accumulated amount of nuclide in the downstream biosphere is calculated from:

$$\frac{\partial I_{DBio}^i}{\partial t} = \left[-\lambda_r^i \cdot I_{DBio}^i(t) + \lambda_r^p \cdot I_{DBio}^p(t) + F_{OutLake}^i(t) + F_{DegasSoil}^i(t) + F_{DegasLake}^i(t) \right] \quad (6.20)$$

7. RADIOTOXICITY INDICATORS

In addition to dose rates, two complementary indicators for repository safety are calculated. These indicators may be more reliable for use in the far future because they do not depend upon assumptions regarding biosphere conditions and human lifestyles (Becker et al. 2002).

The two complementary indicators are the radiotoxicity concentration of a radionuclide in lake water and the radiotoxicity flux from the geosphere to the biosphere. A radiotoxicity concentration is defined as the radioactivity concentration of a nuclide weighted by its ingestion dose conversion factor. The indicator value is the sum of the radiotoxicity concentration or flux over all nuclides.

7.1 RADIOTOXICITY CONCENTRATION IN LAKE WATER

The radiotoxicity concentration of nuclide i in lake water, RTC^i [Sv m^{-3}], is:

$$RTC^i = C_L^i(t) \cdot N_{Av} \cdot \frac{\lambda^i}{csa} \cdot DFe^i \quad (7.1)$$

where

$C_L^i(t)$ is the activity concentration of radionuclide i in lake water [mol m^{-3}] from Equation (5.20),

N_{Av} is Avogadro's number [atoms mol^{-1}],

csa is the number of seconds per tropical year 31,556,926 [s a^{-1}],

λ^i is the decay constant of radionuclide i [a^{-1}], and

DFe^i is the ingestion dose conversion factor for radionuclide i [$\text{Sv} \cdot \text{Bq}^{-1}$].

The total radiotoxicity concentration for all nuclides in lake water is RTC_{total} [$\text{Sv} \cdot \text{m}^{-3}$]:

$$RTC_{total} = \sum_i RTC^i \quad (7.2)$$

which can be regarded as a relative safety indicator for the repository that is independent of the human lifestyle, but does depend on surface biosphere conditions insofar as they affect lake water concentrations.

7.2 RADIOTOXICITY FLUX FROM GEOSPHERE

The radiotoxicity flux of nuclide i from the geosphere to the biosphere is RTF^i [$\text{Sv} \cdot \text{a}^{-1}$]:

$$RTF^i = \left(\sum_d X_d^i \right) \cdot N_{Av} \cdot \frac{\lambda^i}{csa} \cdot DFe^i \quad (7.3)$$

where

X_d^i is the flux of radionuclide i from discharge location d [$\text{mol} \cdot \text{a}^{-1}$],

N_{Av} is Avogadro's number [$\text{atoms} \cdot \text{mol}^{-1}$],

csa is the number of seconds per tropical year 31,556,926 [s a^{-1}],

λ^i is the decay constant of radionuclide i [a^{-1}], and

d is the discharge locations, including the well.

The total radiotoxicity flux from geosphere to biosphere for all nuclides is RTF_{total} [$\text{Sv}\cdot\text{a}^{-1}$]:

$$RTF_{total} = \sum_i RTF^i \quad (7.4)$$

which can be regarded as a relative safety indicator that is independent of biosphere conditions and human lifestyles.

7.3 REFERENCES

Becker, D.-A., D. Buhmann, R. Storck, J. Alonso, J.-L. Cormenzana, M. Hugli, F. van Gemert, P. O'Sullivan, A. Laciok, J. Marivoet, X. Sillen, H. Nordman, T. Vieno and M. Niemeyer. 2002. Testing of safety and performance indicators (SPIN). European Commission report FIKW-CT2000-00081. Brussels, Belgium.

ACKNOWLEDGEMENTS

This report was extensively based on descriptions prepared by Atomic Energy of Canada Limited as part of their documentation of the Environmental Impact Statement and Second Assessment Case studies. We would particularly like to acknowledge the authors of the main models – Robert Lemire and Frank Garisto (container solubility), Dennis LeNeveu (container release and vault transport), Ted Melnyk (streamtube network geosphere), Marsha and Steve Sheppard (soil), Brian Amiro (atmosphere), Glen Bird and M. Stephenson (lake), Reto Zach and Steve Sheppard (food-chain pathways), and Phil Davis and Michael Stephens (overall).

Significant update and editing were provided by P. Gierszewski, T. Melnyk, S. Sheppard, J. Tait, F. Garisto, C. Kitson, and B. Goodwin.

APPENDIX A: CONVOLUTION AND COMPARTMENT MODELS

A.1 CONVOLUTION MODEL

A convolution integral describes the output of a given system to a defined input as follows:

$$G(t) = \int_0^t F^{IN}(t') \cdot R(t-t') \cdot dt' \quad (A.1)$$

where

$F^{IN}(t)$ is the input "driving" function which can vary with time;
 $G(t)$ is the desired output of the system as a function of time;
 $R(t)$ is the "response function" - the response of the system to a delta function input at $t=0$.

A.2 COMPARTMENT MODEL

In several of the calculations in this report, a simple mass balance model, called a "compartment model", is used to represent a portion of the system that is considered to be homogeneous or "well mixed". For example, the compartment might represent the inventory of a nuclide in the container. The compartment model accounts for inflow, radioactive decay and ingrowth within the compartment, and release.

The mass balance for the amount of nuclide i accumulated in the interior of the compartment at time t is $A_i(t)$, where

$$\frac{dA_i(t)}{dt} = [F_i^{IN}(t) + \lambda_p A_p(t)] + [F_i^{OUT}(t) + \beta_i A_i(t)] \quad (A.2)$$

Input is due to some arbitrary input rate $F_i^{IN}(t)$ plus ingrowth from its parent nuclide p with decay constant λ_p that is present in the compartment in the amount $A_p(t)$. Loss is due to an arbitrary loss term $F_i^{OUT}(t)$ plus linear loss terms that are proportional to the accumulated amount of nuclide i present. The constant β_i defines the linear loss rate. In the cases considered here, the only linear loss is radioactive decay so $\beta_i = \lambda_i$, the radioactive decay constant. The initial condition is that there is no nuclide i initially present inside the compartment; that is, $A_i(0) = 0$. The general solution to this mass balance equation is:

$$A_i(t) = \int_0^t [F_i^{IN}(\tau) + \lambda_p A_p(\tau) - F_i^{OUT}(\tau)] \cdot \exp(-\lambda_i(t-\tau)) d\tau \quad (A.3)$$

This equation is solvable if $F^{IN}(\tau)$ and $F^{OUT}(\tau)$ are known. However, while $F_i^{IN}(t)$ may be known; in general the outflow is a function of $A_i(t)$ and is not known. We consider one particular case of interest.

Specifically, the compartment model as used here applies two conditions on $F_i^{OUT}(t)$. First, if there is no amount of i accumulated in the compartment, then the output rate $F_i^{OUT}(t)$ from the compartment is equal to the total input rate (the input plus the ingrowth from parent nuclide). Second, $F_i^{OUT}(t)$ is limited to a pre-defined maximum output rate $F_i^{MAX}(t)$.

$$F_i^{OUT}(t) = \begin{cases} \min\{F_i^{max}(t), [F_i^{IN}(t) + \lambda_p A_p(t)]\} & \text{if } A_p(t) = 0 \\ F_i^{max}(t) & \text{if } A_p(t) > 0 \end{cases} \quad (\text{A.4})$$

Thus, nuclide i accumulates when the input rate into the compartment is greater than $F_i^{max}(t)$, and depletes when the input rate is less than $F_i^{max}(t)$. Defining an individual case for the compartment model is done by defining the input flow rate $F_i^{IN}(t)$, the accumulated amount of parent $A_p(t)$, and the maximum output rate $F_i^{max}(t)$. If these functions have a simple form, then an analytical solution to the compartment model may be obtained. If $F_i^{IN}(t)$ and $F_i^{max}(t)$ are not simple or are known only numerically, then numerical techniques must be used to evaluate the solution.

APPENDIX B: LAPLACE TRANSFORM INVERSION

B.1 LAPLACE TRANSFORM INVERSION

The vault model transport was defined as analytical solutions in Laplace transform space, Section 4. The approach adopted to numerically inverting these Laplace transform was a modification of the Talbot algorithm (Talbot 1979).

Specifically, in using the Talbot algorithm as published, some problems were identified.

- $F(s)$ could not be evaluated to sufficient accuracy at some values of s .
- The inversion of $F(s)$ for some times t was inaccurate.
- The inversion required too many evaluations of $F(s)$. Rizzardi (1995) has shown that it is possible to reuse some of these function evaluations to estimate $f(t)$ at different times. When this method works it saves considerable computer time. Unfortunately, this technique frequently exacerbated the first two problems listed above.

A study of potential modifications to the Talbot algorithm was carried out. The modified algorithm adopted as a result of this study uses a suite of fixed contours in the complex plane so that $F(s)$ can be called a minimum number of times when inverting $F(s)$ at multiple time points, in a way similar to that described by Rizzardi (1995). A contour is defined by three parameters: ν , σ , and λ . Based on the study, several heuristic rules were found that improve the use of the Talbot algorithm.

- Keep $\nu = 1$. Talbot recommends this value for functions having all their singularities on the real axis.
- Set σ to the real value of the largest singularity. Variations of this setting can be important for getting good convergence at late times but seem to have little effect at early times. If the value of the largest singularity is not known, since the singularities usually lie on the negative real axis for problems of this type, set $\sigma = 0$.
- Start λ at Talbot's recommended value, then search for a better value. For a time t , assuming that σ is set as recommended above, Talbot's recommendation for λ is given by $\lambda_t = \omega/t$ where ω is a machine-specific constant. The study showed that this recommended value works well for medium and large times. However Talbot's recommended contour does not work well with the sample function used for a small t and an algorithm was devised to locate a better value.
- Use a set of standard contours. The strategy above for selecting λ can be modified slightly to use one of a set of standard contours, rather than a contour specific to time t . This approach works since the range of contours giving satisfactory results is fairly broad. If T is the largest time to be dealt with, N contours would be defined with times separated by a factor of 2 belonging to the sequence $\{4T, 2T, T, T/2, T/4, T/8, \dots, T/2^{N-2}\}$.
- Retain use of trapezoidal integration. Several other integration techniques were examined, including Simpson's rule and Gaussian quadrature, both of which usually work much better than trapezoidal integration. However, trapezoidal integration, as originally recommended by Talbot, gave the best result. Use of a higher density of points in small regions of the integrand where the function is changing rapidly and a sparser scattering of points in other parts of the interval was also examined. In this application, this approach does not work well at all. Accelerated convergence of trapezoidal integration using Talbot's method seems to require an even distribution of points.
- Estimate error by comparing integrals along neighbouring contours. With a factor of 2 for λ between contours as described above, the line integral will typically converge on at least two

adjacent contours. This is not necessarily the case with larger factors, and smaller factors require too many contours. By finding the optimal pair of contours with the least difference between their estimates of $f(t)$, one obtains two independent estimates of this value. The estimates are independent because they are based on different data points. The difference between these two estimates is an estimate of the error in either estimate. By averaging the two estimates, one can cut this error estimator in half.

B.2 REFERENCES

- Rizzardi, M. 1995. A modification of Talbot's method for the simultaneous approximation of several values of the inverse Laplace Transform. *ACM Transactions on Mathematical Software* 21(4), 347-371.
- Talbot, A. 1979. The accurate numerical inversion of Laplace transforms. *Jrnl. Inst. Maths. Applics.* 23, 97-120.

APPENDIX C: BIOSPHERE SUBMODEL PARAMETERS

C.1 IDENTIFICATION OF STATE-DEPENDENT AND STATE-INDEPENDENT PARAMETERS

Tables C.1 and C.2 identify parameters used by the biosphere submodel that are dependent and independent of the biosphere state, respectively. The former would change from state to state, and potential sources of data include the following:

- A temperate state would be similar to the conditions modelled in several contemporary studies, including Davis et al. (1993), Zach et al. (1996) and Garisto et al. (2004a).
- A permafrost state would be accompanied by changes to the properties of local plants and animals, affecting the food intake of the critical group. Irrigation would likely not be practised. Sources of data include Garisto et al. (2005), Environment Canada (2008), and Garisto et al. (2010, Appendix A).
- A proglacial lake state would include a very large lake formed in part from glacial meltwater. It would also be accompanied by changes to the properties of local plants and animals, affecting the food intake of the critical group. In particular, the critical group might ingest larger quantities of local fish. Sources of data include Garisto et al. (2005b), Environment Canada (2008), and Garisto et al. (2010, Appendix A).
- Ice sheet states are characterized by a thick sheet of ice extending over a wide area around the repository, precluding the presence of humans. We recommend setting the overall occupancy factors to zero for human and non-human biota. Values for most other biosphere parameters are not relevant in this case.

Sources of state-independent parameters data may be found in Garisto et al. (2004b) and Garisto et al. (2011).

Table C.1 State-dependent Parameters in the Biosphere Submodel

Symbol	Definition [and dimension]
α_{sed}^i	rate constant for net transfer of nuclide i from the lake water to the lake sediments [a^{-1}]
λ_{vol}^i	rate constant at which volatile or gaseous of nuclide i are released from the lake's surface and enter the atmosphere [a^{-1}]
λ_v^e	volatilization rate constant for element e degassing from soil [a^{-1}]
$A_{watershed}$	watershed area of the lake [m^2]
A_L	lake surface area [m_{water}^2]
CR_{nhfood}^e	plant-to-soil concentration ratio of element e for crop or garden plants used as human food [-]
CR_{nhfood}^e	plant-to-soil concentration ratio of element e for forage plants used by domestic animals or non-human biota [-]
Cym^j	carbohydrate content (concentration) of food type j [$g \cdot kg^{-1}_{wetbio}$]
ff_{Afire}	frequency of agricultural fires [s^{-1}]
ff_{Lfire}	frequency of land fires [s^{-1}]
f_L	leaching rate fraction for upland soils [-]
$f_{downwind}$	fraction of time that a person is downwind from the house and can be exposed to contaminated air plume from the chimney [-]
$F^{e,j}$	terrestrial transfer coefficient for element e and food type or biota j

Symbol	Definition [and dimension]
	$[\text{d} \cdot \text{kg}^{-1}_{\text{wetbio}}]$
$F^{i,j}$	terrestrial animal inhalation transfer coefficient for nuclide i and food type or biota j $[\text{d} \cdot \text{kg}^{-1}]$
Fym^j	fat content of food type j $[\text{g} \cdot \text{kg}^{-1}_{\text{wetbio}}]$
H_b	building height [m]
H_s	soil ingestion rate from hands $[\text{kg}_{\text{drysoil}} \cdot \text{a}^{-1}]$
li	man's inhalation rate $[\text{m}^3_{\text{air}} \cdot \text{a}^{-1}]$
I_{MLA}	iodine aquatic mass-loading parameter $[\text{m}^3_{\text{water}} \cdot \text{m}^{-3}_{\text{air}}]$
I_p	duration of use of irrigated field [a]
I^f_{wref}	irrigation rate for field f [m/a]
K_{Rn}	indoor radon transfer coefficient $[(\text{mol}_{222\text{Rn}} \cdot \text{m}^{-3}_{\text{air}}) / (\text{mol}_{226\text{Ra}} \cdot \text{kg}^{-1}_{\text{drysoil}})]$
K_{water}^{Rn}	Rn transfer coefficient from fresh water to air: $[\text{m}_{\text{water}} \cdot \text{s}]$
N_{crit}	number of persons in the critical group [-]
Ob	building occupancy factor [-]
Og	ground occupancy factor [-]
Oh	overall human occupancy factor [-]
Onh	overall non-human occupancy factor [-]
P_{total}	total annual precipitation rate [m/a]
Pr_{peat}	probability of peat used as fuel [-]
Pr_{sed}	probability of sediment used as soil [-]
$p_{domestic.water}$	flag indicating the source of domestic water [-]
p^f_{irr}	flag indicating whether field f is irrigated [-]
q_{Rn}	radon flux density per unit ^{226}Ra concentration in the soil $[\text{mol}_{222\text{Rn}} \cdot \text{m}^{-2}_{\text{soil}} \cdot \text{s}^{-1} \cdot \text{mol}^{-1}_{226\text{Ra}} \cdot \text{kg}_{\text{drysoil}}]$
Pym^j	protein content of food type j $[\text{g} \cdot \text{kg}^{-1}_{\text{wetbio}}]$
Q_{pc}	annual water demand per person for drinking and domestic use $[\text{m}^3_{\text{water}} \cdot (\text{person} \cdot \text{a})^{-1}]$
Q^j_{dw}	animal drinking water ingestion rate for food type or biota j $[\text{L}_{\text{water}} \cdot \text{d}^{-1}]$
Q^j_s	animal soil ingestion rate for food type or biota j $[\text{kg}_{\text{dry soil}} \cdot \text{d}^{-1}]$
$Q^j_{f,an}$	forage feed consumption rate of each animal for food type or biota j $[\text{kg}_{\text{wetbio}} \cdot \text{a}^{-1}]$
Q^j_a	animal inhalation rate for food type or biota j $[\text{m}^3 \cdot \text{d}^{-1}]$
r^j_{air}	atmospheric plant interception fraction for food type j [-]
r^j_{irr}	irrigation plant interception fraction for food type j [-]
R_{runoff}	watershed average runoff from precipitation (P - ET) [m/a]
R_{melt}	total melt-water from glaciers [m/a]
t_{hwbm}	holdup time for wood building materials [d]
t_{peat}	duration of fuel peat use [a]
$thdw$	holdup time for human drinking water [d]
thp	holdup time for fish [d]
thf^j	terrestrial animal feed or forage holdup time between harvest and consumption for food type j [d]
t_{for}	forest renewal time [a]

Symbol	Definition [and dimension]
te^{jk}	time of above-ground exposure for food type j and pathway k during the growing season, or return time for pasture [d]
t_{hibm}	holdup time for inorganic building materials [d]
tpb	plant environmental half time for non-human biota [d]
tpf	forage plant environmental half-life [d]
tpg	plant environmental half time [d]
U_w	annual average wind speed at the repository site [m/s]
U_{dw}	input human drinking water rate [L/a]
U_{in}^j	input human ingestion rate of food type j [$g_{wetbio} \cdot d^{-1}$]
V_d	dry deposition velocity [$m^3_{air} \cdot (m^2_{soil} \cdot s)^{-1}$]
W_b	building width [m]
Y_p^{garden}	garden plant biomass density (yield) [$kg_{wetbio} \cdot m^{-2}$]
Y_j^{forage}	forage plant biomass density (yield) for food type j [$kg_{wetbio} \cdot m^{-2}$]
Y_{pb}	plant biomass density (yield) for wood (for building or fuel) [$kg_{wetbio} \cdot m^{-2}$]
Z_s	depth of soil normally accessed by plant roots [m]
Z_d	depth to water table [m]
Z_L	mean depth of the lake [m]

Table C.2 State-independent Parameters in the Biosphere Submodel

Symbol	Definition [and dimension]
λ_{bt}	loss due to bioturbation by flora and fauna [a^{-1}]
ϵ_{dsed}	deep sediment porosity [-]
θ_s	volumetric water-content of the surface soil [$m^3_{water} \cdot m^{-3}_{soil}$]
ρ_{dsed}	deep sediment bulk density [$kg_{drysed} \cdot m^{-3}$]
ρ_{soil}	dry soil bulk density [$kg \cdot m^{-3}_{drysoil}$]
$\rho_{soil}^{organic}$	soil bulk density for organic (peat) soil [$kg_{drysoil} \cdot m^{-3}_{drysoil}$]
b	Exponent in Equation (5.44), equal to about 3 for a fine sandy loam [-]
B^{ij}	aquatic concentration ratio for nuclide i and food type j [$L_{water} \cdot kg^{-1}_{wetbio}$]
$B^{i,fish}$	aquatic concentration ratio for nuclide i and biota $m = fish$ [$L_{water} \cdot kg^{-1}_{wetbio}$]
B_{C12}	carbon content of soft tissues in a human [kg]
B_{Cl}	chlorine content of soft tissues in a human [kg]
B_H	average hydrogen concentration in humans [$g \cdot kg^{-1}$]
B_m	soft tissues mass in a human [kg]
Ca_{dw}^{H3}	average 3H concentration in drinking water [$Bq \cdot m^{-3}_{water}$]
C_{C12}	annual average groundwater concentration of <u>stable</u> carbon [$kg_C \cdot L^{-1}_{water}$]
C_{Cl}	annual average groundwater concentration of <u>stable</u> chlorine [$kg_C \cdot L^{-1}_{water}$]
C_I	annual average groundwater concentration of <u>stable</u> iodine [$kg_C \cdot L^{-1}_{water}$]
CB_{C12}^m	concentration of carbon in biota m [$kg_C \cdot kg^{-1}_{wetbio}$]
CB_{Cl}^m	concentration of chlorine in biota m [$kg_C \cdot kg^{-1}_{wetbio}$]
CB_H^m	concentration of hydrogen in $m = plant, mammal, bird and fish$ [$g_H \cdot kg^{-1}_{wetbio}$].

Symbol	Definition [and dimension]
CB_i^m	concentration of iodine in biota m [$\text{kg}_C \cdot \text{kg}^{-1}_{\text{wetbio}}$]
C_{Cl}	average stable chlorine concentration in the surrounding water [$\text{kg}_{Cl} \cdot \text{L}^{-1}_{\text{water}}$]
cda	is the number of days per tropical year 365.2422 [d a^{-1}]
$cdws$	dry/wet soil conversion factor [$\text{kg}_{\text{drysoil}} \cdot \text{kg}^{-1}_{\text{wetsoil}}$]
Cec	carbohydrate fuel value [$\text{kJ} \cdot \text{g}^{-1}$]
C_H	concentration of hydrogen in water [$\text{g} \cdot \text{m}^{-3}$]
clm	conversion factor from m^3 to L [$0.001 \text{ m}^3 \cdot \text{L}^{-1}$]
csa	is the number of seconds per tropical year 31,556,926 [s a^{-1}]
DFa^i	air immersion dose conversion factor for nuclide i [$\text{Sv} \cdot \text{a}^{-1} / (\text{Bq} \cdot \text{m}^{-3}_{\text{air}})$]
DFb^i	building material exposure dose conversion factor for nuclide i [$\text{Sv} \cdot \text{a}^{-1} / (\text{Bq} \cdot \text{kg}^{-1}_{\text{drv}})$].
DFB_{int}^{C14}	internal dose conversion factor for ^{14}C [$(\text{Gy} \cdot \text{a}^{-1}) / (\text{Bq} \cdot \text{kg}^{-1})$]
DFB_{int}^{Cl36}	internal dose conversion factor for ^{36}Cl [$(\text{Gy} \cdot \text{a}^{-1}) / (\text{Bq} \cdot \text{kg}^{-1})$]
DFB_{int}^i	internal dose conversion factor for nuclide i [$(\text{Gy} \cdot \text{a}^{-1}) / (\text{Bq} \cdot \text{kg}^{-1}_{\text{wetbio}})$]
DFB_{int}^{I129}	internal dose conversion factor for ^{129}I [$(\text{Gy} \cdot \text{a}^{-1}) / (\text{Bq} \cdot \text{kg}^{-1})$]
$DFB_{int}^{i, \text{fish}}$	dose conversion factor for internal exposure of fish to nuclide i [$(\text{Gy} \cdot \text{a}^{-1}) / (\text{Bq} \cdot \text{kg}^{-1}_{\text{wetbio}})$]
DFB_{int}^{H3}	internal dose conversion factor for ^3H [$(\text{Gy} \cdot \text{a}^{-1}) / (\text{Bq} \cdot \text{kg}^{-1})$]
$DFB_{int}^{i,m}$	internal dose conversion factor for nuclide i [$(\text{Gy} \cdot \text{a}^{-1}) / (\text{Bq} \cdot \text{kg}^{-1}_{\text{wetbio}})$]
$DFB_{a, \text{ext}}^{i,m}$	air immersion dose conversion factor for m = bird, plant or mammal for nuclide i [$(\text{Gy} \cdot \text{a}^{-1}) / (\text{Bq} \cdot \text{m}^{-3}_{\text{air}})$]
$DFB_{a, \text{ext}}^{i,m}$	dose conversion factor for nuclide i and m = bird or mammal, for external exposure to vegetation [$(\text{Gy} \cdot \text{a}^{-1}) / (\text{Bq} \cdot \text{m}^{-3}_{\text{wetbio}})$]
$DFB_{\text{ext}}^{i,m}$	water immersion dose conversion factor for m = bird, plant or mammal for nuclide i [$(\text{Gy} \cdot \text{a}^{-1}) / (\text{Bq} \cdot \text{m}^{-3}_{\text{water}})$]
$DFB_{s, \text{ext}}^{i,m}$	soil or sediment immersion dose conversion factor for m =bird, plant or mammal for nuclide i , [$(\text{Gy} \cdot \text{a}^{-1}) / (\text{Bq} \cdot \text{m}^{-1}_{\text{drysoil}})$]
DF^{C14}	internal dose conversion factor for ^{14}C [$\text{Sv} \cdot \text{a}^{-1} / (\text{Bq} \cdot \text{kg}^{-1})$]
DFe^i	ingestion dose conversion factor for nuclide i [$\text{Sv} \cdot \text{Bq}^{-1}$]
DFg^i	ground exposure dose conversion factor for nuclide i [$\text{Sv} \cdot \text{a}^{-1} / (\text{Bq} \cdot \text{kg}^{-1}_{\text{wetsoil}})$]
DFh^i	water immersion dose conversion factor for nuclide i [$\text{Sv} \cdot \text{a}^{-1} / (\text{Bq} \cdot \text{m}^{-3}_{\text{water}})$]
DFi^i	inhalation dose conversion factor for nuclide i [$\text{Sv} \cdot \text{Bq}^{-1}$]
En	man's total energy need [$\text{kJ} \cdot \text{d}^{-1}$]
E_{peat}	convertible energy content of dry fuel peat [$\text{MJ} \cdot \text{kg}_{\text{drypeat}}^{-1}$]
E_{wood}	convertible energy content of fuel wood [$\text{MJ} \cdot \text{kg}_{\text{wetbio}}^{-1}$]
f_{cl}	fraction of crop elemental composition lost each year [-]
Fec	fat fuel value [$\text{kJ} \cdot \text{g}^{-1}$]
ff_{crop}	cropping frequency of garden and forage fields [a^{-1}].
$f_{ss}^{f,d}$	fractional area of field f that is on aquatic discharge location d [-]
ff_{woodlot}	cutting frequency of woodlot field [a^{-1}]
Fi^m	terrestrial animal inhalation transfer coefficient for nuclide i and biota m [$\text{d} \cdot \text{L}^{-1}$] or [$\text{d} \cdot \text{kg}^{-1}$]

Symbol	Definition [and dimension]
f_{ie}	input leaching rate fraction for upland soils (i.e., fraction leaching relative to total input minus evapotranspiration [-])
F^m	ingestion transfer coefficient for nuclide i for biota $m =$ mammal and bird [$d \cdot kg^{-1}_{wetbio}$]
fr_{Afire}^i	emission fraction from agricultural fires [-]
fr_{Efire}^i	emission fraction from energy fires [-]
fr_{Lfire}^i	emission fraction of nuclide i from land fires [-]
fr_{iw}^i	fraction of nuclide i released to indoor air from the water [-]
f_{sbc}	soil/inorganic building material conversion factor [-]
f_{wdw}	wet/dry wood conversion factor [$kg_{wetbio} \cdot kg^{-1}_{dryveg}$]
gb^i	mass/radioactivity conversion factor for nuclide $i = {}^{14}C$ [$kg \cdot Bq^{-1}$]
gb^i	mass/radioactivity conversion factor for nuclide $i = {}^{36}Cl$ [$kg \cdot Bq^{-1}$]
gb^{129}	mass/radioactivity conversion factor for ${}^{129}I$ [$kg \cdot Bq^{-1}$]
I_{bldg}	building infiltration rate [s^{-1}]
$I_{irr}^{f,stype}$	rate of irrigation for each field f and soil type $stype$ [$m^3_{water} \cdot m^{-2}_{soil} \cdot a^{-1}$]
$I_{irr}^{garden,stype}$	garden irrigation rate for the soil type $stype$ [$m \cdot a^{-1}$]
In^i	human total intake of stable iodine [$kg \cdot a^{-1}$]
$K_{d, sed}$	sediment solid/liquid distribution coefficient [$m^3 \cdot kg^{-1}_{drysed}$]
K_d^i	sorption coefficient of nuclide i in the surface soil [$m^3 \cdot kg^{-1}$]
Ki_{Rn}	indoor radon transfer coefficient from ${}^{226}Ra$ [$(mol_{222Rn} \cdot m^{-3}_{air}) / (mol_{226Ra} \cdot kg^{-1}_{drysoil})$]
K_k	plume wake entrainment parameter [-]
M_w^i	molecular weight [$kg \cdot mol^{-1}$]
N_{AV}	Avogadro's number [mol^{-1}]
Oe	water immersion occupancy factor [-]
Pec	protein fuel value [$kJ \cdot g^{-1}$]
Ps	amount of soil on plants [$kg_{drysoil} \cdot kg^{-1}_{wetbio}$]
Q_{fuel}	energy requirement from the fuel [$MJ \cdot a^{-1}$]
Q_{fuel}	energy required to heat the critical group's dwelling for a year [$MJ \cdot a^{-1}$]
$Q_{bs}^{f,d}$	water flow from the subsoil to surface soil for field type f and location d [$m \cdot a^{-1}$]
Q_{sed}	rate of accumulation of (dry) sediment per unit area of lake [$kg_{dry} \cdot m^{-2} \cdot a^{-1}$]
Q_{ss}	flow of uncontaminated water from other areas of the catchment [$m^3 \cdot a^{-1}$]
Q_{swd}	summer water deficit [m/a]
$R_{fac}^{d,i}$	retardation factor for nuclide i in the last geosphere layer preceding discharge to the biosphere at discharge location d [-]
R_t	total watershed runoff [$m^3_{water} \cdot m^{-2}_{watershed} \cdot a^{-1}$]
r_{pb}	plant interception fraction for wooden building material [-]
r_{air}^{plant}	atmospheric plant interception fraction for plant biota [-]
$stype$	soil type (sand, loam, clay, organic)
$t_{1/2}$	half life of an unspecified radioactive isotope [a]; related to decay rate by $\lambda = \ln(2)/t_{1/2}$.

Symbol	Definition [and dimension]
$t_{1/2,fc}$	highest daughter half life, used in association with Equation (5.82) and set equal to 20 [a].
t_{eb}	time of above-ground exposure for wooden building material [d]
te^{jk}	time of above-ground exposure for food type j during the growing season, or return time for pasture [d]
$te^{plant,k}$	time of above-ground exposure for the plant during the growing season, or return time for pasture [d]
th	holdup time between harvest and consumption of plants [d]
Tha^j	terrestrial animal inhalation holdup time for food type j [d]
Thi	iodine content of thyroid [kg]
Thm	mass of thyroid [kg]
ths^j	terrestrial animal soil ingestion holdup time for food type j [d]
thw^j	terrestrial animal drinking water holdup time for food type j [d]
thw^j	plant holdup time for food type j = aquatic plant [d]
$U_{w,ref}$	annual average wind speed across the Canadian Shield, used in Equation (5.63) and assumed to equal 2.36 m/s
W_r	washout ratio [-]
W_{sed}^0	initial mass of (dry) sediment per unit area of sediments [$kg_{dry} \cdot m^{-2}$]
Y_w	plant yield for wood (for building or fuel) [$kg_{wetbio} \cdot m^{-2}_{soil}$]
$Y_{p,min}^f$	minimum plant biomass yield for field f [$kg_{wetbio} \cdot m^{-2} \cdot a^{-1}$]
Y_{for}	forest yield [$kg_{biomass} \cdot m^{-2}$]
Y_{an}^j	average dressed yield of animal j [$kg_{wetbio} \cdot a^{-1}$ or $L_{milk} \cdot a^{-1}$]
Z_{biosed}	bioturbated sediment thickness accumulated over a 50 year period [m]
Z_{sed}	thickness of sediment that can be accessed [m] (generally, this is the same as Z_s)
Z_{ssl}	shallow soil limit [m]

C.2 REFERENCES

- Davis, P.A., R. Zach, M.E. Stephens, B.D. Amiro, G.A. Bird, J.A.K. Reid, M.I. Sheppard, S.C. Sheppard and M. Stephenson. 1993. The disposal of Canada's nuclear fuel waste: The biosphere model, BIOTRAC, for postclosure assessment. Atomic Energy of Canada Limited Report, AECL-10720, COG-93-10. Pinawa, Canada.
- Environment Canada. 2008. Southern Artic Ecozone. (<http://www.ec.gc.ca/soerre/English/vignettes/Terrestrial/sa/default.cfm>)
- Garisto, F., J. Avis, N. Calder, A.D'Andrea, P. Gierszewski, C. Kitson, T.W. Melnyk, K. Wei and L. Wojciechowski. 2004a. Third case study – Defective container scenario. Ontario Power Generation Report 06819-REP-01200-10126-R00. Toronto, Canada.
- Garisto, F., J. Avis., T. Chshyolkova, P. Gierszewski, M. Gobien, C. Kitson, T. Melnyk, J. Miller, R. Walsh and L. Wojciechowski. 2010. Glaciation scenario: Safety assessment for a deep geological repository for used fuel. Nuclear Waste Management Organization Technical Report NWMO TR-2010-10. Toronto, Canada.

- Garisto, F., A. D'Andrea, P. Gierszewski and T. Melnyk. 2004b. Third case study - Reference data and codes. Ontario Power Generation Report 06819-REP-01200-10107-R00. Toronto, Canada.
- Garisto, F., M. Gobien, E. Kremer and C. Medri. 2011. Fourth case study: Reference data and codes. Nuclear Waste Management Organization Technical Report NWMO TR-2011-18. Toronto, Canada. (In Progress)
- Garisto, N.C., Z. Eslami and F. Bhesania. 2005. Alternative Exposure Groups, Characteristics and Data for the Post-Closure Safety Assessment of a Deep Geological Respository. Ontario Power Generation Report 06819-REP-01200-10150-R00. Toronto, Canada.
- Zach, R., B.D. Amiro, G.A. Bird, C.R. Macdonald, M.I. Sheppard, S.C. Sheppard and J.G. Szekely. 1996. The disposal of Canada's nuclear fuel waste: A study of postclosure safety of in-room emplacement of used CANDU fuel in copper containers in permeable plutonic rock; Volume 4: Biosphere Model. Atomic Energy of Canada Limited Report, AECL-11494-4, COG-95-552-4. Pinawa, Canada.